DOE/JPL-1060-69
(DE84008503)

Energy

SOLAR

# PROCEEDINGS, FIFTH PARABOLIC DISH SOLAR THERMAL POWER PROGRAM ANNUAL REVIEW

March 1, 1984

Work Performed Under Contract No. AM04-80AL13137

Jet Propulsion Laboratory
California Institute of Technology
Pasadena, California

Technical Information Center
Office of Scientific and Technical Information
United States Department of Energy

## DISCLAIMER

## DISCLAIMER



This report has been reproduced directly from the best available copy.

Available from the National Technical Information Service, U. S. Department of Commerce, Springfield, Virginia 22161.

Price: Printed Copy A12
Microfiche A01

Codes are used for pricing all publications. The code is determined by the number of pages in the publication. Information pertaining to the pricing codes can be found in the current issues of the following publications, which are generally available in most libraries: *Energy Research Abstracts (ERA); Government Reports Announcements* and Index (*GRA* and I); *Scientific and Technical Abstract Reports (STAR);* and publication NTIS-PR-360 available from NTIS at the above address.

DOE/JPL-1060-69
(CONF-831274)
(DE84008503)
Distribution Category UC-62

5105-133
Solar Thermal Power Systems Project
Parabolic Dish Systems Development

# Proceedings
# Fifth Parabolic Dish Solar Thermal Power Program Annual Review

December 6-8, 1983
Indian Wells, California

March 1, 1984

Prepared for
U.S. Department of Energy
Through an Agreement with
National Aeronautics and Space Administration
by
Jet Propulsion Laboratory
California Institute of Technology
Pasadena, California

JPL Publication 84-13

THIS PAGE

WAS INTENTIONALLY

LEFT BLANK

## ABSTRACT

The Fifth Parabolic Dish Solar Thermal Power Program Annual Review was held December 6-8, 1983, at the Erawan Garden Hotel, Indian Wells, California, under the sponsorship of the U.S. Department of Energy, and conducted by the Jet Propulsion Laboratory.

The primary objective of the Review was to present the results of activities within the Parabolic Dish Technology and Module/Systems Development element of the Department of Energy's Solar Thermal Energy Systems Program. The Review consisted of nine technical sessions covering overall Project and Program aspects, Stirling and Brayton module development, concentrator and engine/receiver development, and associated hardware and test results to date; distributed systems operating experience; international dish development activities; and non-DOE-sponsored domestic dish activities. A panel discussion concerning business views of solar electric generation was held.

These Proceedings contain the texts of presentations made at the Review, as submitted by their authors at the beginning of the Review; therefore, they may vary slightly from the actual presentations in the technical sessions.



## ACKNOWLEDGEMENT

This conference was conducted by the Jet Propulsion Laboratory and was sponsored by the U.S. Department of Energy through Interagency Agreement DE-AM04-80AL13137 (NASA/JPL TASK RE-152, Amendment No. 327).

THIS PAGE

WAS INTENTIONALLY

LEFT BLANK

TABLE OF CONTENTS
AND SUMMARY OF PRESENTORS

# FIFTH PARABOLIC DISH SOLAR THERMAL POWER PROGRAM REVIEW

## WELCOMING REMARKS

John W. Lucas
General Chairman

Jet Propulsion Laboratory
Pasadena, CA 91109

Welcome to the Fifth Parabolic Dish Solar Thermal Power Program Annual Review. During the next three days, reports on the many significant accomplishments that have occurred during the past year will be presented by the involved contractors. In addition, we have arranged what should be an outstanding panel discussion.

Robert San Martin, Deputy Assistant Secretary for Renewable Energy, Department of Energy, will highlight the first session with an authoritative overview of alternate energy activities.

Also on Tuesday, domestic dish activities not sponsored by DOE will be reported upon.

There will be a field trip to the nearby Vanguard Stirling module site on Wednesday.

John Stolpe, Supervising Research Energy, Southern California Edison Company, will lead the panel, discussing issues affecting solar thermal electric dish development on Wednesday. Manufacturing, utility, and financial perspectives will be represented.

A session on Thursday will present operating experience from the three dish plants currently operational in the world. Also on Thursday, several of our foreign visitors will report on parabolic dish development in their respective countries.

# A BRIEF HISTORY

A. T. MARRIOTT

Jet Propulsion Laboratory
Pasadena, California 91109

The conversion of solar energy to electricity using paraboloidal collectors in conjunction with focal point-mounted heat engines is unique to the JPL managed DOE Solar Thermal Technology Program. This concept, developed by JPL, has evolved in seven years to become a viable candidate for the production of electricity on a commercial basis. The dish-electric project is now being transferred from JPL to Sandia National Laboratories, Albuquerque (SNLA) and it is an opportune time to look back at its short history.

The idea of producing thermal energy from the sun using a dish collector is not new; early dishes were used for irrigation purposes but could not compete with less expensive fossil fuels. However, interest was renewed after the oil crisis in 1973. JPL, as a result of experience in energy conversion and dish structures in the space program and a growing involvement in civil system activities, began to look at alternatives - one of which was a distributed collector system concept. This idea emerged from work done for NASA between 1974 and 1976 in a comparative assessment of orbital and terrestrial solar central power stations. In 1976 a proposal to the Energy Research and Development Agency (ERDA) was accepted to look at distributed systems as an alternative to the central receiver concept and to perform studies in support of the ERDA solar thermal office.

The parabolic dish project developed and went through several stages including a rather broad charter that included small solar thermal power systems employing a variety of technologies. By 1980 it had evolved to the point that three distinct activities comprised the project and the technology was limited to parabolic dishes. Advanced Subsystem Development was responsible for determining the feasibility of advanced components and materials for future generation systems. Module Development performed the detailed engineering, fabrication and testing of complete power producing modules. Applications Development was responsible for complete power systems and the demonstration of the dish technology through a series of engineering experiments. During this time the groundwork was laid for the Parabolic Dish Test Site (PDTS) at Edwards Air Force Base and the test bed concentrators (TBC) were installed. Also, many contracts were initiated with industry for the development of concentrators, receivers and engines, and for system level activities in preparation for the Small Community Experiments.

In 1981 several major activities were underway. General Electric was designing PDC-1 and Acurex was doing panel development for a concentrator that was to become PDC-2. Garrett Turbine Engine Company and United Stirling of Sweden were involved with the solarization of Brayton and Stirling engines, respectively. Ford Aerospace and Communications Corporation (FACC) was well into Phase II of Small Community Experiment No. 1, using an organic Rankine cycle (ORC) engine being developed by Barber-Nichols.

Fiscal year 1982 saw a cessation of funding for the Advanced Subsystem Development activity with most of this work going to SERI. The project consolidated to include two major areas: Technology Development and Module/System Development. At the same time, the major emphasis was shifted to the three module development activities associated with the Stirling, Brayton and ORC engines, and supporting component and subsystem development. It was during this year that the most significant test results were achieved at PDTS. The United Stirling (USAB) 4-95 engine was tested in conjunction with a USAB receiver on a TBC and produced electricity at a record efficiency of 29% from sunlight to power out of the generator. The ORC was also run on a TBC in a successful test that verified the system including receiver and controls. Sanders Associates and Advanco Corporation were under contract to design, build and test Brayton and Stirling modules, respectively. Power Kinetics Incorporated under contract to Applied Concepts successfully installed and tested a thermal dish at Capitol Concrete in Topeka, Kansas.

Significant progress was made during FY 1983. The Stirling module design was completed as was most of the subsystem fabrication; installation at Rancho Mirage was started. The ORC bearing problem was solved and steps taken toward the completion of a qualification test program. Acurex completed the design of PDC-2 and started fabricating test panels. Sanders Associates selected the LaJet concentrator for the Brayton module and the first one was built late in the year. JPL and GRI reached an agreement whereby two subatmospheric Brayton cycle engines would be made available to the solar thermal program. In other respects, FY 1983 was one of transition. JPL's system contract with FACC was completed and a contract was established between FACC and DOE to continue the ORC development. In July, a decision was made by JPL management to withdraw from the solar thermal project. Subsequent discussions with DOE and SNLA resulted in an approved plan to transfer the dish-electric project to SNLA during FY 1984.

While this is a point of departure for the JPL program, as well as for the people involved over the past several years - we feel confident that the transition will be made smoothly and we rest assured that the dish project will be in good hands as SNLA assumes responsibility for its management.

# FUTURE DISH PROJECT ACTIVITIES *

SAND83-2315A

James A. Leonard
Sandia National Laboratories
Albuquerque, New Mexico 87185

## ABSTRACT

The transition of the lead lab responsibility for the DOE Dish Electric Program from JPL to Sandia will create both problems and opportunities. In the near-term the schedule and budget of some of the project elements are being adversely affected. The DOE, JPL, and Sandia are dedicated to minimizing the impact of the transition. We at Sandia are pleased and gratified with the level of dedication, support, and cooperation displayed by the JPL staff. Likewise, we have been impressed with the patience and forbearance of the contractors in the program as we have imposed on most of them to help us familiarize ourselves with their projects.

The opportunity mentioned above has to do with the Dish Program now being planned and managed in a more unified way relative to the spectrum of applications for dish technology - a technology which can collect more energy at a given mid-to-high temperature than any other, bar none. This will allow more of the program budget to be devoted to R & D and less to administration and management.

The applications to be investigated in the future include distributed dish-electric, centralized dish-electric, cogeneration, industrial process heat, and fuels and chemicals production; materials and process development, and component and subsystem development will be pursued for all dish elements such as the concentrator, receiver, controls (including tracking and drive), engines and turbines, and thermal energy transport.

The strategy will generally be to pursue applications at higher and higher temperatures and to pursue technology development in an orderly process from materials studies through component development and field experiments. This does not mean that several of the above elements would not co-exist in the program - some development areas are ahead of others now and some development areas will move ahead more rapidly than others.

Relative to emphasis, it seems justifiable to place high priority on solar specific components such as the concentrator and the receiver. Engine development is inherently expensive and time-consuming. The foreseeable solar thermal budget will not support all-out R & D from the ground up. The current program philosophy of "tagging along" with developers in other

*This work supported by the U. S. Department of Energy

sectors appears prudent. The key technical issue of thermally connected fields of dishes is the thermal transport system. Encouraging progress in development of cost-effective thermal transport systems will be required before substantial commitments to dish-thermal applicatons are made.

Last, but not least, system-level tests and evaluations in realistic settings are an essential final step in any R & D process. In solar these are particularly important, not only because interface problems not foreseeable otherwise can be identified and corrected, but also because credibility and public acceptance and confidence are crucial to industry's ability to market systems commercially. The commitment to real-world sites must be carefully considered and must follow careful system-level shakeout and rigorous non-public qualification tests.

Sandia National Laboratories is pleased to be a part of the Dish Program, albeit disappointed to lose the suport of our good friends at JPL. We look forward to a productive relationship with all the other program participants.

Sandia Laboratories

Solar Energy

## PARABOLIC DISH TECHNOLOGY DEVELOPMENT

- SYSTEMS ENGINEERING AND ANALYSIS
- ENERGY TRANSPORT AND STORAGE
- RECEIVER DEVELOPMENT
- CONTROLS DEVELOPMENT
- DISTRIBUTED RECEIVER TEST FACILITY
- ENGINE DEVELOPMENT
- FIELD EXPERIMENT TECHNICAL SUPPORT
- CONCENTRATOR DEVELOPMENT

# IMPORTANT AREAS OF DISH PROGRAM FUTURE INVESTIGATION

- SYSTEM ENGINEERING AND ANALYSES

  NEEDED TO EVALUATE TRADEOFFS, SCOPE MARKET POTENTIAL, AND IDENTIFY THE MOST ATTRACTIVE FUTURE SYSTEM DEVELOPMENTS

THERMAL APPLICATIONS
- MID-TEMP ($<600^{o}C$) INCLUDING LOW-PRESSURE STEAM
- HIGH-TEMP - IS THERE AN UPPER TEMPERATURE BOUND?
- FUELS AND CHEMICALS - COORDINATE WITH CENTRAL RECEIVER APPLICATION STUDIES AND F & C RESEARCH

ELECTRICAL POWER APPLICATIONS
- HIGHER TEMPERATURE DISH-ELECTRIC STUDIES
- DISH-THERMAL BULK POWER WITH CONVENTIONAL STEAM CONDITIONS AND LARGE TURBINE GENERATORS
- SUPPORT DOE SCSE (EVALUATION & TECHNICAL CONSULTATION)

COGENERATION
- UTILIZE SHENANDOAH EXPERIENCE
- ALTERNATIVE SYSTEMS, APPLICATION, TEMPS

## IMPORTANT AREAS OF DISH PROGRAM FUTURE INVESTIGATION

ENERGY TRANSPORT AND STORAGE DEVELOPMENT - KEY TECHNICAL ISSUE FOR HIGH-TEMPERATURE DISH-THERMAL

- SENSIBLE HEAT - ESTABLISH BASELINE
- PHASE CHANGE - SCREENING STUDY
- CHEMICAL TRANSPORT - SIGNIFICANT NEAR-TERM EFFORT
  - LABORATORY SCALE EXPERIMENTS
  - FIELD EXPERIMENTS WITH HEATERS
  - FIELD EXPERIMENTS WITH COLLECTORS

## IMPORTANT AREAS OF DISH PROGRAM FUTURE INVESTIGATION

- RECEIVER DEVELOPMENT

  MID-TEMPERATURE THERMAL RECEIVER (>600°C)
  HIGH-TEMPERATURE RECEIVER FOR DISH-ELECTRIC AND THERMAL
  EXTERNAL RECEIVER
  RECEIVER/REACTOR
  HEAT TRANSFER FLUIDS (GASES, SALTS, LIQUID METALS, SOLID PARTICLES)
  APERTURE GLAZING AND AR COATINGS
  TERMINAL TRACKING SENSORS
  COLLATERAL BEAM DAMAGE PREVENTION (WALKOFF PROBLEM)
  HEAT PIPE RECEIVER

## IMPORTANT AREAS OF DISH PROGRAM FUTURE INVESTIGATION

- CONTROLS DEVELOPMENT - (IMPORTANT BUT NOT A NEAR-TERM EFFORT)
  - INTEGRATED COLLECTOR/SYSTEM CONTROLS/USER INFO
  - PROCESS CONTROLLERS
  - ADVANCED (SMART) CONTROLS TO MAXIMIZE ANNUAL COLLECTION
  - POWER CABLE CARRIER SYSTEMS

## IMPORTANT AREAS OF DISH PROGRAM FUTURE INVESTIGATIONS

- DISTRIBUTED REVEIVER TEST FACILITY (DRTF)
  - TEST AND EVALUATE COMPONENTS AND SUBSYSTEMS
  - CONDUCT SYSTEM-LEVEL TEST AND EVALUATIONS AS PRECURSORS TO (OR IN LIEU OF) FIELD PROJECTS
  - MAINTAIN CAPABILITY FOR CONTINUING TROUGH SYSTEMS TESTS (MISR FACILITY)
  - EVALUATION SUPPORT TO PRIVATE SECTOR DEVELOPERS

## ENGINE DEVELOPMENT

- UPGRADES
- FOLLOW-ON TESTING & EVALUATION
- HIGHER OPERATING TEMPS
- DESIGNS FOR HIGH VOLUME
- CENTRALLY LOCATED ENGINES

## IMPORTANT AREAS OF DISH PROGRAM FUTURE INVESTIGATION

- CONCENTRATOR DEVELOPMENT

  HIGH PERFORMANCE/LOW COST POTENTIAL

  REFLECTIVE CONCENTRATORS
  - SILVERED GLASS
  - SILVERED METAL
  - SILVERED FILM
  - STRETCHED MEMBRANE
  - CASSEGRAINIAN
  - HIGH RIM ANGLE (EXTERNAL RECEIVER)

  REFRACTIVE CONCENTRATORS
  - FRESNEL LENS (SINGLE OR MULTIPLE)

  OPTIMUM DIAMETER TRADEOFF FOR VARIOUS APPLICATIONS

# CONCENTRATOR DEVELOPMENT

William A. Owen
Jet Propulsion Laboratory
Pasadena, California

During the six years of technology development by the Parabolic Dish program, the problems peculiar to tracking dishes have been explored in depth with particular emphasis on economics. Starting with the Precursor Concentrator, testing techniques and apparatus such as calorimeters and the flux mapper were developed. At the same time, mirrors were developed to have a long operating life as well as high performance. Commercially available equipment was evaluated as well. Building on all these elements, the Test Bed Concentrators were designed and built. With a peak intensity in the focal plane of over 17,500 suns and an average concentrator ratio over 3,000 on an eight inch diameter aperture, they have proven to be the work horses of the technology. With a readily adjustable mirror array, they have proved to be an essential tool in the development of dish components, receivers, heat transport systems, instrumentation, controls, engines, and materials, all necessary to cost effective modules and plants. Utilizing the lessons learned from this technology, more cost effective systems were designed. These included Parabolic Dish Number 1 (PDC-1) and PDC-2 currently in final design by Acurex Corporation. Even more advanced concepts are being worked on, such as the Cassegranian systems by BDM Corporation.

# PARABOLIC DISH CONCENTRATOR (PDC-1)

Edwin W. Dennison/Maurice J. Argoud
Jet Propulsion Laboratory
Pasadena, California

The design, construction and installation of the Parabolic Dish Concentrator, Type 1 (PDC-1) has been one of the most significant JPL concentrator projects because of the knowledge gained about this type of concentrator and the development of design, testing and analysis procedures which are applicable to all solar concentrator projects. The need for these procedures was most clearly understood during the testing period which started with the prototype panel evaluation and ended with the performance characterization of the completed concentrator. For each phase of the test program practical test procedures were required and these procedures defined the mathematical analysis which was essential for successful concentrator development. The concentrator performance appears to be limited only by the distortions resulting from thermal gradients through the reflecting panels. Simple optical testing can be extremely effective, but comprehensive mechanical and optical analysis is essential for cost effective solar concentrator development.

# PARABOLIC DISH CONCENTRATOR (PDC-2) DEVELOPMENT

D. Rafinejad
Acurex Corporation
Mountain View, California
for
Fifth Parabolic Dish Solar Thermal Power Program Review
December 6-8, 1983

## ABSTRACT

Acurex Corporation has completed the design of the point-focus Parabolic Dish Concentrator (PDC-2). The fabrication of the prototype dish has begun.

The PDC-2 is a high-flux, 12.2m-diameter dish with a thermal output of 96.5 $kW_t$. The concentrator consists of a lightweight space-frame structure and 64 highly accurate reflective panels. The structurally efficient panels are comprised of cellular glass cores sandwiched between thin backsilvered mirror glass on the front and unsilvered glass on the back. The concentrator tracks the sun in elevation and azimuth axes and is mounted on a single embedded pedestal foundation.

This paper describes the concentrator design and status of the development project.

## INTRODUCTION

Acurex developed the PDC-2 design as a subcontractor to Ford Aerospace and Communication Corporation, under the sponsorship of the Department of Energy. The objective of the program is to develop a 12.2m parabolic dish concentrator for use in the Small Community Solar Experiment (SCSE No. 1). The program scope includes the design, fabrication, and testing of one concentrator at Sandia test facilities in Albuquerque, New Mexico.

Although PDC-2 development is intended for electrical power generation at a small community, it can be used in a much broader area of application. PDC-2 is a highly accurate concentrator that can be used in a distributed solar system for thermal and electrical power generation. The power conversion unit can be mounted at the focal plane or be centrally located. Its modular nature makes it suitable for applications in all system sizes.

Acurex has designed several generations of parabolic dish concentrators under JPL sponsorship. Extensive conceptual design studies have been performed over several years to optimize the design. The optimized concept has now been successfully carried through the detailed design and component prototyping stage.

The optimization studies were based on the overall installed system life cycle cost and performance and incorporated relevant improvements in related technologies such as heliostats. The PDC-2 design reflects several years of dish development and represents the state of the art in high performance solar dish technology.

The following sections describe the PDC-2 design and update the project status.

## PDC-2 DESIGN

The PDC-2 is a single reflection point-focusing, two-axis tracking solar concentrator with a reflective surface aperture of 12.2m in diameter. The focal length to aperture diameter ratio (f/D) of the dish is approximately 0.54. The reflected solar radiation focuses onto a receiver aperture of 10 to 15 in. in diameter, depending upon application. The dish concentration ratio ranges from 1,000 to 2,300. PDC-2 is shown in figure 1.

PDC-2 produces a minimum of 96.5 kW thermal power (100 $kW_t$ nominal) at the receiver aperture at 1,000 $W/m^2$ insolation and 10 mph wind.

The PDC-2 concentrator is designed for minimum fabrication and installation cost and is adaptable to low cost at high volume production. The concentrator has a design life of 20 years for reliable and safe operation.

The PDC-2 operates safely at winds up to 25 mph. At winds greater than 25 mph the concentrator will move to stow position facing the zenith.

The PDC-2 consists of five subsystems, as shown in figure 1:

- Reflective surface
- Support structure
- Pedestal/foundation
- Drive subsystem
- Electrical and controls

These subsystems are described in the following sections.

## REFLECTIVE SURFACE SUBSYSTEM

The concentrator surface consists of two concentric rings of independent reflective elements (panels) which form a physically discontinuous parabaloidal reflective surface with a common focal point. The inside ring is made up of 24 panels, and 40 panels comprise the outside ring. The reflective panel consists of a lightweight cellular glass core bonded to a thin glass mirror in front and a narrow strip of unsilvered thin glass in the back spar. The mirror glass and the spar cap carry the major portion of the bending loads of the composite structure. The reflective panel design is shown in figure 2.

The high quality reflective surface has a slope error of less than 1 mrad rms due to manufacturing tolerances and worst-case operating conditions. Cellular glass is a low-cost, noncritical material with a very high stiffness-to-weight ratio. It is easily machinable to provide the highly accurate optical surface and closely matches the coefficient of thermal expansion of the front and back glass. The panel back is shaped to minimize weight while maintaining the minimum thickness for structural integrity.

Each panel is supported at three points via support pads that are bolted to the ring truss structure. The support pads are made of precipitation

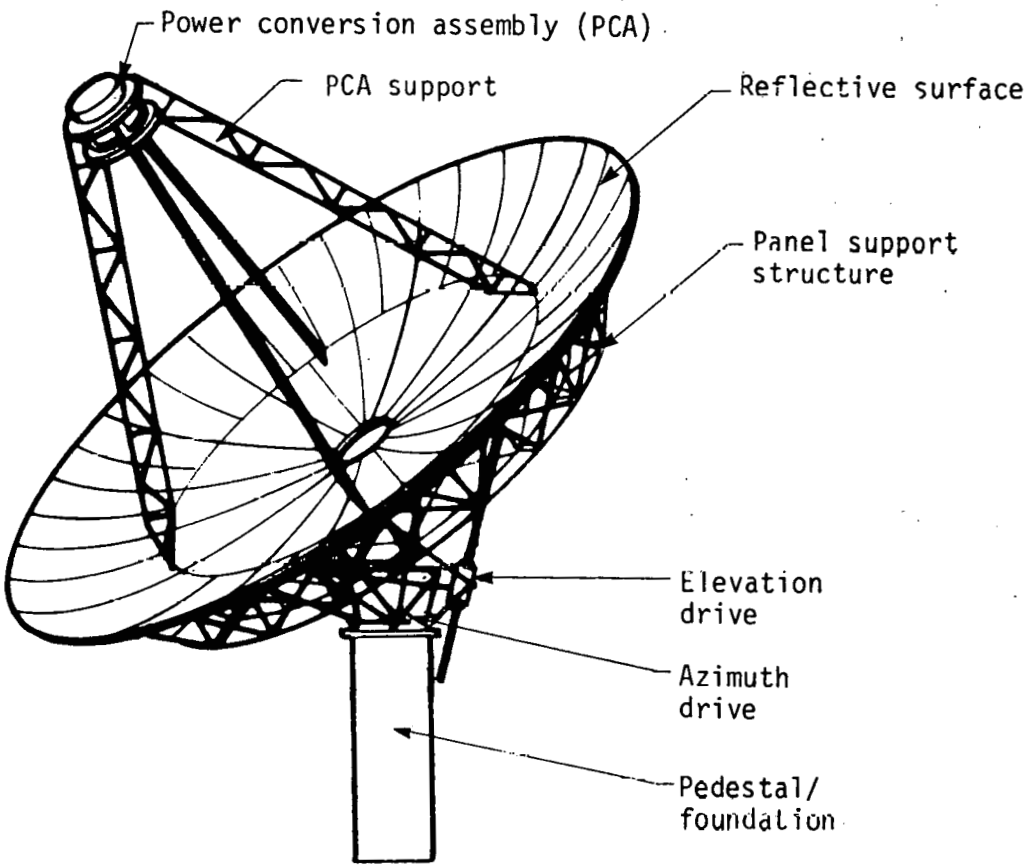


Figure 1. PDC-2

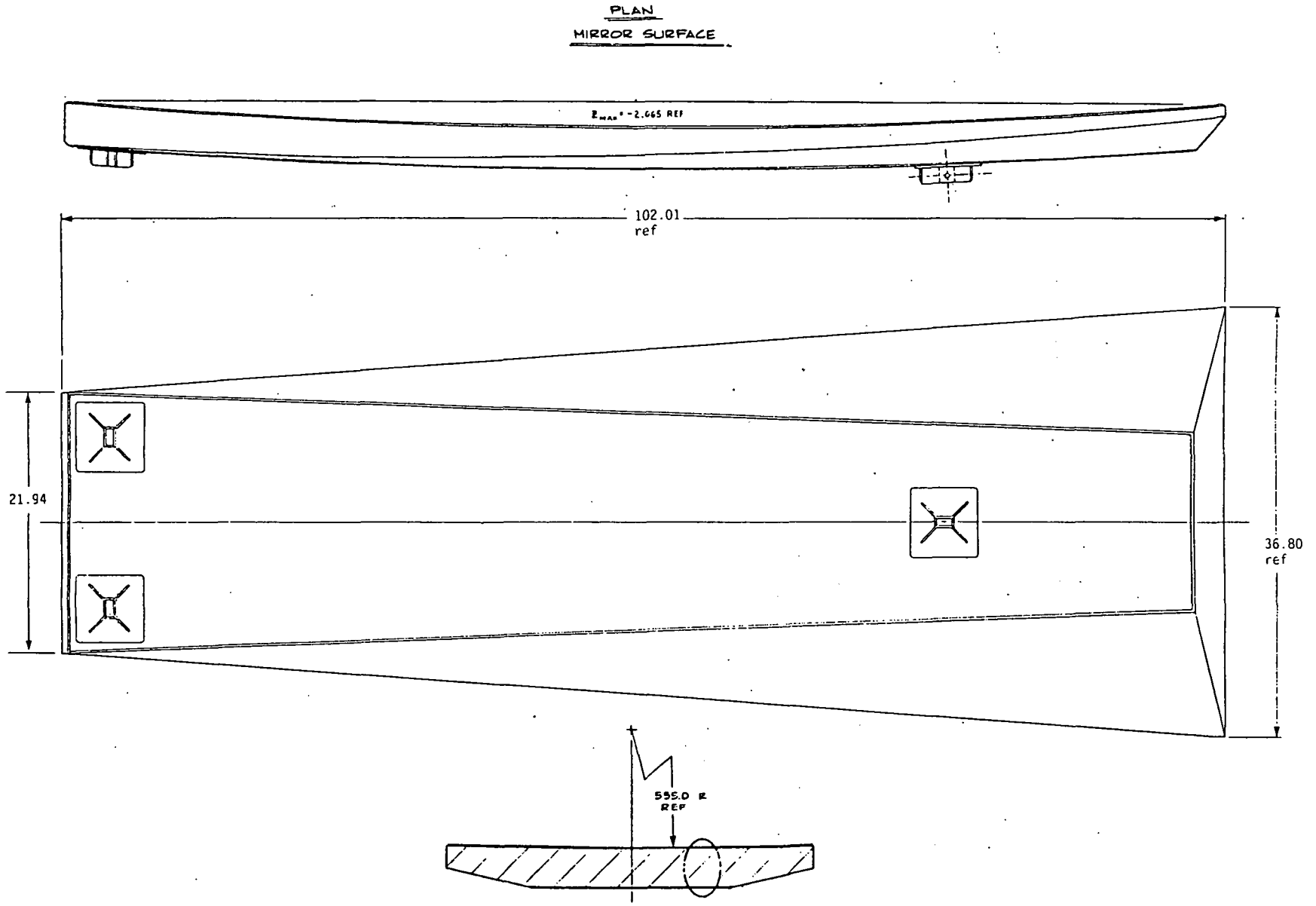


Figure 2. Outer Reflective Panel

hardened steel (ph 15-7 mo) for a good match with coefficient of thermal expansion of the glass.

The reflective surface mirror is a 0.040- to 0.058-in. thick chemically strengthened backsilvered glass. Acurex investigated availability of thin solar mirror glass in the desired length (108 in. for inner panel) from various U.S. and European suppliers.

Although it was determined that mirror in the desired size could be obtained from one European supplier it was deemed prudent early in the project to develop an alternate panel design to minimize program risk. A spliced joint reflective surface configuration was designed. In this design, two shorter (50 in. long) glass mirrors are butted together with a narrow piece (6 in.) of overlapping thin clear glass. The prototype PDC-2 panels will be made of full size (single sheet) corning 0317 glass that is 0.058 in. thick and is currently available in limited quantities.

The standard 24 in. by 18 in. by 5 in. foamglass blocks are currently mass produced by Pittsburgh Corning. The supplier will not manufacture large pieces (full size) of foamglass unless very large quantities are ordered. Therefore, for prototype and low-volume production of PDC-2 panels, 10 standard blocks are bonded together and cut to shape. The foamglass front surface is machined in a sanding operation to the paraboloidal configuration.

SUPPORT STRUCTURE SUBSYSTEM

The support structure subsystem consists of three parts as shown in figure 3:

a. Power conversion assembly (PCA) support
b. Panel support
c. Drive support

The overall support structure weight is 8,000 lbs and supports the 1,500-lb PCA, 5,400 lb of reflective panels and 600 lb of cabling and miscellaneous hardware.

The PCA support is a quadripod structure using laced legs and is of thin-wall steel tubing construction. Sixteen 5/16-in. diameter guy cables contribute to structure stability. The quadripod also provides a means of routing cables and lines to the equipment located at the focal point. The structure has a detachable PCA mounting frame required for installation and removal of the PCA. The quadripod legs are rigidly attached to the panel support structure at four flange mounting points located 45° with respect to the vertical and horizontal dish axis. The PCA support structure is designed for minimum shading or blocking to the incident and reflected insolation.

The panel suport structure is a space frame ring truss made of structural steel tubing. The triangular truss ring has outrigger attachments to support the reflective panels (see figure 3).

The 64 reflective panels are installed on the ring truss structure with statically determinant three-point attachment. These attachments have

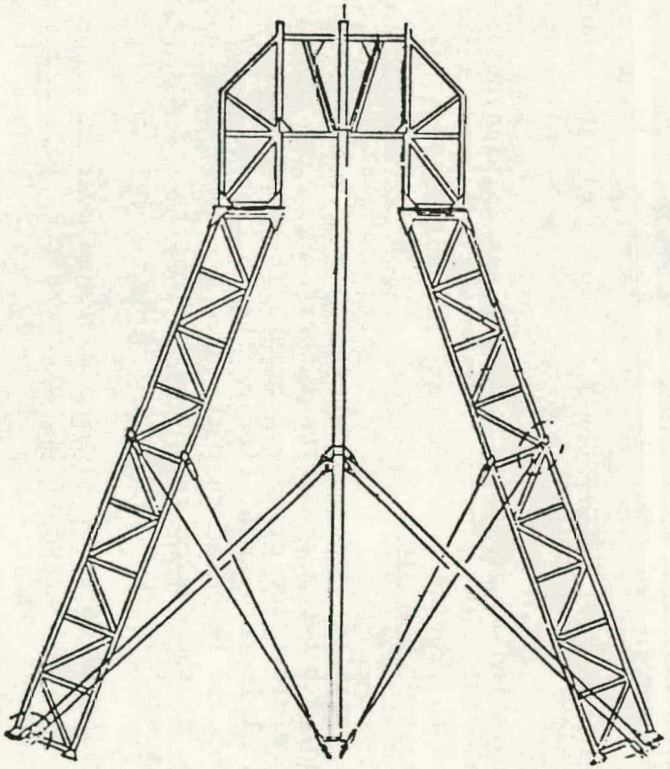

a. PCA support

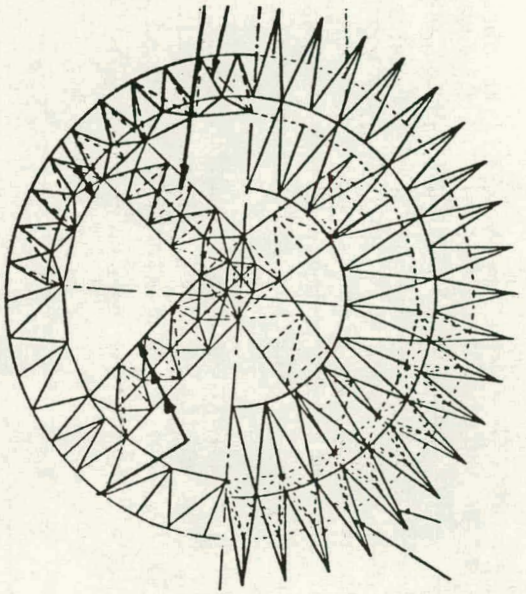

b. Panel support

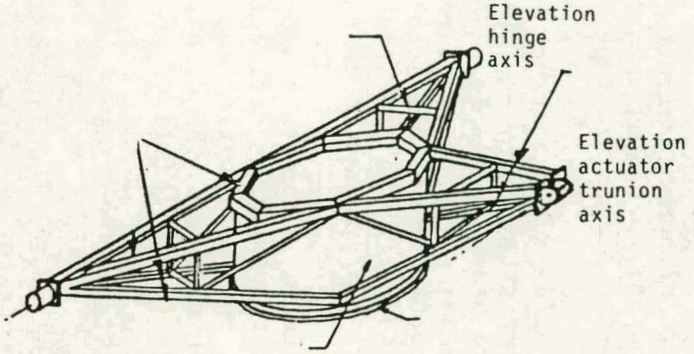


c. Drive support

Figure 3. PDC-2 Structure

sufficient degrees of freedom to allow fine tuning of the composite reflective surface for installation and optical alignments and allow for the panel/structure differential thermal displacements.

The panel support structure is fabricated in five detachable segments for shipment; four ring truss segments and one center frame segment. The segments are bolted together in the field.

The drive support structure serves as an intermediate structure between the reflector assembly and the pedestal. The center hub contains the azimuth drive assembly and is pivoted about the azimuth axis at the top of the pedestal. The space frame arms of the drive support structure provide supports for the elevation hinge about which the dish is pivoted. The third arm supports the elevation actuator trunion. The azimuth drive turntable bearing is connected to the mounting flange on the top of the pedestal.

The PDC-2 structure has been analyzed to determine the contribution of the support structure deflection to the dish optical error. It is determined that the contribution due to gravity loading is approximately 1.5 mrad in the worst case when the dish is facing the horizon. The effect of operating wind loads is negligible.

PEDESTAL/FOUNDATION

A single pier foundation of the PDC-2 provides a fixed axis about which the concentrator assembly is pivoted. The pedestal is a 30-in. pipe that is embedded approximately 16 ft in poured-in-place concrete. The mounting flange is field-levelled and welded to the embedded pedestal.

DRIVE SUBSYSTEM

The PDC-2 can be driven independently about the elevation and azimuth axes at two speeds: slew and tracking.

The azimuth rotation is provided by a ring gear/pinion drive mounted at the top of the pedestal. The pinion is driven by a 5-hp DC motor through a 724:1 gear reduction to provide the necessary mechanical advantage. Azimuth travel range is between 0° and 310°.

The elevation rotation is accomplished with a 30-ton inverted ball screw jactuator mounted between the drive support structure and panel support structure. The elevation drive motor is a 15-hp DC motor. The range of elevation travel is between 0° (facing the horizon) and 90° (facing the zenith). It should be noted that the normal concentrator duty cycle requires small fraction of the design rating of the motors and the paresitic energy consumption is small.

DC motors were found to offer clear advantages over AC motors for this application. The advantages of DC motors as they relate to the PDC-2 application include: wider range of speed control, ease of speed, acceleration/decelleration and torque control, higher torque capacity, quick reversing and braking and lower cost in the 5 to 15 hp size range.

The drive control provides dynamic braking to bring the concentrator to a stop. In addition, a mechanical brake is provided for elevation drive to hold the concentrator stationary once it has come to a stop under the stow and operating conditions.

ELECTRICAL AND CONTROL SUBSYSTEMS

The electrical subsystem provides power to the concentrator drives and transmits the output power from the PCA to a rectifier box mounted on a rack near the pedestal.

The concentrator control subsystem consists of:

a. Central controls that provide the plant level control interface with the concentrator
b. Power conversion system interface controls
c. Local concentrator control subsystem

The local concentrator control elements consist of a sun sensor, azimuth and elevation positional feedback devices (encoders), limit switches, drive controller, and the remote control interface assembly (RCIA).

The drive controller consists of the azimuth and elevation motor speed controllers and a manual control station. The controls are set up for two-speed operation from the panel or RCIA. The azimuth and elevation drive speeds in tracking and stow are 0.1°/sec and 1.2°/sec, respectively, with speed control repeatability of $\pm$10 percent. The drive controller also provides independently adjustable acceleration and deceleration controls. It is housed in a NEMA 3 double door cabinet with heat exchanger for high-temperature outdoor operation.

The RCIA contains the control algorithms and logic for sun tracking and interface with the central controls. The sun tracking is a hybrid system. RCIA calculates ephemeris data to provide coarse tracking signals to the concentrator. The sun sensor provides the fine "sun track mode" signal. During intermittent cloud coverage, the concentrator goes into the ephemeris track mode where it follows the sun path. The concentrator can also follow the sun path in the offset track mode where it performs ephemeris track with an angle bias. Other concentrator control modes include acquisition and detrack from sun and stow command. The concentrator control is a fail safe system and causes the concentrator to go to stow if there is a power or software failure. An emergency back-up generator is required at the system level to provide power in case of grid power failure. Limit switches are provided to stop movement of the concentrator beyond certain position in each direction.

PROJECT STATUS

The PDC-2 design development is complete and the detailed design drawings have been prepared. Specifications for procurement of all concentrator components have been prepared and issued for competitive bidding. The subcontracts for delivery of the support structure, reflective surface mirror glass, drive motors and controllers, elevation drive jactuator, azimuth drive

speed reducer and the ring gear turret, have been placed and they are currently at various stages of fabrication.

A semi-automated technique for fabrication of the reflective panels has been developed, including the cellular glass sanding and mirror bonding and sealing. Two partial full-scale prototype panels have been fabricated to verify the design and demonstrate the viability of the foamglass sanding technique. The partial full-scale prototype panel was designed as a true section of the full size outer panel to simulate the features of the full panel as closely as possible.

The partial full-scale panels are scheduled for optical, structural, and environmental testing at Sandia. The factory layout and tooling design requirements for production of the reflective panels have been prepared. The long lead factory equipment have been ordered.

The final stage and remaining task in the PDC-2 development will be the completion of fabrication and testing of a prototype module.

# A Transmittance-Optimized, Point-Focus Fresnel Lens Solar Concentrator

Mark J. O'Neill
ENTECH, INC.
P. O. BOX 612246
DFW Airport, Texas 75261

## INTRODUCTION

ENTECH, INC. (a new company which purchased E-Systems Energy Technology Center in October 1983) is currently developing a point-focus Fresnel lens solar concentrator for high-temperature solar thermal energy system applications. The concentrator utilizes a transmittance-optimized, short-focal-length, dome-shaped refractive Fresnel lens as the optical element. This unique, patented (Ref. 1) concentrator combines both excellent optical performance and a large tolerance for manufacturing, deflection, and tracking errors.

Under Jet Propulsion Laboratory (JPL) funding, ENTECH has completed the conceptual design of an 11-meter diameter concentrator which should provide an overall collector solar-to-thermal efficiency of about 70% at an 815°C (1500°F) receiver operating temperature and a 1500X geometric concentration ratio (lens aperture area/receiver aperture area).

In the following paragraphs, a review of the Fresnel concentrator development program will be presented, including a description of the concentrator, a summary of its expected performance, the key features of the lens, a parquet approach to lens manufacturing, a description of a prototype lens panel, the results of optical testing of the prototype lens panel, and a discussion of a practical mass production approach for the lens panels.

## CONCENTRATOR DESCRIPTION

The point-focus lens concentrator is shown in Figure 1 and described in Table 1. The optical element is a convex, dome-shaped, acrylic Fresnel lens. The dome consists of ten conical-segment rings, which are each flat in the radial direction and curved in the circumferential direction. The rim angle of the lens (from optical axis to outermost prism) is 45 degrees. Each of the conical-segment rings is about 61 cm wide, with a smooth outer surface and a prismatic inner surface. The lens is made of uv-stabilized acrylic plastic, about 2.4 mm thick. Steel space-frame structure is employed for both the basic concentrator and the pedestal. Reinforced concrete is used for the foundation. The tracking system provides full two-axis sun-tracking and inverted (lens-down) stowage. The Fresnel concentrator will be adaptable to a wide variety of receivers currently under development by JPL and others. The air volume between lens and receiver is enclosed with a thin aluminum conical shroud to minimize dirt and moisture accumulation on the inner surface of the lens. A slight pressurization of this air volume may be desirable for dust infiltration prevention. The total concentrator weight is about 13,000 pounds (13 pounds per square foot of aperture).

## CONCENTRATOR PERFORMANCE SUMMARY

The point-focus Fresnel concentrator performance is summarized in Table 2 for two cases of practical importance. The first case corresponds to a high-temperature receiver which would be required for a Brayton or Stirling engine application. For this case, a 1500X geometric concentration ratio is utilized (corresponding to a receiver aperture diameter of 0.28 meter). After treating reflection/absorption losses in the acrylic lens, 90% of the sunlight is transmitted. Of this transmitted sunlight, about 92% is contained within the limited 0.28 meter receiver aperture circle; i.e., 92% is the receiver intercept factor. About 6% of the lens aperture is blocked by structure; thus the blocking/shading factor is 94%. After all of these loss mechanisms are considered, the overall optical efficiency is 78%. Still considering Case I, this 78% optical efficiency for an 11-meter diameter concentrator (aperture area = 95 $m^2$) corresponds to a black-body receiver energy absorption rate of 59 kw (thermal) under a direct insolation of 800 $w/m^2$. Assuming an 815°C receiver temperature, the black body thermal radiation loss will be 5 kw (thermal). Thus, the net collector output will be 54 kw (thermal), corresponding to a 71% overall collector efficiency.

For the second case in Table 2, a lower temperature receiver is assumed, corresponding to a Rankine engine application. For this lower temperature, a lower geometric concentration ratio (500X) provides better overall collector performance. After considering the same loss factors described above, the concentrator optical efficiency is 83%, this higher value being attributable to a better receiver intercept factor for the larger receiver aperture diameter (0.49 meter). After subtracting the 2 kw (thermal) black-body radiation loss corresponding to a receiver temperature of 371°C, the net collector output will be 61 kw (thermal), equivalent to an overall collector efficiency of 80%.

## KEY LENS FEATURES

The patented ENTECH concentrator is a dome-shaped Fresnel lens with a smooth outer surface and a prismatic inner surface. The lens is a convex, non-spherical-contour lens, in which each prism transmits direct solar rays with equal angles of incidence and excidence, as shown in Figure 2. This incidence/excidence symmetry (also called the minimum deviation condition) provides each prism with the lowest possible reflection losses, and thereby the highest possible transmittance, for that prism's light deviation (turning) angle, as proven rigorously in Reference 1. In addition to maximal transmittance, this minimum-deviation-prism lens also provides a maximal tolerance for lens contour errors (slope errors), an improved tolerance for lens manufacturing errors (prism angular errors and rounded prism peaks), and a smaller solar image size (including finite solar disk angular diameter and chromatic aberration effects), when compared to previous flat and spherical contour lenses. The optical performance superiority of the new lens is fully described in References 2 and 3. Perhaps the most important attribute of the new transmittance-optimized lens is its high slope error tolerance, which allows a substantial relaxation of the support structure stiffness requirements, and thus a significant reduction in weight and cost of the concentrator. Compared to a reflective concentrator (e.g., a 45 degree rim angle parabolic dish), the Fresnel lens concentrator is more than 100 times more tolerant of radial slope errors, as dramatically illustrated in Figure 3.

## PARQUET LENS MANUFACTURING APPROACH

One potentially low-cost manufacturing approach for the point-focus lens is the parquet approach of Figure 4. The dome consists of conical segments which are curved in the circumferential direction and straight in the radial direction. This approach allows the acrylic plastic lens material to be made in flat form and mechanically held in the conical geometry in the completed concentrator. The unfolded flat conical segments can be subdivided into a number of identical lens panels. While these panels would ideally utilize prisms running circumferentially along concentric circles, current manufacturing approaches for lens tooling can not achieve these large-radius non-linear prisms. Fortunately, proven manufacturing approaches are available for making linear prismatic tooling. Thus, the lens panel of Figure 4 is configured to approximate the ideal curved-prism geometry by utilizing a parquet of linear prism elements. The two key variables of this parquet lens approach are the element width (w) and the gap width (g) between elements, since the element width causes a focal plane image enlargement and since the gap width causes transmittance losses. Prototype fabrication efforts have proven that the gap width can be maintained at about 0.5 mm. Element width selection is based on optical analyses discussed below.

Optical analyses of the parquet lens concentrator have been completed. These analyses are based upon cone optics; i.e, the theoretical mapping of the conical bundles of radiation which originate at the solar disk, which are incident upon the lens outer surface, and which form elliptical images in the focal plane, as shown in Figure 5. Because of dispersion (chromatic aberration), the solar images of different wavelengths are spread across the focal plane, as shown in Figure 5. For any fixed receiver aperture diameter and any particular prism in the lens, the design wavelength can be selected to minimize the energy missing the receiver aperture, and thus to maximize the intercept factor. The current lens has been tailored for a 1500X design concentration ratio by properly varying the design wavelength for the various prisms comprising the lens.

For the parquet lens approach, the effect of the parquet element on lens focussing is the formation of a linear solar image in the transverse direction of Figure 5, with the total image transverse length being equal to the parquet element width (w) plus the solar disk image width. The computer model treats this parquet element effect and calculates the radiant flux profile in the focal plane by integrating over all contributing portions of the lens (treating the local lens transmittance), and over all contributing wavelengths, to define the total radiant flux concentration at each point in the focal plane. Results of such a flux profile calculation for several parquet element widths are shown in Figure 6. The radiant flux is normalized by the one-sun direct solar flux incident on the lens, while the radial position in the focal plane is normalized by the lens aperture radius, for the results shown in Figure 6. As expected, the larger the parquet element width, the more spread out the image becomes. However, the image spreading effect is small for element widths of 5 inches and less, when one notes that a 1500X geometric concentration ratio corresponds to a receiver normalized radius ( $\rho/R$) of $26 \times 10^{-3}$ in Figure 6. The flux profile labeled W=0 represents the ideal lens with non-linear prisms.

The flux profiles of Figure 6 can be integrated over various size receiver circles to define the overall energy interception rate for various geometric concentration ratios. The results of such an integration are shown in Figure 7, wherein the intercepted energy rate has been normalized by the energy rate incident on the lens outer surface; thus the effective transmittance (optical efficiency) is shown as a function of geometric concentration ratio for lenses with various parquet element widths. (The results of Figure 7 do not include absorption losses within the thin acrylic lens, which are expected to be 1-2%, based upon measurements for similar acrylic Fresnel lenses. Also, the results in Figure 7 do not include structural blocking/shading losses, although this 6% loss was included in Table 2.) Note that wide parquet element widths work well for low geometric concentration ratios, but not well for high geometric concentration ratios, due to the image spreading effect of the parquet width. Note also that there exists an optimal element width for each value of geometric concentration ratio, this optimum corresponding to the best tradeoff of image spreading losses (which increase with element width) and gap losses (which decrease with element width since g/w represents the lost gap area fraction). For 1500X geometric concentration ratio, element widths of 2, 3, and 4 inches provide essentially equal performance. To minimize lens complexity, the 4-inch element width has been selected for prototype fabrication, as discussed below.

## PROTOTYPE LENS PANEL

A prototype lens panel, using the parquet lens manufacturing approach, has been fabricated for optical testing. This panel is described in Table 3. The panel represents one part of the conical ring located between 27.9° and 32.1° of local rim angle, measured from the lens optical axis. This segment was selected for prototype fabrication because its optical performance is typical of the full dome lens performance. A nominal 2 foot by 4 foot panel size was selected for prototype fabrication, using 12 linear prismatic parquet elements of 4 inch average element width (w) to form the 4 foot curved dimension of the panel. The linear prismatic elements were made by 3M Corporation to ENTECH's specification, using 3M s low-cost lensfilm process. The twelve elements were solvent-bonded to a single piece of extruded acrylic sheet to form the final panel. The entire laminated panel thickness is about 0.1 inch.

## LENS PANEL OPTICAL TESTING

Optical performance testing of the prototype lens panel has been successfully completed. The panel and a focal-plane radiant flux measurement system were mounted on a two-axis tracking structure, which was manually pointed at the sun. The geometrical arrangement of the panel and focal plane was maintained according to the design of the full dome lens. The radiant-flux measurement system consisted of eight independently wired silicon photovoltaic cells mounted in a line on a water-cooled heat sink. The cells were specially designed for concentrated sunlight by Applied Solar Energy Corporation. The linear array of cells was motor-driven to scan the focal plane at the rate of about 1 inch per second.

Prior to each test run, the cells were individually calibrated to determine the proportionality factor between short-circuit current and irradiance. This calibration was done two ways. With the panel covered to prevent focussing onto the cells, the structure was pointed at the sun and

sunlight while allowing direct sunlight to reach the cell. The cell short-circuit current was then divided by a pyrheliometer direct insolation measurement to obtain the proportionality constant. The second calibration was done with a shading disk over each cell, instead of the collimating cylinder. The difference in cell short-circuit current between fully illuminated (no disk) and shaded (with disk) conditions was divided by the pyrheliometer direct insolation measurement to obtain the proportionality constant. Both constants agreed with one another for each cell, verifying the calibration.

An actual test run consisted of first measuring the total irradiance on each cell with the panel covered and the structure pointed at the sun. This provided the baseline irradiance on each cell. Next, the panel was uncovered and the cells were driven across the focal plane, while monitoring their short-circuit-current outputs with an eight-channel strip-chart recorder. The measured radiant flux profile minus the baseline irradiance thus provided a two-dimensional flux map for the focal plane. This flux map was then integrated over various size receiver circles to provide the intercepted energy transfer rate. The projected area of the panel times the measured direct insolation provided the incident energy transfer rate. The ratio of intercepted to incident energy transfer rate is the optical efficiency of the panel for each receiver circle, which relates to geometric concentration ratio.

Key results of the testing are presented in Figure 8 and Table 4. Figure 8 shows the intercept factor versus receiver circle radius. Intercept factor is here defined as the optical efficiency for a given receiver radius divided by the optical efficiency for a large receiver radius of 13.66 inches. Table 4 shows the measured versus predicted optical efficiency for various geometric concentration ratios. (For the dome lens, geometric concentration ratio is of course the square of the ratio of lens aperture radius (18 feet) divided by receiver circle radius.) The prototype lens panel had a continuous linear defect covering about 3.7% of its area due to poor lamination of the lensfilm to the acrylic superstrate. This defect was not optically transparent. If the defective area is subtracted from the lens panel area, the corrected efficiency numbers become those shown in the final column of Table 4. Note that for the design concentration ratio of 1500 X, the predicted optical efficiency was 82%, not accounting for absorption or scattering losses. The measured efficiency was 77%, while the corrected measured efficiency was 80%. This close correlation between measured and predicted optical efficiency verifies the following points:

(1) The dome lens will perform efficiently at high concentration ratios.

(2) The dome lens can be made as a parquet of linear lens segments.

(3) The optical effect of manufacturing and alignment errors on dome lens performance is negligible, since these errors were not included in the analytical predictions, while the prototype was crudely assembled and aligned.

(4) The dome lens optical performance is accurately predicted with a simple dispersive cone optics computer code.

## PRACTICAL MASS PRODUCTION OF DOME LENS PANELS

While the method of manufacturing of the prototype panel was labor-intensive, requiring the linear lens segments to be cut into trapezoidal shapes and laminated to a single-piece superstrate, the parquet geometry provided excellent optical performance. If the lens parquet panels could be made without the cutting and integration of the small segments, the dome lens approach would be far more practical. Fortunately, such a practical mass-production approach is now available, as described below.

3M Company, under Sandia National Laboratories - Albuquerque funding, has this year adapted their low-cost, continuous lensfilm process for making prismatic sheet to lens designs without linear prism geometry. 3M has successfully made parquets of annular-prism point-focus lenses by the lensfilm process. This achievement means that the dome lens panels could also be made by the lensfilm process. The lensfilm tooling would include the parquet of linear lens elements in the tooling itself. Thus, the lensfilm produced on the tooling would consist of a continuous strip of acrylic sheet with dozens of panels (like the one shown at the bottom of Figure 4) reproduced one after the other on the strip. These panels could be easily cut out of the strip, since lensfilm is only 0.5 mm thick. The completed panel could be laminated to a thicker superstrate if required; however, with the large error tolerance of the dome lens, it is quite possible that the lensfilm could be used without a superstrate, especially so if the dome interior is slightly pressurized.

## REFERENCES


1. O'Neill, M.J., "Solar Concentrator and Energy Collection System," U.S. Patent No. 4,069,812, 24 January 1978.

2. O'Neill, M.J., "A Unique New Fresnel Lens Solar Concentrator," Silver Jubilee Congress of the International Solar Energy Society, Atlanta, Georgia, May 1979.

3. O'Neill, M.J. and R.A. Waller, "Analytical/Experimental Study of the Optical Performance of a Transmittance-Optimized Linear Fresnel Lens Solar Concentrator," Annual Meeting of the International Solar Energy Society, Phoenix, Arizona, June 1980.


## FIGURES AND TABLES

Figures and tables are located on the following pages.

FIGURE 1

# POINT FOCUS
# FRESNEL LENS CONCENTRATOR

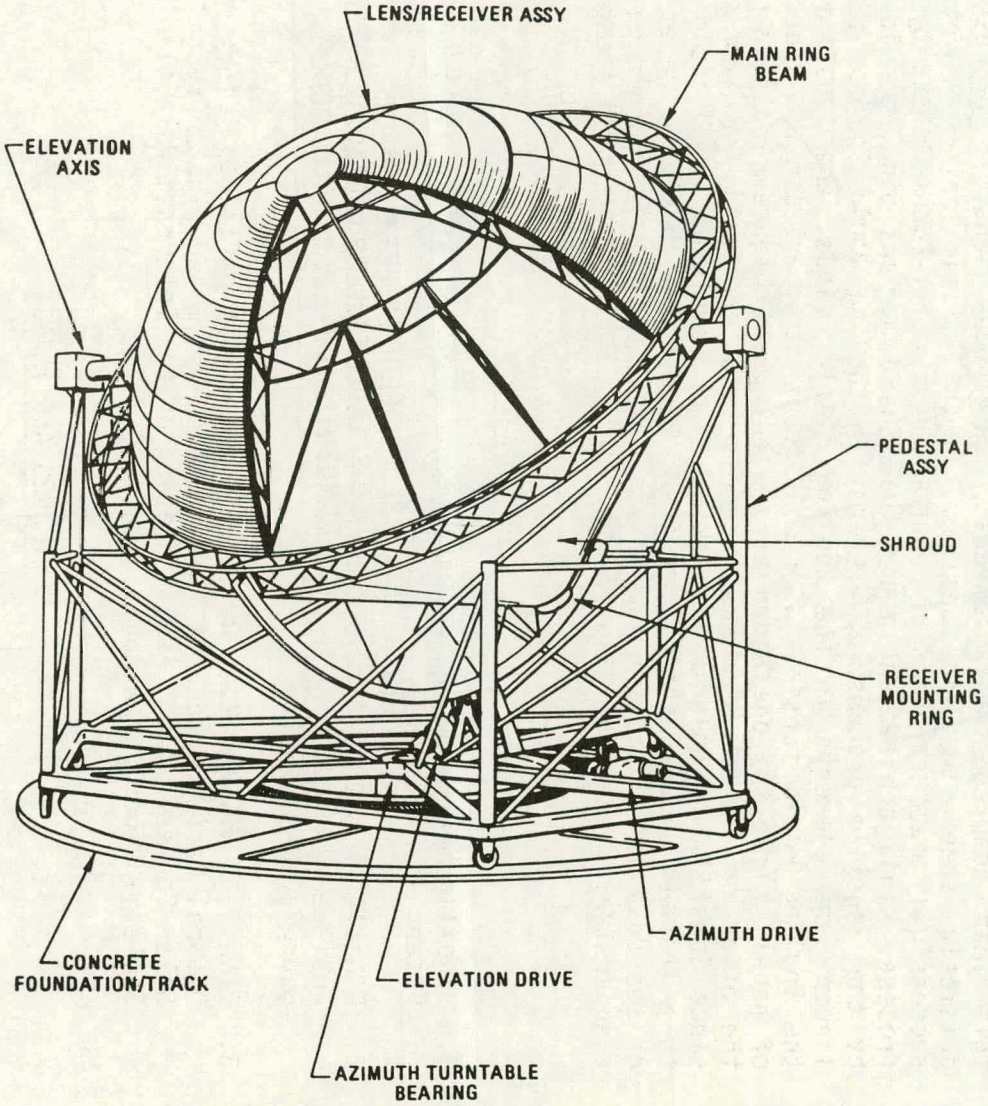

FIGURE 2 -

## PRISM FACE OVER-EXTENSION TO MINIMIZE OPTICAL LOSSES

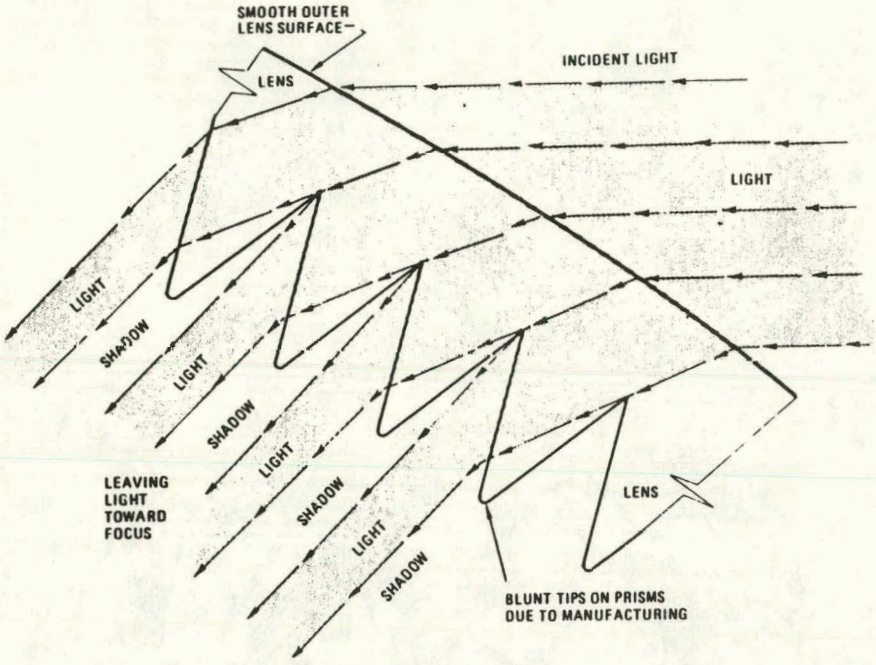


FIGURE 3 - SLOPE ERROR EFFECT ON IMAGE DISPLACEMENT FOR FRESNEL CONCENTRATOR vs PARABOLIC DISH

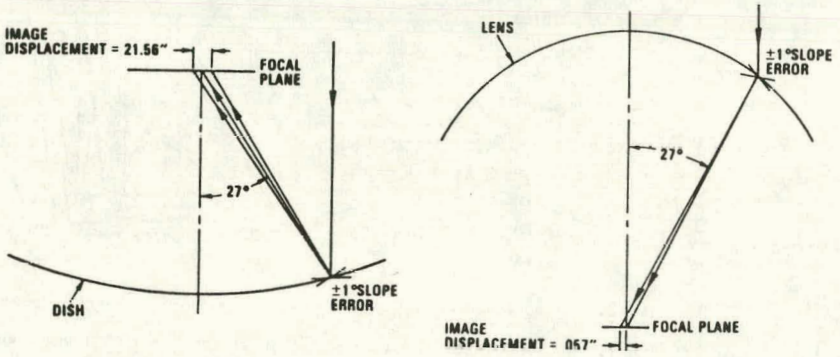


**PARABOLIC DISH**

- 45° RIM ANGLE
- 36 FOOT APERTURE
- ±1° SLOPE ERROR AT 27° LOCAL RIM ANGLE
- PLUS AND MINUS SLOPE ERRORS CAUSE EQUAL DISPLACEMENTS IN OPPOSITE DIRECTIONS

**FRESNEL LENS**

- 45° RIM ANGLE
- 36 FOOT APERTURE
- ±1° SLOPE ERROR AT 27° LOCAL RIM ANGLE
- PLUS AND MINUS SLOPE ERRORS CAUSE EQUAL DISPLACEMENTS IN SAME DIRECTION

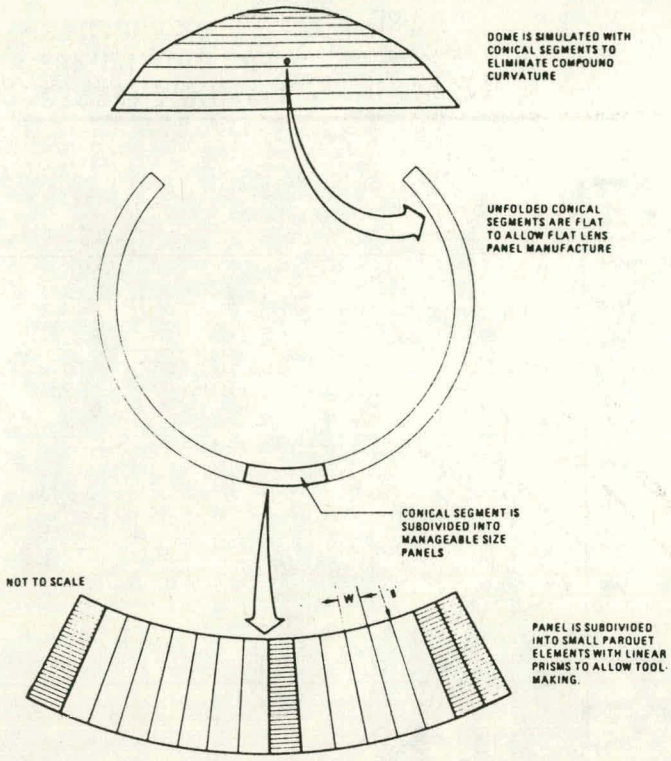


FIGURE 4 - *GEOMETRY INVOLVED IN USING FLAT LINEAR FRESNEL LENS ELEMENTS TO MAKE DOME POINT FOCUS LENS*

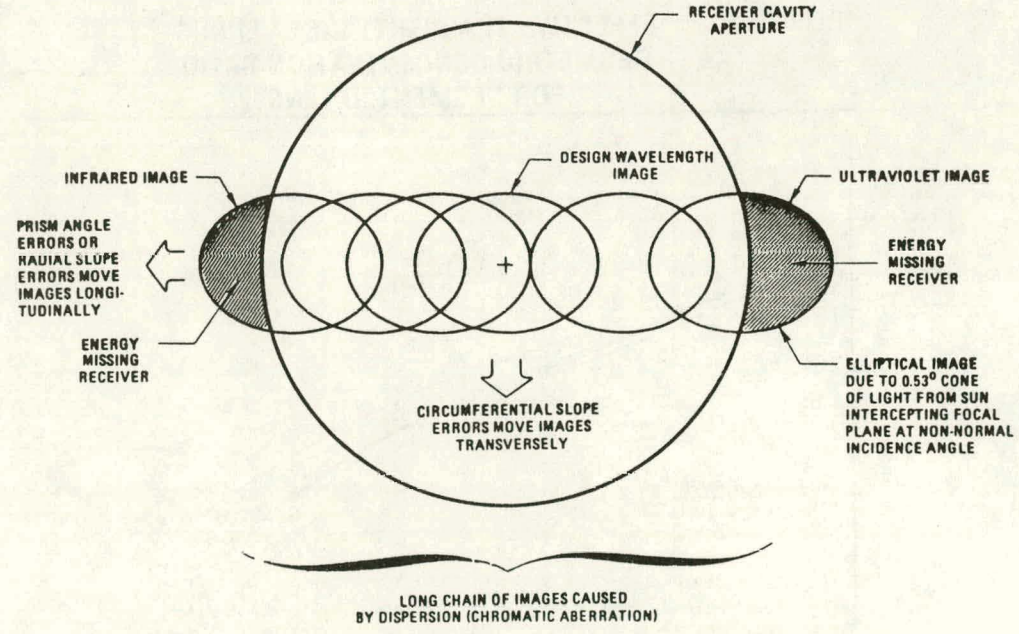


FIGURE 5 - *TYPICAL IMAGE PATTERN PRODUCED BY DIFFERENTIAL ELEMENT OF LENS SHOWING EFFECTS OF DISPERSION AND ERRORS – NOT TO SCALE*

FIGURE 6 - **FLUX PROFILES FOR OPTIMAL 45° RIM ANGLE LENSES**

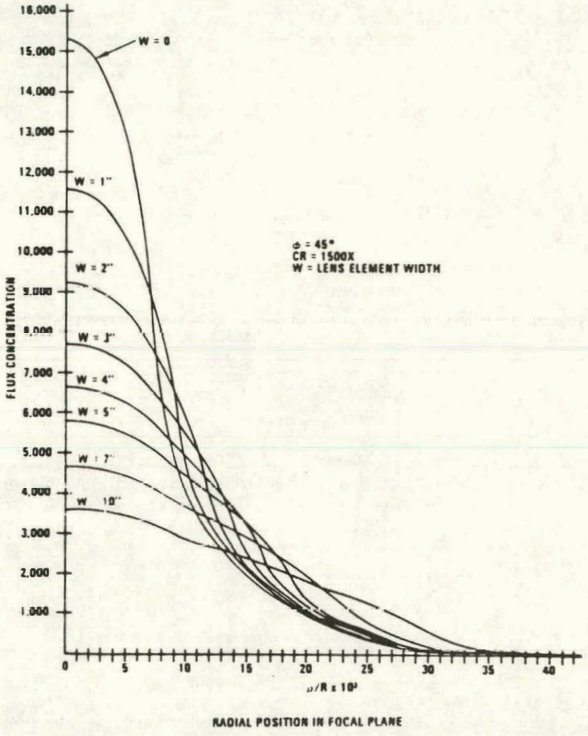


FIGURE 7 - **EFFECTIVE TRANSMITTANCE VERSUS GEOMETRIC CONCENTRATION RATIO FOR SEGMENTED LENS**

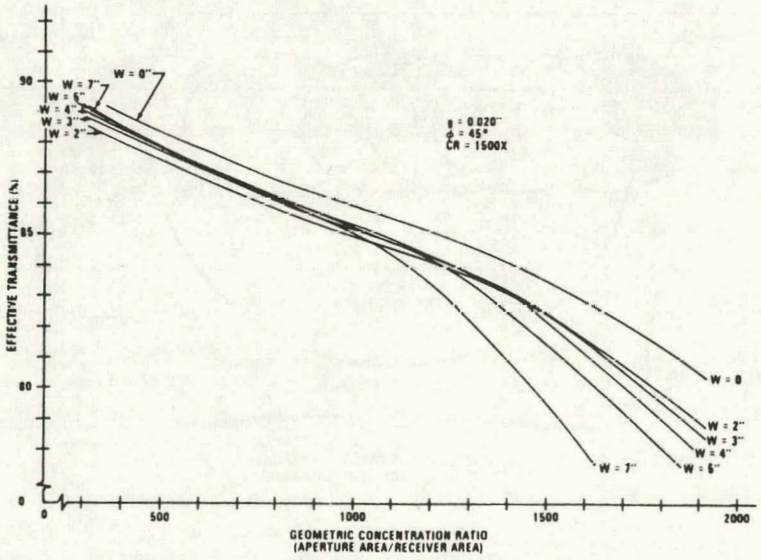

FIGURE 8

# ENTECH, INC.

## POINT-FOCUS LENS PANEL TEST RESULTS - INTERCEPT FACTOR

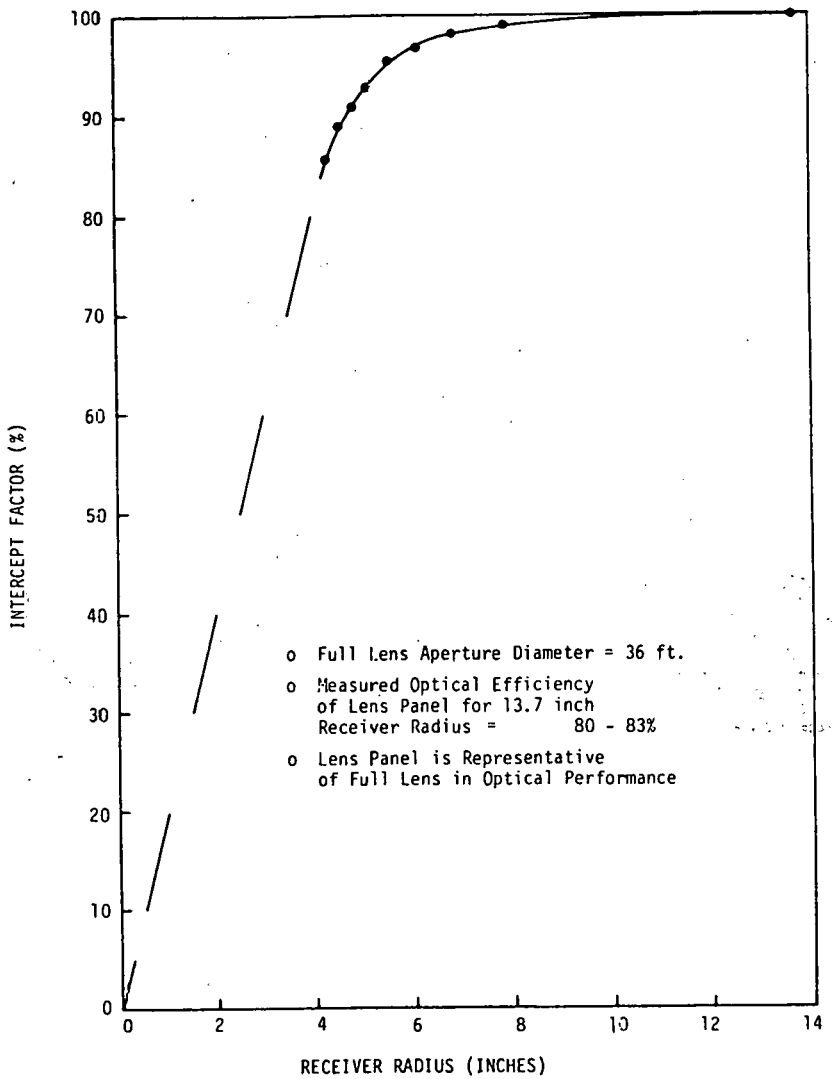

TABLE 1

## RECOMMENDED SYSTEM DESCRIPTION

| | |
|---|---|
| • PHYSICAL | |
| CONCENTRATOR APERTURE DIAMETER | 11M (36 FT.) |
| CONCENTRATOR RIM ANGLE | 45 DEGREES |
| OVERALL COLLECTOR WEIGHT | 13,000 POUNDS (EXCLUSIVE OF RECEIVER) |
| • LENS PANELS | |
| REFRACTIVE MATERIAL | ACRYLIC (2.4 MM NOMINAL) |
| PANEL CONSTRUCTION | BONDED CONICAL SEGMENT PANELS |
| DUST PROTECTION | PRESSURIZED INTERIOR (BETWEEN LENS AND SHROUD) |
| • LENS/RECEIVER ASSEMBLY | |
| LENS SUPPORT STRUCTURE | STRUCTURAL STEEL SPACE FRAME WITH MAIN RING BEAM, 12 RADIAL BEAMS, AND INTERMEDIATE SUPPORTS. |
| RECEIVER SUPPORT STRUCTURE | BIPOD AND SWAY BRACES, WITH PRESSURIZED SHROUD |
| • PEDESTAL (ALIDADE) | |
| AXIS CONFIGURATION | EL OVER AZ, WHEEL TRACK |
| CONSTRUCTION | STRUCTRUAL STEEL SPACE FRAME |
| • FOUNDATION | |
| TRACK | CIRCULAR REINFORCED CONCRETE RING |
| AZIMUTH AXIS | CONCRETE PIER FOR AZ BEARING MOUNT, CONCRETE BEAMS INTEGRATING PIER AND RING TOTAL CONCRETE 7CU. YDS. |
| • DRIVES AND TRACKING | |
| AZIMUTH RANGE | ±180 DEGREES |
| AZIMUTH DRIVE | CABLE WINCH, POSITIVE ACTION |
| MAX. AZIMUTH VELOCITY TO STOW | 2,000 DEG/HOUR |
| AZIMUTH MOTOR | AC SYNCHRONOUS STEPPER, 1800 IN-OZ @ 72 RPM |
| ELEVATION RANGE | ±90 DEGREES |
| ELEVATION DRIVE | CABLE WINCH, POSITIVE ACTION |
| MAX. ELEVATION VELOCITY TO STOW | 2,000 DEG/HOUR |
| ELEVATION MOTOR | 1800 IN-OZ @ 72 RPM, AC SYNCHRONOUS STEPPER |
| • RECEIVER | |
| WEIGHT (JPL DEFINED) | 705 POUNDS |

TABLE 2

## SYSTEM PERFORMANCE SUMMARY

| • OPTICAL PERFORMANCE | CASE I | CASE II |
|---|---|---|
| GEOMETRIC CONCENTRATION RATIO | 1500 | 500 |
| LENS TRANSMITTANCE | 90% | 90% |
| RECEIVER INTERCEPT FACTOR | 92% | 99% |
| BLOCKING/SHADING FACTOR | 94% | 94% |
| OVERALL OPTICAL EFFICIENCY | 78% | 83% |
| • THERMAL PERFORMANCE (@ 800 WATTS/M² INSOLATION) | | |
| RECEIVER CAVITY TEMP | 815°C (1500°F) | 371°C (700°F) |
| RECEIVER RADIATION THERMAL LOSS | 5 KW (THERMAL) | 2KW (THERMAL) |
| COLLECTOR NET OUTPUT | 54 KW (THERMAL) | 61 KW (THERMAL) |
| COLLECTOR OVERALL EFFICIENCY | 71% | 80% |

TABLE 3

PROTOTYPE LENS PANEL

# ENTECH, INC.

| | | |
|---|---|---|
| LOCATION WITHIN DOME LENS | - | CONICAL SEGMENT BOUNDED BY LOCAL RIM ANGLES OF 27.9° AND 32.1°. |
| PANEL SIZE | - | 4 FEET AVERAGE CIRCUMFERENTIAL ARC LENGTH BY 2 FEET STRAIGHT LENGTH. |
| CONFIGURATION | - | 12 LINEAR PRISMATIC ELEMENTS. 4 INCH AVERAGE WIDTH BY 2 FEET LENGTH. |
| MATERIALS | - | LINEAR PRISMATIC ELEMENTS MADE OF 3M ACRYLIC LENS-FILM. SOLVENT-BONDED TO SINGLE PIECE OF EXTRUDED ACRYLIC SHEET - TOTAL PANEL THICKNESS = 0.1 INCH. |

TABLE 4

PREDICTED VERSUS MEASURED DOME LENS OPTICAL EFFICIENCY

# ENTECH, INC.

| GEOMETRIC CONCENTRATION RATIO | PREDICTED OPTICAL EFFICIENCY | MEASURED OPTICAL EFFICIENCY | CORRECTED* MEASURED OPTICAL EFFICIENCY |
|---|---|---|---|
| 1000 X | 85% | 79% | 82% |
| 1250 X | 84% | 78% | 81% |
| 1500 X | 82% | 77% | 80% |
| 1750 X | 80% | 75% | 78% |
| 2000 X | 77% | 74% | 77% |

* CORRECTING FOR A 3.7% NON-TRANSPARANT DEFECTIVE AREA ON THE PROTOTYPE LENS PANEL.

# OPTICAL ANALYSIS OF CASSEGRAINIAN POINT FOCUS CONCENTRATORS

S. S. Waterbury and W. E. Schwinkendorf
The BDM Corporation
1801 Randolph Road S.E.
Albuquerque, New Mexico 87106

## ABSTRACT

A Cassegrainian solar concentrator, using a 7-meter diameter primary reflector, is analyzed in three forms: 1) an unmodified Cassegrainian, 2) the Ritchey-Chretien configuration, and 3) the unmodified Cassegrainian with a nonimaging tertiary reflector. Performance was not significantly improved with the Ritchey-Chretien; however, the tertiary resulted in significant improvement in intercept factor and optical efficiency.

## INTRODUCTION

The Cassegrainian optical configuration consists of a parabolic primary reflector and a hyperbolic secondary mirror. A solar concentrator designed using this configuration can benefit by allowing a more flexible receiver design, since it no longer has to be supported at the primary focal point. The main disadvantages of the Cassegrainian configuration are the additional reflection and blocking due to the secondary.

In addition to the "true" Cassegrainian described above, a variant, referred to as the Ritchey-Chretien, has been studied. The Ritchey-Chretien (R-C) has a slightly hyperbolic primary with the secondary adjusted accordingly. These modifications correct the system for the off-axis aberration referred to as coma. Since the sun is not a point source, much of the incoming insolation is off of the optical axis, causing coma. Elimination of coma should decrease the overall spot size at the focal plane, increasing the intercept factor for a given concentration ratio.

A nonimaging tertiary reflector, added at the focal point of the system, can improve the optical performance of the Cassegrainian. The configuration considered for this application is the hyperbolic flowline concentrator, as described by Winston (1). This design has the advantage over other nonimaging concentrators such as the compound elliptic concentrator (CEC), of affecting only the edges of the beam, thus reducing the overall reflection losses.

## METHOD OF ANALYSIS

This study has used a Monte-Carlo ray trace computer program originally developed by Honeywell (2). This code is modular in nature, and allows modeling of any concentrator system by writing appropriate subroutines describing the geometry of the system to be studied. It has the capability to include the effects of RMS surface imperfections on system performance and a finite sun size with nonuniform flux distribution.

The approach used in this study was to perform a parametric study on the true Cassegrainian, compare the performance of the R-C to the true Cassegrainian for selected parameters, and then analyze a tertiary reflector added to the Cassegrainian system. Finally, an analysis was performed to determine the sensitivity of the optical performance to misalignment of the secondary and tertiary reflectors.

GEOMETRY

As stated previously, the Cassegrainian consists of a confocal parabola and hyperbola, as shown in figure 1. The convex secondary reflector increases the focal length of the optical system, and thus reduces the angle of the extreme rays reflected from the secondary to the system focal plane. Since the optical extent of the system must be conserved, an increased focal length reduces the maximum concentration ratio that can be achieved. The theoretical concentration ratio for a system of axial symmetry is defined in equation 1.

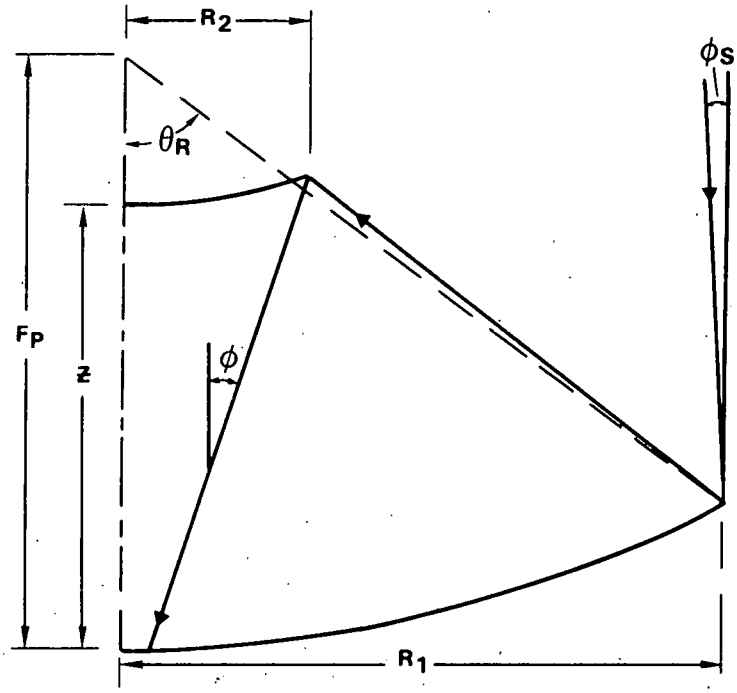


Figure 1. Cassegrainian Geometry

$$CR = \left(\frac{\sin \phi}{\sin \phi_s}\right)^2 \tag{1}$$

where $\phi$ is the entrance angle of the extreme rays and $\phi_s$ is the sun angle. As can be seen, $\phi$ determines the maximum CR possible.

The variation in system focal length is related to the primary focal length ($F_p$) and the eccentricity (e) of the secondary by the magnification factor (M), defined as

$$M = \frac{e_2 + 1}{e_2 - 1} \tag{2}$$

The system focal length is the product of M and $F_p$. Likewise, the extreme ray angle $\phi$ is related to the primary rim angle. These relationships can be used to determine M and the theoretical concentration ratio.

There are several factors that do not allow the theoretical concentration ratio to be reached. In a perfect optical system (i.e., free from errors on the reflector surfaces) the limitations are caused by various aberrations.

It is possible to design an optical system to reduce or eliminate some of these aberrations. One such design is the Ritchey-Chretien, which is corrected for spherical aberration and coma. There have been several derivations of the relationships required for this configuration. The one chosen for this study is by Wetherell, et al (3). This development results in a "sag" equation for the two surfaces as a function of the primary reflector focal length, the system aperture area, the system focus position, and the vertex-to-vertex spacing between the two reflectors.

Another major source of degradation in concentrator performance is imperfections on the reflector surfaces. They have the effect of increasing the size of the cone of light reflected off of each surface.

It is advantageous from a cost standpoint to design a concentrator system with large slope errors on the reflectors and a small primary rim angle. Also, from an efficiency standpoint it is advantageous to reduce the size of the secondary to reduce the blocking factor by increasing the spacing between the primary and secondary reflectors. Unfortunately, these design decisions tend to spread the beam of radiation impinging on the focal plane, reducing the concentration ratio possible for a given intercept factor.

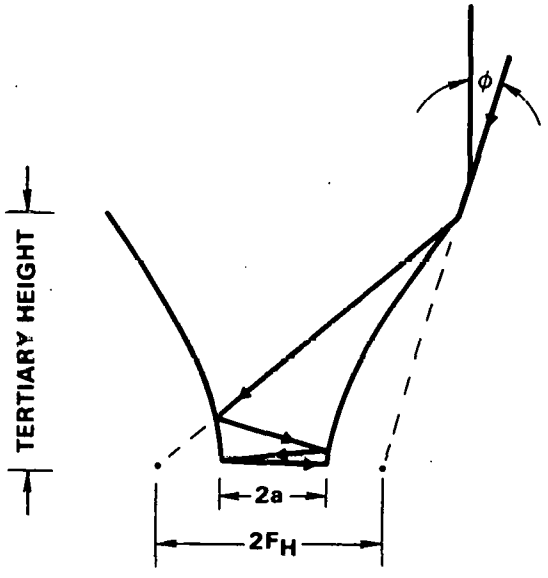


Figure 2. Tertiary Geometry

To increase the concentration ratio for a given intercept factor, a hyperbolic tertiary reflector may be added at the focal plane of the system. The geometry for this nonimaging concentrator is shown in figure 2. One property of a hyperbola is that any ray directed at one of the focal points will be reflected towards the other focal point. After an infinite number of reflections, the ray will exit through the bottom of the concentrator. Rays that would intersect the focal plane within the $2F_H$ diameter exit with correspondingly fewer reflections, while those outside $2F_H$ would be rejected out the top of the concentrator. The concentration ratio of the tertiary is defined as:

$$CR = \frac{F_H^2}{a^2} \tag{3}$$

For a given spot radius "$F_H$", there exists a family of hyperbolas with varying concentration ratios. The rule that governs the shape of the hyperbola is:

$$\sin^{-1}\left(\frac{a}{F_H}\right) \leq \phi \tag{4}$$

This restriction is the limiting factor for the maximum concentration ratio possible for this concentrator. However, to intercept the entire beam at the limit, the required height of the concentrator would be infinite.

There are two additional restrictions that are in effect for integrating the tertiary into the Cassegrainian design. They are:

The radius of the tertiary at the truncation height must not block any rays that are reflected from the primary towards the secondary.

The radius of the tertiary, at the truncation height must intersect all rays reflected from the secondary.

These two restrictions place a maximum and minimum height restriction on the tertiary, respectively. This, together with the required shape of the tertiary for a given concentration ratio, limits the maximum concentration ratio that can be attained.

## RESULTS

### Cassegrainian Only

A parametric study was performed for the Cassegranian concentrator. Figure 3 illustrates the existance of an optimum Z/F for a particular geometric concentration ratio. The optical efficiency is defined as the product of the intercept factor and 1 minus the blocking factor.

As was discussed earlier, the beam incident on the focal plane spreads as Z/F increases, reducing the intercept factor for a given CR. The shift of optimum optical efficiency due to rim angle is caused by the reduction in primary focal length at higher rim angles, which increases the angle of extreme rays ($\phi$) reflected from the secondary. This increase in $\phi$ reduces the beam size at the focal plane, according to conservation of optical extent, thereby increasing the intercept factor for a given CR. Reducing Z/F also results in an increase in $\phi$, and therefore an increased intercept factor, but at the expense of an increased blocking factor, reducing the optical efficiency. Increasing the primary surface error results in a shift of the optimum Z/F to the left, in essence trading increased blocking to obtain a higher optical efficiency.

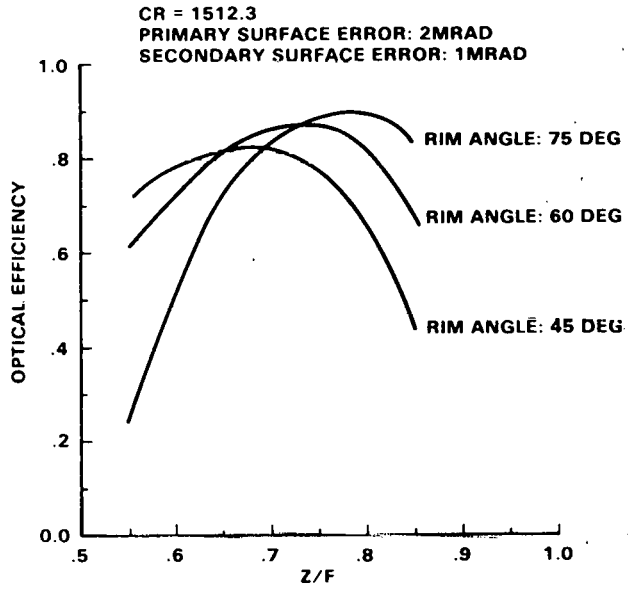


Figure 3. Optical Efficiency Versus Z/F

Table 1 lists the performance of the true Cassegrainian at maximum optical efficiency and maximum intercept factor at a rim angle of 60 degrees for various combinations of primary and secondary surface errors. Results for 45 and 75 degrees are not shown since performance at 45 degrees is low, and 75 degrees results in higher primary costs. The optical efficiency listed assumes 100 percent reflectivity on the primary and secondary reflectors, and 95 percent reflectivity on the tertiary.

Several results are apparent from this table. They are:

Primary surface errors ($\sigma_p$) affect the performance of the system much more than errors on the secondary ($\sigma_s$).

It is not possible to achieve the acceptance criteria of CR = 1200 at IF $\geq$ .96 at maximum optical efficiency except for the case of $\sigma_p$ = 2 mr.

A primary surface error of 8 mr will not produce an acceptable IF.

Table 2 lists the performance of the Ritchey-Chretien configuration in the same format as above. Comparing the Ritchey-Chretian to the true Cassegranian shows no significant improvement in optical efficiency. The major reason for this is that the improvement resulting from elimination of coma is masked by the effects of surface errors. Figure 4 shows the intensity distribution for the true Cassegrainian and the R-C for a typical set of parameters. The most noticeable difference between the two configurations is the higher intensity of radiation in the center for the Ritchey-Chretien due to the elimination of coma. If this is a desirable feature in the overall design of a concentrating system, then perhaps the Ritchey-Chretien should be considered. If not, then there is little, if any advantage to using the Ritchey-Chretien.

Cassegrainian with Tertiary Reflector

The main parameter required to integrate the tertiary into the Cassegrainian design is the radius of the spot on the focal plane, $F_H$. This parameter, along with the desired concentration ratio, defines the required shape of the tertiary. However, it is not necessarily advantageous to set $F_H$ equal to the maximum radius of the spot, since this would require a relatively tall, narrow concentrator. Examination of figure 4 reveals that the intensity distribution is very close to a normal distribution. This fact can be used to determine an appropriate $F_H$. The procedure for determining $F_H$ is as follows:

Determine the standard deviation of the flux distribution ($\sigma_D$).

Calculate $F_H$ by determining the desired fraction of the total energy available to be captured. These calculations have been performed for a capture ratio of .995 and .975. It is apparent that as the capture ratio decreases, the required tertiary height decreases.

Blockage of rays reflected from the primary reflector must also be avoided. At high tertiary heights, this becomes a problem, and limits the concentration ratio of the system.

TABLE 1. CASSEGRAINIAN PERFORMANCE

Rim Angle: 60°

$\sigma_p$ = 4mr , $\sigma_s$ = 2mr

| CR | IF | ηmax | z/F | r(cm*) | P(kW)** | IFmax | z/F | $\eta_o$ | P(kW) |
|---|---|---|---|---|---|---|---|---|---|
| 1200 | 0.9 | 0.77 | 0.7 | 10.2 | 30 | 0.98 | 0.55 | 0.58 | 22.5 |
| 1500 | 0.85 | 0.73 | 0.675 | 9.0 | 28 | 0.96 | 0.55 | 0.55 | 22 |

$\sigma_p$ = 8mr , $\sigma_s$ = 2mr

| CR | IF | ηmax | z/F | r(cm) | P(kW) | IFmax | z/F | $\eta_o$ | P(kW) |
|---|---|---|---|---|---|---|---|---|---|
| 1200 | 0.69 | 0.54 | 0.65 | 10.2 | 20.7 | 0.79 | 0.55 | 0.45 | 17.5 |
| 1500 | 0.63 | 0.49 | 0.65 | 9.0 | 18.8 | 0.73 | 0.55 | 0.42 | 16.5 |

$\sigma_p$ = 4mr , $\sigma_s$ = 1mr

| CR | IF | ηmax | z/F | r(cm) | P(kW) | IFmax | z/F | $\eta_o$ | P(kW) |
|---|---|---|---|---|---|---|---|---|---|
| 1200 | 0.90 | 0.77 | 0.70 | 10.2 | 30.0 | 0.98 | 0.55 | 0.58 | 22.5 |
| 1500 | 0.89 | 0.73 | 0.675 | 9.0 | 28.5 | 0.965 | 0.55 | 0.57 | 22.5 |

$\sigma_p$ = 2mr , $\sigma_s$ = 1mr

| CR | IF | ηmax | z/F | r(cm) | P(kW) | IFmax | z/F | $\eta_o$ | P(kW) |
|---|---|---|---|---|---|---|---|---|---|
| 1200 | 0.98 | 0.90 | 0.75 | 10.2 | 34.4 | 0.997 | 0.7 | 0.87 | 33.4 |
| 1500 | 0.96 | 0.87 | 0.75 | 9.0 | 34.0 | 0.99 | 0.65 | 0.81 | 31.0 |

*r = receiver radius
**p = power entering the receiver plane in kilowatts

TABLE 2. RITCHEY-CHRETIEN PERFORMANCE

Rim Angle: 60°

$\sigma_p$ = 4mr , $\sigma_s$ = 2mr

| CR | IF | ηmax | z/F | r(cm) | P(kW) | IFmax | z/F | $\eta_o$ | P(kW) |
|---|---|---|---|---|---|---|---|---|---|
| 1200 | .91 | 0.77 | .70 | 10.2 | 29.5 | .94 | .65 | .71 | 27.3 |
| 1500 | .87 | 0.73 | .70 | 9.0 | 28.0 | .90 | .65 | .68 | 26.0 |

$\sigma_p$ = 2mr , $\sigma_s$ = 1mr

| CR | IF | ηmax | z/F | r(cm) | P(kW) | IFmax | z/F | $\eta_o$ | P(kW) |
|---|---|---|---|---|---|---|---|---|---|
| 1200 | .986 | 0.89 | .75 | 10.2 | 34.4 | .998 | .70 | .85 | 32.9 |
| 1500 | .967 | 0.88 | .75 | 9.0 | 33.7 | .993 | .70 | .85 | 32.7 |

Analysis of the radiation on the secondary reflector indicates that the diameter can be reduced with a small gain in performance. This is because the flux of reflected energy on the outer ring of the secondary is very low, and by not intercepting that energy, it is possible to decrease the blocking factor. Reducing the secondary diameter also benefits the tertiary reflecter design. Since the "source" for the radiation that the tertiary intercepts is now smaller, the height of the tertiary can be reduced for a given concentration ratio, or conversely, a higher concentration ratio can be achieved for a given height.

Results for the Cassegrainian with the tertiary reflector are listed in table 3 for a reduced secondary diameter. The most significant result is that the optical efficiency does not peak as a function of z/F. The tertiary reflector redirects the beam to the desired receiver aperture regardless of the size of the beam on the tertiary. The major penalty for redirecting a large beam is a tall tertiary.

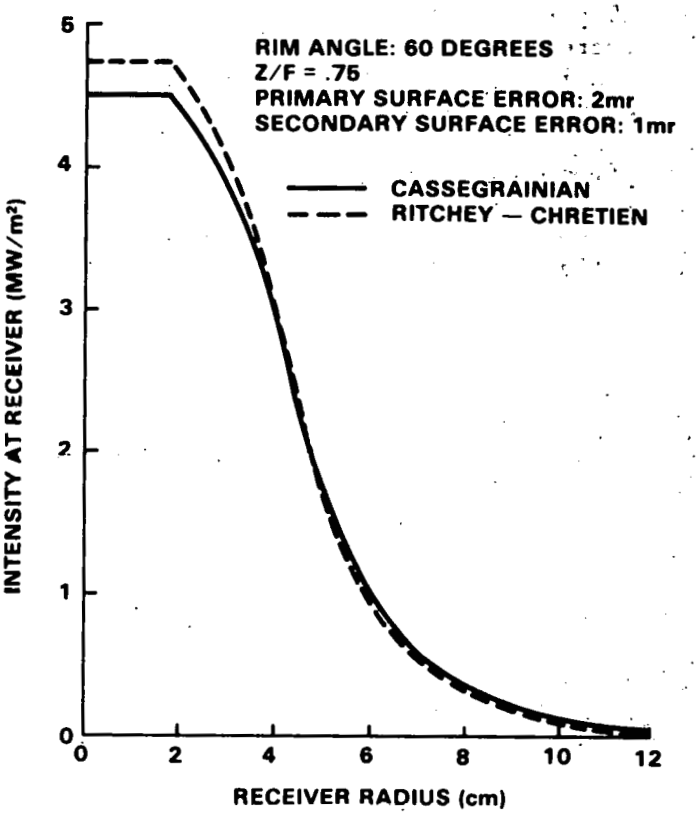


Figure 4. Comparison of Intensity Distributions.

TABLE 3. CASSEGRAINIAN PLUS TERTIARY PERFORMANCE

Rim Angle: 60° $\sigma_p$ = 4mr $\sigma_s$ = 2mr $\sigma_T$ = 2mr z/F = 0.75
Secondary Diameter = 1.96 m

Capture Ratio: .995

| CR | r(cm) | IF | $\eta_{max}$ | $Z_T$(cm)* | P(kW) |
|---|---|---|---|---|---|
| 1200 | 10.1 | .98 | .89 | 99.0 | 34.4 |
| 1300 | 9.7 | .98 | .89 | 114.0 | 34.4 |
| 1500 | 9.0 | - | - | - | - |
| 2200 | 7.5 | - | - | - | - |

Capture Ratio: .975

| CR | IF | $\eta_{max}$ | $Z_T$(cm) | P(kW) |
|---|---|---|---|---|
| 1200 | .97 | .88 | 42 | 33.7 |
| 1300 | .97 | .88 | 47 | 33.7 |
| 1500 | .96 | .87 | 60 | 33.6 |
| 2200 | .96 | .87 | 118 | 33.3 |

*$z_T$ = height of the tertiary

Comparing the maximum efficiencies for the Cassegrainian only and the Cassegrainian plus tertiary yields a 17 percent increase at CR = 1200 and a 19 percent increase at CR = 1500. These increases in efficiency result from increasing the intercept factor. Additionally, it is possible to increase the concentration ratio without significantly degrading the efficiency when using the tertiary.

Effects of Misalignment

There are three loss mechanisms that affect the performance of the tertiary reflector. They are:

Rejection of rays through the inlet aperture.

Absorption of energy caused by multiple reflections.

Non-interception of radiation by the inlet aperture.

Another loss mechanism, introduced by the reduction of the secondary diameter, is non-interception of radiation by the secondary reflector.

Rotational misalignment has the largest effect on increased loss, followed by axial alignment. Positive axial misalignment reduces the percentage of radiation not intercepted by the secondary. Perhaps the secondary diameter could be increased, resulting in less sensitivity to axial misalignment.

Figures 5 and 6 show the effects of multiple misalignments on optical efficiency and intercept factor. The criteria chosen for determining the maximum amount of misalignment permissible was to set the minimum optical efficiency equal to the maximum efficiency attainable without the tertiary with perfect alignment. This is an arbitrary decision, although it does give a rational bound on system efficiency. Using this criteria, the maximum combined misalignment is:

| | |
|---|---|
| Axial: | ± .0254m (1") |
| Radial: | ± .0254m (1") |
| Rotational: | ± .5° |

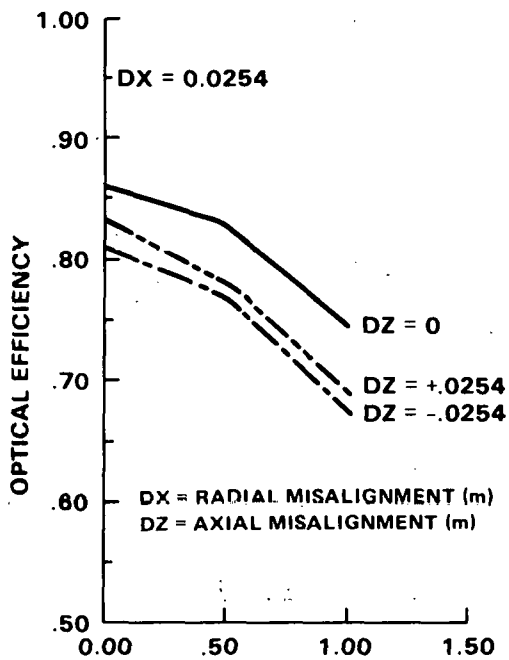


Figure 5. Effect of Misalignment on Optical Efficiency

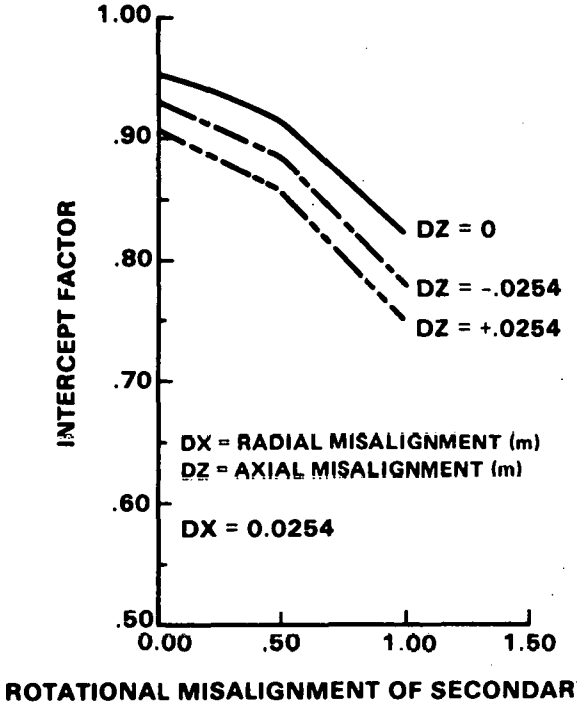


Figure 6. Effect of Misalignment on Intercept Factor

This results in a decrease in optical efficiency and intercept factor of approximately 11 percent, such that the minimum optical efficiency is 77 percent, with an intercept factor of 85.5 percent.

## CONCLUSIONS

The Cassegrainian concentrator is a viable system for the 7-meter dish studied.

The Ritchey-Chretien modification does not significantly improve the performance of the Cassegrainian configuration due to the presence of surface slope errors that largely mask improvements produced by the elimination of coma.

A non-imaging tertiary reflector significantly improves the optical performance of the Cassegrainian, and should be integrated into the design.

## REFERENCES

1. Winston, R., Welford, W. T. "Geometrical Vector Flux and Some New Nonimaging Concentrators", J. Opt. Soc. Am., Vol. 69, No. 4, April 1979.

2. Survey: Mirrors and Lenses and Their Required Surface Accuracy. Honeywell, Inc. Minneapolis, MN, DOE/CS/35348-T1, January 1980.

3. Wetherell, W. B., Rimmer, M. P. "General Analysis of Aplanatic Cassegrain, Gregorian, and Schwartzchild Telescopes", Applied Optics, Vol. 11, No. 12, December 1972.

# ENGINE/RECEIVER DEVELOPMENT

Taras Kiceniuk

Jet Propulsion Laboratory
Pasadena, CA 91109

Solar parabolic dishes require small, high efficiency heat engines. These engines need to be compact and to have low operating cost.

The first paper describes development of an organic Rankine engine. Resolution of two key problems - excessive bearing wear and arcing within the alternator were reported.

The second paper reviews development of several small engines and their possible use with dishes.

Since solar receivers are in the efficiency train with engines, high efficiency receivers are also required.

The third paper discusses the technological status of solar dish receivers and suggested a number of approaches to improving their design.

The fourth paper reports on testing of various materials relative to their use on aperture plates of receivers.

# CURRENT STATUS OF AN ORGANIC RANKINE CYCLE ENGINE DEVELOPMENT PROGRAM

Robert E. Barber

Barber-Nichols Engr. Co.
Arvada, CO 80002

This paper presents the steps taken to achieve improved bearing life in the organic cycle (ORC) engine being developed for use on solar parabolic dishes. A summary of recent test results is also given.

The Power Conversion Subsystem (PCS) consists of an air-cooled, regenerative 25 $kW_e$ ORC engine/generator unit mounted at the focus of a parabolic dish concentrator. The working fluid, toluene, is circulated in a hermetically-sealed, closed loop system. Toluene vapor at 750 to 800°F drives the turbine-alternator-pump assembly (TAP) at speeds up to 60,000 rpm. Liquid toluene is used as the lubricant in the hydrodynamic fluid-film bearings in the TAP.

Excessive bearing wear was experienced during solar testing of the PCS at the JPL Parabolic Dish Test Site in February and March 1982. As a result, a program was undertaken to diagnose the cause of bearing failure and remedy the problem. This effort was successful and the specific testing approaches and design changes which led to the current successful bearing system configuration are discussed in the paper.

The first series of tests in the Bearing Life Development Program was designed to characterize the performance of the radial bearing and thrust bearing designs (as individual bearings) under various combinations of controlled load, speed, lubricant flow rate and temperature.

The next series of tests utilized the actual TAP assembly. The shaft was mechanically driven at speeds up to 60,000 rpm by a special test rig. Optical proximity probes were installed to monitor shaft orbit behavior. Evidence of rotor dynamic instability (subsynchronous whirl) was observed; this led to further analyses and specific design changes in the radial bearings and lubrication feed system. However, bearing surface damage continued to appear even after the rotor instability problem was solved. This was traced to electrical pitting caused by electromagnetically-induced shaft voltage arcing across the fluid film and was corrected by design changes.

The most recent test series included operation of the entire PCS (with the TAP installed) for 100 hours of total run time in a ground test facility at Barber-Nichols Engr. Co. (B-N) which realistically simulated operation on the sun. Rotor dynamic behavior was recorded continuously during the 100 hours and the TAP was disassembled at predetermined intervals for bearing inspection. Performance of both the 5-shoe, tilting-pad radial bearings and the gimbal-mounted thrust bearings was entirely satisfactory. This test demonstrated that the objective of solving the "infant mortality" bearing problem has been accomplished. The Power Conversion Subsystem also demonstrated reliable operation over a wide range of test conditions.

# PROGRAMS AND IMPLICATIONS FOR SOLAR THERMAL ELECTRIC APPLICATIONS

Donald Alger

NASA Lewis Research Center
Cleveland, OH 44135

The DOE automotive advanced engine development projects managed by the NASA Lewis Research Center were described. These included one Stirling cycle engine development and two air Brayton cycle developments. Other engine activities include 1) an air Brayton engine development sponsored by the Gas Research Institute, and 2) plans for development of a Stirling cycle engine for space use. Current and potential use of these various engines with solar parabolic dishes were discussed.

# ADVANCED SOLAR RECEIVERS

William A. Owen
Jet Propulsion Laboratory
Pasadena, California

Even though more small cavity solar receivers have been designed, fabricated and tested in recent times, the perennial problem of low thermal efficiency has not gone away. Most solar receivers have not been as efficient as the analysis that went into their design predicted. Energy losses have been 5 to 50 percent greater than anticipated. Perhaps this should have been expected since little optimization was done in the formative periods of system design due to the relatively low cost of the receiver compared to the entire system cost. Recent system designs, however, have paid greater attention to receiver efficiency as a route to greater system efficiency recognizing too that there is a higher probability of good improvement per design dollar here than with already optimized subsystems.

Receiver losses result from all three modes of heat transfer, radiation, convection and conduction. Table 1 indicates how these might be distributed and shows where future improvements could be expected. These are of course temperature dependent, the numbers shown are for a receiver with a cavity temperature about 870°C (1600°F).

At this meeting last year, I showed data which indicated that even though there was not a lot of active receiver development in progress, the prospect of producing a very efficient i.e. greater than 90 percent, small cavity solar receiver was good. As new data became available, that analysis has been kept reasonably up to date and today I can give you a progress report.

The basic thesis that a highly efficient cavity receiver is practical is still a good one. And how we get to that goal is a little clearer. Test runs at the JPL Parabolic Dish Test Site on a Brayton cycle receiver built for us by Garrett AiResearch and a series of tests run for us by Sanders Associates at their Merrimack, New Hampshire test facility have given us better numerical insight into exactly how the losses from small cavity receivers are distributed.

Figure 1 is a cut-away drawing of the Sander's receiver. It was mounted on a test stand and preheated air ($T_2$) supplied at about 0.25 kg/sec (0.56 lb/sec), a rate typical of the Brayton engines under consideration. The small numbers on the figure indicate thermocouples and the q numbers bracket various zones of the receiver from which heat losses were measured. Table 2 summarizes the results obtained. Several facts are immediately evident from the numbers. The most obvious is that about two-thirds of all losses are in the window frame area $q_M$. This

should easily be reduced by redesigning the insulation inside the cavity and adding external insulation in the frame area. Additional heat could be retained by better insulation systems in the flange area ($q_{A3}$) and in the outlet duct area ($q_C$). The overall lesson to be learned here is that conduction losses are not negligible and should receive adequate attention.

To estimate the overall efficiency of the receiver, it was allowed to reach thermal equilibrium and overall losses established from the temperature drop of the air stream. Typical temperature data is shown in Figure 2 and the losses calculated in Table 3. These data allow an overall receiver efficiency to be estimated. Thus, for a 75 kW capacity receiver operating at about 870°C (1600°F), when an 8 percent window loss of 6 kW due to Fresnel reflection is added to the 6.58 kW thermal loss, the overall efficiency is about 83 percent. This value agrees well with previous measurements and suggests that a highly efficient receiver is more likely to be windowless.

The disadvantage of not having a window is cavity convection. While considerable work has been done on this problem for the very large central receivers, not much confirmatory evidence exists for small cavities. This needs to be done especially since it is affected by so many variables such as wind speed and direction, cavity configuration, attitude, temperature, mounting geometry, and others. The highly efficient receiver must have these well under control.

Another major loss mechanism, usually the largest, is radiation out the aperture. But even though it is a large loss, very little work has been done recently. I think this is, at least in part, due to the misperception that there is not much you can do about it. But many routes exist to reduce this loss.

The most obvious of these is to reduce the size of the aperture. Very good systems engineering is essential to balance concentrator performance against costs for a minimal focal plane spot diameter. This also allows for the optimal spillage allowance to be established. Other techniques such as using terminal concentrators should be evaluated.

Within the cavity, several techniques are available to reduce reradiation. Figure 3 illustrates a number of these including overall cavity size ratio, cavity wall configuration, heat exchanger placement, thermal characteristics of the casvity components especially using absorbers and reflectors in an optimal fashion, using secondary heat exchangers as preheaters while cooling cavity elements, and others. Good radiation management is essential and should result in significant performance improvements.

In summary, if careful attention is paid to the overall thermal systems design especially to conductive losses about the window and areas of relatively thin insulation; and if the cavity design is carefully managed to insure a small, minimally reradiating aperture, the goal of a very high efficiency cavity receiver is a realistic one.

EXPECTATIONS

| | PREVIOUS LOSS-WATTS | IMPROVED |
|---|---|---|
| RADIATION | 6000 | 1000 - 2000 |
| CAVITY CONVECTION | 2500 | 1000 |
| CONDUCTION | 2000 | 500 |
| EXTERNAL CONVECTION | 750 | 500 |
| REFLECTION | 500 | 200 |
| EXTERNAL RADIATION | 250 | 200 |
| | 12000 | 3400 - 4400 |
| EFFICIENCY | 85% | 94 - 95% |

Table 1: Receiver Losses

FIGURE 1: COMPOSITE HEAT FLOW ANALYSIS
FOR SAGT-1A RECEIVER

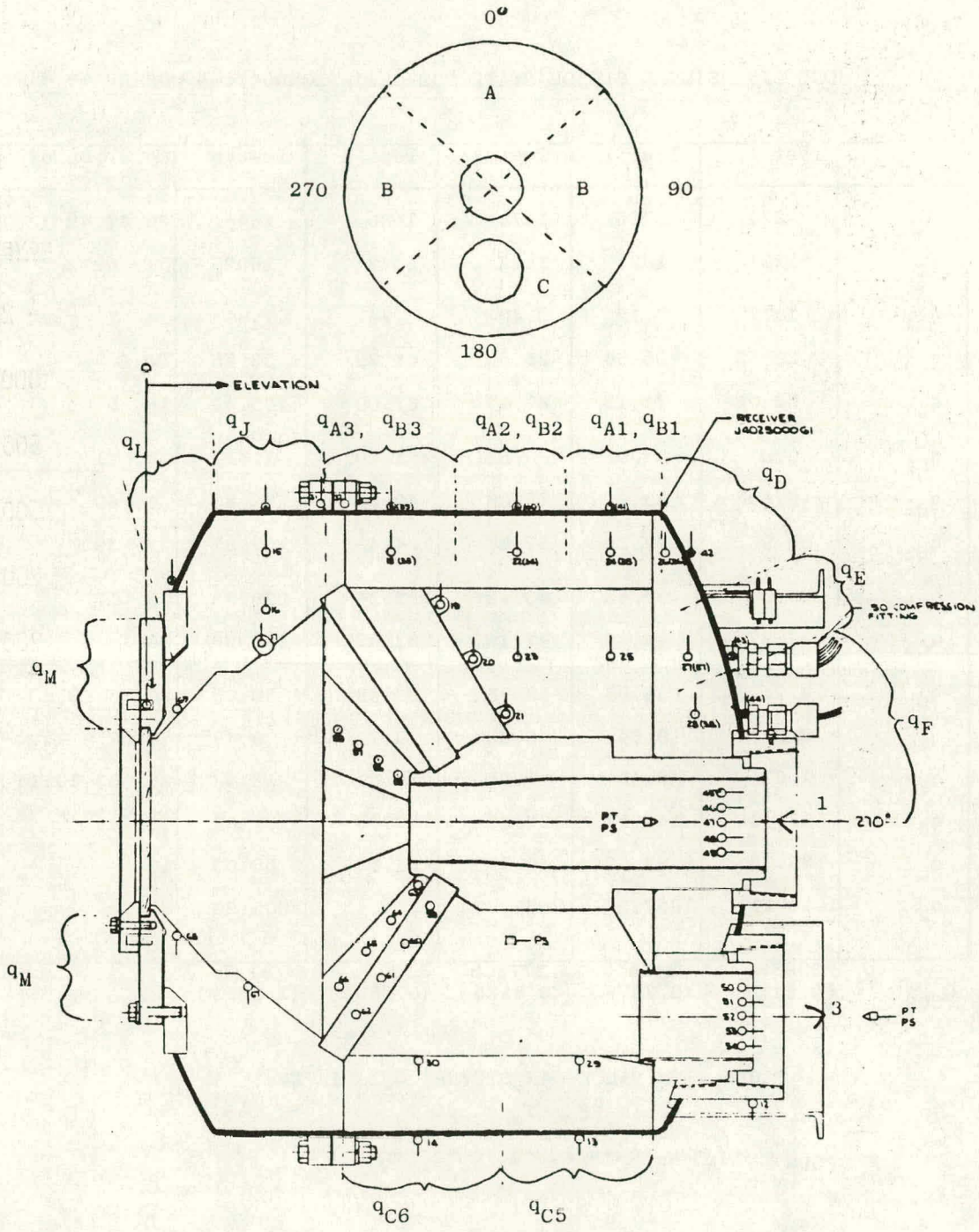

ONE DIMENSIONAL STEADY STATE COMPOSITE CONDUCTION MODEL

| | Test 1 | Test 2 | Test 3 | Test 4 | Test 5 | Location of TC Nodes |
|---|---|---|---|---|---|---|
| $T_1$ | 1271 | 1360 | 1478 | 1580 | 1648 | 46,47,48 |
| $T_2$ | 1221 | 1323 | 1442 | 1542 | 1602 | 51, 53 |
| $q_{A1}$ | 1.77 | 3.12 | 2.40 | 4.74 | 2.69 | 24, 7 |
| $q_{A2}$ | 20.35 | 25.64 | 25.59 | 41.29 | 33.75 | 22,6 |
| $q_{A3}$ | 62.08 | 71.13 | 87.47 | 97.09 | 105.59 | 18, 5 |
| $q_{B1}$ | 0.07 | 0.30 | 0.51 | 1.40 | 1.61 | 35, 41 |
| $q_{B2}$ | 19.80 | 23.67 | 25.06 | 40.50 | 32.80 | 34, 40 |
| $q_{B3}$ | 69.98 | 77.35 | 87.81 | 104.4 | 107.81 | 33, 39 |
| $q_{C4}$ | 34.03 | 38.43 | 43.48 | 212.24 | 229.35 | 29, 13 |
| $q_{C5}$ | 37.87 | 42.42 | 47.15 | 51.83 | 260.36 | 30,14 |
| $q_{D}$ | 2.24 | 38.99 | 59.25 | 33.49 | 39.90 | 26,36,42,8 |
| $q_E$ | 2.29 | 6.64 | 6.83 | 6.73 | 9.49 | 27,37,9,43 |
| $q_F$ | 1.63 | 2.45 | 1.96 | 13.69 | 18.42 | 28, 38,10,44 |
| $q_J$ | 93.44 | 104.57 | 123.07 | 139.98 | 137.38 | 15, 4 |
| $q_L$ | 33.93 | 38.57 | 49.72 | 51.80 | 55.00 | 17,3 |
| $q_M$ | 1613.71 | 1837.26 | 2099.77 | 2354.45 | 2605.20 | 69,2 |
| $Q_{SUM}$ | 2083.0 (0.6110) | 2413.0 (0.7078) | 2773.3 (0.8135) | 3300 (0.9680) | 3781.7 (1.1093) | |

TABLE 2: q VALUES IN BTU/HR, $Q_{SUM}$ in KWt, T IN $^{o}F$, $T_{\infty}$ = $80^{o}F$

$$Q_{SUM} = q_A+2q_B+q_C+q_D+q_E+q_F+q_J+q_L+q_M$$

FIGURE. 2

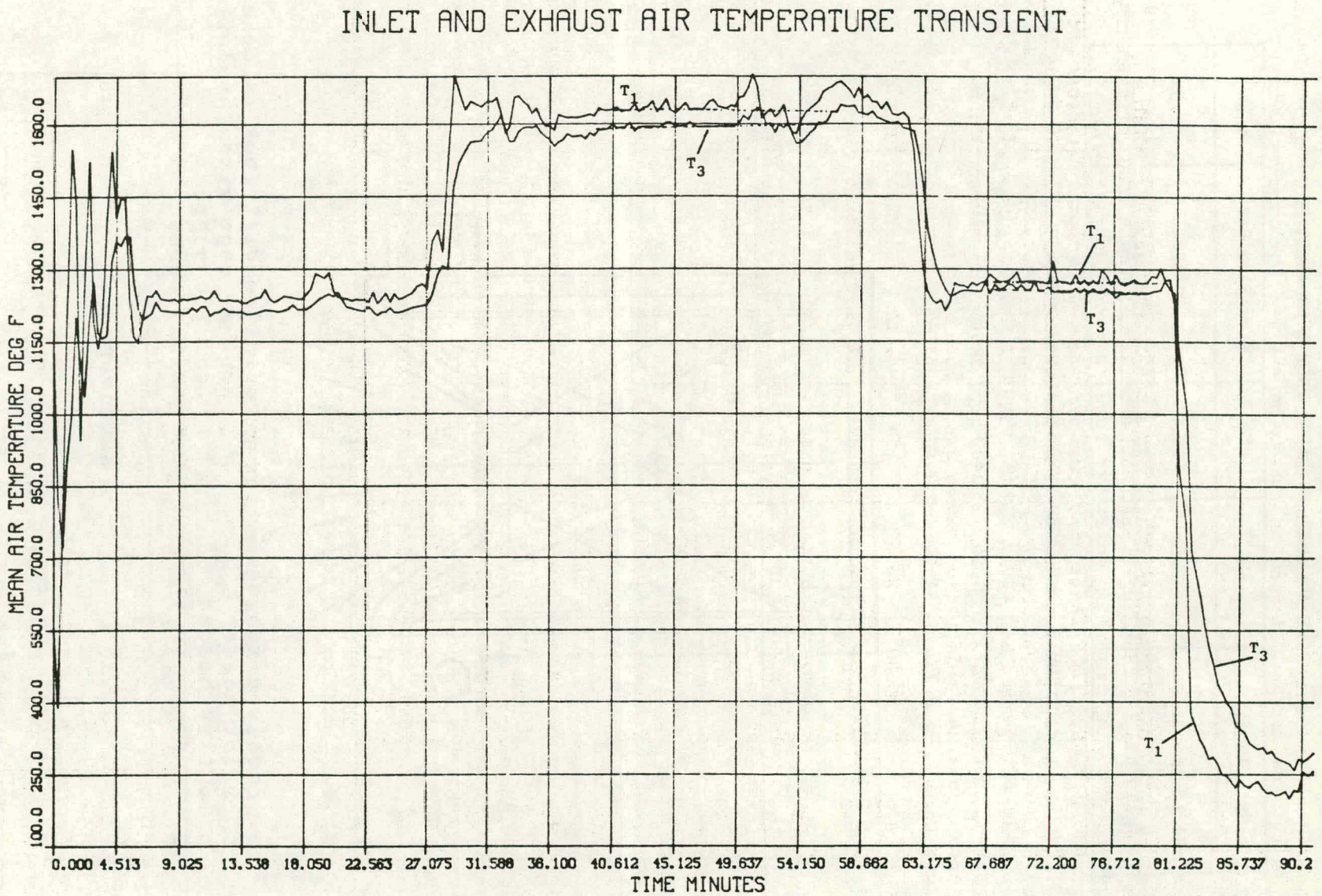
INLET AND EXHAUST AIR TEMPERATURE TRANSIENT
MEAN AIR TEMPERATURE DEG F
100.0
250.0
400.0
550.0
700.0
850.0
1000.0
1150.0
1300.0
1450.0
1600.0
0.000 4.513 9.025 13.538 18.050 22.563 27.075 31.588 36.100 40.612 45.125 49.637 54.150 58.662 63.175 67.687 72.200 76.712 81.225 85.737 90.2
TIME MINUTES
T1
T3
T1
T3
T3
T1

TIME AVERAGED ENTHALPY DROP OVER RECEIVER

| Time (min.) | $T_1$ Ave $^oF$ | $\Delta T$ $^oF$ | Mass Flow Rate | q $Kw_t$ |
|---|---|---|---|---|
| 34 to 56 | 1276 | 16.0 | 0.572 | 2.62 |
| 67 to 80 | 1631 | 38.5 | 0.564 | 6.58 |

TABLE 3 - AVERAGED OVER PERIODS SHOWN IN FIGURE 2

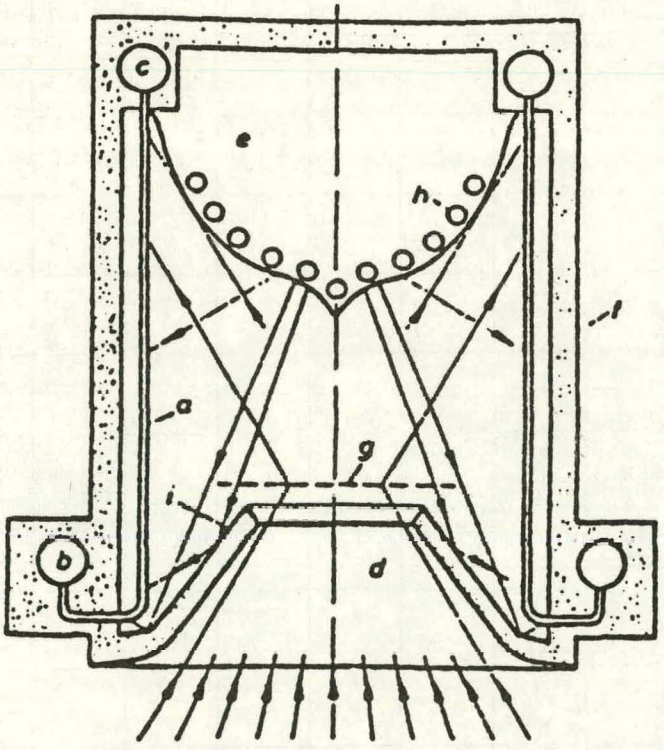


a receiver tubing
b inlet header
c outlet header
d window
e radiation distribution cone
f receiver cage with insulation
g focal plane area
h cooling tubes
i reflective wall

Receiver.

Figure 3: Cavity Shape Optimization

# Solar Tests of Aperture Plate Materials for Solar Thermal Dish Collectors

Leonard D. Jaffe
Jet Propulsion Laboratory
Pasadena, CA 91109

## ABSTRACT

In parabolic dish solar collectors, walk-off of the spot of concentrated sunlight can be a hazard if a malfunction causes the concentrator to stop following the sun. A test program was therefore carried out to evaluate the behavior of various ceramics, metals, and polymers under solar irradiation of about 7000 kW/m$^2$ (peak) for 15 minutes. The only materials that did not slump or shatter were two grades of medium-grain extruded graphite. High-purity slip-cast silica might be satisfactory at somewhat lower flux. Oxidation of the graphite appeared acceptable during tests simulating walk-off, acquisition (2000 cycles on/off sun), and spillage (continuous exposure of a receiver aperture lip).

## INTRODUCTION

If a malfunction occurs in a solar thermal point-focus distributed receiver power plant while a concentrator is pointed at the sun, motion of the concentrator may stop. As the sun moves relative to the Earth, the spot of concentrated sunlight then slowly "walks off" the receiver aperture, across the receiver face plate, and perhaps across adjacent portions of the concentrator. Intense local heating by the concentrated sunlight may damage or destroy these parts.

Methods of protection against walk-off damage are discussed in Ref. 1. Use of materials that can withstand the concentrated sunlight without active cooling has the advantage of providing passive protection, which should increase reliability and may be less costly than alternative techniques.

The peak flux density at the focus is typically 1,000 to 15,000 kW/m$^2$. With such input, a gray body losing heat only by reradiation may reach an equilibrium temperature as high as 3750°C (6800°F). Because the spot moves at the Earth's rotation rate of 15 deg/h, typical times for the spot to move its own diameter are 5 to 15 minutes (except in polar regions). For passive protection, a material and design that can withstand these conditions is needed.

Ability to withstand walk-off is only one of the requirements for an aperture plate. In most designs, the spot of sunlight traverses the aperture plate each time the concentrator is swung to point it at or away from the sun during normal operation. The exposure time during normal sun acquisition or "deacquisition" is much shorter than during walk-off: typically 1 to 2 seconds for the spot to move its own diameter. However, sun acquisition and deacquisition occur once or several times a day during operation, whereas

walk-off occurs only through malfunction. An aperture plate that is exposed to the sun during acquisition should withstand many cycles of acquisition and deacquisition.

An additional requirement of any aperture plate is that it must withstand "spillage" or lip heating. The flux density at the lip during normal operation is usually less than one percent to a few percent of the peak flux density of the spot, but the lip is exposed to this spillage at all times when the concentrator is pointed at the sun.

Some work has been reported on the ability of uncooled materials to withstand concentrated sunlight for short periods of time. Except for some limited tests, this prior effort was not oriented toward dish concentrators, and either the flux densities or exposure times used were lower than those of interest for walk-off of dish concentrators. Considerable work has been done on materials for high-speed reentry bodies and for resistance to nuclear explosions, but applicability of this work to solar concentrators is uncertain because of the different modes of energy transfer. It therefore appeared worthwhile to undertake tests to evaluate candidate materials. In particular, there was interest in finding a suitable aperture plate material for passive protection for the organic Rankine system. A more detailed account of the work, with extensive literature references, is given in Ref. 2.

## TYPES OF MATERIALS TESTED

The general types of materials tested included graphite, silicon carbide, silica, silicates, alumina, zirconia, steel, and polytetrafluoroethylene. Also tested were aluminum and copper with temperature-resistant coatings, and graphite with temperature-resistant coatings. About 45 samples were tested.

The preferred sample size selected was 200 x 200 x 25 mm (8 x 8 x 1 in.), to have samples large enough when compared to the solar spot size and thick enough to provide reasonable protection. A few thicker samples were tested to see if greater thickness improved performance. Because many samples were provided free of charge rather than purchased, they were often smaller than preferred. Some were as thin as 0.4 mm (0.017 in.); these samples were provided more because of the supplier's interest in using them for protection during normal operation, acquisition, and deacquisition than for possible walk-off protection.

## TEST EQUIPMENT

Solar tests were made on Test Bed Concentrator 1 at J.P.L.'s Parabolic Dish Test Site. As part of the setup for testing a major portion of the organic Rankine module, a water-cooled aluminum shield had been mounted near the focal plane of the concentrator. This shield had a central opening 400 mm (16 in.) in diameter. A water-cooled aluminum sliding shutter, installed on the side of the shield closest to the concentrator mirrors, could be opened or closed to permit concentrated sunlight to pass through the shield opening or to block it off.

## Solar Walk-off And Solar Acquisition

For the materials walk-off and acquisition tests a fixture was designed which mounted against the aluminum shield, on the side away from the mirrors. The test fixture was made of graphite in the form of a "window frame" with an opening 230 mm (9 in.) square, in which the sample was placed. The sample was retained by graphite rods 10 mm (3/8 in.) in diameter, which fitted loosely through holes in the upper frame of the fixture and rested in blind holes in the lower frame. During exposure, the center of the solar spot was close to the center of one face of the sample.

The flux pattern used for walk-off and solar acquisition tests was designed to simulate the pattern then planned for use with the organic Rankine module. The distribution of solar flux in the materials test plane was measured with a flux-mapper (Ref. 3). The peak measured flux density in this plane was 9,700 $kW/m^2$ at an insolation of 1 $kW/m^2$. The total concentrated solar power at 1 $kW/m^2$ was approximately 78 kW, as measured by a cold-water calorimeter. In the materials tests the actual insolation was lower than 1 $kW/m^2$; at an insolation of 720 $W/m^2$, the peak flux density was 7,000 $kW/m^2$.

## Solar Spillage

For spillage tests, one edge of the samples was tapered and rounded to form a lip. Two chromel-alumel thermocouples, wire diameter 0.25 mm (0.010 in.), were inserted through the back of the 26 mm (1.0 in.) thick samples, terminating 0.5 mm (0.02 in.) from the lip. The samples were mounted at various radial and axial positions to simulate spillage conditions (such as flux levels) that might be encountered with various solar thermal power modules. Samples were mounted off center so that only the edge of the solar spot struck the sample.

# TEST PROCEDURES

In all solar tests, the samples were observed on television utilizing a black-and-white TV camera; imagery was recorded on a video cassette recorder. Insolation was recorded digitally using Eppley and Kendall pyroheliometers. Direct normal insolation during tests was 530 to 960 $W/m^2$.

## Walk-off Tests

All of the materials investigated were tested for their ability to sustain walk-off. The test duration was 15 minutes unless the sample failed earlier. The test was more severe than an actual walk-off because the spot of maximum solar flux was held fixed on the sample, whereas in walk-off the spot would traverse across the plate.

Several samples were tested wet to simulate exposure to rain followed by sunlight and walk-off. They were soaked in water at a depth of 15 to 30 cm (6 to 12 in.) for at least 30 minutes prior to solar testing.

## Acquisition Tests

Tests aimed at evaluating behavior under acquisition and deacquisition conditions and under spillage conditions were conducted only on graphite. These

tests were run because some grades of graphite appeared promising in the walk-off tests, but there was concern that the rate of loss of graphite by oxidation might be excessive under the long cumulative exposures associated with acquisition-deacquisition and spillage.

Two graphite samples were tested under conditions simulating repeated acquisition and deacquisition. They were mounted in the same way as the samples for walk-off testing. The acquisition-deacquisition tests consisted of multiple cycles of opening and closing the shutter, each approximately 1 second open, 10 to 19 seconds closed. Maximum exposure was 2000 cycles. Insolation in these tests was 780 to 960 $W/m^2$; acquisition and deacquisition in service probably would be primarily at low sun elevation, when insolation would be lower.

Spillage Tests

Solar tests of oxidation of graphite under conditions simulating many thousand hours of spillage exposure were beyond the scope of this work. Instead, to allow estimation of the long-time oxidation rate, measurements were made of the temperature of graphite samples simulating a tapered aperture lip. The lip, with thermocouples inserted, was placed 75 to 175 mm (3 to 7 in.) from the center of the spot of sunlight (representing aperture diameters of 150 to 350 mm, 6 to 14 in.) and at various axial positions. Flux density at the lip position nearest the spot center varied from less than 1 to over 1000 $kW/m^2$ depending on sample position.

## WALK-OFF TESTS: MELTING AND FRACTURE RESULTS AND DISCUSSION

Results of the walk-off tests are summarized in Table 1 and tabulated, with accompanying measurements and photographs, in Ref. 2.

Graphites

Grade G-90. Graphite grade G-90 was the only material that consistently survived a 15-minute simulated walk-off without melting, slumping, or cracking. A sample of G-90 survived two 15-minute tests without cracking. Another sample of this material was tested wet, and did not crack.

Grade G-90 is an extruded material that is reimpregnated several times with coal-tar pitch and regraphitized to reduce its porosity and increase its bulk density. Grade G-90 is a premium grade and somewhat expensive for a graphite: about $45/kg ($20/lb).

Grade CS. During the standard walk-off test, all six samples of uncoated graphite grade CS 14 to 37 mm (0.5 to 1.5 in.) thick developed a single crack extending from near the midpoint of an edge to near the center of the specimen. This reproducibility was striking, particularly because the samples came from three different lots of graphite. Of two samples that were 50 mm (2 in.) thick, one survived the simulated walk-off test without cracking or other failure; the other cracked from an edge to somewhat beyond the center. None of the CS graphite specimens fell apart into two or more pieces. Four samples of CS graphite that cracked halfway during initial exposure were retested for total times up to 45 minutes without further observed crack

advance. Apparently the first crack, halfway across, was sufficient to relieve the thermal stresses and prevent further cracking. With proper segmenting, this grade should perform satisfactorily. (Bank and Owen (Ref. 4) reached a similar conclusion on the basis of earlier tests.) Grade CS is a commercial grade of extruded graphite that costs about $4.50/kg ($2/lb).

Like most graphites fabricated by extrusion, grade CS has markedly anisotropic properties, with its coefficient of thermal expansion being lower and its strength higher in the direction parallel to the grain (parallel to the extrusion direction) than in the direction perpendicular to the grain (perpendicular to the extrusion direction). It is very likely that cracking occurred perpendicular to the grain.

Effect of Water. Graphite grades G-90 and CS absorbed very little water on immersion and their subsequent performance in simulated walk-off tests was unaffected by this wetting.

Other Graphite Grades. Other grades of conventional graphite tested were 3499, 8826, and HLM-85. All samples of these grades cracked apart or shattered in test; the 3499 at exposure times of 1-1/2 to 8 minutes, the 8826 and HLM-85 in 1 to 1-1/2 minutes.

Walk-off Performance and Other Characteristics of Graphite Grades. Graphite grades G-90 and CS, which performed well, are extruded grades with medium grain size (maximum particle size nominally 750 micrometers). Grades 3499 and 8826 are fine-grained molded graphites (maximum particle size nominally 75 micrometers); they shattered in test. This suggests that fine grain (and possibly molding) is less desirable than medium grain (and extrusion?) in graphites for walk-off protection. Such an interpretation of the grain size effect is consistent with the general belief that coarser-grained graphites have better resistance to thermal shock than fine-grained.

Many graphite grades are available besides those tested. Perhaps some further testing of grades with a wider range of characteristics would be worthwhile.

Graphite Cloth. One sample of a "graphite cloth," graphitized polyacrylonitrile, was tested under simulated walk-off conditions. The sample, 0.43-mm (0.017-in.) thick, developed slits and holed through in 30 seconds. Examination under the microscope indicated that the material had not melted, but that woof fibers, especially, had disappeared, presumably by oxidation. Similar results have been reported (Refs. 4,5).

If one assumes that multiple layers would behave independently, an assembly of 30 plies, 13-mm (0.5-in.) thick, might last 15 minutes. This is rather speculative in the absence of a multi-layer test. Such a graphite cloth assembly would be considerably lighter than conventional graphite of the same dimensions: 4.5 kg (10 lb) for an aperture plate for the collector mentioned above. Material of this type costs about $150/kg ($70/lb).

Coated Graphite. Three samples of graphite were coated with boron nitride, which is white, and two with commercial high-temperature white paints. The

samples behaved like uncoated samples of the same grade, except that one CS sample cracked all the way across, rather than halfway.

### Silica

Samples of high-purity slip-cast fused silica with fine particle size survived 4 minutes at insolation of 670 $W/m^2$ and 1-1/2 minutes at 740-790 $W/m^2$ before slumping. The longer survival at the lower insolation suggests that high-purity slip-cast silica would be satisfactory at somewhat lower flux levels than those used in this test program. The cost of a segmented aperture plate of high-purity slip-cast silica for the collector discussed would be about $12/kg ($6/lb) in quantities of a hundred or so.

### Other Materials

None of the other materials survived more than 3 minutes. Most failed within a few seconds. Comparison of the behavior of the various materials in the walk-off tests emphasizes the importance of melting point. The only materials tested that did not melt or slump were graphite and silicon carbide. Neither of these materials melts at atmospheric pressure. Silicon carbide was nevertheless unsatisfactory because it shattered in thermal shock. Silicon carbide has lower thermal conductivity than graphite, which is doubtless a major factor in its poorer performance.

## WALK-OFF TESTS: OXIDATION RESULTS AND DISCUSSION

During walk-off tests the loss in thickness due to oxidation for grades CS and G-90 varied from 0.2 mm (0.008 in.) to 8 mm (0.3 in.) per 15 minutes of exposure. The corresponding loss in mass was 2 to 22% (normalized to a standard sample size, 25 x 200 x 200 mm (1 x 8 x 8 in.), assuming that the mass loss in grams is independent of sample size). This loss rate will probably be acceptable for walk-off protection because walk-off is expected to be an infrequent event and the test was more severe than the expected service.

The effect of wind speed on the oxidation loss was significant (Fig. 1), and accounts for a large part of the variation in loss between samples. Interestingly, insolation did not have a significant effect upon mass loss rate. The literature indicates that, at the temperatures encountered in walk-off, the rate-limiting process is mass transfer through the boundary layer. Insolation level would be expected to have only a small effect on mass transfer, whereas wind speed would have a major effect.

The difference in mass loss rate between grade CS graphite and grade G-90 was not statistically significant. Neither a boron nitride coating nor prior immersion in water had a statistically significant effect.

## ACQUISITION TEST RESULTS AND DISCUSSION

The repeated on-sun/off-sun cycles used for some samples of grade CS graphite were intended to give an indication of the extent of graphite oxidation during normal sun acquisitions and deacquisitions. In 700 to 2000 cycles,

which might represent a year or two of service, the samples lost 5 to 7 mm in thickness and 0.15 to 0.2% of their weight (normalized to a thickness of 25 mm, 1 in.). This appears to be tolerable. Wind speed during the simulated acquisition-deacquisition test was 2 to 10 m/s, 4.5 to 22 mi/h), representative of the wind conditions likely to be encountered during operation.

## SPILLAGE TEST RESULTS AND DISCUSSION

The various positions of the sample edge in the spillage tests were used to indicate the temperatures attained by the lip of a graphite aperture plate exposed to various levels of spillage. One test represented, approximately, the conditions that were planned for the organic Rankine receiver with an aperture diameter of 350 to 380 mm (14 to 15 in.). The flux density at the lip was about 10 $kW/m^2$; the lip temperature was 107°C (225°F). At this temperature the oxidation of graphite would be negligible even over periods of many years.

Tests of other samples represented conditions on receiver aperture plates having diameters of 150, 200, and 250 mm (6, 8, and 10 in.), positioned close to the focal plane. Flux densities at these positions were approximately 400, 70, and 40 $kW/m^2$. Temperatures reached were, respectively, 312, 173, and 133°C (594, 343, and 271°F). According to data of Ref. 6, the oxidation rate for grade CS graphite below 750°C (1400°F) is given by

$$dm/dt = 5.26 \times 10^8 e^{-42,900/RT_K} \qquad (1)$$

where $dm/dt$ = mass loss, $g/m^2s$
$R$ = universal gas constant = 1.986 cal/K-mol
$T_K$ = temperature, K

For the 200 and 250 mm (8 and 10 in.) apertures, the calculated oxidation rate is negligible. For a 150 mm (6 in.) aperture, the calculated rate of less than 1 μm/y certainly appears acceptable.

According to the literature, graphite oxidation at temperatures up to 750 to 850°C (1400 to 1600°F) is reaction-rate limited. Loss rates due to spillage, therefore, should not be significantly affected by wind speed.

## SUMMARY AND CONCLUSIONS

A test program was carried out to evaluate behavior of materials under conditions simulating walk-off of a parabolic dish solar collector. Each test consisted of exposure to concentrated sunlight at a peak flux density of about 7,000 $kW/m^2$ for 15 minutes. Types of materials tested included graphite, silicon carbide, silica, various silicates, alumina, zirconia, aluminum, copper, steel, and polytetrafluoroethylene. Of these, the only material that neither cracked nor melted was grade G-90 graphite, a premium grade. Grade CS graphite, a lower cost commercial grade, cracked half-way across, but did not fall apart. Both of these grades are medium-grain extruded graphites. A graphite cloth (graphitized polyacrylonitrile) showed fair performance when tested as a single thin ply; it might be useful as a multi-ply assembly.

The only other material tested which appeared promising was high-purity slip-cast silica; samples survived one and one-half to four minutes. This duration is inadequate for walk-off protection, but the material may well be satisfactory at flux densities somewhat lower than those used in these tests.

The other grades of graphite and silica tested, and all the samples of other materials, either melted, slumped or shattered quickly during the walk-off tests.

Coatings of white high-temperature paint or boron nitride did not improve the performance of graphite samples. Immersion in water prior to test, simulating rain, did not affect their performance.

Oxidation of grades CS and G-90 graphite per 15-minute simulated walk-off varied from 0.2 to 8 mm (0.008 to 0.3 in.) of thickness, from 2 to 22% of the mass (normalized to 25 mm (1 in.) thickness). The amount of oxidation varied strongly with the wind speed.

Grade CS graphite was tested for up to 2000 cycles simulating 1-second periods of acquisition at the same flux density as the walk-off test. Loss in moderate to high winds was about 5 mm in thickness or 0.15% of the sample mass. Tests under simulated spillage conditions were limited to measurements of the temperature of the lip of a simulated aperture plate of grade CS graphite. They indicate that the oxidation rate of this material will be negligible at a flux density of 400 $kW/m^2$ on the lip, for the graphite geometry and flux distribution used in test.

## ACKNOWLEDGMENTS

William Owen, Richard Smoak, and Terry Hagen contributed to planning of the work. George Lynch helped greatly in arrangements to obtain and prepare samples. John Woodbury and Dennis Maciej provided major support in the solar testing. Toshio Fujita, Frank Surber, Robert Hale, and Wayne Phillips suggested significant improvements in the manuscript.

Test materials were provided by Maurice Argoud, Herman Bank, J. A. Barry, David Lawson, William Owen, Wayne Phillips, Kudret Selcuk, and Jack Stearns of JPL, Joseph Harris of Georgia Institute of Technology, Wilson Schramm of Lockheed Missiles and Space Company, David Wells of United Stirling, Inc., John Davidson of Airco-Speer Carbon Co., Y. Harada of Illinois Institute of Technology Research Institute, and David Page of Union Carbide Corp.

## REFERENCES

1. L.D. Jaffe, R.R. Levin, P.I. Moynihan, B.J. Nesmith, W.A. Owen, E.J. Roschke, M.K. Selcuk, D.J. Starkey, and T.O. Thostesen, "Systems Approach to Walk-off Problems for Dish-Type Solar Thermal Power Systems," JPL Doc. 5105-97, 1981, and Proc. I.E.C.E.C., Orlando, FL, Aug. 1983, Am. Soc. Chem. Eng.

2. L. D. Jaffe, "Solar Tests of Aperture Plate Materials for Solar Thermal Dish Collectors," JPL Doc. 5105-121, 1983.

3. W. A. Owen, Internal communications, JPL, 1981-1983.

4. H. Bank and W. Owen, Internal communication, JPL, 1980.

5. R. Smoak, Internal communication, JPL, 1980.

6. Carbon Products Division, Union Carbide Corp., "Oxidation of CS-312 in Dry Air," Union Carbide Corp., Palma, Ohio.

Table 1
Summary of Results of Walk-off Tests

| Material Type | | Thickness mm | Failure Mode | Time |
|---|---|---|---|---|
| Graphite | 3499 | 26 | Shattered | 1 to 8 min |
| | 8826 | 26 | Shattered | 1 to 1-1/2 min |
| | CS | 14-50 | Cracked halfway (1 of 10 survived) | 10 s to 14 min |
| | HLM-85 | 24-26 | Shattered | 1 to 1-1/2 min |
| | G-90 | 24-25 | (Survived) | 30 min |
| | Cloth | 0.4 | Holed | 30 s |
| SiC | | 6-32 | Shattered | 1 s |
| $SiO_2$ | Slipcast, high purity | 18-21 | Slumped | 1-1/2 to 4 min |
| | Slipcast, commercial | 20-26 | Dripped | 10 s |
| | Fibrous, glazed | 41 | Dripped | 7 s |
| Silicates | Mullite | 32-38 | Melted | 1 to 4 s |
| | Processed kaolin | 27 | Melted | 3 s |
| | Cordierite | 25 | Melted | 2 s |
| | Alumina-boria-silica | 0.5-0.7 | Melted | 1 s |
| $Al_2O_3$ | Paper | 0.4-1.4 | Melted | 2 to 6 s |
| $ZrO_2$ | Cast and sintered | 29 | Melted | 20 s |
| | Fibrous board | 25 | Melted | 1 min |
| | Cloth | 0.5 | Melted | 8 s |
| Copper | | 26 | Melted | 1 to 3 min |
| Aluminum | | 1.8 | Melted | 1 s |
| Steel | | 2 | Melted | 2 s |
| Polytetrafluoroethylene | | 38 | Melted | 2 min |

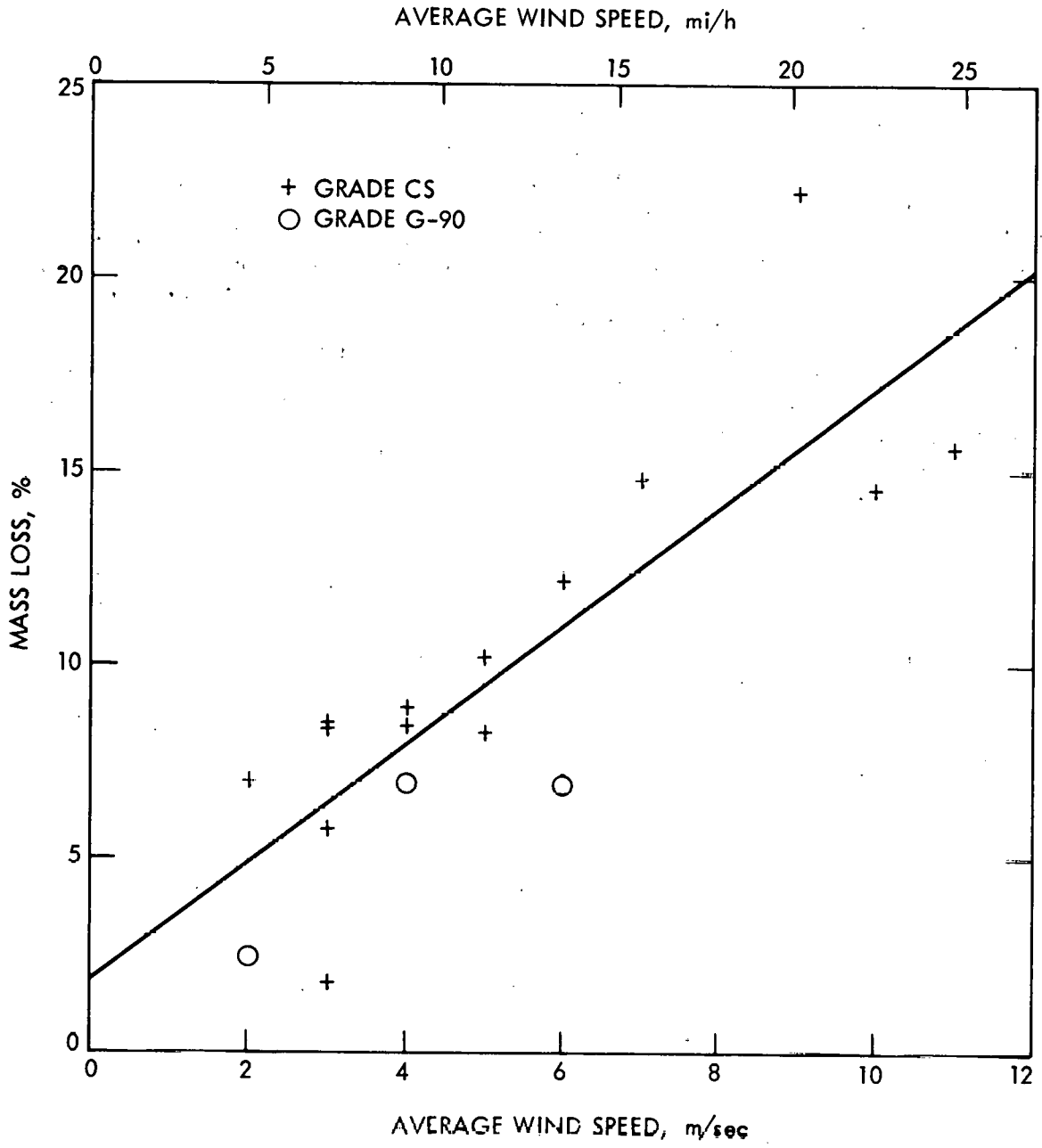


Fig. 1 Effect of wind speed upon mass loss by oxidation, for graphite, Grades CS and G-90, in walk-off tests. (Mass losses normalized to 15 minutes exposure and 25 x 200 x 200 mm (1 x 8 x 8 in.) sample.

# NON-DOE-SPONSORED DOMESTIC DISH ACTIVITIES

Toshio Fujita

Jet Propulsion Laboratory
Pasadena, CA 91109

The papers in this session are devoted to parabolic dish development activities being undertaken within the private sector of the United States. The primary emphasis of these non-DOE-sponsored activities is placed on the development of commercial products that can penetrate the market in the near term. The exchange of information between these activities and the complementary DOE-sponsored work directed toward developing advancements in technology is considered to be of major importance. The experiences and problems encountered in the private sector serve as inputs that will help guide in the planning of the DOE program. In turn, a principal objective of the DOE program is the transfer findings of its technological development activities to the private sector.

Activities in the private sector are characterized by their diversity in terms of both product design and marketing approach. This diversity is reflected in the five domestic dish activities covered in this session. The differences in the design concepts and the sizes of the dish concentrators under development are particularly noteworthy.

# Advanced Solar Power Systems

John H. Atkinson and John M. Hobgood

Advanced Solar Power, Inc.

Anaheim, California 92806

## Abstract

Advanced Solar Power, Inc. (ASPI) has developed a demonstration prototype of a point focusing solar power system. The concentrator is a modified Cassegrain system (10th order generalized aspheric mirrors) producing 10,000 suns at the focal point. The integral receiver is an extended, pressurized black-body cavity designed to operate at 700 psi and 503 °F. The system tracks on two axes under microprocessor control. The demonstration prototype has a 4 kilowatt thermal (kWt) mirror mounted on a 40 kWt receiver system and is trailer-mounted (freeway legal) for experimental use.

Because of the patented black-body cavity receiver design, high thermal efficiencies of 80% with aluminimum and 90% with silver on the mirrors are calculated. Energy is transferred directly from photons to the molecules of the working fluid (water). The design system efficiency for this technology is virtually constant in the working range of 350 °F to 2000 °F and 135 psi to 10,000 psi because reradiation is negligible.

Commercial units are sized at 40-50 kWt (highway transportable), 500 kWt (helicopter transportable) and 1 MWt (mirrors manufactured on site). While tooling is expensive, quantity manufacturing is inexpensive and designed to be automated. The 40 kWt to 50 kWt (136,00 to 170,000) units will cost about $20,000 per unit with an available steam engine at a production rate of 300 units per year. A cogeneration version may cost on the order of $2,300 per kilowatt electric (kWe) for 1 to 10 kWe and 120,000 BTU/hr for a thermal load. The 500 kWt to 1 MWt units are estimated to cost $100,000 to $150,000 at a production rate of 500 units/year with the high likelihood of using conventional team turbine generator technology to achieve $600 to $1,000 per kWe of capacity installed cost.

All sizes of ASPS units have the inherent capability of buffer storage of abouat 1 hours of energy collection. Applications for ASPS units range from irrigation pumping, cogeneration and inudstrial process heat to heater/treater operations in oilfields. The larger units are designed to be competitive with fossil fuel as oilfield steam generators, large-scale chemical production, particularly in conjunction with geothermal wells, and electric power production. Since any transparent or translucent working medium can be used, possibilities exist for very efficient systems using helium, air, tolulene or sewage sludge as a working medium.

## Introduction

The Advanced Solar Power System (ASPS) uses a technically sophisticated design and extensive tooling to produce very efficient (80-90%) and versatile energy supply equipment which is inexpensive to manufacture and requires little maintenance. The advanced optical design has two 10th order generalized aspheric surfaces in a Cassegrainian configuration which gives outstanding performance and is relatively insensitive to temperature changes, wind loading and manufacturing tolerances have been achieved.

A 4 kilowatt thermal (kWt; 14,000 BTU/hr) freeway transportable demonstration prototype unit has been designed, constructed and tested. The system, illustrated in Figure 1 uses automatic two-axis tracking, focusing and alignment under microprocessor control to give high geometric efficiency and low manufacturing and maintenance costs. The required mechanical motions are provided by hydraulic actuators which have stored energy to provide high power levels for an emergency scram or during high wind conditions. Routine power requirements are very low.

The key to the ASPS is the direct absorption of concentrated sunlight in the working fluid by radiative transfers in a black- body cavity. This heat transfer mechanism is 100% efficient by physical law. Thus the thermodynamic efficiency of the system is determined by the reflectivity of the two mirror surfaces and the transmission of the pressure window surface. Heat losses through the optical cavity walls can be limited by insulation to any desired economic value.

A broad range of temperatures (350 to 2000 deg F) and pressures (0 to 10,000 psi) are efficiently obtainable with this system which makes it very effective for many unique applications. The first commercial prototype ASPS will supply 40 to 50 kWt (136,000 to 170,000 BTU/hr) in the form of high temperature and pressure steam (350 to 700 deg F at 300 to 700 psi).

## Basic ASPS Design Concepts

Figure 2 illustrates the basic design concepts underlying the ASPS technology. The key patented element of the ASPS is the black-body cavity receiver where photons are absorbed directly in the working medium. Max Planck's insight in 1899, explained the observed distribution of energy in a black body cavity at temperature T, by limiting permissible energy values to $E_n = nhf$ (Verh.d.D.Phys.Ges. 2, 237 (1900); Ann.d.Physik 4, 553 (1901)).

Albert Einstein developed a sounder mathematical basis for the quantization of matter and radiation (Ann. d. Physik 17, 132 (1905); Phys. Zeits., 18, 121 (1917)). The result of the quantization condition is that energy enclosed in an insulated cavity will always produce a given wavelength and intensity distribution dependent only on the absolute temperature (T) and not on the working fluid or the wall materials.

A typical black-body cavity is externally heated and has black walls and a small exit hole allowing the escape of black body radiation. Based on the principle that almost all optical phenomena are reversible, the ASPS

introduces concentrated solar radiation into an enclosed, insulated cavity through a small pressure window. A sophisticated optical system is required to give high concentration ratios ($10^4$) and keep the entrance aperture area a small part (less than 1%) of the total cavity surface area. The entrance window must be highly transparent to the solar spectrum to prevent local heating. Energy is dispersed down the pressure tube by a turning mirror to prevent hot spots and to prevent direct reflections back out the window for any incoming rays. The walls of the cavity are highly reflective (specular and/or diffuse) to aid wall insulation and to permit preferential absorption of solar photons in the working medium (e.g.,water). All photons are absorbed and reradiated by the medium and cavity walls with a typical time constant of $10^{-8}$ seconds until the black-body curve for the equilibrium temperature (T) is achieved in less than a microsecond.

By the principle of Conservation of Energy, the radiative transfer of energy from photons to the working fluid is 100% efficient. To prevent direct reflection of sunlight out the entrance aperture, the minimum ray path in the working fluid is designed to be an absorption length for a green photon. This is about 10 feet for tap water. A minimum length for the optical cavity is established since a reflected ray would be attenuated by at least $1/e^2$.

For reradiation to effectively establish thermal equilibrium in the optical cavity, the working fluid must be transparent or translucent to the equilibrium temperature spectrum as well as the solar spectrum. The minimum temperature for tap water appears to be about 350 degrees F. At higher temperatures, equilibrium will be established faster. At lower fluid temperatures, an expanding 350 degree F. bubble is formed at the inside of the entrance window and at the adjacent turning mirror. Since the turning mirror and window do not melt on start- up, this has been demonstrated to be an effective heat transfer mechanism.

Energy, will of course, be reradiated out the entrance aperture. However, since the entrance aperture sees only the suns disk (the optical system is reversible), a net transfer of energy from the cooler cavity to the hotter sun would violate the first and second laws of thermodynamics. The high concentration ratio of $10^4$ to 1 also makes reradiation losses negligible. Because no energy must be transported through an absorbing surface ( the window is transparent and a thermal insulator) the optical cavity can be insulated as well as desired with cost as the limiting factor. Vacuum insulation in a Dewar construction has been chosen as an economic and convenient insulation method in the 4 kWt demonstration prototype. The microtherm spacers used are effective, but other insulation can be used without compromising the system principles in any way.

To provide precise temperature control of the working fluid without losing sun track, a movable baffle is provided in the optical cavity of the larger systems. This baffle blocks light, which travels in straight lines, but does not block fluid pressure. Since this is not a circulating system the system pressure is set by the feed pump which pumps cold fluid. If more energy is entering the cavity than is being removed, the baffle is moved down the pressure tube, increasing the size and the heat capacity of the cavity and maintaining a constant temperature. If more energy is being removed from the cavity by withdrawing fluid than is entering the cavity from the sun, then the baffle is moved up the tube. This decreases the size of

the cavity and the heat capacity while maintaining a constant temperature of the working fluid. In this way, ideal engine or turbine operating conditions can be achieved and the Carnot efficiency of the system can be maximized.

System Efficiency

Because the ASPS has no appreciable reradiation losses, the only significant energy losses are from the two mirror reflections and the reflection at the surface of the pressure window. Because of the steepness of the mirror curves, 25% of the primary mirror intercept area is at ray angles of less than $45^{o}$, and a large part of the secondary mirror area has ray angles of less than $45^{o}$. Since at acute angles the reflectivity of the aluminum (or silver) layer and the plastic outer surface approaches 1 at the critical angle, for a given wavelength, the total reflectivity exceeds 80% for aluminum and 90% for silver coatings. Use of dichroic coatings could increase these reflectivities but may not be economic. The pressure window does have a dichroic coating which transmits better than 99.5% of the solar spectrum incident in an f/1.0 cone. After energy is inside the window, it is in the black body-cavity and will contribute to the equilibrium temperature by radiation or conduction.

The high vacuum insulation proposed, if properly designed, can give losses of less than 1% per day for a single Dewar design maintained at $10^{-6}$ Torr. Additional insulation can be added to reduce thermal losses to any desired value. In further testing of the 4 kWt unit, calorimetric analysis will primarily measure the efficiency of the cavity insulation. The reflectivity of the mirrors can easily be measured separately as a function of incident angle and wavelength integrated over the solar spectrum. Tracking efficiency is not a factor because it is either adequate to keep the sun's image on the pressure window or parts of the system melt or burn. However, the calorimetric analysis directly measuring the ratio:

$$\frac{\text{Energy in fluid}}{\text{Direct solar insolation}} = \text{efficiency}$$

will give an easily understood measure of system efficiency.

Moreover, the start-up variations of temperature as a function of position along the tube will give an indication of the working fluid opacity as a function of equilibrium temperature. This is a difficult number to calculate accurately for water and many other fluids, although a lower operating limit of about 350 degrees F. is expected in water.

A unique advantage of the ASPS is the essential independence of thermal efficiency from equilibrium operating temperature or the external environment. Thus the system can be operated to optimize the performance of external devices or processes. The practical upper limit for a fused quartz window operated at pressures to 10,000 psi is about 2,000 degrees F. Crystaline quartz windows would be limited to about 3,000 degrees F.

## ASPS Optical System

Conventional telescopes are designed to resolve a point source (star) at infinity and have parabolic prime mirrors as derived by Sir Isaac Newton (1671). A conventional Cassegrain system has a parabolic primary and a hyperbolic secondary to give a more convenient focus for spectrographic studies of stars as derived by N. Cassegrain (1672). However, the sun subtends 1/2 degree of arc at the earth's orbit and is thus not a point source at infinity. This observation is taken into account in the design of the ASPS. The two reflective optical surfaces were designed using the full power of the Optical Researach Associates (ORA) of Pasadena, California proprietary software programs and hardware. The optimized surfaces are given by:

$$Z = \frac{(curv)y^2}{1 + (1-(1+k)\ (curv)^2y^2)^{\frac{1}{2}}} + Ay^4 + By^6 + Cy^8 + Dy^{10}$$

The ORA optical design programs are generally recognized as the best available for systems containing reflective elements.

Figure 3 shows the optical diagram for the 4 kWt ASPS which was constructed using two hyperbolas. The improvement over the conventional design is significant at the edge of the field (sun's rim) which is the area of primary concern. Because the objective is to put light through a hole, the energy distribution in the center of the sun's image is of little concern. The demonstration unit design was limited to conic sections because these simpler equations were presumed to simplify manufacture and testing of the mirrors.

However, the manufacturing and testing methods developed during the fabrication and testing of the demonstration 4 kWt system revealed that using conic sections was not an advantage. Numerically controlled machine tools used to generate the sweep template for constructing mirror molds point fit anyway and can accept the 10th order curve. Conventional testing methods do not work for our very fast systems (4 kWt;f/1, 40 kWt;f/0.8) because there is no prime focus but only a volume defined by rays from the primary mirror. Figure 4 shows the optical diagram 10th order design of the 40 kWt mirrors. The more sophisticated design provides steeper curves with higher reflectivity and more mechanical strength. In addition, this design has a lower obscuration ratio (11.2% - 14.4%) and better manufacturing tolerances.

The obscuration ratio is deliberately kept larger than 10% to permit the use of a plastic secondary mirror rather than the stainless steel secondary originally proposed. Obscuration ratios in the range used also give better manufacturing tolerances. The mirror design is tolerant of the primary environmental effects of temperature changes and wind loading. Temperature increases bring up the rim of the mirror, increasing the curvature and thus shortening the focal length. This effect can be corrected by automatic refocussing. The wind loading changes the pointing of the mirror which can be corrected by the fine-tracking system.

Manufacturing tolerances required for the 4 kWt unit have been achieved and will scale linearly with size for the proposed 40 kWt unit. The key tolerance is 1 milliradian random deviation on the mean slope of the primary mirror. Achievement of this tolerance on the demonstration unit was measured on a Cordax unit and also shown by the optical performance of the complete

system. The sun's image on the face of the pressure window was calculated to be 1.1 inches in diameter with the allowable tolerances. The actual diameter was measured to be 1.08 inches.

To provide this superior optical performance at minimum construction and maintenance cost, these mirrors must move as a unit without unpredictable changes in figure. Thus all the materials used in a mirror must have similar coefficients of expansion, the mirror must be damped to avoid standing waves, and it must be of monocoque construction to avoid continuing adjustment. The ASPS mirrors are made of fiberglass and paper honeycomb with a slightly stretched reflective surface of aluminum or silver with a slippery plastic outer protective layer. This lightweight construction is economical because the materials are inexpensive ($1.50/lbd.), fabrication can be automated, there are no labor intensive subassemblies and there is no need for continuing alignment adjustments.

## Controls

The ASPS features automatic tracking and focusing under microprocessor control primarily for economic reasons. The coarse tracking system located on the back of the secondary mirror is a simple quadrant detector. The system is constructed using four photo sensors (photo transistors) that are located under diffusing domes (pilot light covers). The sensors detect the shadow cast by a black hat. Since the system optical axis is boresighted to the coase detector equal shadows cast on all four sensors mean the detector is perpendicular to the sun's rays. This sytem will acquire the sun within 180 degrees (2 steradians) and lock on within 15 seconds.

The fine tracking and focusing system looks through 4 quartz fibers at the sun's image on the face of the pressure window. Again this arrangement is a quadrant dectector which centers the image on the window. Additional algorithms are used to minimize the size of the image, thus insuring proper focus. A clock is also contained in the microcomputer permitting rough tracking without a visible sun. This sophisticated but inexpensive control system permits less rigidity in the mount, prime mirror and secondary mirror support (spider) than a conventional telescope drive would require This results in enormous savings in system weight and cost. Maintenance is also greatly reduced since there are no manual adjustments required for changing environmental or operating conditions.

The microcomputer also performs critical performance monitoring and remote control from any location with a communication link (e.g., telephone). Energy production is monitored for billing purposes and tampering with the unit could be detected. Whenever dangerous temperatures or pressures are measured or sun-track is lost, the unit is programmed to scram by rotating 90 degrees off the sun within 5 seconds. If the unit is not moved off the sun within 15 seconds, of course parts of the system burn or melt. Strain gauges will be used to sense excessive wind loading and instruct the control software to move the unit into a zenith stow position.

## Mount

An equatorial mount as illustrated in Figure 5, is the most economic design for the limited support requirements of the ASPS. The sun position is well known as the earth rotates daily about its inclined (23 - 1/2 degrees) polar axis and completes a yearly elliptical orbit around the sun. The daily rotation is most efficiently accomplished about an axis parallel to the earth's axis (i.e., a north-south axis inclined at the latitude angle). The seasonal variations then require a 23 1/2 degree inclination range perpendicular to this axis.

Because the ASPS needs a long absorption path in the working fluid, a cylindrical receiver reaching from the ground to the Cassegrainian focus is our efficient collection vessel. The pressure tube provides a very rigid axis of rotation inclined at the latitude angle without additional expense. The system is designed to operate in up to hurricane force (65 mph) winds and to survive in a stowed position (horizontal) for winds of 150 mph. The mirrors are fabricated to meet military requirements for wind survival since the technology used was developed for military use. The horizontal stow position is chosen to give negative lift: the Bernoulli forces are down. Thus hurricane winds would tend to force the stowed mirror into the ground. Since the mount is strong in compression, only superficial damage to the unit would be anticipated.

Hydraulic actuators are used for tracking and focusing functions because they are effective, reliable and economical. Minimal power is required for routine tracking and focusing. On the 4 kWt demonstration prototype, a small (0.1 HP) electric pump intermittently replenishes an accumulator tank which stores energy. Hence, large instantaneous power demands can be met for emergency scram functions, rapid solar acquisition after losing track, and slewing to the stow position in case of high winds. Additionally, the fluid characteristics of a hydraulic system can absorb mechanical shocks generated by wind gusts, also provide desired damping in the tracking and focusing functions and prevent "hunting".

The pressure tube receiver is inclined at the latitude angle with the north end raised in the northern hemisphere. Since the mirror must clear the ground at sunrise and sunset, there is substantial ground clearance which would permit other land uses such as farming beneath the collectors. The support structures can be made adaptable to the installation location and terrain. Flat land is not required and installation on top of buidlings appears to be economic. The supporting piers must be adequate to counter the wind shear forces generated by the drag coefficient of the mirrors in hurricane force winds; otherwise, pier materials can be selected on a cost basis.

## Applications

Commercial units of the ASPS are sized for transportability and effectiveness for particular applications. The smallest practical unit produces 40 kWt with a round mirror and 50 kWt with a square mirror (see Figure 5). The mirrors are transportable in two sections over the interstate highway system

without a special permit. With a production volume of at least one unit per day, 300 units per year, direct costs with an available steam engine are estimated to be about $20,000.

A cogeneration version of the ASPS would provide 20% of the available power (10 kilowatt electric; kWe) for electrical generation or pumping and 70% of the power for thermal loads at an estimated cost of about $2,300 per kWe of capacity with 120,000 BTU per hour of commercial grade steam as a byproduct. Such a system would be competitive with diesel electric systems and oil field boilers operating in remote areas. Installation costs are minimal in large part because only two piers are required on a north-south axis.

Economics of scale can be achieved through other ASPS unit designs that would produce 500 kWt with a direct insolation of 1 kW per square meter. In this case, the prime mirrors are helicopter transportable at a reasonable cost. This system was originally designed for solar thermal oil recovery (STEOR) applications. Each unit would produce 1.7 Million BTU per hour of steam at any desired temperature and pressure; however, it is desirable to operate the ASPS at or above the critical point (705 $^{o}$ F, 3204 psi). Thus a cogeneration system producing 150 kWe along with 1.2 Million BTU per hour of 500 $^{o}$ F. steam is feasible and very attractive. System costs at production rates of one per day are estimated to be on the order of $100,000 per system. This gives a cost of approximately $667 per kWe of capacity for electrical generation. The same system with a variety of operating parameters is economic for industrial process heat and cogeneration applications.

The largest sized units economically producible with our patented technology appear to be 130 feet in diameter with an output of 1 MWt. With the mirrors produced on site in quantities of 500 or more, the steam producing system is estimated to cost $150,000 per unit. The installed cost of a large electrical generation plant would be in the range of $600 to $1,000 per kWe of capacity.

These large 1 MWt units are also useful for large-scale chemical production, particularly in conjunction with geothermal wells. Because any transparent or translucent working medium can be used, possibilities exist for very efficient systems using helium, air, toluene and sewage sludge as a working medium. As a final point, all sizes of ASPS units have inherent buffer storage of about 1 hour of energy collection. Constant temperature and pressure steam storage is also available at a 50% system cost increase for 24 hours of energy collection storage.

Figure 1

# ASPCO DEMONSTRATION UNIT SCHEMATIC

THIS UNIT IS TRAILER MOUNTED AND FREEWAY TRANSPORTABLE WITHOUT PERMITS FOR EASE OF FIELD TESTING. THE MIRRORS COLLECT 1/10TH THE ENERGY OF THE FIRST COMMERCIAL INDUSTRIAL SOLAR STEAM UNIT.

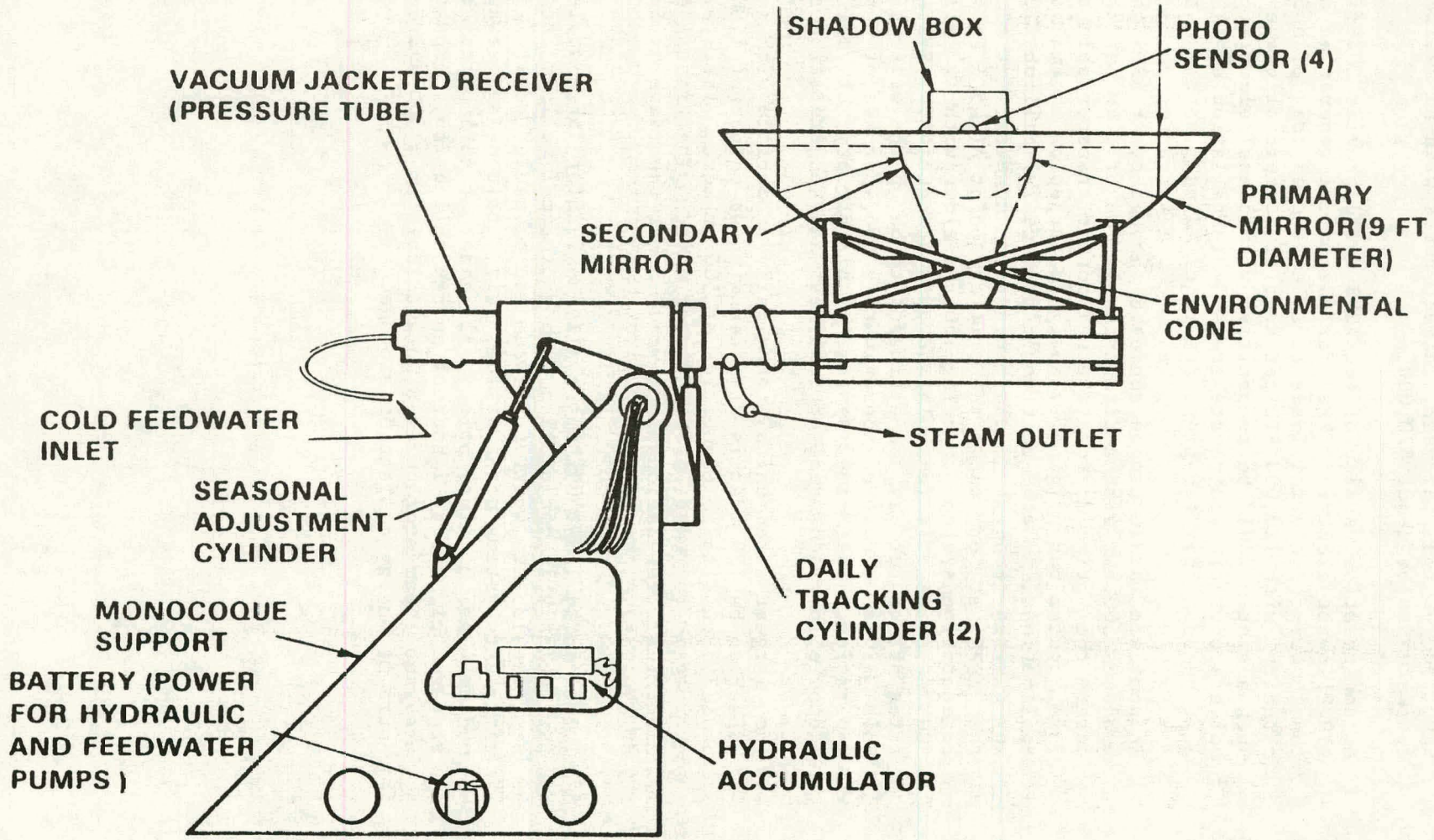

Figure 2

# BASIC CONCEPTS OF THE ASPCO TWO AXIS TRACKING AND FOCUSING INDUSTRIAL SOLAR STEAM SYSTEM

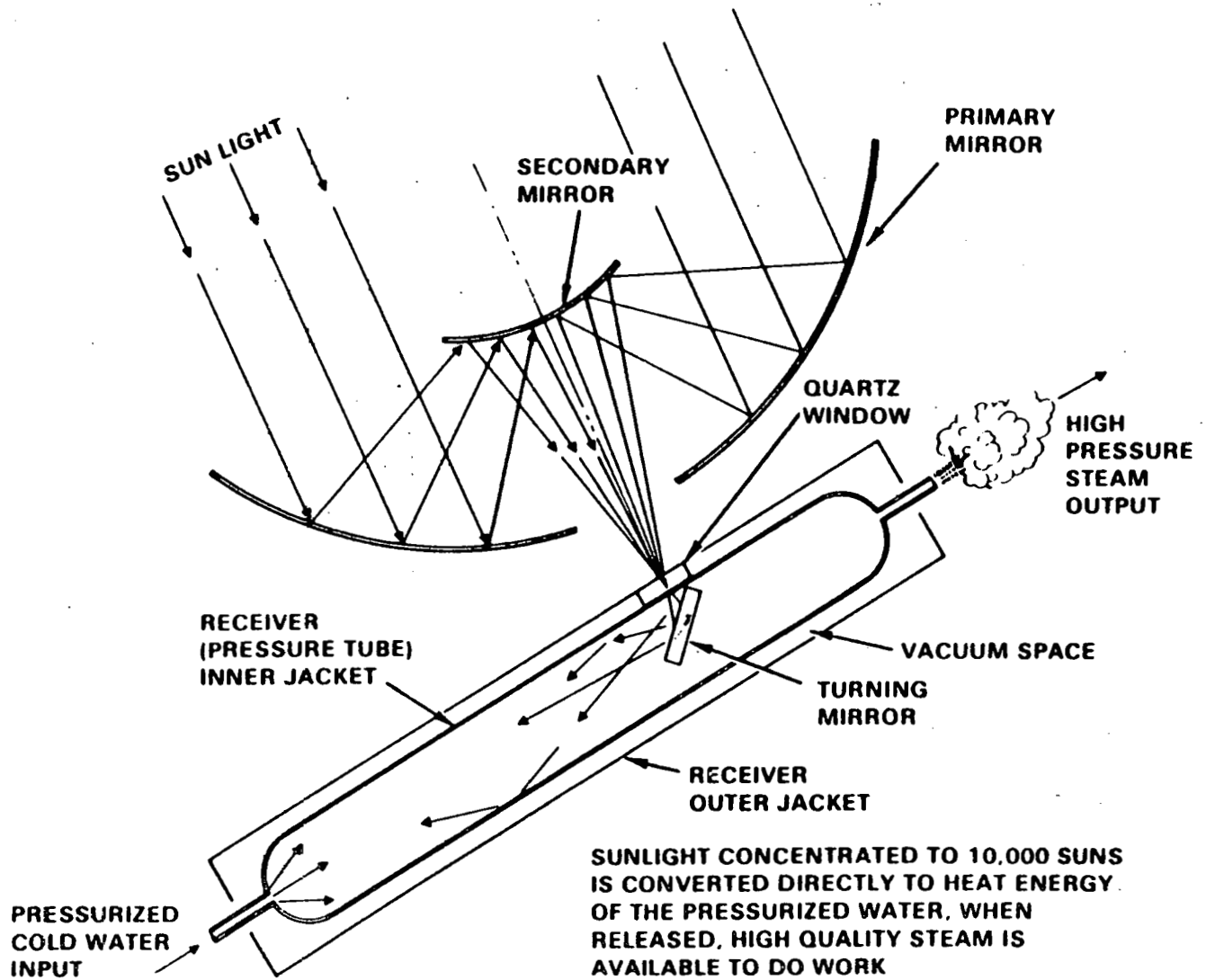

FIGURE 3

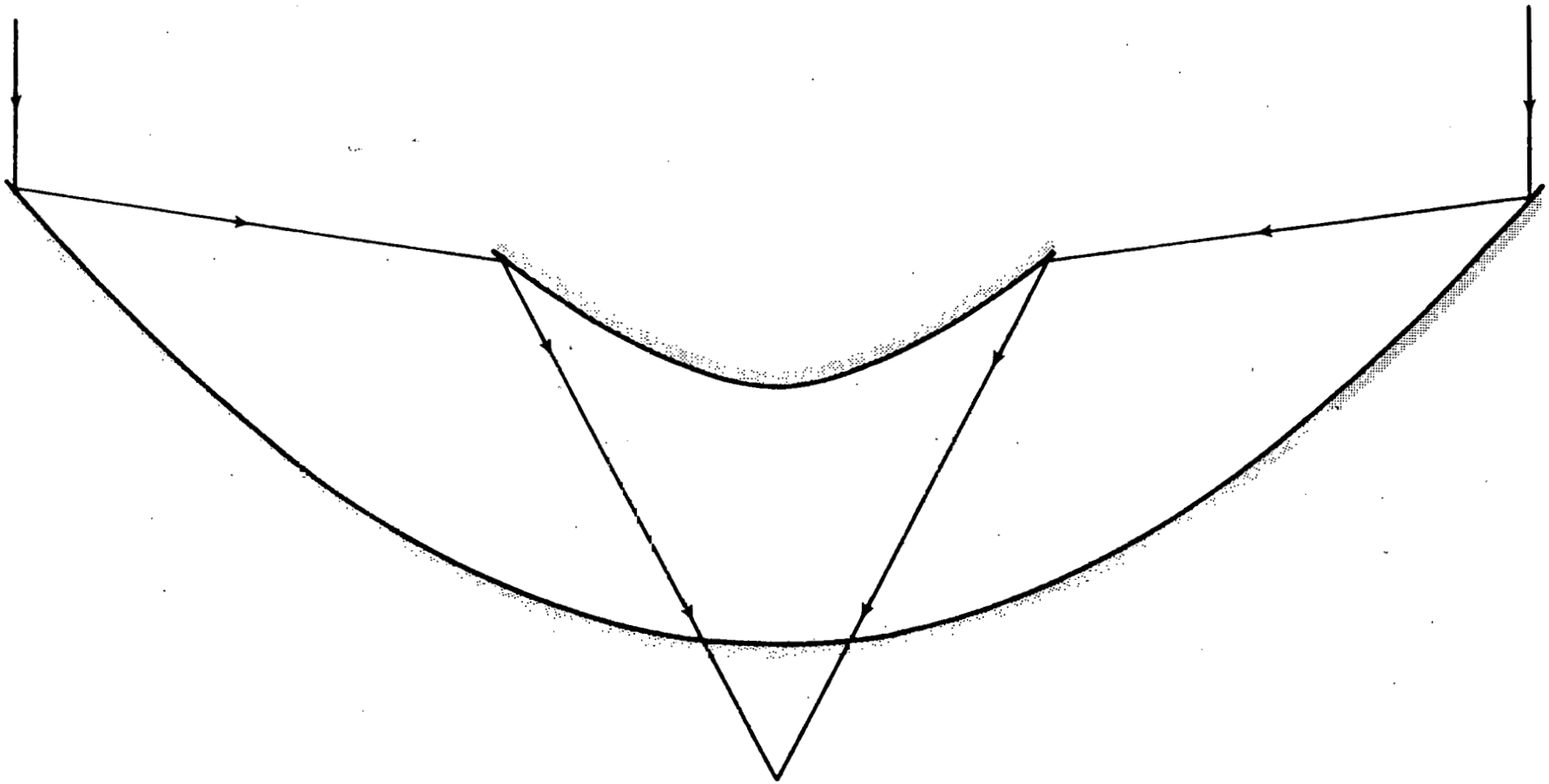

4 kW DEMONSTRATION MIRROR

FIGURE 4

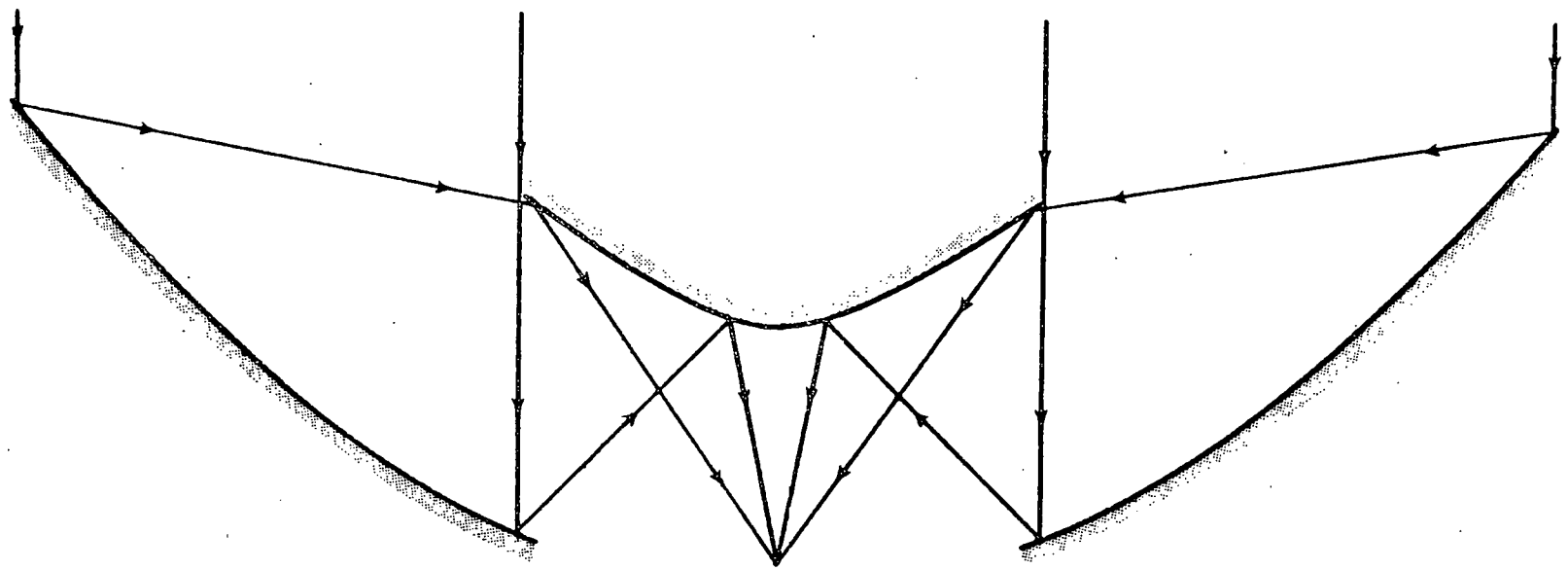

40 kW SYSTEM MIRROR

Figure 5

# ASPS COMMERCIAL PROTOTYPE DESIGN SCHEMATIC

THIS IS A LOW-COST TWO-PIER GROUND SUPPORT MOUNTED UNIT PERMITTING SEASONAL AND DAILY TRACKING BY USING HYDRAULIC MOTORS. THE PRIMARY IS 28 FEET IN DIAMETER COLLECTING 40 kwt (136,000 BTU/HR) OF ENERGY TO PRODUCE HIGH QUALITY STEAM FOR INDUSTRIAL PROCESS HEAT AND ELECTRIC POWER PRODUCTION.

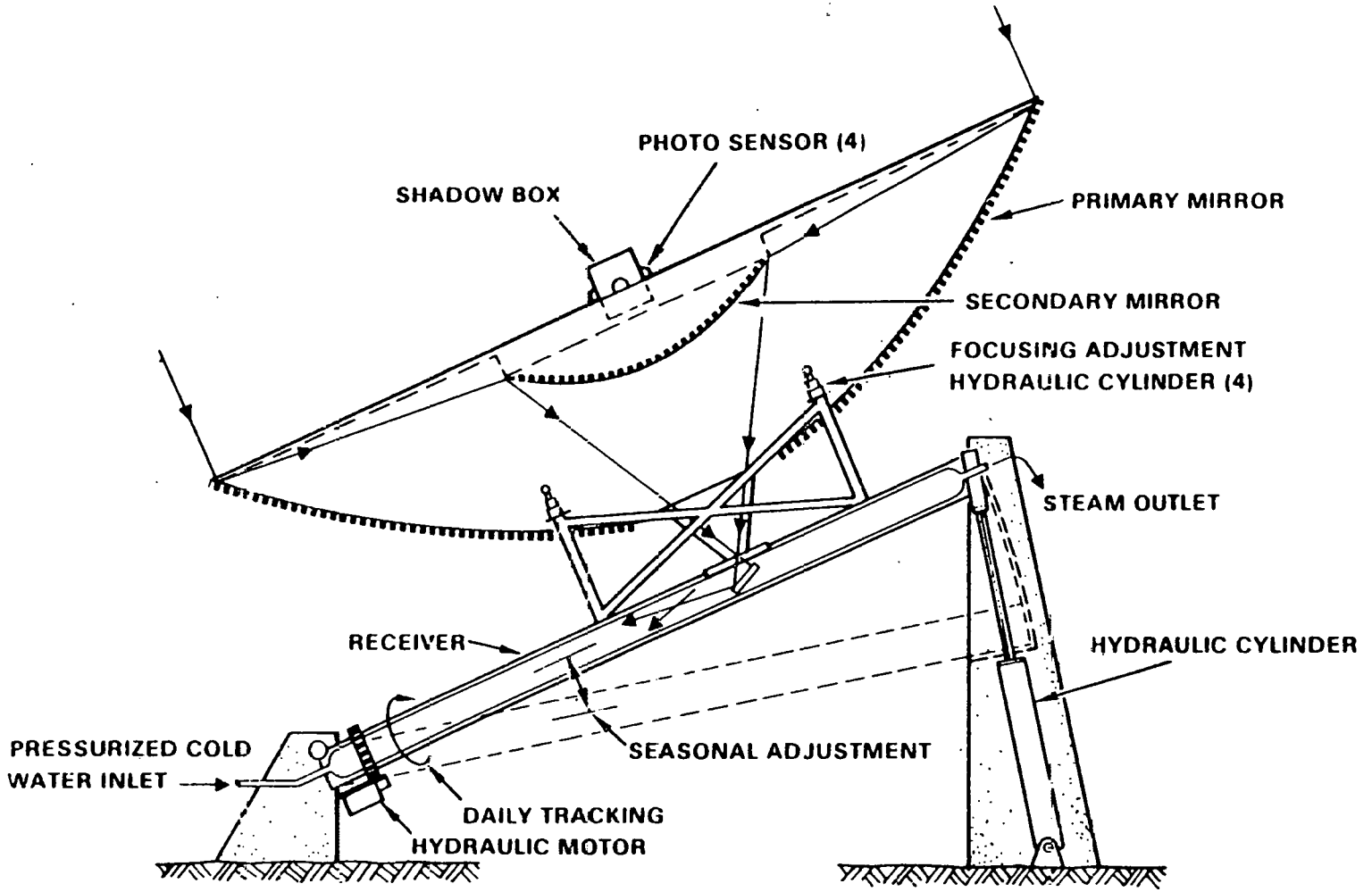

# On Solar Thermal Electric Power Capacity Sizing

Jeffrey S. Clark
Deltatemp Energy Corporation
Fort Wayne, Indiana

Parabolic dish technology has for the most part to date been borrowed from existing and expensive microwave dish technology rather than designed to accomodate electrical generating schemes with a good probability of success in practical applications. Studies by this author of the possible uses of various engine/generator designs and sizes with dishes, show that the most immediate possibilities for implementation are in a 3Kw (10m2) size capable of versatility of application and marketing, which assists also in compensating for inadequate developmental funding availability.

Innovation in dish design has produced a $10m^2$ dish at a cost level compatible with DOE goals under STPP for 1990 in conjunction with a 3Kw generator design. The production cost problems of a 3Kw size module may soon be solved. It remains for a suitable generator to be developed and tested at what are reasoned to be comparable cost levels in order to achieve the over-all DOE objectives.

(1) The $10m^2$ range has a simplicity and ease of maintenance which is a function of its size.
(2) Existing labor forces and plant capacity now unused are readily available and adaptable to the production of small modules.
(3) Off-site construction will contribute to lower capacity costs.
(4) Average residential energy requirements in the U.S. @ 600+w/Hr make a 3Kw a slight producer in the consumer/retail market.
(5) Versatile markets are available: utility, commercial, and retail consumer - which will speed implementation.
(6) Component hardware is readily available and compatible.
(7) The smaller size is a more productive use of a given land area.

In summary, over-all economic conditions now extant indicate that a 3Kw $10m^2$ dish/generator module stands up against the larger sizings as lending itself to the most rapid development and the greatest marketing versatility. It therfore stands the best chance of success over the next five to ten years for commercialization.

# RECENT DEVELOPMENTS -- PKI SQUARE DISH FOR THE SOLERAS PROJECT

WILLIAM E. ROGERS

POWER KINETICS, INC.
TROY, NY 12180

In 1983, Power Kinetics, Inc. fabricated, tested and shipped 18 PKI "Square Dish" solar collectors for the SOLERAS Project in Saudi, Arabia. The installation uses 730°F syltherm 800 to power a desalination facility.

In the course of completing the project, the PKI Square Dish was subjected to rigorous design attention regarding corrosion at the site, and certification of the collector structure to meet A.I.S.C. codes. The microprocessor controls and tracking mechanisms were improved in the areas of fail-safe operations, durability, and low parasitic power requirements (less than 1 kw hr per day). Prototype testing required by the project contract demonstrated performance efficiency of approximately 72% at 730°F outlet temperature.

This project provided an opportunity for PKI to make significant studies including developing formal engineering design studies including developing formal engineering design drawing and facrication details, establishing subcontracts for fabrication of major components, and developing a rigorous quality control system. The improved design has proven to be more cost effective to produce and the extensive manuals developed for assembly and operations/maintenance result in faster field assembly and ease of operation.

The PKI factory, established in early 1983 at Green Island, New York, is now capable of producing 100 to 250 collectors per year with expansion capacity to over 500 per year. At 500 units per year, cost per unit is expected to be $35,000.

# CONTINUING RESEARCH AT SOLAR STEAM, INC.

DOUG WOOD

SOLAR STEAM, INC.
TACOMA, WA 98402

Solar dish technology could become cost competitive with conventional energy sources. This potential for a multi-billion dollar industry has attracted an international group of innovative dish developers resulting in a number of different dish designs for various specified applications and temperature goals.

Solar Steam, Inc. is wholly committed to the research and development of a mid-temperature dish system which can compete effectively with conventional energy technologies.

The Solar Steam 30 foot diameter glass dish was prototyped in 1979 and concluded our dish geometry development.

The dish was tested by SERI to have a gross concentration ratio of about 123 to 1 (adequate for a 750 Farenheit thermal steam system). However, the prototype could not be mass produced as is and be cost effective without tax subsidies.

Since 1979, the Solar Steam R&D effort has focused on design analysis and on the research being conducted by the national laboratories. Federally funded research and development programs supplied information and test results on various systems and helped our private research efforts. The work done at JPL in materials, concentrators, applications, and systems has been invaluable in shaping our first dish. Much of what was learned at JPL will be used in our second prototype.

A second glass prototype is currently being detailed which is 40 feet in diameter and uses a single post wind abatement support carriage. The entire system (less counterweights) may weigh less that 6 pounds per square foot. This dish will be prototyped and tested as soon as possible. If the dish can be commercialized cost competitive with conventional energy sources then the dish design will be marketed. Much research remains to be done.

Our best wishes to others developing dish concentrators and dish applications. And a special thanks to JPL for inviting our participation.

# SPIKE-2 - A Practical Stirling Engine For Kilowatt Level Solar Power

William T. Beale
Sunpower, Inc.
Athens, Ohio USA

## ABSTRACT

Recent advances in the art of free piston Stirling engine design make possible the production of 1-10kW free piston Stirling-linear alternator engines, hermetically sealed, efficient, durable and simple in construction and operation. These machines can operate either as independent units or ganged together for higher power. They may also operate directly connected to the grid without need of any intermediary.

Power output is in the form of single or three phase 60 Hz. AC, or DC. The three phase capability is available from single machines without need of external conditioning. Engine voltage control regains set voltage within 5 cycles in response to any load change.

The existing SPIKE-2 design has the following characteristics and measured performance.

Weight - 38kg
Length - 50cm
Diameter - 25cm
Power - 1.5kW
Working Gas - helium at 7 bar pressure
Engine-Alternator Efficiency - 25% at 650°C heater wall temperature
Life - over three years in solar service
Cost in Production - less than $1,000

The same system can be scaled over a range of at least 100 watts to 25kW.

For longer life, non contact bearings may be used without adding to system complexity or failure modes.

## INTRODUCTION

The very rapid advance in the art of free piston Stirling design has recently made possible the construction of these machines at low cost with attractive performance characteristics, making them suitable as electric power generators in many applications, especially with concentrating solar collectors. The distinguishing features of this new generation of Stirling machines are low pressure, usually between 5 and 30 bar, relatively short stroke and large piston diameter, and relatively high frequency, 50 to 60 Hz.

The design described here was intended from the beginning as a simple, low cost and producible free piston Stirling of minimum complexity, but

with reasonably good over all thermal efficiency at moderate temperatures. The target was 25% at a heater head temperature of 650C. These design goals were met, and the engine is entering the preproduction prototype stage with a delivered electrical power output of 1.5kW maximum. Its life is expected to be at least three years in solar service, and probably much longer.

## ADVANTAGES OF LOW PRESSURE OVER HIGH PRESSURE FPSE

The use of low charge pressure, about one order of magnitude lower than typically used in the past, permits very large clearances between sliding surfaces and consequent ease of fabrication of components. Whereas a 70 bar 30 hz. engine requires clearances on the order of 10 microns to avoid excessive losses from gas leakage, the 7 bar engine can acceptably use over 50 micron gaps without serious penalty. This makes it much less susceptable to damage from foreign particles inside the pressure enclosure. In addition these loose fits make repair and rework of bearing surfaces much easier.

With low internal pressure, it is possible to more readily use plastic and ceramic components. While these are not used in the existing prototypes, they may be worked into the production versions with consequent advantages of lower weight and cost, and higher efficiency.

In addition to the structural advantages, low pressure large diameter designs enjoy an additional benefit from the fact that the working space spring effect is strong enough to resonate the piston and alternator at the desired frequency, thus obviating the need for an additional spring. This considerably reduces the system complexity and cost.

## DESCRIPTION OF ENGINE

Figure 1 shows the external appearance of the engine-alternator, and Figure 2 the internal arrangement. There are only two primary moving parts, the displacer and the coaxial piston with its attached alternator magnets. The heater head is internally and externally finned, and the heat sink is a liquid circulated around the cooler section which contains a large number of gas flow passages. A central rod provides a multiple service of alignment of the moving parts and bearing surface, as well as the gas spring piston for the displacer. Teflon based solid lubricants are used on all moving parts.

A more detailed description of the engine is given in Reference 1.

## ALTERNATOR CHARACTERISTICS

The alternator is a very simple device using a light moving magnet (Samarium Cobalt) directly attached to the piston. Its structure allows the use of conventional flat transformer laminations and makes its fabrication no more complex than that of ordinary rotating machines. Alternator power/mass ratio is approximately 7kg/kw.

At the cost of nominal increase in complexity, the alternator may be designed to produce three phase power. The method by which this is achieved is proprietary and cannot be revealed at this time, but it results in power

output indistinguishable from that of conventional three phase rotating machinery.

The alternator responds to load change rapidly with the aid of a simple control system. It will recover set voltage in 3 to 4 cycles after and 80% load variation. Newer control schemes give promise of recovery in two cycles from a 100% load change. The control system does not add significantly to the engine-alternator complexity or number of failure modes. In the reduced load condition, system efficiency is reduced only a moderate amount.

## OPERATING CHARACTERISTICS

The engine is started by a small electric impulse to the alternator after the heater head has reached about 450C. At this temperature its power is only about 300 watts, which rapidly rises to the set power and voltage as the heater head temperature rises to about 550C. As temperature rises above this, power rises rapidly, but voltage is held constant by the controller, or if the engine is on the electric grid, the uncontrolled current increases while voltage remains at the grid value.

Changes in solar input simply change engine power with only relatively small changes of heater head temperature. Engine efficiency remains relatively constant as delivered power varies between maximum and .5kW. This operation does not require any change in engine pressure and hence needs a minimal control, or none except a disconnect in the case of a grid connection (Figure 3).

When the solar input is below the minimum, engine voltage drops below the set (or grid) value, and the engine idles, producing no power until the heat input is once again adequate. The engine will run down to a very low heater head value, about 80 degrees above coolant temperature, before it actually stops oscillating. This is because of the extremely low mechanical friction in the free piston machine.

Operation is very quiet, and cylinder oscillation is very low in amplitude, about 1mm excursion. This low amplitude vibration can easily be isolated by mounting springs.

The cooling system may be mounted on the engine, or on the ground as preferred. Engine efficiency is of course affected by coolant temperature, which should be as low as reasonably achievable, unless it is desired to use the hot coolant for some other purpose.

## SPIKE-2 FOR SOLAR USE

A SPIKE-2 solar system can be expected to have an overall conversion efficiency of about 17% when used with a good quality concentrator and absorber and a well designed heat rejection system. This is high enough to warrant consideration for use in some applications, and is also attractive for experimental or evaluation purposes. For this system a dish between 3.5 and 4 meters would be required to produce a net 1.5kW to a load.

Expected cost of the engine-alternator in reasonably large scale production is about $800, but the presently available prototype costs much more.

A more advanced version, producing three kW, three phase is expected to be available for experiment and evaluation in late 1984.

REFERENCE

David Berchowitz - The Development of a 1kW Electric Output Free Piston Stirling Engine Alternator Unit. Presented at the 18th IECEC, Orlando, Florida, August 1983.

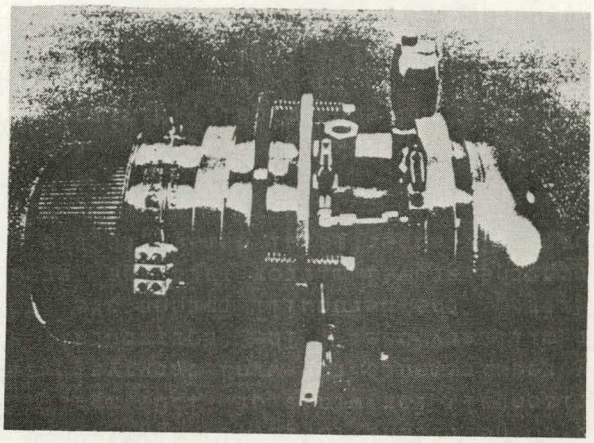

Engine-Alternator
Figure 1

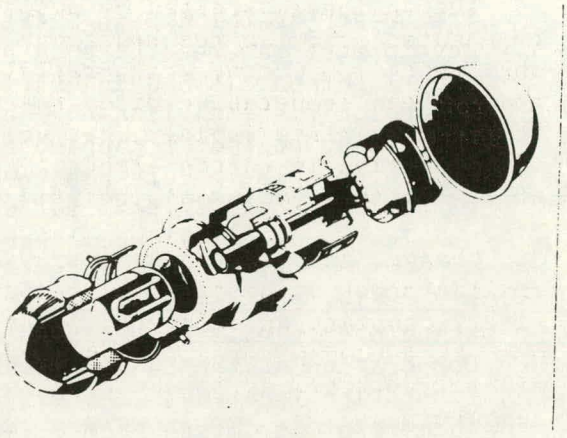

Exploded View
Figure 2

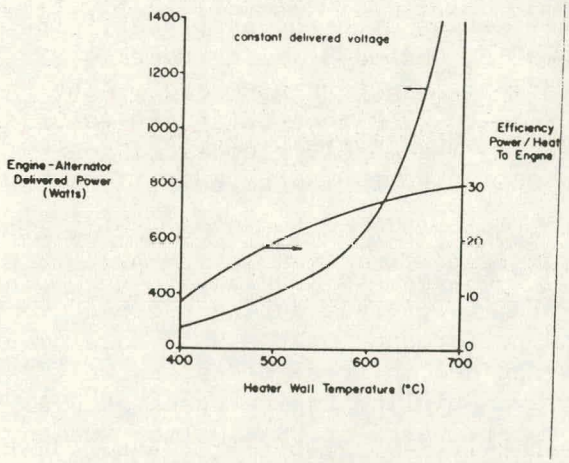


Efficiency and Power Vs
Temperature
Figure 3

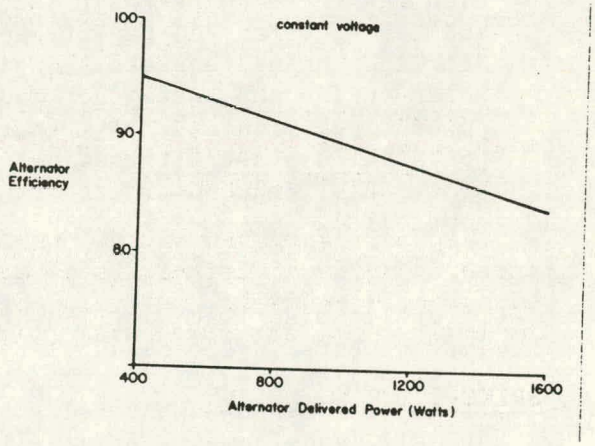


Alternator Efficiency Vs
Power
Figure 4

# STIRLING MODULE DEVELOPMENT OVERVIEW

Floyd R. Livingston
Jet Propulsion Laboratory
Pasadena, California

## I. Summary

The Solar Parabolic Dish-Stirling Engine Electricity generating module development has been pursued by the Department of Energy with Government laboratories and industrial participants since FY 1978. The solar parabolic dish-Stirling engine electricity generating module consists of a solar collector coupled to a Stirling-engine powered electrical generator. The module has been designed to convert solar power to electrical power in parallel with numerous identical units coupled to an electrical utility power grid.

Presently, the solar parabolic dish-Stirling engine electricity generating module exists as a commercial prototype erected by the Advanco Corporation at the Southern California Edison Company's Santa Rosa Substation located in the city of Rancho Mirage, California. If the commercial prototype, named Vanguard, tests prove the equipment to be effective and reliable, then the participants have planned to construct an electricity generating plant.

In order to prepare for the Vanguard module erection, Advanco Corporation has worked with their subcontractors to design, fabricate, assemble and test the many components and subsystems over the past year. The Stirling engine/generator consists of an United Stirling Model 4-95 solar engine and a Reliance Model XE286T induction generator. The power conversion assembly generates up to 25 kilowatts at 480 volts potential/3 phase/alternating current. The module electrical power system has been constructed by the Onan Corporation to be fully self-controlled.

The United Stirling/JPL have tested two test bed modules at the Parabolic Dish Test Site, Edwards AFB, California during the past year. Improvements in the reliability and performance of the USAB Model 4-95 solar engine results from knowledge gained in these tests, as well as from the DOE/NASA sponsored Automotive Stirling Engine tests at USAB and MTI, and from the private laboratory tests at USAB Malmo, Sweden. The joint USAB/JPL solar tests of the two Model 4-95 engines provide the only actual environment for function, performance and endurance measurements needed to improve the hardware and software, and to project the commercial value.

The testing has been very successful during the FY 1983 period. Piston rings and seals with gas leakage have not occurred, however, operator failures resulted in two burnt out receivers, while material fatigue resulted in a broken piston rod between the piston rod seal and cap seal.

## II. Commercial Prototype - Vanguard

The prototype 20-kWe Solar Parabolic Dish-Stirling Engine System Module (Vanguard) in Rancho Mirage, California, is the world's most effective solar-electric generating station. Design, fabrication, assembly and testing of the prototype Vanguard module represents a cooperative effort between government and private industry to commercialize the advanced technology developed over the past several years by the Solar Thermal Power Technology Division, United States Department of Energy. The solar-electric generating station is located in the northern Imperial Valley on the Southern California Edison Company's (SCE) Santa Rosa Substation. The Vanguard module can generate up to 25 kWe net electrical power at 480 V/3 /60Hz, however, the module is rated at a net electrical power of 20 kWe with direct insolation of 850 watts per square meter. All of the above module net power will be divided between supplying the station parasitic power requirement and power to the utility grid. As an estimate of the module effectiveness when operated continuously for one year in the Mojave desert, the module is estimated by the author to generate 60,000 kWhe while converting an average of 27 percent of all direct insolation on the mirror surfaces to net electrical energy. The Prototype Solar Parabolic Dish-Stirling Engine System Module is a joint project of the Department of Energy, and the Advanco Corporation. Principal organization working with Advanco in addition to SCE are United Stirling, Inc., KB. United Stirling (Sweden) AB and Company, Onan Corporation, Rockwell International - Energy Systems Group, Electrospace Systems Inc., Modern Alloys Inc., Winsmith, and the Georgia Tech Research Institute. The Jet Propulsion Laboratory assists the Department of Energy in its Cooperative Agreement participation by providing technical consultants since prior development at JPL resulted in a test bed Solar Parabolic Dish Stirling Engine System Module.

### A. Collector System

A collector system consists of 32 solar parabolic dish concentrators. Each collector is a solar parabolic dish concentrator with a reflective net area of 83 square meters (893 square feet) consisting of 328 back-silvered fusion glass mirrors cold sagged and bonded to a spherically ground foam-glass substrate. These 5-cm (2-in.) thick, (46-cm) (18 in.) by 61-cm (24 in.) mirror facets have been individually mounted on 16 steel rack assemblies. Of ten mirror facets tested, all survived accelerated environmental tests at JPL and SNLA with no trace of failure. The 16 mirror rack assemblies are mounted on a geared drive unit for azimuth and elevation control. With the skewed elevation axis passing through the center of gimbaled mass, the elevation drive has demonstrated very small torque requirements.

The collector control system consists of individual microprocessor concentrator controllers and a central controller for groups of up to 32 concentrators. Each concentrator can be controlled individually or in groups in either the manual or automatic modes through the central controller in the plant control room. Also,

# VANGUARD DISH - STIRLING MODULE

**OVERALL MODULE FEATURES**

DIAMETER: 11 m (36 ft - 1 in.)
HEIGHT: 12 m (39 ft - 4 in.)
WEIGHT: 7980 kg (17,560 lb)
SYSTEM EFFICIENCY: 25.4%
ELECTRICAL POWER: 20.8 kWe

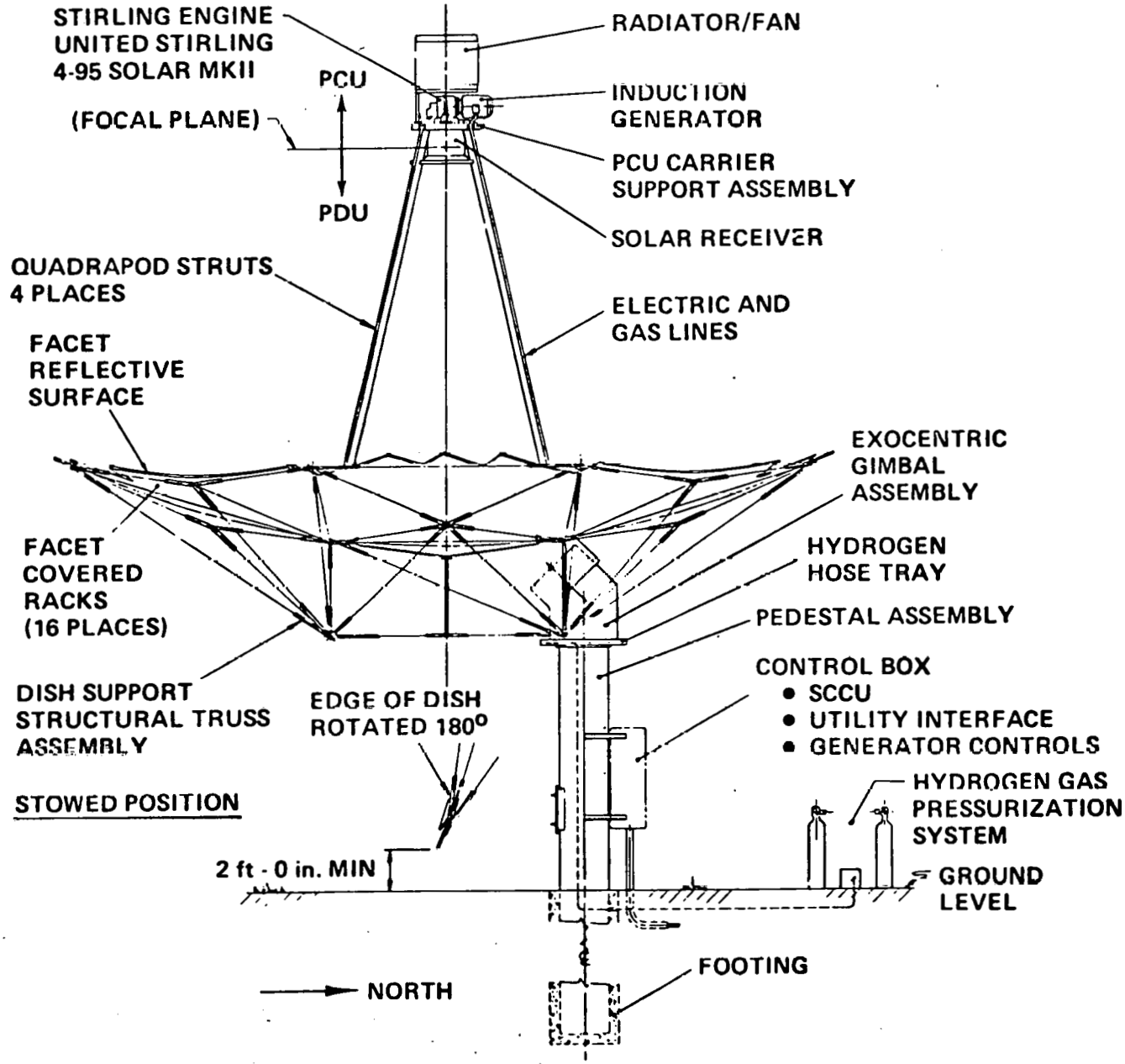

each concentrator can be controlled at the individual concentrator controller. The concentrators have been designed to operate in steady winds of 13 m/sec (30 mi/h) with 2 sec gusts up to 22 m/sec (50 mi/h). In the stowed position, the concentrator has been designed to survive 40 m/s (90 mi/h) short duration gusts. Soon after the prototype concentrator was erected, it withstood up to reportedly 17 m/s (40 mi/h) gusts with no noticeable ill effect.

Of those JPL technical consultants engaged in the Cooperative Agreement activity, all agree the reflective facets, the rack assemblies, the geared drive units, the remaining structure and foundation, the individual concentrator microprocessor control, and the group microprocessor controller have been expertly designed, fabricated, tested, installed and operated by the Advanco Corporation with their several subcontractors.

B. Engine/Generator System

Each individual United Stirling Model 4-95 Solar MK II engine with Reliance Model XE286 induction generator is rated at 25 kWe with a normalized direct insolation value of 1000 $W/M^2$. A group of 32 units would be rated at 800 kWe, electrical power less the power required for parasitic loads. Overall direct insolation to electricity conversion efficiency is estimated to be 27% for the solar year. From test results obtained by the Jet Propulsion Laboratory with the United Stirling Model 4-95 Solar MK I engine with the ASEA induction alternator these performance estimates have been essentially verified. The engine operates at a solar receiver temperature of 700°C (1290°F) with a coolant temperature of 50°C (122°F) with several grams of hydrogen as the working medium. The present commercial engine represents an improvement in 30% reduced production cost and increased reliability by a factor of at least 2 while maintaining the performance level of the prior test bed engine. Reduced production cost and increased reliability has yet to be verified by the U.S. Department of Energy. The electrical power system control uses a simple reliable design with all commercial components. Standard design practices have been used to satisfy electrical codes and utility requirements.

C. Group Control System

The group control system is one master microprocessor that controls the plant from a plant control room. The plant/group control is ultimately fully automatic with an operator override option. For individual system control to augment the group control, each individual system has its own distributed process controller. Two of these process controllers are digital, the concentrator controller and the engine controller, while one is hard-wired, the electrical power system controller. The process controllers are located near or within the respective system's hardware in the distributed systems. There is strong reason for

JPL to believe group control system and/or the process controllers will function properly because the simple and proven components and software have been integrated into prior and proven systems.

## III. Solar Engine Development

United Stirling funded the construction of an engine/generator with 5 experimental solar only receivers for evaluation at the Parabolic Dish Site in Edwards AFB, California. The test program was jointly funded by United Stirling and the DOE. The objectives of the test program are to gain practical fabrication and operating experience, and to establish the capability of building commercial solar receivers. Early results of tests performed between January and March 1982 may be found in Reference 1. Later results of tests performed during the period of May 1982 through July 1983 are published in Reference 2. Another current paper describing the solar engine development by United Stirling has been published in Reference 3. Also, previous proceedings of the Parabolic Dish Solar Thermal Power Program Review includes early progress reports of the present activity.

### A. Experimental Solar Only Receivers

United Stirling has tested 5 different experimental solar only receivers (BSORs) on the two engine/generator units at Edwards Air Force Base. The principal difference between these receivers was in the tube-manifold construction of the heater. The different heaters were --

- ESOR I, the standard combustion system heater.
- ESOR IIA, a new designed solar only receiver, including a manifold.
- ESOR IIB, a new designed solar only receiver with only single tubes.
- ESOR III, a new designed solar only receiver with only single tubes but with increased diameter and specially designed tubes of "hair pin" type.
- ESOR IV, a new optimized receiver for solar application with production cost considered.

All of these receivers except the last have operated for many hours on the test bed concentrators at the Parabolic Dish Test Site, EAFB, California with no failures other than burnout of three receivers due to operator mistakes. Burnout of tubes was readily repaired by brazing in replacement tubes - usually one per quadrant.

### B.

Model 4-95 engine and generator United Stirling provided one engine/generator especially configured for these tests. Through JPL, the Department of Energy provided another Model 4-95

engine/generator previously purchased from United Stirling.

The engine/generator furnished by United Stirling operated flawlessly through about 300 hours of solar testing. The government furnished engine/generator twice experienced the breakage of a piston rod in the same cylinder due to material fatigue. Mal-alignment of cylinder-seal-piston components may have subjected the rod to unusual stresses.

C. Engine Control System

United Stirling provided two digital electronic control units for the two test engines. The control system provided automatic totally remote, unattended operation of the engine/generator systems. Software provided with the digital electronic control units was modified and further developed as the tests progressed. There were no problems encountered with the engine control systems.

D. Radiator System

Early tests were conducted without an engine cooling system mounted on the engine.

Later the government provided engine was equipped with a complete radiator system furnished by United Stirling. The radiator has four heat exchange matrices built up in a square form with a radial fan in the center. A water pump circulates water from the engine through heat exchanger matrices. At full engine power a fan power of 790 W and water pump power of 200 W provides adequate cooling. A comparable ground mounted cooling system required a power of 4000-5000 W to operate a cooling fan and water pump.

References

1. Nelving, H-G, "Performance Test of 4-95 Solar Stirling Engine with Two Different Solar Only Receivers", United Stirling AB, Malmo, Sweden, September 7, 1982.

2. Nelving, H-G, "Testing of 4-95 Solar Stirling Engine in Concentrator at Edwards Air Force Base During Period May 1982 - July 1983", United Stirling AB, Malmo, Sweden, September 7, 1983.

3. Holgersson, Sten, and Worth H. Percival, "The 4-95 Solar Stirling-Engine - A Progress Report", Proceedings of the Twentieth Automotive Technology Development Contractor's Coordination Meeting, Society of Automotive Engineers, Inc., April 1983.

# PARABOLIC DISH STIRLING MODULE

Byron Washom

Advanco Corporation
El Segundo, CA

Advanco Corporation and its subcontractors have completed the design, manufacture, and assembly of the first commercially designed parabolic dish Stirling 25 kWe module. The module will begin testing in December 1983 and commence power the following month. The project has been funded by two Cooperative Agreements between Advanco Corporation and the U.S. Department of Energy and Southern California Edison Co. Discussed during this session were the cost, expected performance, design uniquenesses, and future commercial potential of this module, which is regarded as the most technically advanced in the parabolic dish industry.

# United Stirling's Solar Engine Development — the background for the Vanguard Engine

Author: Sten Holgersson
United Stirling AB Sweden

## Abstract

The Vanguard project engine, named 4-95 Mk II Solar Stirling Engine, represents the result from four years of solar engine development at United Stirling. In these development activities United Stirling has participated in programs on contracts from JPL and DOE, the latest being the Vanguard project. A major part of the development has also been internally funded.

The development started in 1979 based on the then existing 4-95 laboratory test engine which thru the 4 years has been converted to a solar version and significantly improved in several areas. The conclusion of the Vanguard project results in a new engine generation of a design that can be regarded as a preproduction prototype.

The major part of the solar engine development has been concentrated to the three different areas, the receiver, the lubrication system and the control system, but improvements have been made on most components. The new components were first tested on engines in United Stirling's laboratory in Malmö. Five such engines are on test within the solar project. Thereafter the function of the components has been validated in actual solar tests. These tests started at Georgia Institute of Technology in 1981 and have then from the beginning of 1982 been performed at JPL's test station at Edwards Air Force Base.

This paper describes the development and testing resulting in the Vanguard engine and some of the caracteristics of the Stirling engine based power conversion unit.

## Introduction

United Stirling is a company within the industrial corporation FFV. The company's task is to develop the Stirling engine for commercial applications.

The development work has been going on since 1969 resulting in engines in different sizes of our own designs. The present engine family is shown in figure 1. United Stirling is now concentrating the efforts on four different application projects. One is the Automotive Stirling project with the ASE engine, a second one is the Submarine project mainly concentrating on a 4-275 engine, a third is the Auxiliary Power Unit project with the V160 engine and the fourth is the Solar project with the 4-95 Solar engine, the subject for this presentation.

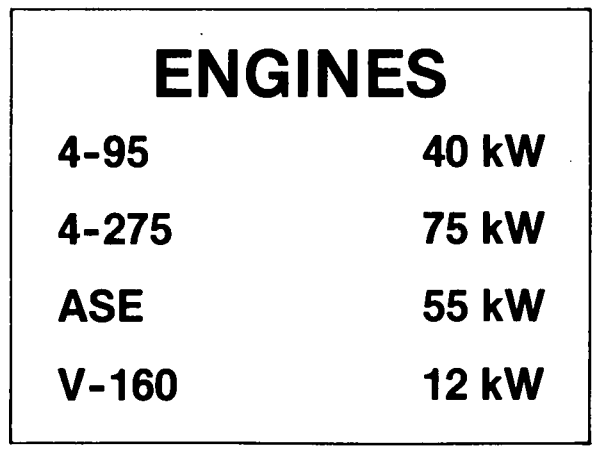


*Fig 1. United Stirlings engine family*

## Solar development programs

Although it of course has always been an awareness at United Stirling of the possibility to use the Stirling engine for solar energy conversion our activities in the field were very low until 1978. We then became participants in a NASA-funded study together with MTI. This study identified both the kinematic and the free-piston Stirling engine as viable candidates for the solar application. The next year, 1979, we accepted participation in a JPL-program. Our task was to redesign the drive unit to fit to and be able to operate in the EAFB test bed concentrator and to deliver one drive unit while JPL developed the receiver. Participation in this program rose our interest in receiver design and we decided in 1980 to develop a receiver design of our own. This was a natural step since in the Stirling engine the receiver is an integral part of the engine and our intention was to be capable to deliver a complete Stirling engine for an application in which the commercialization of the engine could be realized. From 1980 and on our own extensive solar engine development program has been going on. In addition to that, and as one of the significant components of our solar engine development we 1982 became members of the Vanguard program which now is being realized in hardware in Palm Springs through delivery of the concentrator from Advanco and the PCU from United Stirling. The Stirling engine in the Vanguard project is the first engine in the new generation internally at United Stirling called the 4-95 Mk II Solar SE. This engine is of course a product of the Vanguard project, but in reality the result of a much broader development program at United Stirling. This development program is the combination of the Vanguard project and internally funded solar engine development. A summary of the externally funded solar development programs in which we have participated is given in figure 2.

**USAB SOLAR ACTIVITIES**

- **NASA STUDY 1978 – 1979**

  **15 KW SOLAR STIRLING ENGINE**

- **JPL PROJECT 1979 – 1981**

  **INSTALLATION OF THE FIRST SOLAR STIRLING ENGINE WITH HYBRID RECEIVER IN A PARABOLIC DISH**

- **DOE PROJECT 1982 –**

  **TEAM MEMBER OF THE VANGUARD PROJECT**

*Fig 2. Solar programs*

## The engine choice for solar applications: 4-95

The development of the Solar Stirling engine has during the last 3-4 years been concentrated to the 4-95 engine, figure 3. The reasons for choosing this engine were several. The engine size fits to a concentrator within the size range, 10-18 m diameter, that seems to be most cost effective. The existing JPL test bed concentrator and the 4-95 engine are almost perfect in sizes for each other which means that an opportunity to performe realistic hardware tests existed. The 4-95 engine was one of United Stirling's engines, that had the highest amount of accumulated running hours with rather good results. Figure 4 shows a summary of the present experience with the 4-95 engine.

The 4-95 engine was originally designed as a laboratory test engine in 1975. It has since then been used as the baseline engine in the beginning of the Automotive Stirling Engine program and as the first underwater engine designed by United Stirling. The further developed 4-95 engine is now chosen as the solar Stirling engine.

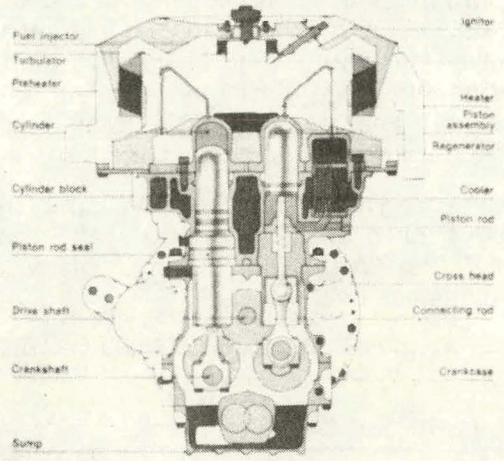


*Fig 3. 4-95 cross section*

| 4-95 ENGINE STATUS | Nov 1983 |
|---|---|
| ● Number of engines built | 27 |
| ● Running hours | |
| ● in total | 41000 |
| ● single engine | 11000 |

*Fig 4. 4-95 Status*

## Main areas of redesign

Although the 4-95 engine in many respects was suitable as a solar energy converter there was also a need to redesign and further develop the engine in a number of areas. The engine must be able to operate in all different orientations from horizontal to upside down when following the movement of the concentrator. In the Advanco concentrator with its gimble mechanism it also rotates around its vertical axis. This means that it was necessary to completely redesign the lubrication system. The original heater was strictly designed as a heat exchanger for convective heat transfer from combustion gases. It was therefore necessary to develop a new heater suitable as a radiative heat exchanger together with a cavity surrounding it and thus fit the engine with a solar receiver. The receiver of a Stirling engine, in contrast to other engines, is an integral engine component. The control systems of the 4-95 engine were designed for applications with other and more complex control functions and with stronger requirements on response times than needed for the solar application. This was the case for both the pressure (power) control system and the electronic control system. Therefore new control systems had to be developed. Also in order to design an autonomous power conversion unit to be placed up in the focal mount a new radiator system had to be developed.

The major development work has been concentrated to the mentioned four areas, but significant changes have also been introduced on a large number of the engine components. So many improvements have been made that the Vanguard engine represents a new engine generation.

**MAIN AREAS OF REDESIGN FOR SOLAR APPLICATION**

- Heat system (receiver)
- Lubrication system
- Control systems
- Radiator systems

*Fig 5. Areas of redesign*

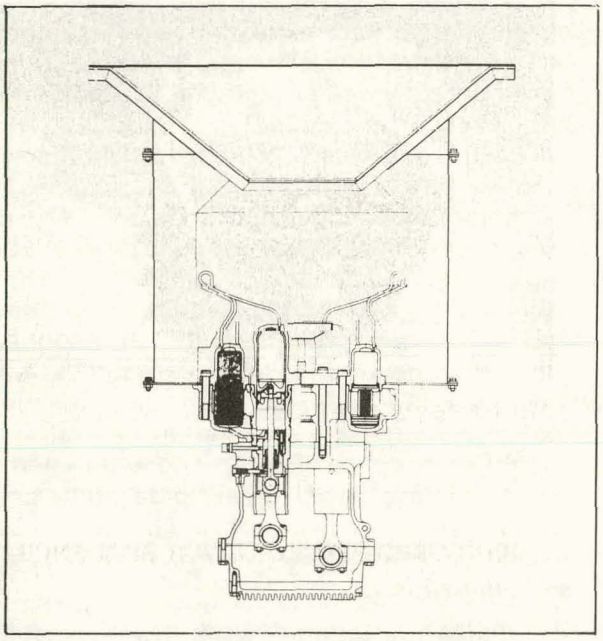

*Fig 6. Vanguard engine cross section*

## Testing at United Stirling

A very vital part of the solar engine development has been engine testing. Six of United Stirling's 4-95 engines have been designated for development tests for the solar application. Fig 8 shows the main content of our development program. In addition during the last year tests have also been performed on JPL's engine, the 4-95 No 21 engine, located at Edwards Air Force Base. Five of United Stirling's engines have been tested in our laboratory in Malmö, Sweden. Two of these engines were used for component development tests, i.e. functional tests, usually of relatively short duration, of redesigned components and subsystems. Three of the engines were used for simulated solar cycle endurance tests. This test cycle, shown in fig 7, was based on loads and transients calculated from insolation statistics from Barstow and Albuquerque.

The lubrication system, the control system and the radiator system were first developed and tested on the engines in our laboratory.

A special engine stand was designed in order to turn the engines in the same way as in the actual concentrator. One of the engines was mowed out on our yard in order to gain experience from the outside environment. During the last three years 13000 hours of solar engine tests have been accumulated in Malmö.

After testing in our facilities all the subsystems have been on verification tests at Edwards Air Force Base, where the sixth of the 4-95 engines has been located.

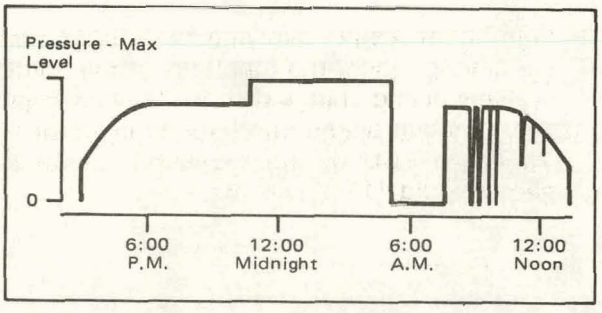


*Fig 7. Simulated solar test cycle*

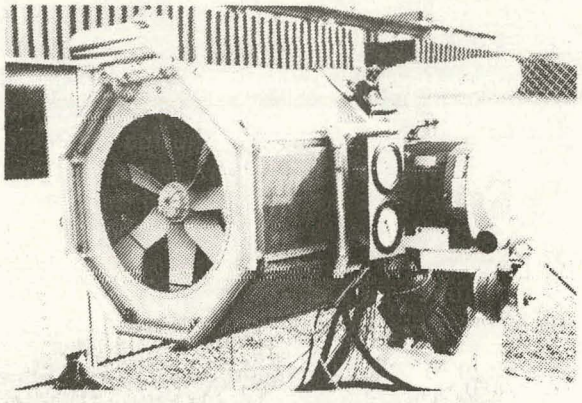

*Fig 8. PCU on test stand*

## Actual solar tests

Testing of engines actually running on solar energy started 1981 at the test facility at Georgia Institute og Technology in Atlanta. This test facility is designed for higher power

than the 4-95 engine but testing was possible to perform by shielding the excessive flux with a watercooled plate. The testing in Atlanta gave very useful information for the further development of the receiver and control systems, but in order to evaluate the function of all components in a matched system there was still a need to test in a parabolic dish. Therefore the testing was transferred to JPL's test station at Edwards Air Force Base early in 1982 where testing has been going on since then jointly with JPL in their test bed concentrator.

Significant results evolving from these tests are among others the functions of the control systems during start, stop and cloud passages. The principal operation characteristics of the Vanguard PCU during these transients are shown in fig 11, 12 and 13.

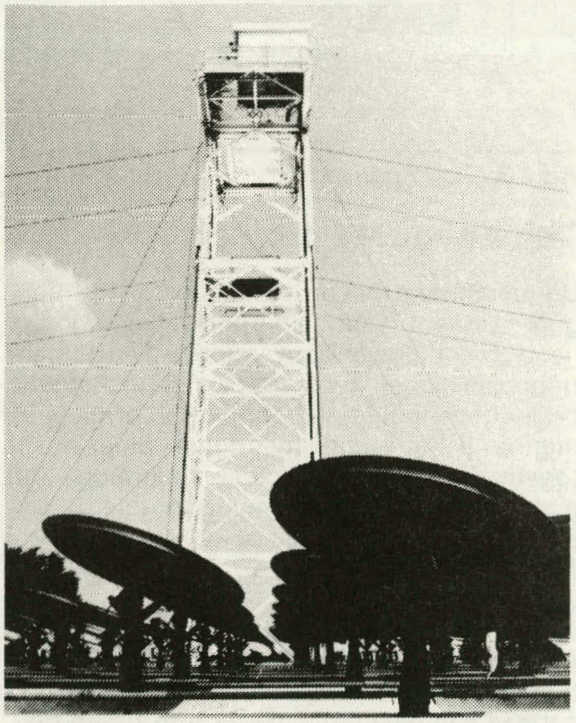

*Fig 9. Tests in Atlanta*

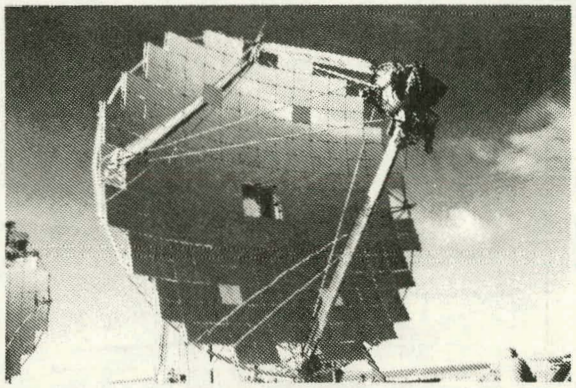

*Fig 10. Tests at EAFB*

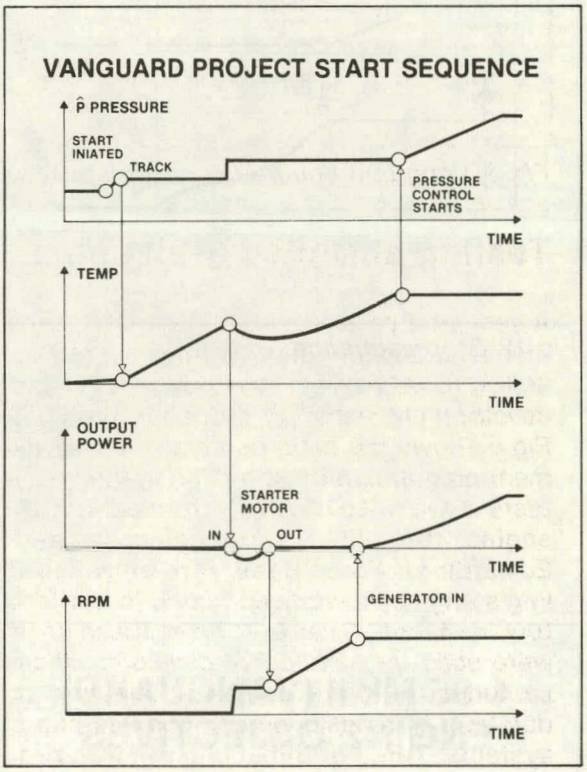


*Fig 11. Start sequence*

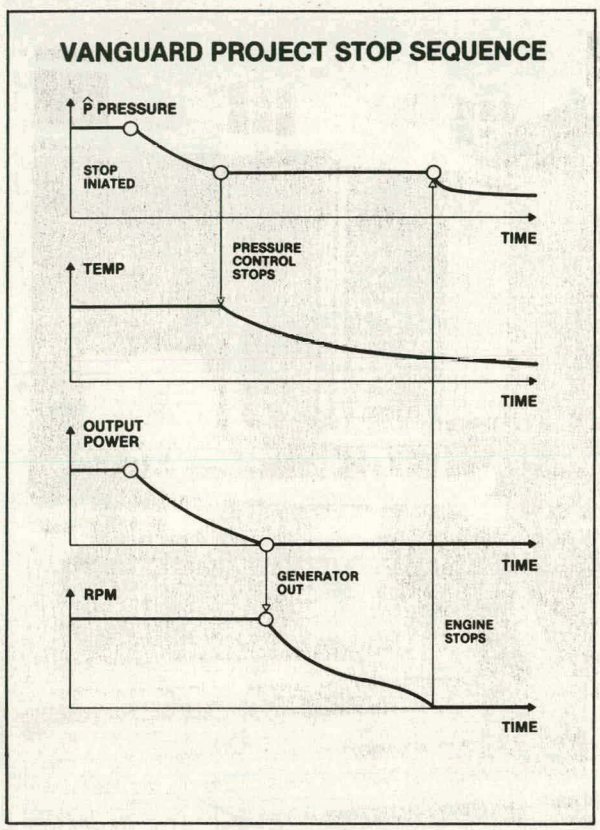


*Fig 12. Stop sequence*

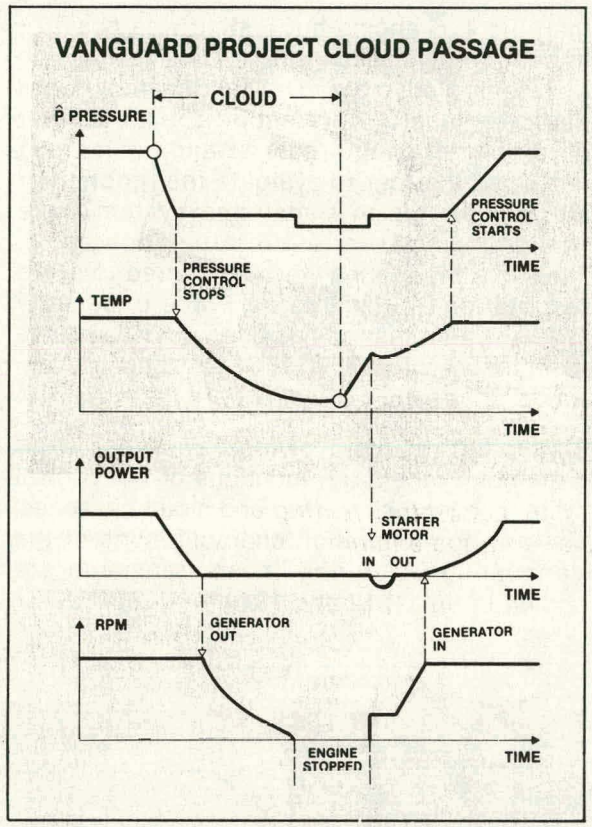


*Fig 13. Cloud passage*

## 4-95 Mk II (VANGUARD) ENGINE OBJECTIVES

- **Keep Mk I performance level**
- **Increase reliability**
- **Reduce production cost**

*Fig 14. Vanguard engine objectives*

## The Vanguard project

United Stirling became member of the Vanguard project responsible for design and delivery of the power conversion unit. The contract was signed in May 1982. Our task in this project has included modification of the 4-95 engine in the earlier mentioned areas to fit together with the Advanco concentrators. The main objectives for the engine for this project are shown in fig 14. Laboratory tests have verified that the performance goals are met and calculations show a reduction of 30% in production costs. Several modifications of components aimed at increased reliability have been introduced. The results of these modifications can only be achieved thru future testing of the engine.

The PCU is now delivered to the test site and ready for testing.

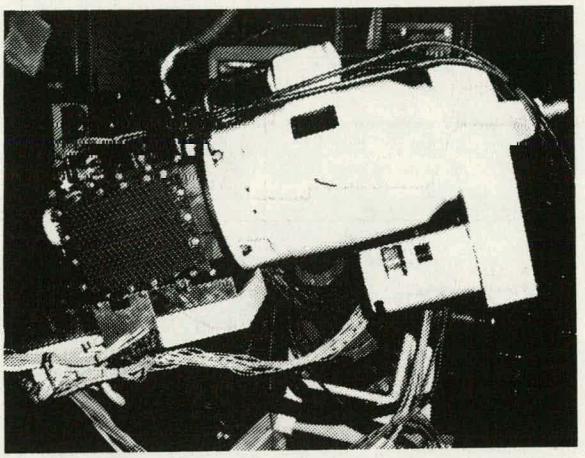

*Fig 15. Laboratory testing of the Vanguard engine*

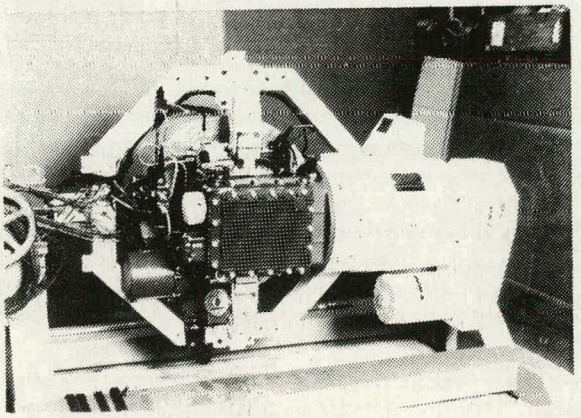

*Fig 16. Vanguard engine with alternator and mounting ring*

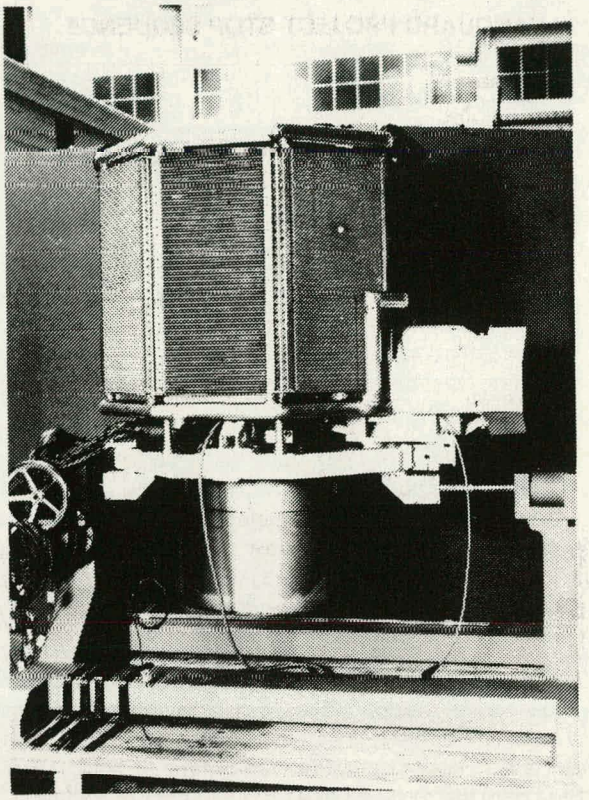

*Fig 17. Vanguard PCU ready for delivery*

UNITED STIRLING

Testing of the United Stirling 4-95 Solar Stirling Engine on Test Bed Concentrator

Author: H-G Nelving,
United Stirling AB, Malmö, Sweden

## Abstract:

Testing of the improved 4-95 solar Stirling engine in a parabolic dish system has been going on in Test Bed Concentrators at Edwards Air Force Base since May 1982. This paper presents the objectives with the testing, test set-ups and component designs and the results of the testing.

Different type of tests have been performed, among the most important have been characterization of receivers, full day performance of complete system, cavity and aperture window test including influence from windeffects, control system tests, radiator system tests and special temperature measurements with infrared camera.

The maximum output from the system — 24 kW module power output, 28% overall conversion efficiency solar to net electric — and the full day performance — 13,5 hours of operation generating over 250 kWh — shows the system capability. Other important results are the influence on performance of flux distribution depending on concentrator alignment, and the optimum receiver operating criteria when balancing flux and temperatures on cooled receiver surface while avoiding flux on uncooled surfaces.

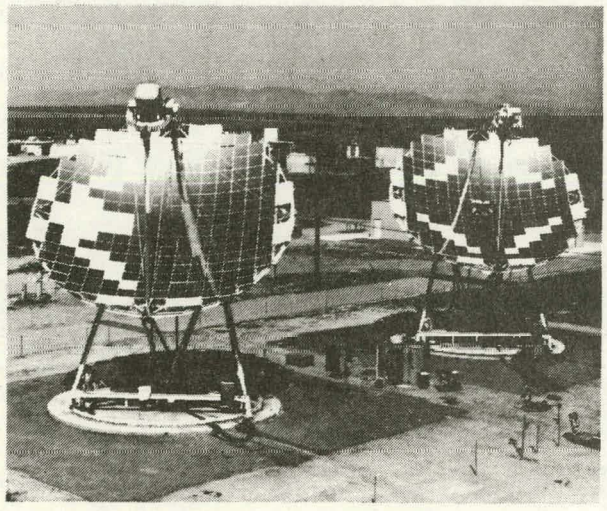

*Fig 1 TBC's with Stirling Modules*

## Introduction

The testing of the solar Stirling engine in Test Bed Concentrator at Edwards Air Force Base started in early 1982 with the first version of engine with receiver system. An improvement of the engine followed as well as an improvement of the concentrator flux distribution and in May 1982 the testing of the new system started.

A second engine was installed in the second concentrator at Edwards Air Force Base in February 1983 and since then parallel testing of the two solar Stirling engines has been going on almost continuously. (Fig 1 ).

The engine used in the testing has been the United Stirling model 4-95, the 4-cylinder double acting Stirling engine with a maximum output of 25 kW in solar application and compatible with an 11 m concentrator. The Stirling engines under testing have been integrated with other components, which are special for the solar application such as receiver system, generator, radiator and electrical and electronic controls.

## Test sequence

The testing in the Test Bed Concentrator No 2 has aimed at the improvement of performance and the development of new components. The concentrator was first realigned to improve input characteristics. Special engine mounting as well as receiver cavity and cone were installed to establish optimum operating conditions. New components including receivers, cavities, aperture window and cone material were installed for development testing. Characterization of engine with these components during different operating conditions has been performed with different temperatures, different ambient conditions and also during different operating sequences such as start, stop, cloud passages, etc.

The testing in the Test Bed Concentrator No 1 has aimed at the installation of a complete, selfsustaining unit including engine, generator, radiator and control system, and to endurance test such a system (Fig 2.). Also characterization of the radiator system was to be performed.

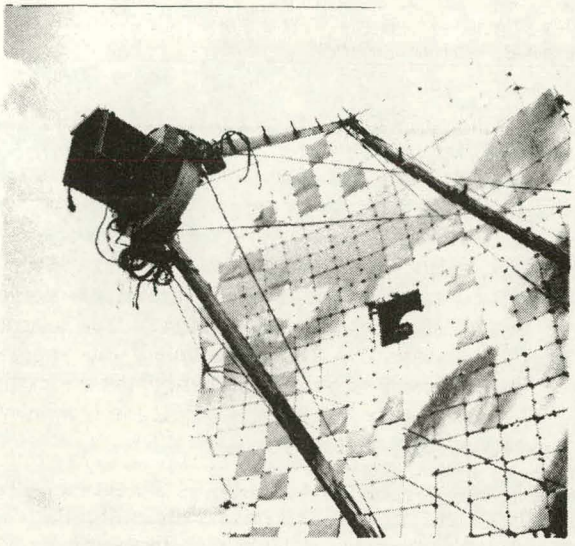

*Fig 2 Module with radiator system*

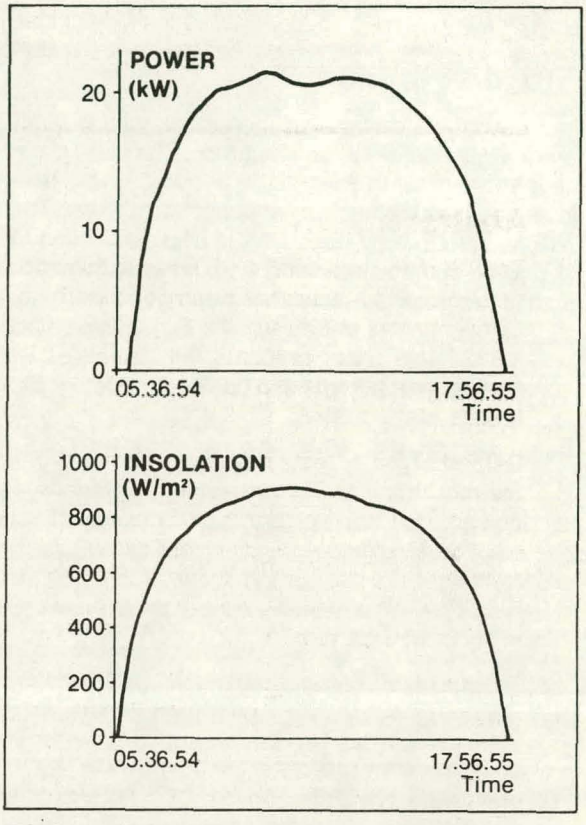


*Fig 3 Insolation and power from a full day test*

## Test results

### Module output

The present power conversion system has shown excellent performance. The module output is the highest so far for any parabolic dish system. The highlights are:

- 24 kW module output
- 28% overall conversion efficiency — solar to net electric
- 13.5 hours of operating with positive power output over a day
- generation of more than 250 kWh over a day

Figure 3 shows the output over a full day with corresponding solar input.

Of special interest is the mean daily efficiency for the system. The Stirling engine has a very high part load efficiency. For example already 1 hour after start, the system efficiency is very close to daily maximum, (Fig. 4). The mean daily efficiency is around 95% of the maximum.

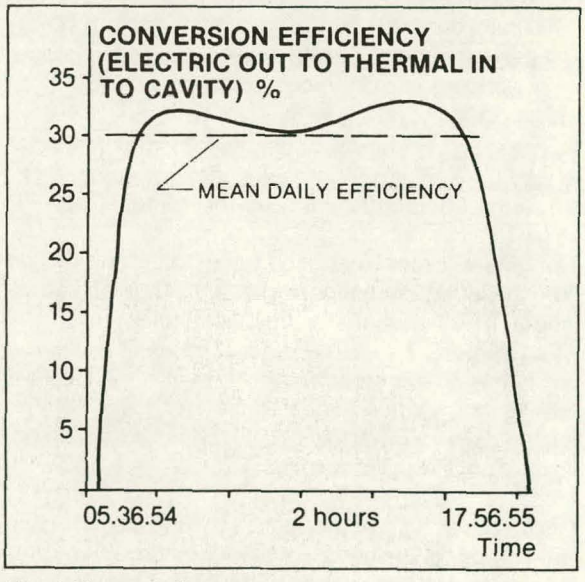


*Fig 4 Mean daily output*

## Flux distribution

The testing has so far been performed with two different aligments of the concentrator. The initial alignment strategy used a single focal point, giving heat flux to all areas in the cavity at nonuniform levels. The realignment strategy used was to allow insolation to fall only on cooled surfaces and to get as uniform distribution as possible. This improves overall performance for the power conversion unit. The basic improvement is the increase in cavity efficiency when limiting cavity wall temperatures. Figure 5 shows a comparison of performance with different flux distributions (March and June/July) for two receivers as well as for helium and hydrogen as working gases.

**EDWARDS TEST DATA**

| RECEIVER TYPE | TIME | WORK GAS | INSOLATION ($W/m^2$) | EL OUTPUT (kW) | EFFICIENCY (%) |
|---|---|---|---|---|---|
| ESOR II A | March | He | 915 | 19.5 | 28.4 |
| ESOR II B | March | $H_2$ | 980 | 20.7 | 28.2 |
| | March | He | 973 | 19.5 | 26.7 |
| ESOR II A | July | $H_2$ | 960 | 24.2 | 33.6 |
| | July | He | 906 | 20.7 | 30.5 |
| ESOR II B | June | $H_2$ | 898 | 22.4 | 33.2 |
| | June | He | 922 | 20.6 | 30.0 |

*Fig 5 Performance comparison at different flux distributions*

## Receiver performance

Three different receiver designs have been tested. Also testing at different distances from the focal point to vary the heat flux input, has been performed to optimize the operating conditions for the receiver.

The different receivers used have conflicting design criteria based on concentrator and engine requirements. The concentrator flux distribution calls for a wide diameter heater cage to achieve uniform, low flux levels on the tubes, but this results in excessive tube lenght which reduces engine performance. The engine calls for relatively short tube lenght which optimizes engine performance.

One receiver type has long tubes, wide diameter and the surface completely covered with tubes. Another receiver has the opposite, short tubes, small diameter, clearance between tubes. Both engines and cavity performance are involved in overall performance.

The third version of the receiver has a medium diameter, mean tube lenght and a surface nearly covered with tubes resulting in optimum receiver performance.

Varying the location of the receiver in relation to the focal point results in varying output if other parameter values are equal. The optimum output is, however, not the only parameter used in evaluation of optimum location. Flux and temperature distribution influencing component life should be involved in the evaluation.

## Cavity, cone and aperture window tests

The cavity and cone are important components in the dish system (Fig 6). The performance of the cavity influences the overall system performance. Losses from cavity, both optical and thermal, depend very much on the design. For example a back up of insulation behind the receiver tubes improves performance and makes controlling more stable. Taking away the cone and cavity totally increases the losses to about twice the base cavity losses which are in the magnitude of 8 kW. Also an introduction of an aperture window can minimize the thermal losses by reducing convection currents. However, when introducing an aperture window, transmission losses are introduced. Depending on the magnitude of the two losses, the system can be optimized. The result from the testing with a flat quartz window shows a lower power output of up to 1 kW at full load. The result depends also on the temperature level used in the cavity system.

Wind direction and speed with respect to the open cavity can have an influence on the output power. When evaluating the two effects together, wind and transmission losses due to aperture window, actual testing has to be made to optimize the system. At present analythical methods are not accurate enough to permit selecting a final design without field testing.

Potential destruction of components in the focal area due to the high flux intensity also influences the design. During the short aperture window tests no damage of the window could be found. Also the cone material is critical when spot traverses the cone during slew off. Successful testing with cast silica has been performed and survival at full insolation under normal tracking was achieved. Lower grade material like ceramic board and Nextel Cloth cannot survive.

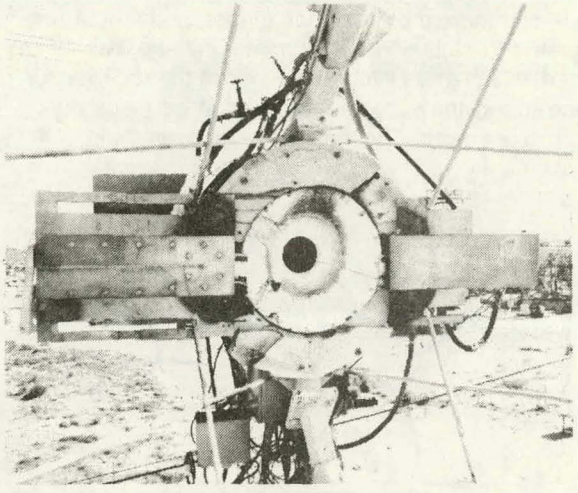

*Fig 6 Aperture cone design*

## Radiator system tests

A complete radiator system installed up in focal mount has been tested. It was built up of 4 matrices in a square form, a radial fan and a waterpump. Performance at full load conditions resulted in a 20°C temperature difference between ambient and coolant temperature.

The parasitic power consumption ranges from 800 W to 1250 W for the fan and 200 W for the water pump. The fan motor has a low and a high power level, which permits the parasitic consumption to be minimized during all operating conditions.

## Control system tests

The USAB microcomputer has been used for controling the module during all operating modes. The microcomputer allows an automatic operation. Numerous emphirical values of different parameters are included in the logics for optimized sequencing and operation. During the past year many tests have been performed to evaluate the control parameters and their optimum values. Figure 7 shows a transient curve corresponding to a start at fairly high insolation level. Shown are temperatures, pressure, speed and power output.

## Temperature measurement

Evaluation of all temperatures in the receiver system is very important, because the temperature level influences the receiver life and performance. The temperature varies somewhat over the heater surface and also around the tube itself, because of the solar input to the front face of the tube only. Temperatures have been measured with 40 thermocouples over the receiver and cavity.

Thermocouples however, cannot cover the entire surface and therefore are limited in measurement of temperature distribution. An infrared camera has been used, which gives information over all the receiver surface facing the sun, and testing can be made during normal operation. The most interesting results from the testing are:

- that no critical hot spots can be found on the receiver surface.
- that all tubes per quadrant show a uniform temperature at the same radial distance
- that the temperature distribution along the tube — warmer at the outer diameter — depends both on internal conditions ( gas flow ) and external conditions ( heat-flux distribution )

Results are shown in figure 8.

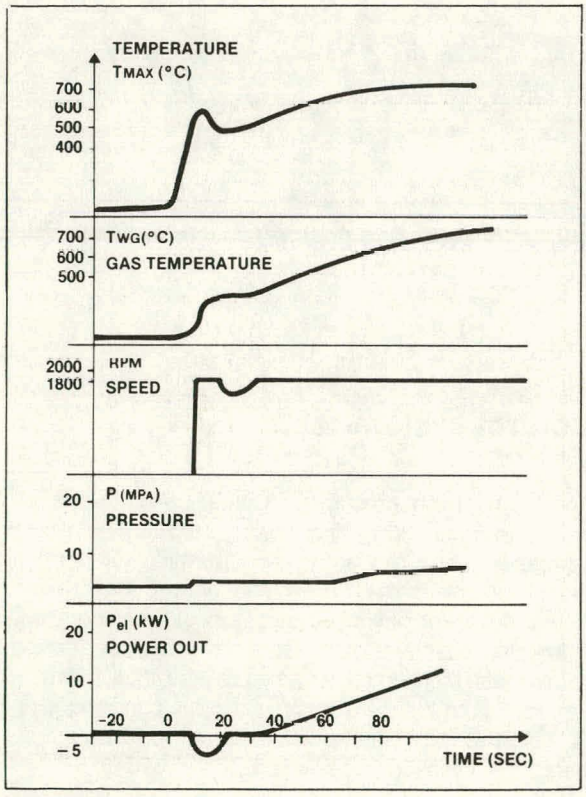


*Fig 7 Transient — start time*

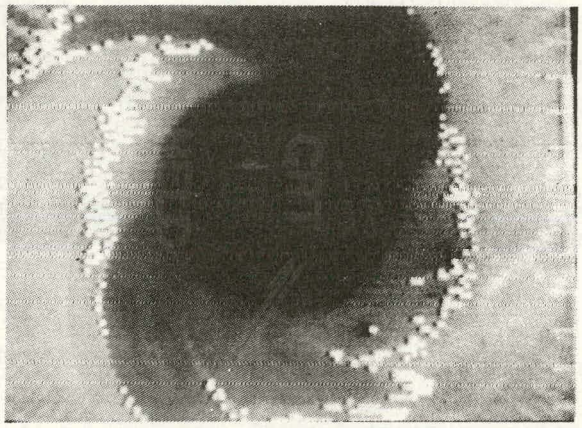

*Fig 8 Infrared camera picture of receiver with quadrants — Isotherm shown*

## Conclusion

The testing at Edwards Air Force Base has been very succesful. Testing has been going continously, except during periods of bad weather. Unfortunately 1983 has been unusual in the respect, causing a severe loss in running hours.

The testing which started in March 1983 with Stirling engines in both concentrators was very impressive. It was the first time when two solar Stirling engines were in solar operation at the same time. (Fig 9).

We now have a much better understanding of solar parabolic dish system and the influence of different parameters. However, more testing is needed and it will continue at Edwards Air Force Base. This testing will include further development of receivers, shutters, cone and aperture window, control system and eventually endurance testing of an optimized system.

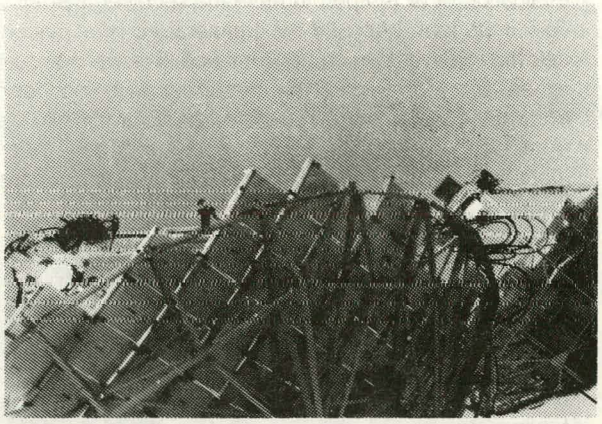

*Fig 9 Two Stirling modules under testing*

## Future action

Additional testing will also go on in Palm Springs within the Vanguard project. This activity is also sponsored by the US Department of Energy under a cost sharing contract. This testing will be done with the second generation of Solar Stirling engines, the Mark II engine, figure 10. This new design had as objectives compared to the Mark I engine to reduce production cost, to increase reliability and to keep the performance level.

The development effort resulted in a simplified design including all experience from the Edwards testing as well as new inventions and development from laboratory testing. The most important new design solutions are:

- the oil system with only internal oilflow
- the build up of cold moving parts allowing accurate alignment of components resulting in improved reliability for seals and piston rings
- the design and material selection of receiver resulting in a cheap receiver with simplified fabrication and improved performance
- the special design of gas control system, guided by the installation of modules together in a farm using one hydrogen compressor and gas storage system including feed lines to each module in concentrators, instead of each module having its own compressor and gas storage and beeing a self-sustaining unit up in focal mount.

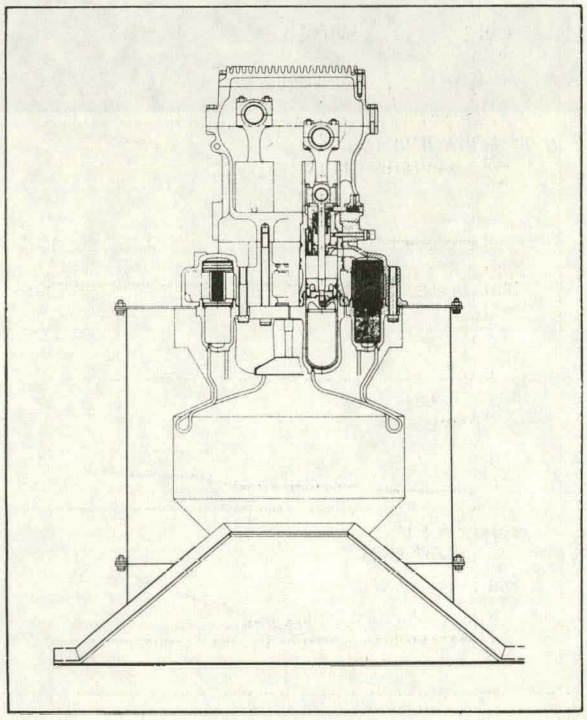

*Fig 10 Mark II Cross-section*

The Mark II engine has been fabricated and assembled and the first engine, intended for the Palm Springs installation, has been laboratory tested for about 200 operating hours (figure 11). The result from the testing shows a slightly better performance than for the Mark I engine. The Mark II engine has been converted for solar operation and assembled with radiator and solar control system, to a selfsustaining unit and is ready for continued solar testing in Palm Springs. (Figure 12).

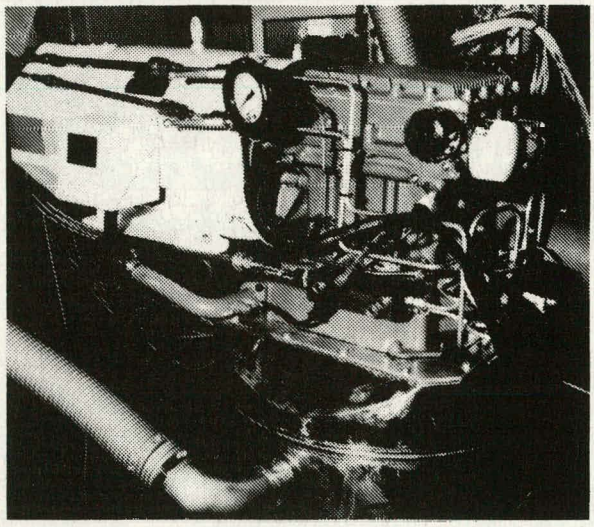

*Fig 11 Mark II in test rig*

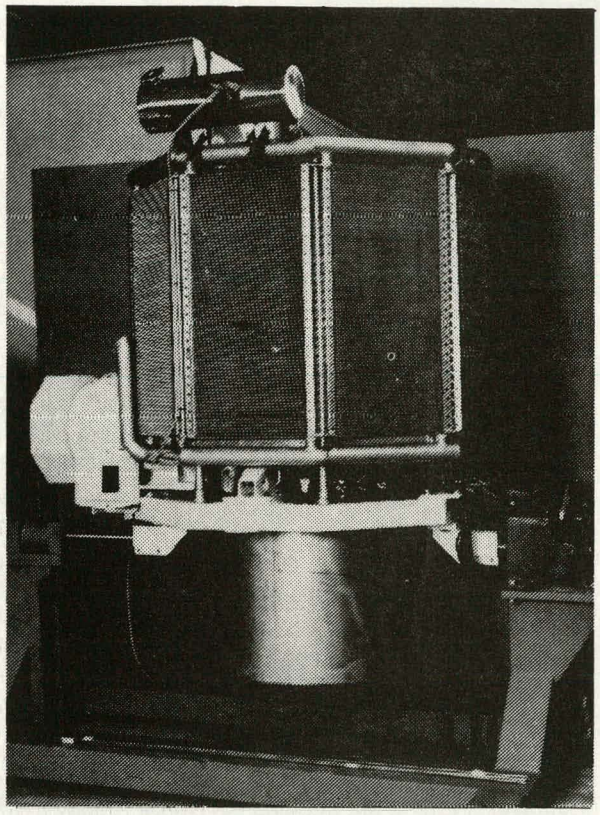

*Fig 12 Mark II Solar module*

Hgn 831024

# VANGUARD CONCENTRATOR

Terry Hagen

Advanco Corporation
El Segundo, CA

Advanco Corporation and the United States Department of Energy (DOE), on May 28, 1982, signed a Cooperative Agreement for the design, manufacture, and test of a "solar only" parabolic dish-Stirling system known as Vanguard 1. As a result of this agreement, a Project effort has developed that combines the extensive research and industrial experience of several participants to develop and produce the Vanguard 1, solar energy, electric-generating module that will technically and economically penetrate the small community market as well as the electrical utility market. The design of the Vanguard 1 dish-Stirling engine system features low risk, simple fabrication and assembly, and minimum cost. Due to the fully self-contained nature and relatively simple size of each power generation module, this solar technology lends itself to rapid commercialization. The concept combines United Stirling's USAB 4-95 Solar II Stirling engine, Jet Propulsion Laboratory's (JPL) developed mirror facets which form the reflective surface of the dish, Rockwell/Advanco's low-cost exocentric gimbal mount with the needed structural stiffness to assure tracking accuracy; a low-cost pedestal foundation; and an automatic un-manned concentrator control system. Reported in this session was a summary of the results achieved by Advanco on the fabrication and erection of the concentrator since the April 83 Detailed Design Review of the Vanguard I program.

# BRAYTON MODULE DEVELOPMENT OVERVIEW

Herbert J. Holbeck
Jet Propulsion Laboratory
Pasadena, California

## Abstract

The Brayton module development effort has involved the solarization of existing gas turbines. At one time parallel developments were contemplated using both the Advanced Gas Turbine (AGT) and the Subatmospheric Brayton Cycle (SABC) engines. The AGT is being developed for automotive applications by the Garrett Turbine Engine Company (GTEC) under contract to DOE and NASA while the SABC has been developed for a gas-fired heat pump application by the AiResearch Manufacturing Company under contract to the Gas Research Institute (GRI). Funding limitations led to a single module development contract with Sanders Associates. In FY 1982 they conducted trade studies of the AGT, the SABC and other existing gas turbines in combinatiuon with various concentrators. The Sanders recommendation from these studies was to use the SABC for near-term module development while following the AGT development for later advanced application. Following JPL and DOE approval of this approach, Sanders completed a preliminary design at the module, and developmental subsystems are being completed.

## Background

Brayton cycle (gas turbine) engines have been considered for solar thermal application because of the large existing experience base, the simplicity of the rotating assembly, demonstrated long life of gas turbines with foil bearings, the simple incorporation of a hybrid combustor with an air receiver, and the potential for high efficiency in high temperature ceramic engines.

The AGT is being developed for automotive application by GTEC under contract to DOE and NASA. In its final ceramic configuration, it will have the capability to produce more than 50 kW of shaft power at more than 40 percent efficiency with turbine inlet temperatures up to 2500°F. The development initially uses a lower efficiency metal engine with a ceramic regenerator at a turbine inlet temperature of 1600°F. This engine is undergoing development testing while the ceramic parts are being rig tested.

The SABC engine is being developed for gas-fired heat pump application by AiResearch under contract to GRI. This is a smaller, 8 kWe, partially closed cycle metal engine, operating at a turbine inlet temperature of 1600°F with the pressure through the turbine dropping from one (1) atmosphere to 0.4 atmospheres. This engine has all foil bearings and is

readily amenable to the incorporation of a shaft mounted permanent magnet alternater (PMA) replacing the heat pump freon compressor.

When reduced DOE funding mandated a single Brayton module development, Sanders Associates, the system Contractor for the Brayton module development, conducted trade studies in FY 1982. These studies considered the AGT, SABC and other existing gas turbines in combination with several concentrators. The results of these studies were reported at the Fourth Annual Parabolic Dish Solar Thermal Power Program Review in December, 1982.

Recommendations Resulting From Trade Studies

The studies indicated potential for the AGT in its eventual, ceramic, high-temperature, high-efficiency development. However, the ceramic engine is several years from fruition, and additional changes such as incorporation of all foil bearings and a shaft-speed PMA will be needed to increase the 3500 hours of automative lifetime to the 50,000 hours desired for the solar program.

The SABC engine, has a lifetime goal of 50,000 - 100,000 hours for the heat pump program, and this is considered a realistic expectation based on engine test results to date and field experience with similar foil bearing units. Cost studies indicate that this engine can meet cost goals even at relatively low production levels of 1000 units per year. These factors show potential for a near term, cost effective application, even though the net efficiency of small, metal Brayton engine/generators is limited to 25 to 30 percent.

The studies identified several small concentrators which were a reasonable match for the 8 kWe engine. These included concentrators developed by PKI, Essco, SKI and LaJet. Tradeoffs on concentrator size have been undertaken in several studies with various results. Sanders identified lower unit weight and cost advantages for small concentrators together with the higher production level for a given power level.

Module Development Program

The FY 1983 Sanders preliminary design identified the following module subsystems:

1. AiResearch SABC (Mark IIIB) engine with permanent magnet alternator.

2. Sanders air receiver based on their High Temperature Solar Receiver (HTSR).

3. LaJet Energy Company LEC 460 concentrator.

4. Sanders system controls using Standard Microprocessor components.

5. Abacus inverter.

The module development will occur in two stages. In the first stage, developmental subsystems have been fabricated and are being prepared for development testing. These results will be used for design modifications with the subsystems for the final module available at the end of FY 1984.

The SABC Mark IIIA development engine has reduced power and efficiency capability as does the 5 kWe, load cell, PMA used in the development unit. However, this developmental engine/generator will allow development testing of combined subsystems and provide data for design modification and controls software development. Meanwhile an improved Mark IIIB engine with an integral shaft, full load PMA is being assembled.

The LaJet 460 concentrator is the fifth version of a multi-faceted membrane concentrator, privately developed by the LaJet Energy Company. Facet tests at JPL together with analyses have indicated the suitability of this concentrator for the presently designed 10 inch receiver aperture. The concentrator already comes close to meeting cost goals in production quantities.

Future Expectations

The Sanders Brayton module using the AiResearch SABC engine/generator and the LaJet Concentrator appears to provide a realistic near-term Brayton module. Following module verification testing in early FY 1985, this technology is expected to be ready for a multi-module field experiment or for field application.

Meanwhile, the AGT automotive program is being monitored with the ceramic version of this engine is expected to provide an advanced Brayton alternative. A solar feasibility test on the reduced performance metal SAGT may occur in FY 1984 with possible readiness of a ceramic SAGT module in FY 1986.

# Near-Term Brayton Module Status

S.B. Davis
Sanders Associates, Inc.
Nashua, New Hampshire

## Summary

Sanders Associates, Inc. was selected as system integrator for this program with the responsibility of integrating subsystem components and testing a Parabolic Dish Module (PDM) to convert solar energy to grid compatible electric power.

By March 1983 Trade Studies had been completed and the PDM system components were selected. System components were selected on a basis of current and projected performance efficiencies, technology readiness, future production probabilities and prices, current cost and availability. Though the PDM program was originally oriented toward an 11-12 meter reflector with a 15-20 kw electric output, the trade study conclusion led us to downsize the system to include a smaller lightweight reflector and to output a rated 8 kw electric. Potential for this near-term, 8 kw derivative of the PDM is adjudged to be superior to that of a 20 kw system.

Major system components are: 1, the AiResearch/GRI Mark III subatmospheric Brayton cycle power conversion assembly; 2, the LaJet LEC-460 point focusing concentrator; 3, the Abacus 8 kw DC-AC inverter; 4, the Sanders/JPL low pressure, high temperature ceramic matrix receiver; and 5, the Sanders 8086 microprocessor based control system.

The PDM is suited to both grid connected and standalone applications, and it may be fired by solar, fossil, or solar/fossil hybrid means.

Current program plans call for delivery by AiResearch of two engines. The early engine will be utilized in The Development Test Model (DTM) which will be tested in March of 1984 at Sanders, in Merrimack, NH. DTM objectives are to complete:

- System Integration
- Development of Control Algorithms and system operating logic
- Establishment of System Performance Baselines
- Demonstration of System Feasibility

Following the PDM Critical Design Review (CDR) in April 1984, assembly of a Final System will commence. An improved engine will be delivered directly to Sandia Laboratories, Albuquerque, NM and final system integration is scheduled for September 1984. Testing will be concluded in the fourth quarter of calendar 1984.

Status

The Parabolic Dish Module (PDM) Experiment is being conducted by Sanders Associates under contract (956039) with Jet Propulsion Laboratories, Pasadena, Ca. With the major technology development near completion, the contract will be transferred to Sandia National Laboratories, Albuquerque (SNLA), New Mexico, in early 1984 for testing and improvement. Development Test Model (DTM) experiments, design updating, and performance validation tests (PVT) will occur under the aegis of SNLA through calendar 1984. See Figure 1.

The DTM testing in early 1984 is oriented toward completing subsystem integration. The control system will be integrated with the major system components: 1, engine assembly; 2, concentrator controller; 3, inverter; and 4, the operator control terminal. The DTM will be extensively instrumented to collect baseline performance data against which the improved system will be measured in the fall. System feasibility will be demonstrated during these tests and will provide the experimental proof of concept needed to pursue widespread deployment of the PDM system.

The DTM test results will be used to define control and hardware improvements that will be incorporated in the second unit, the PDM, along with the already planned improvements: 1, improved engine; 2, simplified controller; 3, corrosion resistant heat sink exchanger; 4, optimized recuperator ducting; 5, lighter weight receiver; 6, and (tentatively) the electric start.

The validation of system improvements and increased efficiency are primary goals of the PVT. Additionally, the testing of automatic algorithms essential for unattended operation is planned. During extended testing, lifetime and reliability data will be collected to identify improvements necessary for large scale deployment of this new alternate energy source.

The current PDM system is comprised of advanced components which will provide economic conversion of sunlight to grid compatible AC power with the high reliability and low maintenance costs characteristic of Brayton (jet) power plants. The engine is a subatmospheric Brayton cycle engine recently developed by AiResearch Manufacturing Company of California for the Gas Research Institute to drive natural gas fired heating/air conditioning heat pumps. The engine employs air bearings to achieve life expectancies beyond 30,000 hours and advanced versions will operate in the 8 - 10 kilowatt range. While the engine is currently developmental, it has successfully operated several hundred hours and has no major technical uncertainties. The MOD IIIA engine that will be used in the DTM test sequence uses a vacuum air start system. The more advanced MOD IIIB engine uses a shaft-mounted alternator integral to the compressor turbine shaft. This IIIB engine will be capable of automatic electric starting.

The ceramic matrix receiver designed and built by Sanders is an inherently long-life component. Developmental work continues to improve its already high efficiency and to reduce cost to production level goals.

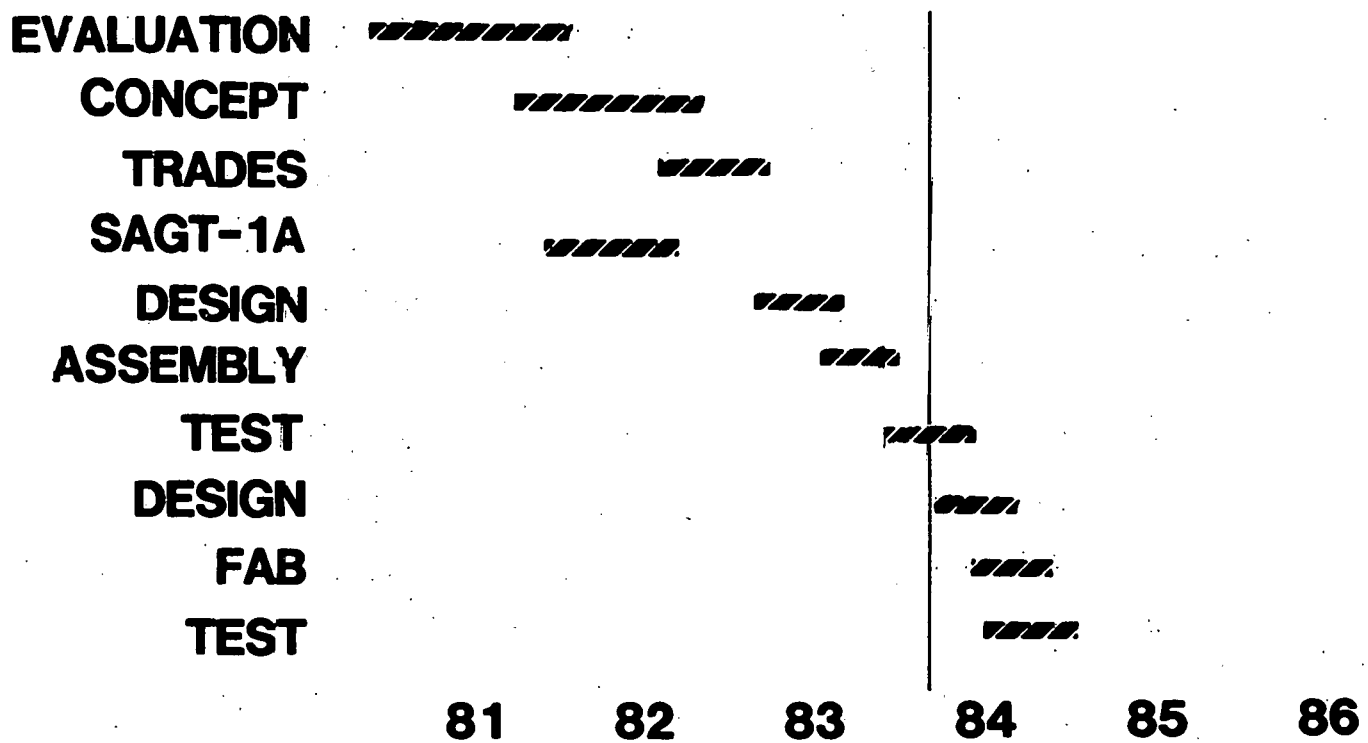


Figure 1. Parabolic Dish Module (PDM) Experiment is Nearing Completion

The lightweight concentrator is equivalent to a 7.4 meter diameter dish and employs 24 closely packed quasi-spherical circular facets to reflect the solar energy through an 8 inch (diameter) aperture into the receiver. The dish has been built in moderate quantities (700+) and meets design to cost (DTC) goals.

The PDM uses an integrally mounted shaft-speed 8 kw permanent-magnet alternator with torque characteristics that allow it to double as a starting motor. The DTM 5 kw alternator from which the 8 kw version is derived has performed reliably during engine testing.

The inverter uses microchips to digitally synthesize the grid-locked output AC from the rectified alternator output. The inverter logic allows signals from the system controller to vary inverter input power requirements and thereby control engine loading.

The PDM control system operates as an executive processor to command the subsystem on-board controllers (concentrator, inverter, and start sequencer.) The controller that was developed for the DTM test will communicate to the operator via a video terminal and will offer a high degree of flexibility to facilitate the developmental testing. Production controllers will be programmed to a more restricted command menu and will consolidate functions to reduce system cost.

The DTM receiver is shown in cutaway Figure 2. It is conceptually similar to the follow-on receiver that will be used with the PDM. Preheated air enters through a central inlet duct and flows through the radiation cavity to the segmented honeycomb silicon carbide panels. The honeycomb panels are heated to approximately 1850°F by the concentrated sunlight that enters the receiver through the fused quartz window. As the 1200°F preheated air flows through the honeycomb, it is further heated to 1600°F. The hot air is then collected in the tapered plenum and delivered to the outlet duct via a stainless steel particulate filter.

The front of the receiver is protected by a passive graphite shield assembly that is inexpensive and requires no parasitic power.

Two DTM receivers have been assembled; one is being used for development tests -- the other has been delivered to AiResearch for integration into the power conversion assembly (PCA).

Packaging and aperture/cavity modifications will be incorporated into the PDM receiver to reduce its weight and improve its thermal performance.

The solar concentrator for the PDM system is an LEC-460, supplied by Lajet Energy Company of Abilene Texas. In this application the PCA is, at 1300#, heavier than the design load for the concentrator. The concentrator was, therefore, analyzed to determine the modifications that would be required to sustain the heavier PCA and expected snow loads. The structure proved to be generally adequate and only limited modifications were required

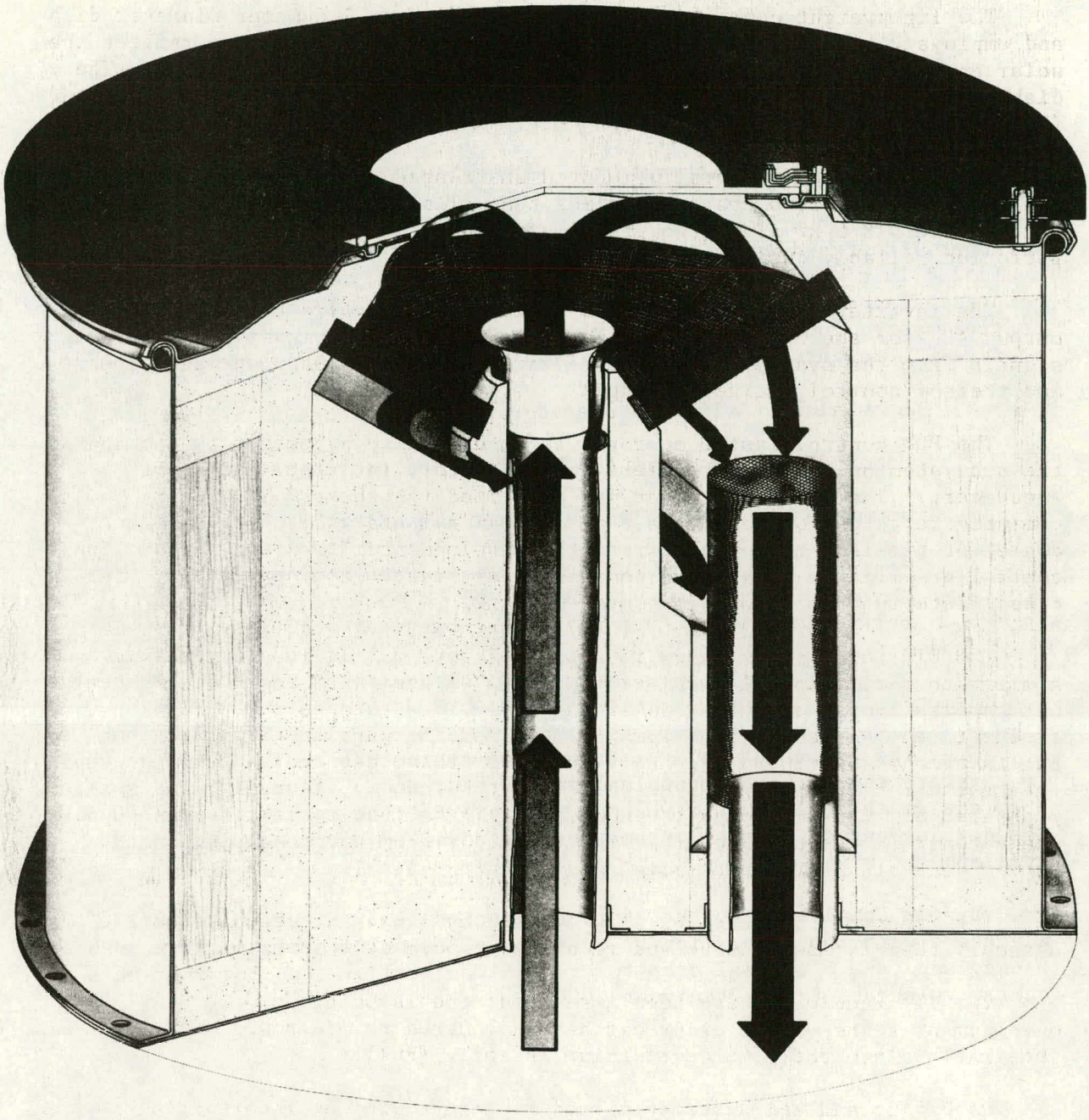

**MEETS DESIGN TO COST GOALS**

Figure 2. Low Pressure-Brayton Cycle Solar Receiver

to meet the desired safety margins with the heavier loading. The modifications have been incorporated and the concentrator is currently being assembled and installed at Sanders' Merrimack, NH facility. Installation will be complete by mid-January and characterization will occur during the ensuing four weeks before DTM testing.

The control system is organized as an executive processor (EP) to expedite the DTM testing and follow-on PVT at Albuquerque. By configuring and programming the EP to use the existing on-board controllers in the inverter, start sequencer, and concentrator, duplication of effort was avoided. This approach reduces contract cost by allowing us to hold to a compressed schedule and complete testing in 1984. Eventually, however, the control system functions will be reallocated to reduce hardware costs and achieve DTC targets. According to Figure 3, the EP:

1, communicates with the operator via CRT or hand-held terminal;

2, commands and monitors the inverter and concentrator;

3, commands the fuel valve and start sequencer:

4, monitors the engine, safety circuits, and weather; and

5, relays data to the recorder for subsequent analysis.

## Conclusion

Over the course of this contract, the system has evolved from concept to hardware that will be practical in the near term, figure 4. The smaller 8 kw system that has been developed will provide the market base to support the development of larger systems as more advanced components become available.

By our commitment to the aggressive schedule of Figure 5, we will advance toward the generation of substantial quantities of truly renewable energy and take a crucial step toward the DOE goal of reducing America's energy vulnerability by the year 2000.

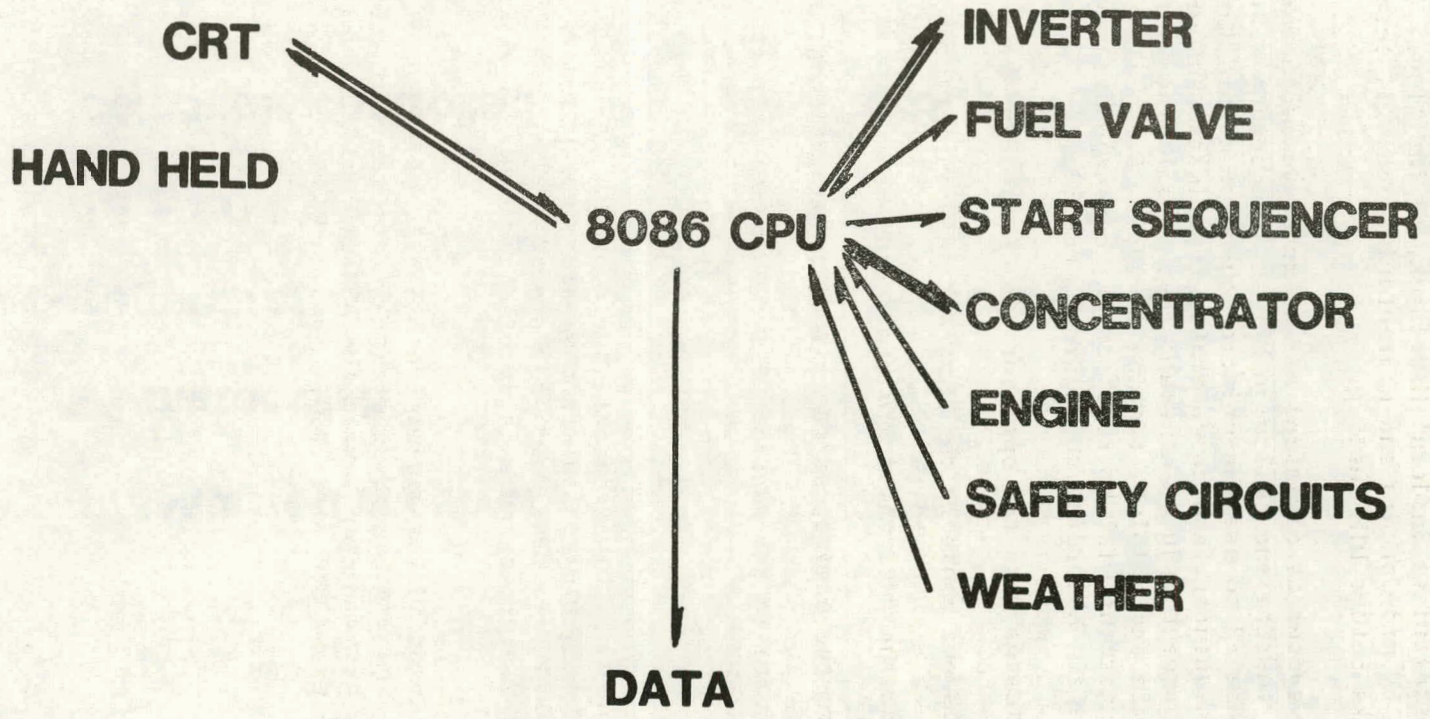


Figure 3. Control System Executive Processor

## PARABOLIC DISH MODULE DESIGN

## HAS EVOLVED FROM CONCEPT

## TO NEAR TERM PRACTICALITY

| | |
|---|---|
| pressurized receiver | atmospheric receiver |
| 11 meter dish | 7.5 meter dish |
| regenerated | recuperated |
| 15 - 20 kW | 7 - 8 kW |
| computer controlled | 8086 mp |

Figure 4. System Evolution

**INSTALLING 8,000 kW BY 12/85**

**1,000 units on line by 6/86**

**2,500 units built by 12/86**

**5,000 units per year in '87 -**

Figure 5. Development Schedule Objective

# Subatmospheric Brayton-Cycle Engine Program Review

Richard L. Johnson
AiResearch Manufacturing Company
Torrance, California

## SUMMARY

This program is to develop a solar-energy-powered electrical generator utilizing an engine developed for the Gas Research Institute (GRI). The generator consists of a subatmospheric, Brayton-cycle engine and a permanent-magnet (PM) alternator. The electrical power is generated by an alternator driven directly by the Brayton-cycle engine rotating group. Unique features that enhance reliability and performance include air foil bearings on both the Brayton-cycle engine rotating group and the PM alternator, an atmospheric-pressure solar receiver and gas-fired trim heater, and a high-temperature recuperator. The subatmospheric Brayton-cycle engine design is based on that of the GRI gas-fired heat pump engine.

Two generators will be supplied in the program: the first, a feasibility demonstration unit using existing GRI hardware, will produce an electrical power output of 5 kW; the second, an upgraded engine and PM alternator, will produce 8 kW.

## INTRODUCTION

The increasing energy shortage has resulted in new developments in energy-saving devices. Utilization of the GRI gas-fired engine which provides onsite power for space conditioning allows full time operation of the solar energy electrical generator. The system offers high performance potential by utilizing air as the working fluid, where high turbine inlet temperatures provide high thermal efficiency. The engine measures 8 ft. by 4.5 ft. by 3 ft. Figure 1 shows the feasibility demonstration system consisting of the modified GRI subatmospheric Brayton cycle engine 5 kW PMA and Sanders solar receiver.

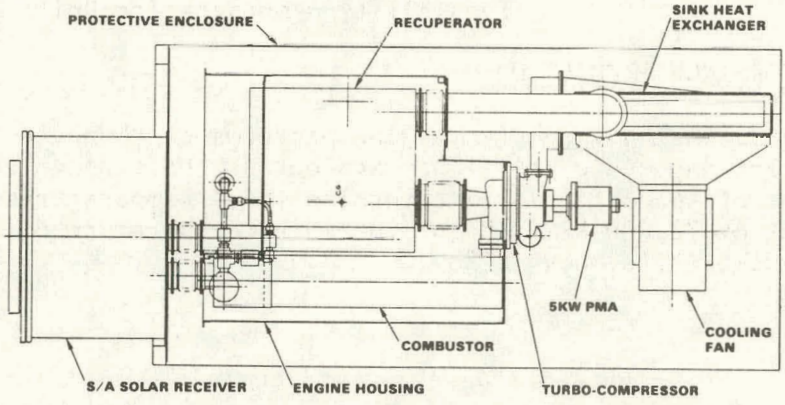


Figure 1. Feasibility Demonstration System

## ENGINE DESCRIPTION

The Brayton cycle engine shown schematically in Figure 2 is a semi-open subatmospheric pressure cycle consisting of a centrifugal compressor, a radial inflow turbine, a recuperator, a sink heat exchanger, and an inline atmospheric combustor. Ambient air is drawn through the recuperator, where it is preheated before being introduced into the solar receiver. The heated air is then passed through the atmospheric-pressure, gas-fired combustor in a mixture that is slightly above stoichimetric. Compressor discharge gas is also cycled through the recuperator and is used as a diluent to provide added flow and the desired turbine inlet temperature. Expansion takes place through the turbine component, from which sufficient power is extracted to drive both the Brayton compressor and PM alternator. The turbine discharge gas, which is at subatmospheric pressure is processed through the recuperator, where is preheats combustor inlet air. The temperature of the low-pressure gas is reduced further by using the sink heat exchanger to reduce compressor power consumption. The compressor pumps the gas back to atmospheric and a small portion is exhausted; remainder is recycled as diluent.

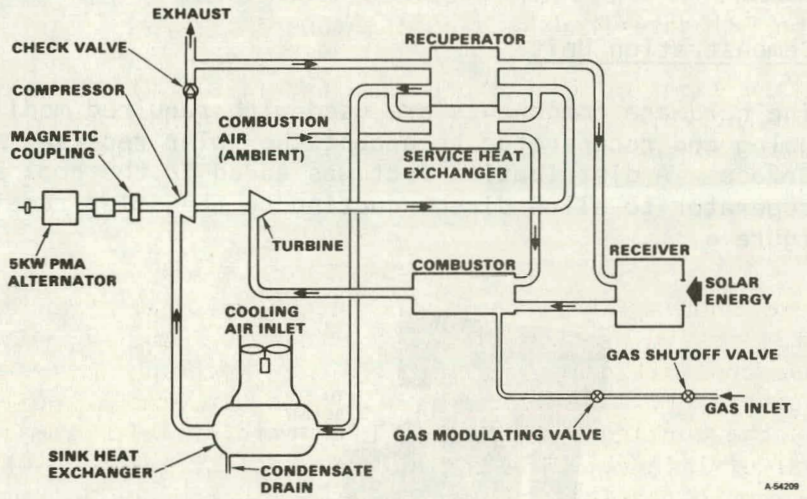


Figure 2. Simplified Schematic of the Feasibility Demonstration Unit

## SYSTEM PERFORMANCE PREDICTIONS

Figure 3 presents the predicted engine performance characteristics for a 55$^{0}$F ambient day cycle efficiency and output shaft power are plotted as functions of speed for varying turbine inlet temperatures. At the design point of 75,000 RPM and turbine inlet temperature of 1600$^{0}$F the predicted cycle efficiency is 25%.

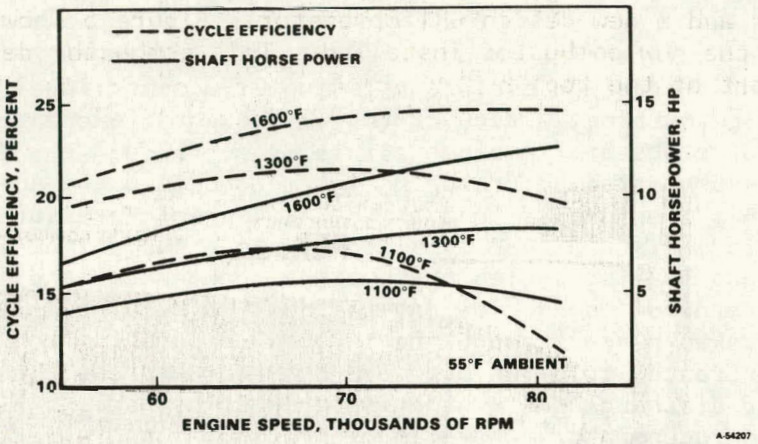


Figure 3. Brayton Engine Performance

## HARDWARE DEVELOPMENT

### 5KW Feasibility Demonstration Unit

Existing GRI engine hardware components are used with required modifications to the engine housing and recuperator to accept the solar receiver and concentrator interface. A distribution duct was added to the cool side outlet of the recuperator to allow direct ducting to the solar receiver inlet shown in Figure 4.

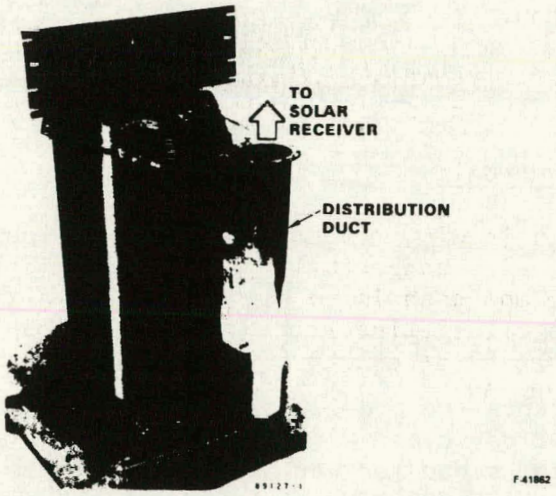


Figure 4. Modified GRI Recuperator

Modifications to the engine housing were required to incorporate the modified recuperator and a new design GRI combustor. Figure 5 shows these modifications with the new combustor installed. This combustor design incorporates an inlet port at the top.

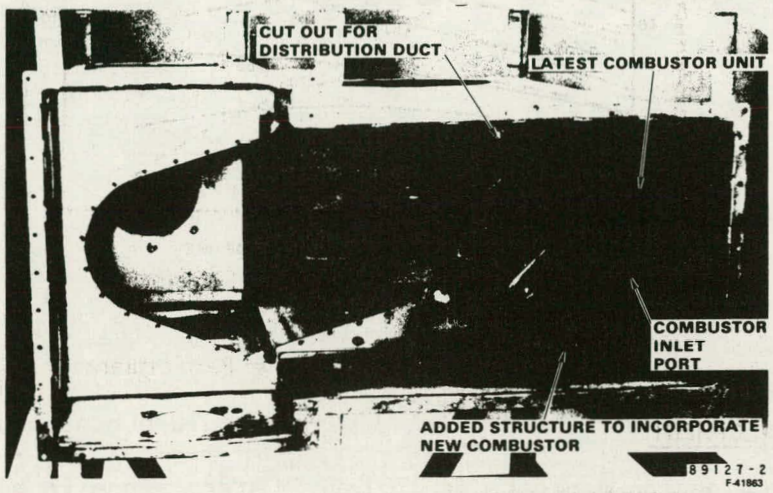


Figure 5. Engine Housing Modifications

This port is aligned directly with the solar receiver outlet port to minimize pressure drop and thermal loss. Additional modifications were required to the engine to realign the sink heat exchanger and provide a cooling air fan.

Hardware modifications are complete and final assembly is in process. Performance testing is scheduled for January and February 1984.

8KW Development Unit

Major redesign is with the PM alternator various approaches are being investigated, with compatibility with electric starting being of primary concern. One approach is to combine the PM alternator and turbocompressor on the same shaft eliminating the magnetic coupling and thrust/journal bearings in the PM alternator. A preliminary sketch of this design is shown in Figure 6.

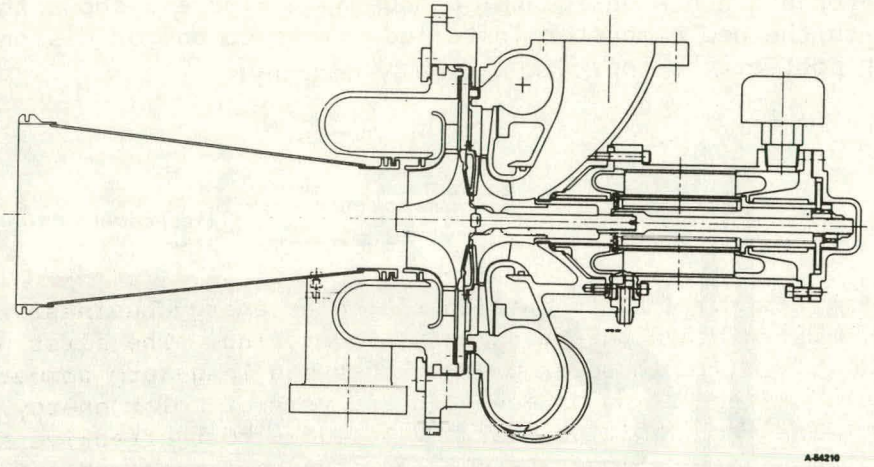

Figure 6. Preliminary Design of Turbogenerator

The alternate design approach is to have a stand alone PM alternator that is driven by a magnetic coupling. This design will require a larger PM rotor and stator plus the addition of a journal bearing and thrust bearing. The combined unit will share bearings with the turbocompressor.

The final design will be selected by mid December and detail design will proceed. System design is scheduled to be complete by March and system delivery in September 1984.

# LEC SYSTEM DEVELOPMENT

David D. Halbert

LaJet Energy Company

Abilene, Texas

LaJet Energy Company ("LEC") entered the solar energy business in early 1978 funded by its then parent company, LaJet, Inc. The first goal of LEC was to identify a viable solar product that had long-term commercial application. After making an economic analysis of solar energy, LEC defined the necessary conditions for developing a cost-effective solar product. With its goal defined, LaJet, Inc. funded a research and development program to create such a product. The result is the LEC System. The latest model of the LEC System is designated the LEC 460.

## Description of the LEC System

The LEC 460 is a parabolic "dish" which incorporates a microprocessor to automatically point it toward the sun from sunrise to sunset. The "dish" is composed of a set of mirrors (made of reflective polymeric film) which focus and concentrate the sun's energy on a receiver, producing intense but controlled amounts of heat. The LEC 460 employs a design concept that permits the use of common and low-cost materials. All major structural components are fabricated from low-carbon, low-alloy steel using methods adaptable to mass production. The mirrors are supported on a steel tubing frame. This frame is attached near its center of gravity to a cantilevered support structure. The mirrors and frame are counterbalanced by the weight of the receiver, thus reducing the energy needed to move the collector (parasitic load) and allowing movement on two axes.

The Reflective Array. Each LEC 460 solar concentrator contains a reflective array consisting of twenty-four 60-inch diameter mirrors. The total reflective surface of each LEC 460 is approximately 460 square feet. Each mirror surface consists of weatherized disposable reflective polymeric film that is drawn to an approximate parabolic shape on a permanently fixed aluminum frame by a continuously applied vacuum (supplied by a small vacuum pump). The depth of the parabolic shape is controlled by an adjustable focusing valve mounted behind the film's surface at the center of the mirror's interior. The solar concentrator flux intensity at the LEC 460's focal point can be varied by adjusting the position of each mirror or by altering the adjustable focal length of the individual mirrors.

The Space Truss Structure and Space Frame. The space truss structure and space frame are designed to support the mirrors and to track the sun from sunrise to sunset. Designed by LEC to overcome the primary obstacles and problems LEC believes are encountered in the design of other solar collectors, they have low-cost, light-weight components and small, low-powered motors to track the sun.

The primary components of the space truss structure and space frame are low-cost, low-carbon steel angle and tubing. When assembled, the space frame is a lightweight, rigid, parabolic-shaped structure. The space frame is mounted on the cantilevered space truss structure, very near its center of gravity, thus minimizing the need for counter-weighting. Because of this design and the low weight, the entire space frame can be driven by a small 1/8 hp motor, thus minimizing the power that must be used to operate the system. The space truss structure is affixed to a concrete foundation.

The Controller. Each LEC 460 is equipped with its own microcomputer-based controller specially designed to operate with the LEC 460. This controller determines the system start-up and shutdown procedures including controlling auxiliary motors, valves, and other support devices, and determines the time of day to perform start-up and shutdown functions. The controller also tracks the sun and automatically adjusts for any errors in positioning or placement to ensure optimum performance. The controller provides for emergency shutdown of the concentrator in case of high wind, fluid flow losses, excessive fluid operating temperatures or other potential operating problems.

The LEC System features advanced engineering focused on reliability, performance, and low cost to produce a sophisticated yet relatively simple product.

**Development of the LEC System**

The development and testing of the LEC System has spanned three years. Six models of the concentrator were designed, built and tested during this period:

| Model | Reflective Surface (square feet) |
|---|---|
| M-1 | 85 |
| M-2 | 190 |
| LEC-200 EM-1 | 210 |
| LEC-300 EM-1 | 330 |
| LEC-400 EM-1 | 410 |
| LEC-460 EM-1 | 460 |

The LEC 460 incorporates a number of refinements and improvements developed through the testing and operation of the previous models, including a reflective surface over 5 times larger than the original model, a substantially stronger space truss structure and space frame, improved mirror design permitting greater efficiencies and durability and a microprocessor control system that governs almost all aspects of concentrator operation.

**Patents**

The LEC System is a unique and innovative technology. To protect the uniqueness and proprietary nature of this technology, LEC has received domestic and foreign patents on the overall conceptual design of the LEC System. Other subassembly patents have been received or have been filed for and are pending.

# PANEL DISCUSSION ON "BUSINESS VIEWS OF SOLAR ELECTRIC GENERATION"

John Stolpe

Southern California Edison Company
Rosemead, CA 91770

Solar power generation systems, including parabolic dishes, are beginning to make headway as income producing business ventures for supplying meaningful amounts of electric power to the utility grid. In doing so, solar developers are making a difficult transition from the emotionally-based justification for solar R&D "to solve the world energy situation" and are now beginning to face the realities of having to justify solar commercialization based on all the tried and proven rules of economics and free enterprise.

For any given solar power technology which has successfully progressed through all the research, development and demonstration steps to prove its technical value to a utility grid, the technology eventually becomes faced with an entirely different set of formidable business questions from the financial community. Such questions are directed toward establishing the financial feasibility of a possible commercial project, and guaranteeing that both lenders and investors will receive their required financial repayment. Because of the multi-million dollar magnitude of typical proposed solar power projects, solar commercialization is truly entering the domain of "big business". The extent to which any solar power technology will succeed in the open marketplace will be determined by its ability to compete with other energy technologies as well as the degree of financial creativity employed by the organizations which undertake to design, construct, and operate future solar plants.

A panel of recognzed experts in the field of solar has been organized to convey views of the continuum of solar business-interests--from the manufacturer to the end-user and the all-important area of finance. Each panelist will offer observations based on his partiacular experience in the overall area of solar and alternate energy systems. These views will be of direct practical value to developers of solar dish hardware.

# ABSTRACT OF REMARKS FOR THE PANEL DISCUSSION
# BUSINESS VIEWS OF SOLAR ELECTRIC GENERATION
# DECEMBER 7, 1983

**EDWARD H. BLUM**
**MERRILL LYNCH CAPITAL MARKETS**

## FINANCING COMMERCIAL SOLAR POWER

- In 1982-3, ML has raised over $200 MM for renewable energy projects totalling roughly $250 MM. The area is attractive.

- Keys to financing are:
  - -Technological quality & guarantees
  - -Strengths of the organizations responsible for the project
  - -Attractive economics, based on reliable numbers

- Technology
  - -Investors' perception is that solar is desirable and attractive, but not yet reliable or economic.
  - -Key concern is technological reliability and performance.
  - -Technological problems have occurred and been widely reported. Investors want evidence and/or assurance that they will not experience problems and/or losses.
  - -Since experience with all solar technologies is necessarily limited, investors want to see strong performance guarantees and financial strength supporting those guarantees.
  - -Time until major failures and overall equipment lifetimes remain open questions.

- Organizational Strength
  - -Failures of small energy companies, and weak financial conditions of some solar/wind suppliers, stimulate a preference for proven financial and management strength.
  - -Smaller firms may need support/guarantees from financially strong companies.
  - -Strength needed not only to support technology, but also to satisfy concerns under securities and tax laws, and for marketing to individuals and to institutions.

- Economics
  - -Need attractive, competitive rate of return -- higher for technologies perceived as riskier or newer.
  - -Financing structures needed to obtain these returns for relatively expensive technologies are sensitive to details of tax law that may change. Deals work now, but may need new structures in 1984 or 1985.
  - -A few wind deals work without state tax credits, but even these still need the Federal ETC. All solar deals still need both the ETC and state credits.
  - -If the ETC is not extended, costs must decrease rapidly to obtain financing after 1985.

# BUSINESS VIEWS OF SOLAR ELECTRIC GENERATION

ROBERT DANZIGER

SUNLAW ENERGY CORP.

The speech focuses on two primary themes: competition and technical risk. Competition is discussed to illustrate the likely business environment developing technologies will encounter. Technical risk is analyzed from the perspective of capital markets.

Inter-fuel competition is highlighted because the economics of private power production hinges upon the power purchasers' alternate cost of energy. For example, oil and gas-fired cogeneration competes with, and will largely displace, utility base and intermediate load oil and gas units. Closed-cycle systems such as coal, coke, biomass or waste-fired fluidized bed systems will compete with the remaining displaceable utility oil and gas units. Therefore, technologies not proven until the 1990's will be competing with the utility's only other displaceable fuel: coal.

Inter-technology competition is just now heating up. For example, solar ponds, point-focusing dishes, solar central receivers, photovoltaics, and all other peak-coincident systems are in direct competition to supply Southern California Edison's summer peak requirements. However, it must be remembered that peak periods are only 16% of the year. As with virtually all plant and equipment, powerplants must generally operate 40% to 80% of the year to be profitable. Thus, even peak-shaving technologies must be able to hold their own against the better utility units in order to make money during these economically vital mid and off-peak hours.

Although inconsistent with generally-accepted views of technology development, it is true that large institutional and corporate funds will not be available until a technology has at least 10 years of good operating experience. Until then capital will come from small, non-brokered limited partnerships. The only proven way to circumvent this problem is to have a vendor or engineering firm take all technical risk including: useful life, consequential damages, performance, and availability. In addition, the guarantor should expect to undertake risks that are technically impossible but financially conceivable. For example, one lender required insurance against a steam turbine rotor twisting twice in 3 years where there had been no such event in 40 years of operation. In the same project the lender wanted an option to truck steam and an engineering report that a gas turbine could not be used as an apartment.

# McDONNELL DOUGLAS ROLE IN SOLAR THERMAL SYSTEMS

Richard J. Faller

McDonnell Douglas Astronautics Co.
Huntington Beach, CA 92647

## CENTRAL RECEIVER SYSTEMS

- 12 years of developing designs and applications for solar central receivers.
  - Seven electric utility and industrial process heat repowering conceptual designs.
  - Advanced conceptual design for electric utility repowering.
  - Total system designs for industrial applications.
  - Proposals for desalination, off-grid electric designs.
- Played major role in technical development of solar central receivers - The Solar One Pilot Plant.
  - Solar One plant design.
  - Integrated microprocessor control system design and hardware.
  - Successful operation to date:
    - Demonstrated 10 MWe net power from receiver 10/82
    - Demonstrated 7 MWe net power from storage 2/83
    - Demonstrated 12.1 MWe net power 6/83
- Playing major role in commercialization of solar central receivers.
  - Joint conceptual design with Edison and Bechtel.
  - Financial/legal development of the demonstration project - Solar 100

- o Played lead role in heliostat development.
  - Five generations of design development.
  - Commercial design.
- o System and heliostat experience springboard for business expansion.

BUSINESS EXPANSION

- o MDC Objectives to introduce commercial products as economics permit.
- o Evaluated several solar energy concept options.
- o Dish electric.
  - Joint MDC/United Stirling study during past year.
  - Evaluated sales potential, design concepts, product costs, operations and maintenance costs, pricing strategies and business economics.
  - Developed agreement for cooperative endeavor between MDC and United Stirling and obtained approval.
  - Started development program.
  - Test program to start in the fall of 1984.
  - Commercialization start targeted for 1986-1988.

# Business Views of Solar Electric Generation

Summary of Remarks
J. Lynn Rasband
Utah Power & Light Company

Between 1975 and 1980, Utah Power & Light Company experienced a load growth rate of approximately 8% per year. During the 1970's, which was a rapid growth era, UP&L placed 400-megawatt, coal-fired generating units on-line in 1974, 1977, 1978, 1980, and 1983.

Recently with reduced economic growth within UP&L's service territory, the load growth has dramatically dropped. We negotiated with all participants in the Intermountain Power Project to half its capacity and also reduced our participation share from 25% of 3,000 megawatts (750 megawatts) to 4% of 1,500 megawatts (60 megawatts). We also rescheduled Hunter No. 4, a 400-megawatt, coal-fired unit, to be operational in 1991 instead of 1985. The annual load growth for the next five years (1983-1988) is expected to be approximately 3.5%.

Although UP&L's margin is above that which would allow for additional capacity additions at the present time, by 1986 small generating units such as parabolic dish solar thermal power units could be justified and would be scheduled to come on-line so that the UP&L system capacity margin or reserve would be held at approximately 20%. Such small generating units would have to produce power competitive with our avoided cost rates which are presently being considered by the Utah State Public Service Commission. In the past, these rates have been below 3 cents per kilowatt hour.

"PGandE View of Solar Electric Generation Development"

C. J. Weinberg

Pacific Gas & Electric

Solar Energy is facing its toughest challenges to date:

- Low projected utility avoided costs due to reduced oil prices and increased availability of natural gas;
- Low projected rates of utility load growth due to effective conservation programs and higher energy costs;
- Expiration of the federal solar tax credits in 1985;
- A difficult road ahead in the 1984 congress for legislation to extend the tax credits;
- Withdrawal of DOE support for bridging solar development costs.

The new National Energy Plan states that we must have a balanced mix of energy sources. What can we do to support the continued development of the solar option? We must continue to push state and federal legislation to extend solar tax credits. The federal government needs to reevaluate DOE's role and reestablish support of solar development costs. Continued development is required to reduce the cost of installation and operation of solar systems, they involve high capital costs since they "buy the fuel up front".

We must also find additional sources of funds to close the development cost gap. Public Utility Commission's must recognize that the cost of closing the economic gap on solar R&D demonstrations must be shared by the residents served. We need to introduce a realistic development program for the future. Much of solar energy was over sold in the 70's.

The road ahead is not going to be easy. It's going to take a real partnership of utilities, government agencies, manufacturers, regulators, financiers and the public to continue the development and growth of solar energy.

# DISTRIBUTED SYSTEMS OPERATING EXPERIENCES

James A. Leonard

Sandia National Laboratories
Albuquerque. NM 87185

Over the past several years, valuable operating experience has been obtained with several distributed systems. The first two papers in this session discuss experience with operations of dish plants in the United States and Australia. The Third paper presents both desirable and undesirable design features of operating systems with troughs as well as dishes.

# SOLAR TOTAL ENERGY PROJECT
# (STEP)
# PERFORMANCE ANALYSIS
# OF
# HIGH TEMPERATURE THERMAL ENERGY STORAGE SUBSYSTEM

D. M. Moore
Georgia Institute of Technology
Engineering Experiment Station
Atlanta, Georgia 30332

The Solar Total Energy Project (STEP) at Shenandoah, Georgia is a cooperative effort between the United States Department of Energy (DOE) and Georgia Power Company to help maximize the potential of solar energy. Sandia National Laboratories provides technical management for the U. S. Department of Energy. The design, operation, and analysis of this point focus system have been supported by a wide range of institutional and industrial organizations. When funded by DOE in 1977 as part of the National Solar Thermal Energy Program, it was the world's largest industrial application of solar cogeneration.

There are 114 twenty-three foot diameter parabolic dishes that track the sun in two axes and provide 11 billion BTUs of energy annually. Heat taken from a heat transfer fluid boils water and superheats steam for a Rankine steam turbine-generator. The design output of the system, under maximum insolation, is 400 kW(e), 1380 pounds per hour of extracted steam for pressing clothes, and 257 tons of air conditioning for cooling the Bleyle garment plant to which the energies are provided.

In 1982 a large number of unexpected electrical and mechanical problems limited experimental operations. However, many lessons were learned from these anomalies that have been totally addressed and resolved. The next generation system should profit greatly by this learning experience. In 1983, system performance tests were initiated, and the thermodynamic design has been validated. Each individual subsystem and component have demonstrated a design basis for future larger systems. A number of prescribed tests associated with this Test Operations Phase have been initiated and will be continued to the middle of 1984. These tests will evaluate total system modes of operation for future commercial type operation.

This technical paper will highlight (1) the 1982 milestones and lessons learned; (2) performance in 1983; (3) a typical day's operation; (4) collector field performance and thermal losses; and (5) formal testing. An initial test that involves characterizing the High Temperature Storage (HTS) Subsystem will be emphasized. The primary element is an 11,000 gallon storage tank that can provide energy to the steam generator during transient solar conditions or can extend operating time. Overnight, thermal losses have been analyzed. The length of time the system can be operated at various levels of cogeneration using stored energy will be reviewed.

## HTS TEST OBJECTIVES

- Energy Storage Capabilities
- Thermocline Stability
- Heat Loss

## HTS TEST # 1

- Heat Tank to 500°F
- Establish 500 - 750°F Thermocline
- Monitor Temperatures Overnight
- Operate System from Storage - 250 kW

## HTS TEST # 2

- Heat Tank to 750°F
- Monitor Temperature Overnight
- Operate System from Storage - 250 kW

## HTS TEST # 3

- Heat Tank to 750°F
- Monitor Temperature Overnight
- Operate System from Storage - 300 kW

# HTS TEST RESULTS

## Energy Storage Capabilities

| | Duration of Test Minutes | Power Level kW | Electricity Produced kWh |
|---|---|---|---|
| Test # 1 | 19 | 250 | 76 |
| Test # 2 | 45 | 250 | 180 |
| Test # 3 | 39 | 300 | 190 |

## Storage Efficiency

| | Energy Stored BTU x $10^6$ | Energy Extracted BTU x $10^6$ | Storage Efficiency % |
|---|---|---|---|
| Test # 1 | 2.60 | 1.89 | 72.7 |
| Test # 2 | 5.63 | 4.41 | 78.3 |
| Test # 3 | 5.58 | 4.51 | 80.8 |

## Heat Loss Analysis

| | Heat Loss 14 Hr. Period BTU | Heat Flux, BTU/HR $FT^2$ |
|---|---|---|
| Design | 168,000 | 15.6 |
| Test # 2 | 326,000 | 30.4 |
| Test # 3 | 228,000 | 26.0 |

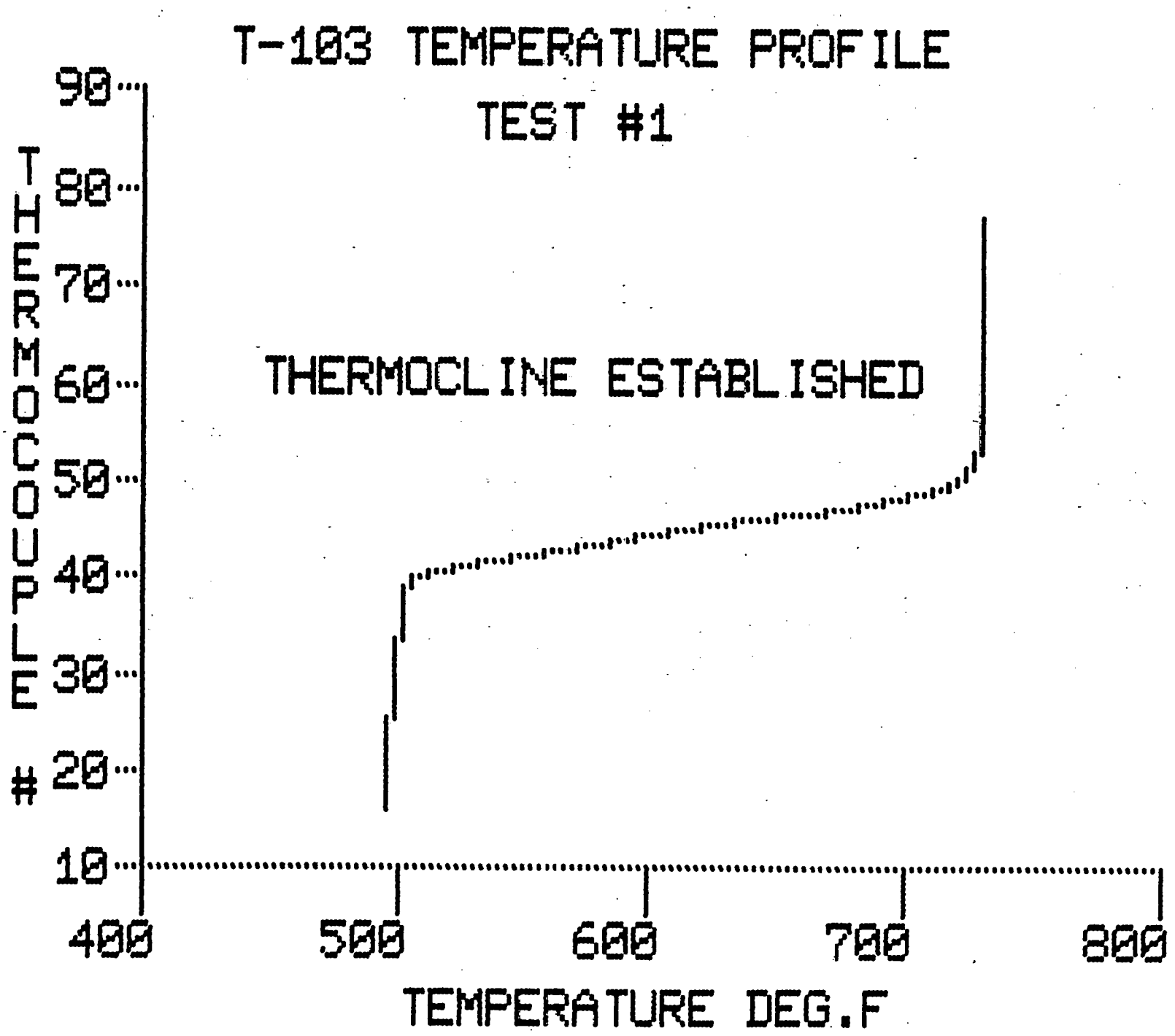
T-103 TEMPERATURE PROFILE
TEST #1
THERMOCLINE ESTABLISHED
# THERMOCOUPLE
90
80
70
60
50
40
30
20
10
400
500
600
700
800
TEMPERATURE DEG.F

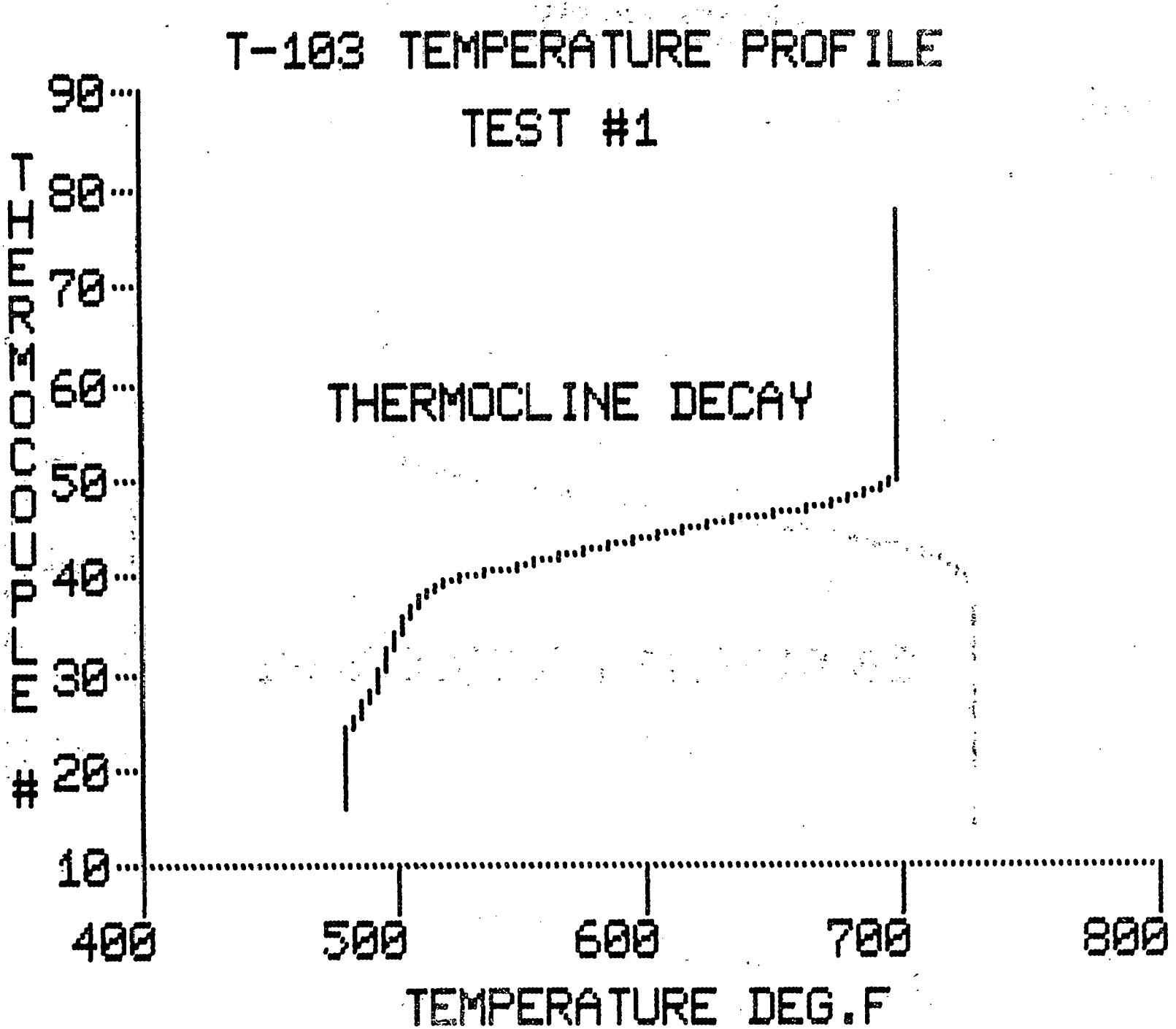
T-103 TEMPERATURE PROFILE
TEST #1
THERMOCLINE DECAY
# THERMOCOUPLE
90
80
70
60
50
40
30
20
10
400
500
600
700
800
TEMPERATURE DEG.F

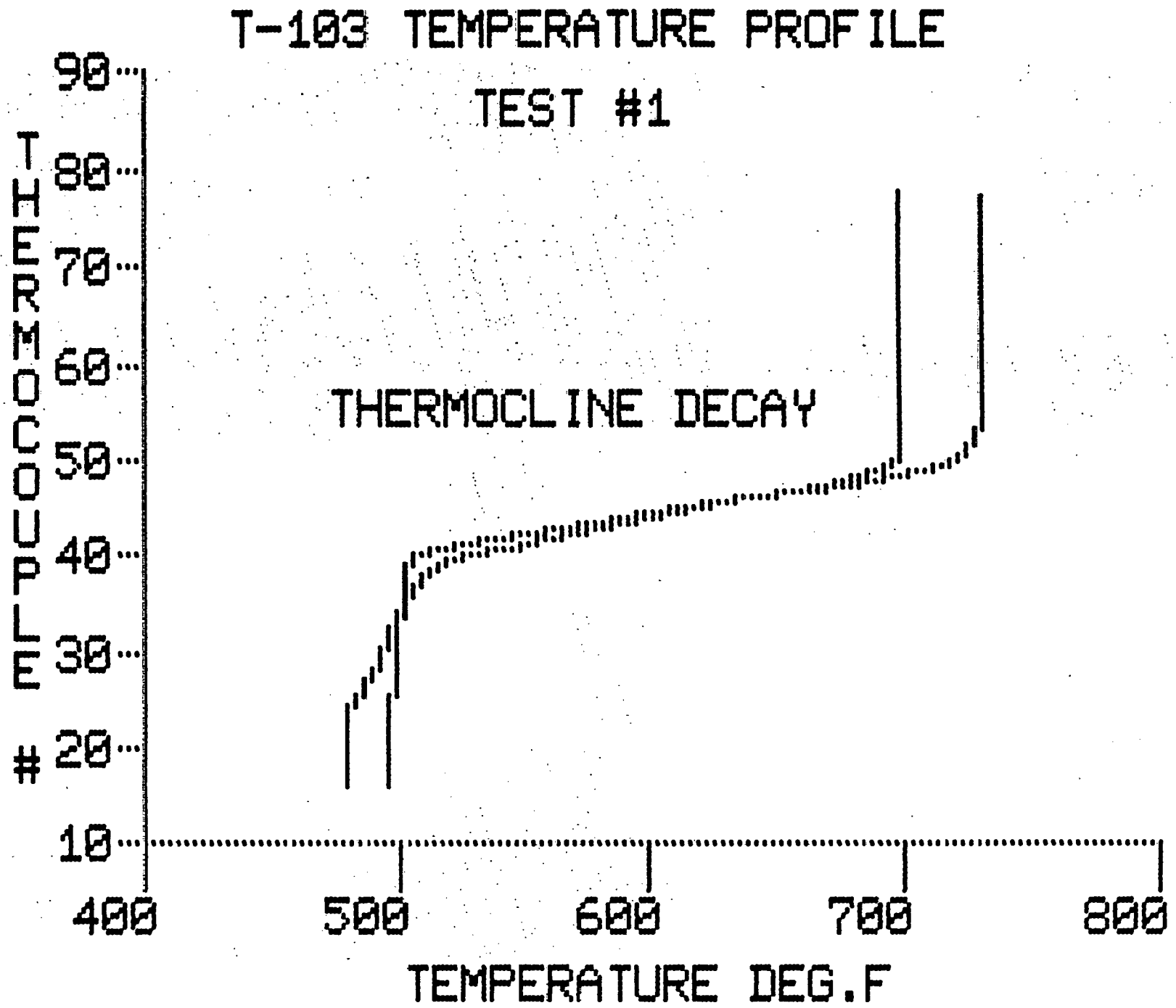
T-103 TEMPERATURE PROFILE
TEST #1
THERMOCLINE DECAY
THERMOCOUPLE #
90
80
70
60
50
40
30
20
10
400
500
600
700
800
TEMPERATURE DEG.F

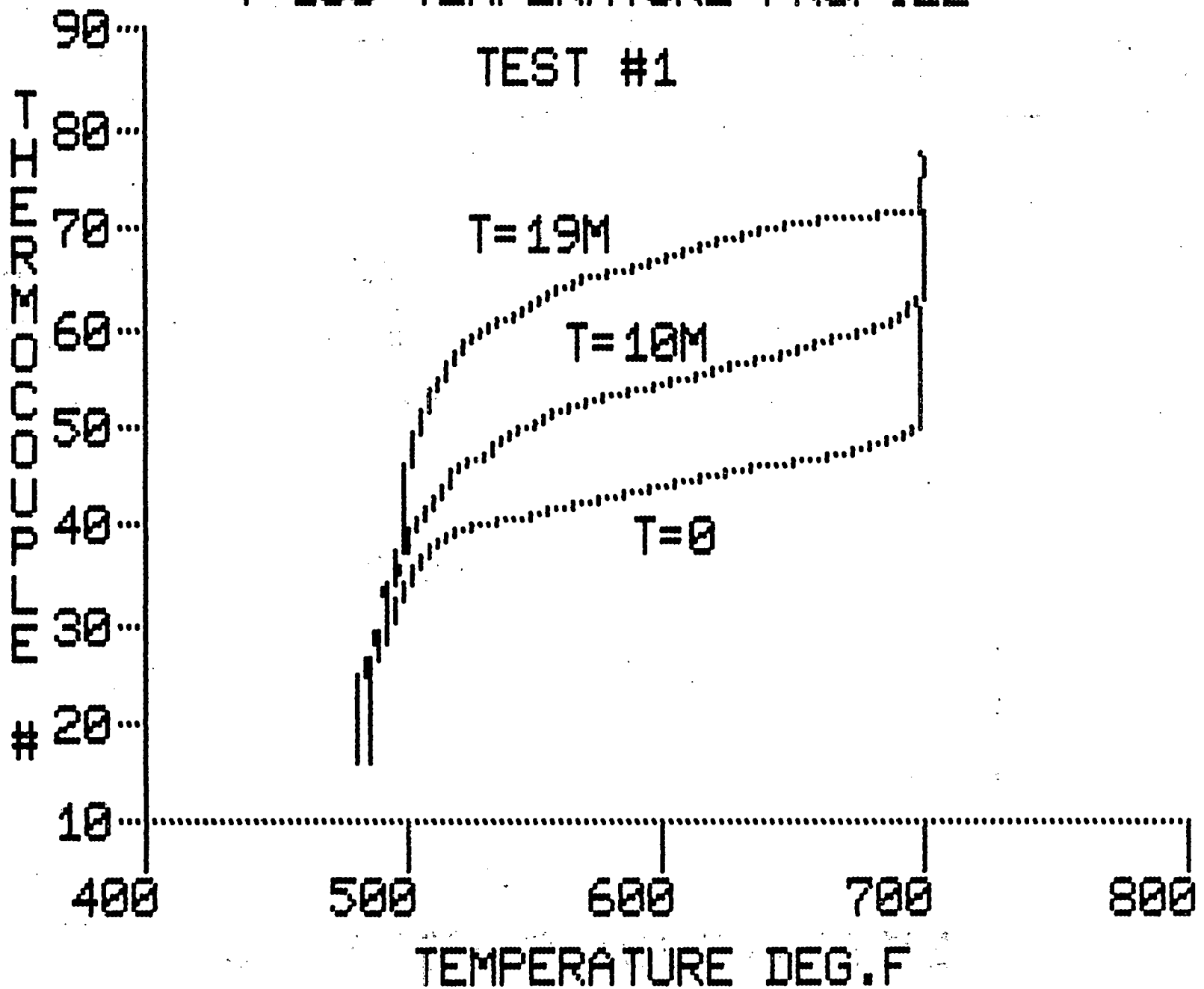
T-103 TEMPERATURE PROFILE
TEST #1
T=19M
T=10M
T=0
THERMOCOUPLE #
90
80
70
60
50
40
30
20
10
400
500
600
700
800
TEMPERATURE DEG.F

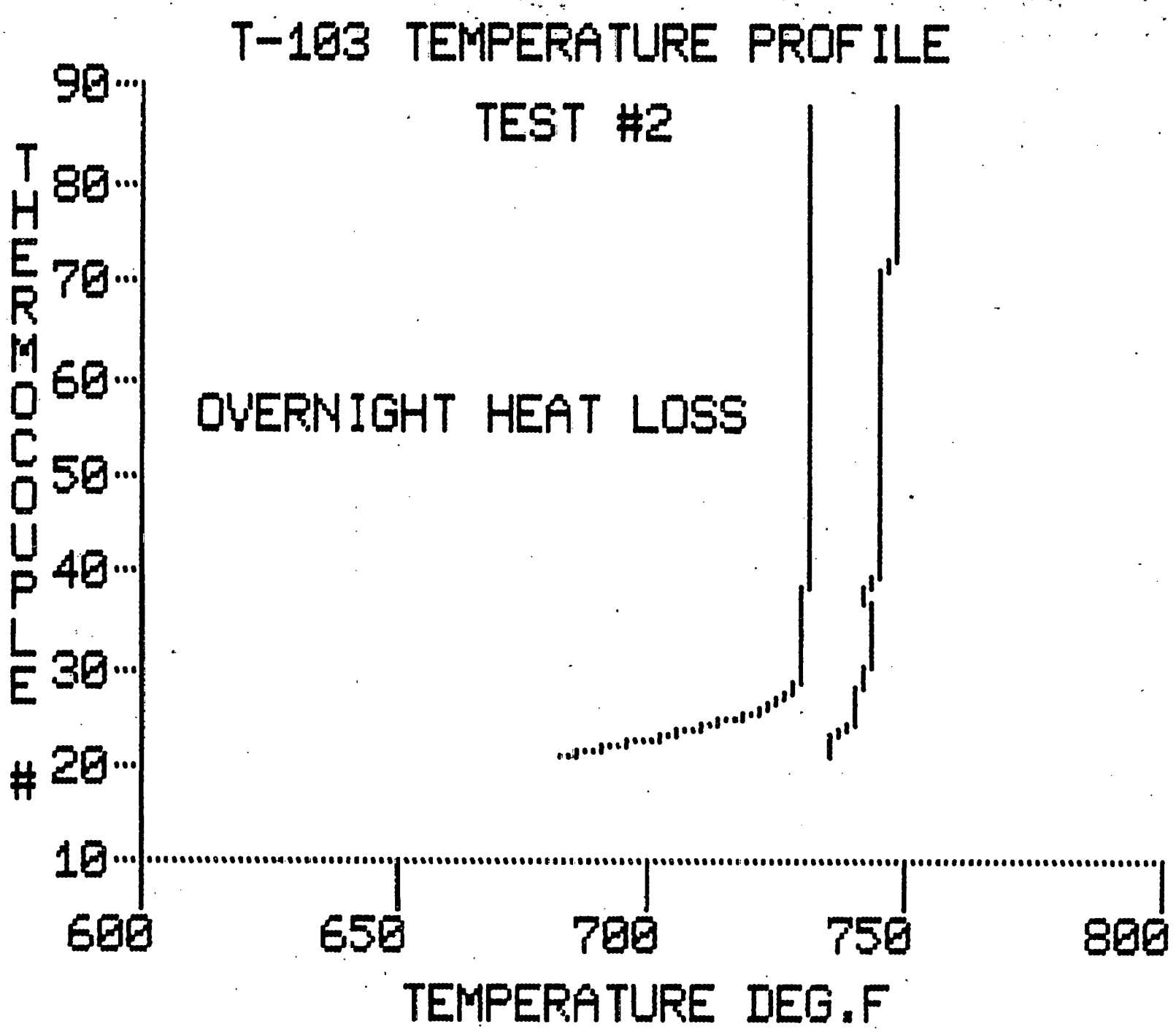
T-103 TEMPERATURE PROFILE
TEST #2
OVERNIGHT HEAT LOSS
# THERMOCOUPLE
90
80
70
60
50
40
30
20
10
600
650
700
750
800
TEMPERATURE DEG.F

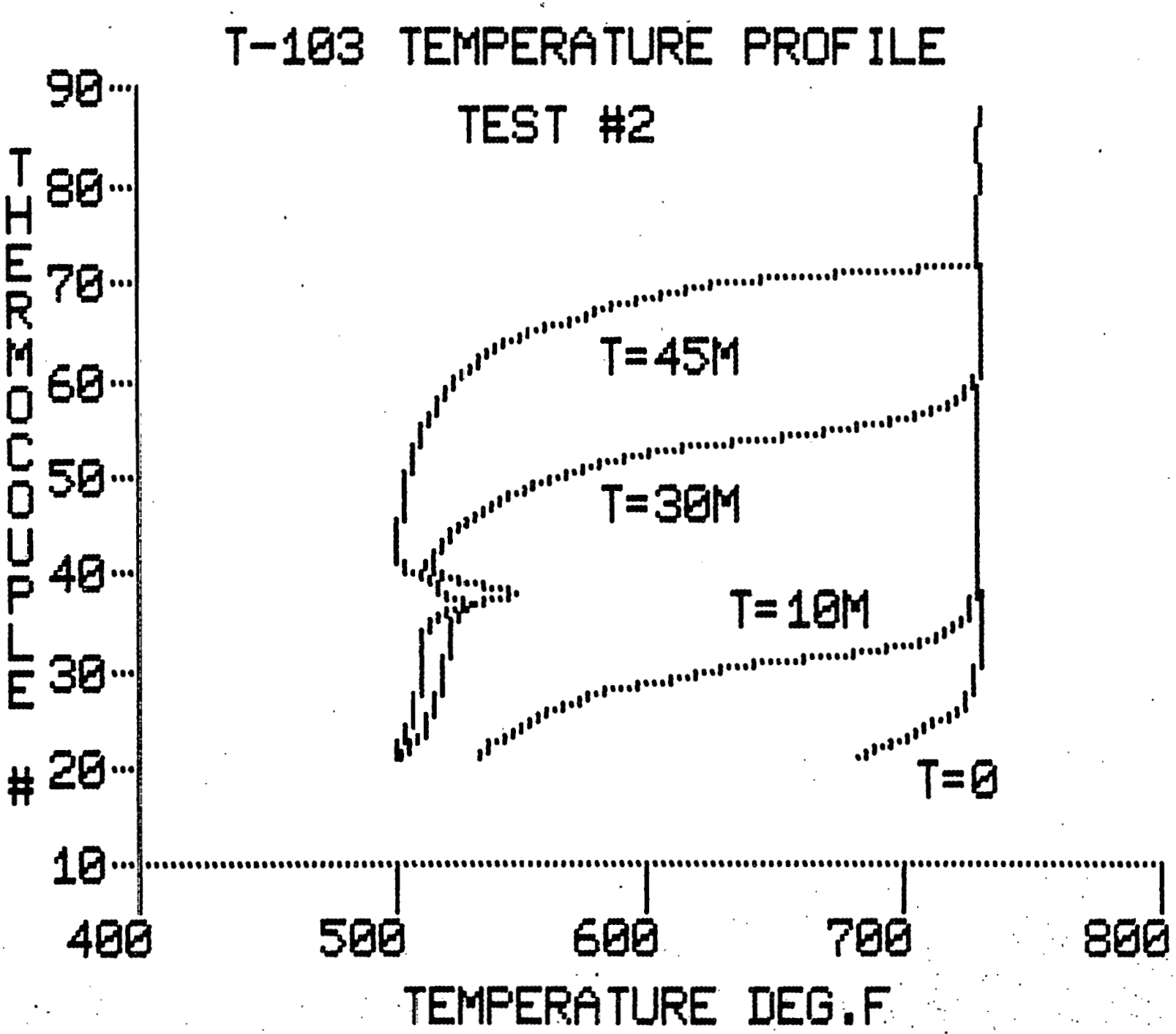
T-103 TEMPERATURE PROFILE
TEST #2
THERMOCOUPLE #
90
80
70
60
50
40
30
20
10
T=45M
T=30M
T=10M
T=0
400
500
600
700
800
TEMPERATURE DEG.F

# WHITE CLIFFS - OPERATING EXPERIENCE

Stephen Kaneff

Department of Engineering Physics
Research School of Physical Sciences
The Australian National University
Canberra. A.C.T. Australia

ABSTRACT

Developmental work for the fourteen dish White Cliffs Solar Power Station commenced in July 1979; engineering design started in August 1980; and construction was completed in December 1981. Experimental running of the full system commenced in March 1982, design specifications were met by June 1982 and robust reliable operation was established by June 1983. The system now supplies the small township on a stand alone basis (with diesel back-up) and runs automatically and largely unattended; handling being by local personnel.

The area is remote and subject to extreme environmental conditions, solution of the associated problems required careful and thoughtful attention and the application of resources. Notwithstanding the wide range and harshness of conditions, the difficulties caused by remoteness and the lack of a technological base and the need for relatively rapid demonstration of success, the project has had a very positive outcome. Qualitative and qunatitative information and lessons are now available to enable considerable simplifications to be made for a new system, reducing both hardware and operation and maintenance costs.

Experience and lessons from the project are presented, particularly in relation to: system performance in various environmental conditions; design philosophies for collectors, the array, control systems, engine and plant; operation and maintenance strategies and cost reducing possibilities. Experience so far gives encouragement for the future of such paraboloidal dish systems in appropriate areas.

## 1. INTRODUCTION

Description and performance information for the White Cliffs Solar Power Station has already appeared elsewhere (for example, Kaneff 1983a, 1983b, 1983c, 1983d); the following details therefore serve as a brief reminder of station details:

The White Cliffs project is intended primarily to help ascertain viability of paraboloidal dish systems in providing energy and water for Australia's inland and remote areas. The small opal mining town of White Cliffs (1100 km west of Sydney) was chosen because it had no existing power supply and is sufficiently remote to provide an authentic environment. Experimental and theoretical investigations commenced in July 1979, engineering design in August 1980 and construction was completed by December 1981; output specifications were met by June 1982 and continuous reliable operation was established by June 1983. The station now supplies the township on a continuous round-the-clock basis

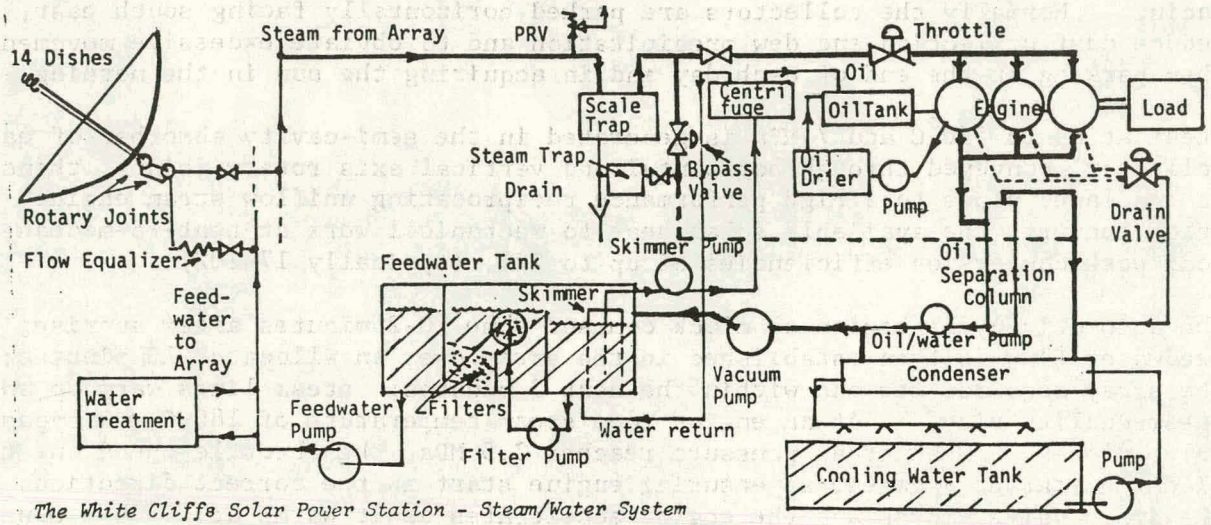


*The White Cliffs Solar Power Station - Steam/Water System*

Figure 1.

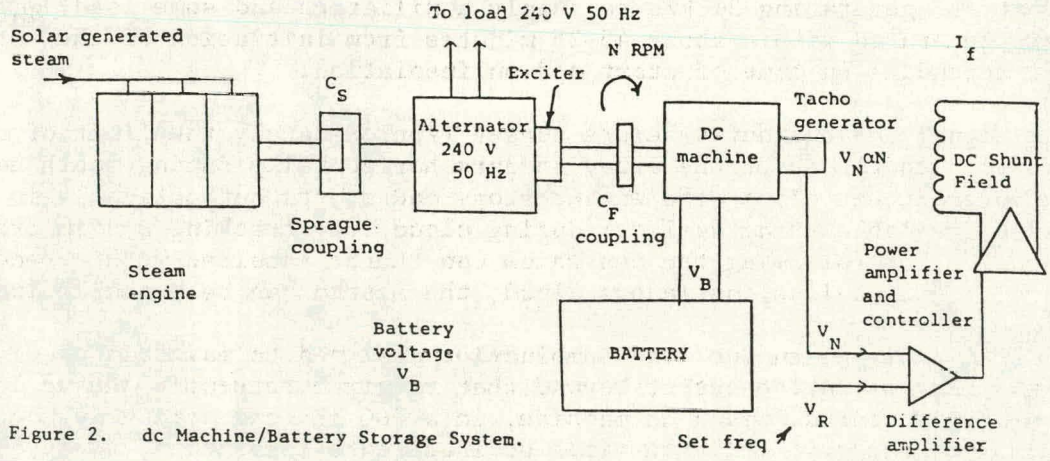


Figure 2. dc Machine/Battery Storage System.

that is, stand alone (with diesel back-up).

## 1.1 System Description

Figures 1 and 2 portray the installation which produces 25 kWe and over 100kW low quality heat at an insolation level of 1 kW/m$^2$ and comprises 14 modular semi-autonomous paraboloidal tracking collectors, each 5 m diameter with fibreglass substrate and plane mirror tile reflecting surfaces(2300 tiles per collector), moving in azimuth and elevation driven by printed circuit motors through actuators and controlled by dish-mounted sun sensor. Each collector carries its own battery supply, charged from the central plant.

A central controller intrudes on the modular units only to give instructions for starting, offsteering (in case of steam or energy flow balance failure), stopping and parking (normal or strong wind mode). In the event of central control failure, each collector can continue operation, close down, park and offsteer (in response to absorber overheat). The collector array operates at wind velocities of up to 80 km/h, above which it parks automatically, vertically

facing. Normally the collectors are parked horizontally facing south east, to reduce dust collection and dew precipitation and to obviate excessive movement when parking at the end of each day and in acquiring the sun in the morning.

Steam at up to 550°C and 7 MPa is generated in the semi-cavity absorber of each collector, conveyed through horizontal and vertical axis rotary joints, thence in insulated pipes to a high performance reciprocating uniflow steam engine which converts the available solar heat to mechanical work at heat-to-mechanical work conversion efficiencies of up to 22%, (typically 17-20%).

The automatic cycle begins on clock command some 10-25minutes after sunrise; feedwater flow is then established in the array over an allocated 10 minutes; the array acquires the sun within the next 3 minutes; steam lines warm up and steam quality rises. At an engine room steam temperature of 180°C, the bypass valve closes. When steam pressure reaches 2.5 MPa, the throttle opens and the electric starter engages, so ensuring engine start in the correct direction; the drain valve closes and the engine accelerates as it warms up. On a sunny day engine start occurs some 12-6 minutes after the array is first tracking; within a further 20-6 minutes, the engine is delivering useful power to the load(that is, generating 3+ kWe to supply auxiliaries and some load). Useful power is generated within about 45-25 minutes from initiation of the 'start' signal, depending on time of start and on insolation.

A clock signal 30-40 minutes before sunset (approximately the limit of useful nett power output) causes the array to park horizontally facing south east. During intermittent cloud, the engine stops and starts automatically in accordance with available steam quality; during cloud, the tracking system provides timed pulses for following the sun which can then be acquired within seconds of emerging. For obvious continuous cloud, the system can be manually locked out.

Figure 2 depicts the engine/load combination designed to maintain energy flow balance. Excess engine output beyond that required to supply the ac load at any moment, is stored, via a dc machine, in a 760 ah lead acid heavy duty traction-type battery, while in times of inadequate insolation, energy is drawn from the battery to drive or help drive the alternator and supply the town. In the absence of sunlight, the battery/dc machine alone drive the alternator, the steam engine being stationary, a situation facilitated by a free-wheel (ratchet) type coupling between engine and alternator. Storage available is intended to cope with overnight requirements but if the battery is discharged before further solar energy is collected, a back-up diesel unit starts automatically to supply the load. A flash boiler permits engine testing and acts as an emergency supply if the diesel set is out of service.

## 1.2 Performance

Robust economical hardware was sought, construction being based on agricultural and automotive practices. Dish manufacturing tolerances were relaxed by permitting a 'fuzzy' focus which nevertheless allows 95% of reflected energy to be intercepted by the semi-cavity absorber 160 mm diameter and 160 mm long, which is accordingly subject to relatively low heat stresses.

Figure 3 shows collector performance as a function of insolation level and steam temperature. Figure 4 is the cascade diagram at stated sun and engine-room conditions; while higher steam quality can be achieved in the engine-room,

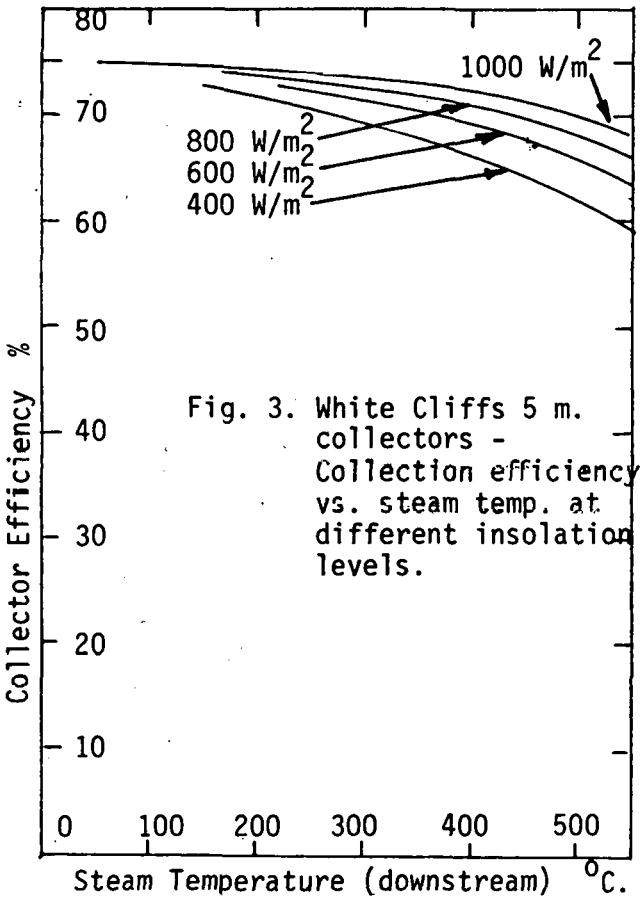


Fig. 3. White Cliffs 5 m. collectors - Collection efficiency vs. steam temp. at different insolation levels.

system output is not necessarily higher and may be lower, due to enhanced losses. Figure 5 shows the generated electrical power profile for operation when peak insolation was 874 W/m$^2$. Useful nett electrical output flows from 50 minutes after sunrise until 30 minutes before sunset in this case and depends on feedwater flow as well as on insolation. (Distortion at the start of the curve for insolation is caused by a small hill). Figure 6 shows the steady state relationship between insolation and gross electrical output.

It may be noted from Figure 6 that at insolation levels below about 400 W/m$^2$, there is inadequate output generated to make up the power taken by auxiliaries (that is, a little over 3 kWe). Generally the array collection efficiency increases as insolation increases (at given steam operating temperature).

Figure 4. WHITE CLIFFS SYSTEM PERFORMANCE AT INSOLATION OF 1 kW/m$^2$ AND STEAM CONDITIONS: 360°C, 6·0 MPa. (into engine)

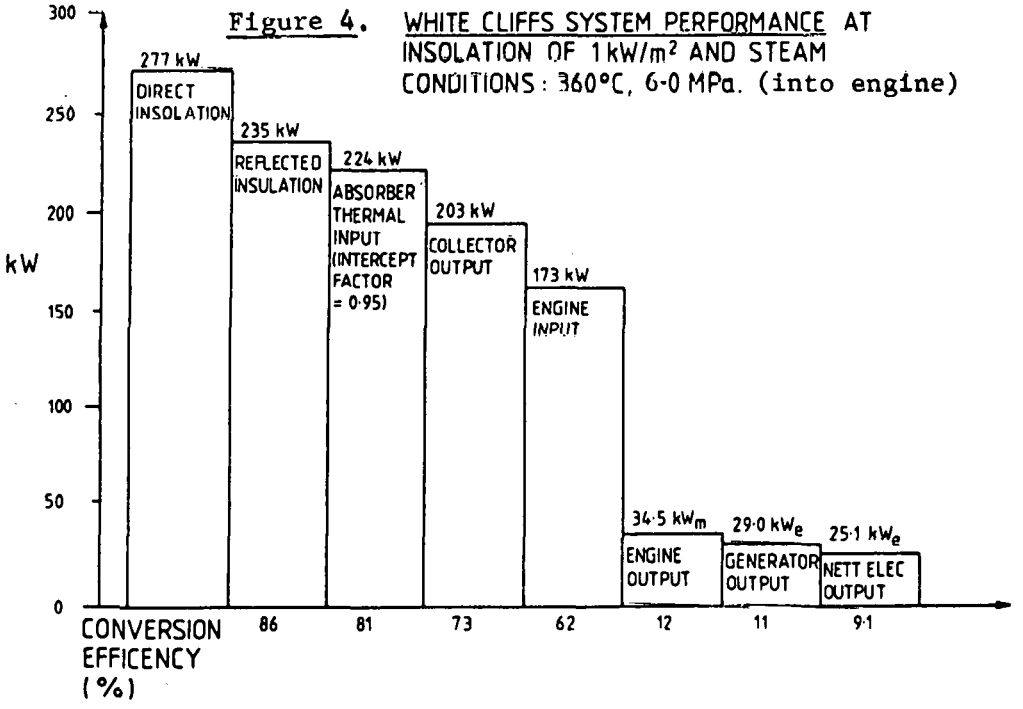

## 2. ENVIRONMENTAL EXPERIENCES

White Cliffs' climate is typical of much of that of inland Australia, with an irregular rainfall whose average is well below 25 cm (10 inches) per annum. Much of this precipitation appears as thunderstorms which cause sporadic flooding at times. During good years (1983 for example), the whole countryside is carpeted with greenery; animal and bird life abound and insolation is more uncertain than normal. At other times (most of the time) conditions become extremely dry and dusty, with much sunshine.

### 2.1 Insolation and Cloud

Figure 7 depicts the hourly and seasonal variations in direct insolation for White Cliffs according to a well known formula. But our records over the past 4 years have frequently recorded higher values than these, especially following rain (suggesting that atmospheric dust plays an important part in the process). It is not uncommon during the period October to March for peak insolation to exceed 1 kW/m2 (even reaching 1.07 kW/$m^2$ on rare occasions.

Meteorological records for the White Cliffs region show approximately 3000 hours of sunshine per year and an incident energy of around 2100 kWh/$m^2$ per annum. Our records for 1980 show some 2400 kWh/$m^2$ per annum, a figure which should be compared with the values of Table Iwhich shows an ideal situation for mean energy/day/$m^2$ and mean peak insolation for each month on the basis of 100% sunny days - total annual incident energy would then be 3390 kWh/$m^2$.

TABLE I. Mean Energy per Day and Peak Insolation Level at White Cliffs for Ideal Conditions

| Month | Jan. | Feb. | Mar. | Apr. | May | June | July | Aug. | Sept. | Oct. | Nov. | Dec. |
|---|---|---|---|---|---|---|---|---|---|---|---|---|
| Mean energy kWh/day/$m^2$ | 11.1 | 10.5 | 9.44 | 8.25 | 7.25 | 7.0 | 7.2 | 8.95 | 9.41 | 10.45 | 11.1 | 11.25 |
| Mean Peak Insolation W/$m^2$ | 947 | 944 | 938 | 920 | 890 | 885 | 890 | 920 | 938 | 944 | 947 | 948 |

But the above figures for incident energy per year disguise the form and content of the available useful insolation. While, as may be expected for areas which are reputedly very sunny, many days over the year are completely sunny, and very few are completely cloudy. But a surprisingly large number of days are only partly sunny: these may be considered in three categories, days in which:

(1) a contunuous band of sunshine is followed by a continuous band of cloud or vice versa (such as occurs when a cloud front arrives or existing continuous cloud clears). The system operation in such circumstances is straightforward.
(2) intermittent cloud is present - a surprisingly frequent phenomenon which can occur at any time of year but particularly in summer. What is often involved is the local formation of a matrix of very slow-moving clouds in the early afternoon lasting until late afternoon. Mechanisms involved

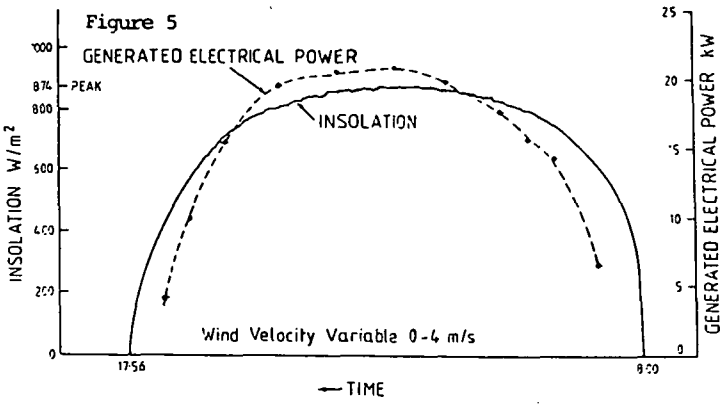


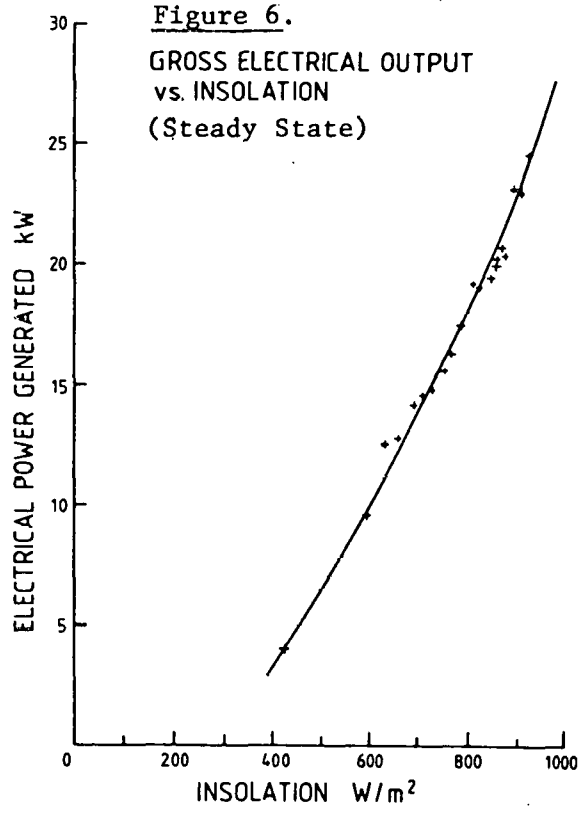


appear to be the formation of 'chimneys' of hot air rising from the ground in a relatively stable pattern accompanied by the formation of a corresponding stable pattern of cloud which moves but slowly, causing insolation at any given point to vary from full sunshine to shadow. The periods of sun and shade vary typically in the range of a few minutes to 20-30 minutes - sometimes the clear periods are longer, and sometimes they are the shorter. In such circumstances the solar steam system operates in accordance with the steam quality available, running and stopping in turn. While the station auxiliaries (especially the feedwater pump, the water and oil circulating and treatment pumps and the cooling water pump) are running continuously, some 3 kWe energy is expended. If there is no steam energy, this quantity has to come from the batteries. It can happen, therefore, depending on the mark-space ratio of the sun/shade, that there may be a nett overall loss of energy while running in this mode, or at least the nett useful energy over the operating period may not be worth the trouble to run.

Even relatively short spikes of shade can cause momentary loss of superheat from which the system takes time to recover. This kind of operation requires special attention.

(3) haze due to sparse cloud, water vapour and/or high level dust is present, lowering the mean insolation level usually with a characteristic 'spikey' profile, with the insolation varying by a significant amount in relation to the total insolation - the spikes are frequent (every minute of so, sometimes less frequent). Apart from lowering steam quality and station output, neither the steam system nor the engine can reach temperature equilibrium and overall efficiency is lowered as is output.

Coping with the above situation presents problems of operating strategy which needs intelligent decisions. A heat store of some tens of minutes' capacity would go some way to improve performance in these conditions (as the current amount of heat stored in the steam system is small, involving only heat capacity of steam lines and insulation)but the cost effectiveness of this has yet

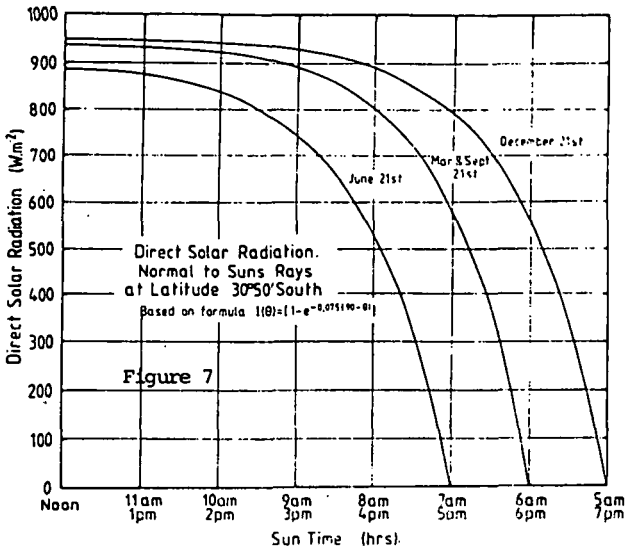


Figure 7

to be resolved and there are grounds for expecting better returns from an automatic fossil fuel burner inserted just before the engine to maintain good superheat.

In the meantime, the station operations manager relies on judgement and prediction of insolation conditions when situations (2) and (3) above arise, as to whether or not to run or continue to run the solar steam system (adding superheat from a fossil fuel in this case is quite efficient, more so than running the diesel back-up system).

Were a new multidish central plant system to be designed, a viable option might be to run all dishes except a small number near the plant at lower temperatures, even wet steam, then to add the superheat from the dishes near the plant; a fossil fuel burner could then be added close to the engine to cope with the abovementioned problems.

2.2 Wind

White Cliffs is located on a relatively flat plain with occasional small hills some tens of metres high. Available meteorological information is sparse and does not provide an adequate or true picture of wind conditions. The area is obviously very windy and local observers report harrowing tales of past storms. Our records over 4 years at the solar site (anemometers at 7 m and 30 m above ground) and on a nearby hill (25 m higher than the site) show that whereas the wind normally dies down at night at the 7 m level, at 30 m above ground and on the hill, the wind almost never stops, with an average velocity of about 7 $ms^{-1}$ (making this an excellent site for wind generators).

The wind can be described as being very strong and gusty during the day quite frequently, strongly buffetting the collectors. Although generally strong, winds are not unduly so and the 80 km/h speed for which the array is designed to park vertically upwards has been exceeded only once on our records at a time when the dishes were already parked vertically; but speeds have approached the park value many times. Although extremely strong winds are uncommon, during its daily operation the array experiences very severe buffetting from the wind especially from late spring to early autumn and steep velocity fronts cause sudden mechanical shocks. Apart from unpleasant effects on people, the wind influences on the solar system include:

(1) perturbation of array tracking - because of general structural resilience (enhanced by the relaxation of rigidity and backlash criteria in order to reduce costs), the presence of strong buffetting winds (particularly from certain directions in relation to collector orientation) can readily cause perpetual hunting of the altitude/azimuth drives, unless appropriate precautions are taken. The designed solution was to permit only intermittent drive, not

continuous - sun sensor signals which denote tracking errors, are allowed to correct the collector orientation to produce zero error but the drive circuits are then inhibited for 10-15 s before further operation is allowed. This strategy has proved extremely satisfactory under all experienced operating conditions and produces a tracking which is more than adequate for the purpose (better than $\pm$ 0.15° pointing error).

(2) the raising of dust clouds and the blowing and depositing of dust onto the collectors - but fine dust particles which settle can also readily be blown off by strong winds, tending to reduce the effect.

(3) the convecting away of heat from the semi-cavity absorbers. This is the most substantial problem from wind and tends to counter the benefits of simplicity of design. In strong winds each absorber can lose more than 1 kW thermal energy above a no-wind condition. This loss is avoidable so that new protected absorbers, closer to a true cavity, are being installed to reduce this substantial loss.

(4) the depositing of large quantities of dust in plant rooms as a result of wind blowing from a particular direction and sometimes by dustladen whirlwinds which more often than seems reasonable, choose a path to the plant.

(5) sudden mechanical shocks on all components arising from wind changes (in some cases wind velocity fronts starting from almost still air to 30 $ms^{-1}$ within one minute or so).

## 2.3 Precipitation

The effect of rain is only slight because of its infrequent occurrence. Most clouds moving over White Cliffs, although reducing solar energy, seem reluctant to part with their moisture. When rain does fall, it is useful in partly washing the dishes but the action is incomplete - some residual dirt remains.
Dew, which is frequent in spring and autumn, and results in several litres of condensate on each dish, acts to consolidate part of the deposited dust on the mirrors.

## 2.4 Dust

Both coarse low level dust blown up by strong winds and high level fine dust occur in abundance in the inland. The former is not a problem since it rarely deposits or remains on the mirrors. The latter often reduces insolation directly and also produces a frequent deposit of fine dust on the dishes and on all other components.
Dust of one kind or another has to be accepted as a fact of life and equipment designed accordingly, either dustproof or dust tolerant. With this in mind, all components have been produced successfully to live with the problem of dust. However the mirrors are regularly affected and, unless cleaned, can suffer an energy loss of up to 20% after a few weeks - this loss removes valuable superheat and is a serious effect.

Cleaning of dishes is therefore considered desirable and is carried out with a frequency of 10-30 days, depending on the state of the mirrors. Because of the absence of grime and due to the fact that the consolidated particles are

very small, cleaning is carried out by manually rubbing with a large lambswool pad mounted on a long flexible tube- this cleans and polishes the mirrors in a time typically 5-10 minutes per dish, depending on its state. To remove tedium, however, we are experimenting with automatic cleaning devices.

2.5 Extremes of Temperature

Temperatures from just below freezing in winter to well above 40°C (up to 47°C) in summer are a feature of the White Cliffs' climate. Humidity in summer can also be a problem. Equipment is not difficult to make tolerant of these conditions and no anti-freeze protection is used in the steam system which is always, to some extent, charged with water when the system is not running.

In summary, although the environment is harsh and inhospitable on occasions, by applying appropriate design and operating strategies, any problems can be coped with reasonably readily.

3. HARDWARE EXPERIENCE

The solar array has presented extremely few problems. During the early phase of collector development, several options were considered and eventually fibre-glass substrates were selected in stead of the initially preferred pressed metal shells due to a perceived inadequate time to perfect the various processes involved. In operation over the past two years no technological changes have been necessary to the array (but we are currently improving the absorbers to improve output by reducing wind convection losses). Tracking performance has been equal to all encountered conditions.

All control, electrical and electronic systems worked from the start and have continued to operate trouble-free. A particularly valuable feature during the commissioning phase has been the facility for manual or automatic operation.

The engine and steam system, on the other hand, required by far the major part of time and resources to develop. In the absence of commercial units of adequately high efficiency, an experimental high performance uniflow reciprocating steam engine was selected on the basis of steam car experience - realised by converting a 3 cylinder Lister diesel engine to steam operation. This was achieved relatively simply and cheaply by retaining engine block, crankshaft and bearings, oil pump and filter, electric starter, flywheel and connecting rods and bearings, but using General Motors' pistons, rings and liners, suitably machined.. Three new cylinder shells were made, each with valve plates, guides and steam chamber and heat shields and three impulse pins were fitted to the tops of each piston. The problem of spare parts was consequently not taxing. Such a converted engine, if produced in relatively small numbers, would cost less than a diesel engine of the same output.

The original conversion, while conceptually sound, required much attention before it emerged as a robust, reliable unit of good performance in everyday operation. Development work was carried out over 18 months on the valve mechanism, the system for extracting oil form the exhaust steam/condensate and on feedwater treatment, all this work being carried out largely on site (1100 km from our laboratory). We consider the steam /engine system is now very satisfactory and applicable in other situations, for example for using crop and other wastes for raising steam and generating elcctricity.

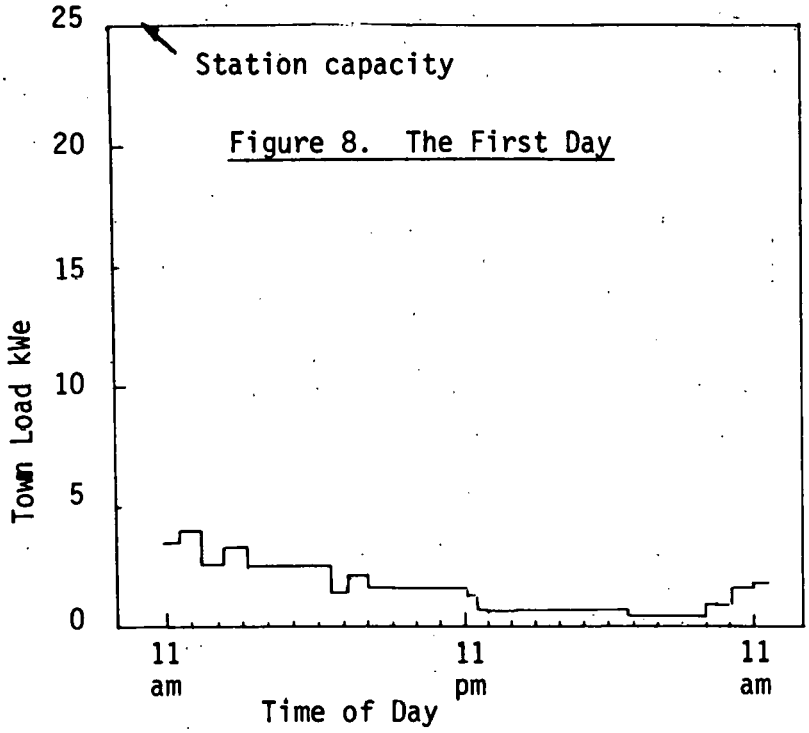


Figure 8. The First Day

### 3.1 Commissioning

Because of the remoteness of the site and the consequent difficulty of carrying out complex maintenance, the New South Wales Government, owners of the station, considered that commercial standard reliability should be established before connecting the supply to the township and leaving it in charge of local people. This phase of the project was completed in June 1983 and the Energy Authority of New South Wales then carried out extensive tests in July and August. Over the approximately 18 months during which the system was operated on 'dummy' load, all manner of operating conditions were successfully coped with. Without change, the system was connected two months later to the town in November.

### 3.2 Supplying White Cliffs

The conventional wisdom in power supply circles suggested that 25 kWe to supply a community of 40-50 people (10 houses, hospital, school, hall and post office as well as street lights) was hardly adequate. The system itself was not sized to power White Cliffs but was determined by other factors; the site was not chosen until some time after other parameters were set.

It was therefore not without some interest that local citizens, Energy Authority and Australian National University personnel gathered at the station site at 11.00 am on November 3 1983. The switch was thrown and the subsequent loads drawn over the next 24 hours were as indicated in Figure 8. When noting the frugal nature of all things in White Cliffs the magnitude of the load is not so surprising. To date the load has not risen above 10 kWe.

Attendance at the station by the operations manager, 7 hours on the first day, has progressively reduced to less than 2 hours per day and should reach less than the1 hour per day targeted in the first few months of continuous operation. Make-up requirements are upt to 10 litres distilled water per day for the steam system and up to 1000 litres of cooling water cooling water on a very hot sunny day.

### 3.3 Practicability

Remoteness of the site has carried with it various logistic problems; but it

did not prove too difficult to establish a field station with adequate resources to handle maintenance and a fair amount of development on site. The level of technology was deliberately chosen to be agricultural/automotive in character so that it would suitably be operated and maintained by local personnel - this philosophy has been vindicated in practice. No problems have arisen over the past 2 years that could not be handled on the spot, except those for which it was decided to change configuration or components and which required machining sophistication. The top end of the engine can be dismantled, adjusted and put together again by one person in less than 4 hours; in 7 hours the engine can be stripped and re-assembled by a person with automotive engine experience.

Confidence has been established that this kind of system is technologically viable for providing continuous electric power on a stand alone basis with diesel back up in areas such as White Cliffs.

3.4 Costs

Overall project costs were approximately $A1 1/4 million, mainly salaries for research and development. Hardware costs for the system as currently on site were $12,500/kWe ($A, Dec. 1981 values). After a period of continuous supply to White Cliffs it is hoped to be able to ascertain the true generation costs.

4. POTENTIAL

White Cliffs has proved robust, reliable and manageable. It has provided valuable experience in two areas of interest which motivated us to carry out the project:

(a) As a means for gaining information towards designing very large paraboloidal arrays for gathering, converting, transporting, storing and utilizing solar energy through the use of thermochemical systems and large central plant with high energy collection efficiency and a range of energy rich products;

(b) to realise a family of modular paraboloidal units suitable as stand-alone systems for remote area supply and for connecting to an electric grid. Our choice of steam Rankine cycle engine was dictated by two factors - no alternative engine was available to us; the engine used was deemed the most likely to be completely maintainable by those living in remote areas.

A new White Cliffs could, by pushing the technology as far as it can go, (better absorbers, better energy transport, shorter lines, more efficient engine, less auxiliary power) might just double its overall efficiency to 18%; so 7 dishes of 5 m diameter would be required, the overall system cost with overnight storage and diesel back-up being about $A6700 (Aug. 1983).

Based on White Cliffs type technology but employing 11 m dishes, and a production run of 15-20 dishes, 30 kWe systems might be produced at around $5000/kWe. An order of magnitude reduction of costs on the current White Cliffs system seems potentially possible through use of the emerging Stirling and Brayton engine technologies when these bacome available.
In the meantime and in the near future, an 11 m dish with azimuth axis mounted steam Rankine cycle engine could have cost and application advantages in the remote areas of Australia.

ACKNOWLEDGEMENTS

The assistance of the New South Wales Government in funding the White Cliffs project, the Asutralian National University for providing resources and facilities and the contributions of the many staff members on the project, are all gratefully acknowledged.

REFERENCES

Kaneff, S. (1983a), "The White Cliffs Solar Power Station", Proceedings Fourth Parabolic Dish Solar Thermal Program Review, Nov. 30-Dec.2, 1982 Pasadena California, Sponsored by U.S. Dept. of Energy, conducted by JPL. DOE/JPL-1060-58, pp. 299-317.

Kaneff, S, (1983b), "The White Cliffs Solar Power Station",Paper 359-3.4.2-D, International Solar Energy Society World Congress, Perth, 14-19 August 1983, 5pp. (To be published).

Kaneff, S. (1983c), "On the Practical and Potential Viability of Paraboloidal Dish Solar Thermal Electric Power Systems", Paper 360-3.6-B, International Solar Energy Society World Congress, Perth, 14-19 August 1983, 5pp. (To be published).

Kaneff, S. (1983d), "The Development of Viable Paraboloidal Collectors for High Quality Heat Production". Paper 361-2.8.1-C, International Solar Energy Society World Congress, Perth, 14-19 August, 1983, 5pp. (To be published).

# Operational Experience from Solar Thermal Energy Projects

Christopher P. Cameron

Sandia National Laboratories

Albuquerque, New Mexico

Over the past few years, Sandia National Laboratories has been involved in the design, construction, and operation of a number of DOE-sponsored solar thermal energy systems. Among the systems currently in operation are several industrial process heat projects and the Modular Industrial Solar Retrofit qualification test systems, all of which use parabolic troughs, and the Shenandoah Total Energy Project, which uses parabolic dishes. Operational experience has provided insight to both desirable and undesirable features of the designs of these systems. Features of these systems which are also relevant to the design of parabolic concentrator thermal electric systems are discussed.

A key design requirement for all solar systems is the ability to operate in and survive a wide range of environmental conditions. In Albuquerque, wind has been observed to increase from less than 20 mph to 60 mph in less than 60 seconds upon the passage of a front while at the same time insolation was adequate for system operation. Since few concentrators can reach a safe stow position in such a short time, the capability to survive wind speeds well above operational limits, typically 25 to 35 mph, when out of the stow position, is highly desirable. Another effect which has been observed is wind-induced oscillation of some concentrators; this has caused significant damage. This possibility as well as the steady state effects of wind (e.g., overturning moments) must be considered in concentrator design. Wind-borne debris, such as small rocks, have apparently caused damage to certain types of glass mirrors. These mirrors have survived hail tests; however, rock can have sharp points which apparently penetrate the surface of the glass. In addition, temperatures well above ambient due to direct insolation on portions of the systems other than the reflectors have led to various problems including damage to the bond in glass-steel laminates and intermittent operation of electronic components.

Other design features discussed are system control functions which were found to be especially convenient or effective, such as local concentrator controls, rainwash controls, and system response to changing insolation. Drive systems are also discussed with particular emphasis on the need for reliability and the usefulness of a manual drive capability.

# OBSERVATIONS ON RATE OF INCREASE OF WIND SPEED

- MISR SYSTEM DESIGN SPECIFICATIONS

  SURVIVAL WITHOUT DAMAGE IN STOW POSITION IN WINDS UP TO 80 MPH.

  OPERATE CONTINUOUSLY IN WINDS UP TO 25 MPH.

  SHUTDOWN AUTOMATICALLY IN HIGH WINDS.

- MISR CONTROL SYSTEM PARAMETERS FOR SHUTDOWN IN HIGH WINDS

  STOW IF WIND CONTINUOUSLY ABOVE SETPOINT FOR A MINIMUM PERIOD OF TIME.

  TYPICAL SETPOINTS
  25 TO 40 MPH
  10 TO 30 SECONDS

- TIME TO STOW FROM FAR HORIZON IS 3 TO 9 MINUTES

- OBSERVED WIND CHANGE AT MISR SITE

  INCREASE FROM LESS THAN 20 MPH TO 60 MPH IN LESS THAN 60 SECONDS.

  THIS RATE OF INCREASE GREATELY EXCEEDS SPEED WITH WHICH SYSTEMS CAN REACH THE SAFE STOW CONFIGURATION; FORTUNATELY, NO DAMAGE TO SYSTEMS OCCURRED.

- RECOMMENDATION - SURVIVAL CRITERIA FOR CONCENTRATOR WHEN OUT OF STOW SHOULD BE ESTABLISHED.

WIND SPEED (MILES/HR)
0
5
10
15
20
25
30
35
40
45
50
14.8
15.0
SOLAR TIME
SNLA
Apr 12, 1983

## WIND-INDUCED OSCILLATIONS

- MANUFACTURERS HAVE SUBJECTED COLLECTORS TO VARIOUS TESTS TO DETERMINE ABILITY OF COLLECTORS TO SURVIVE HIGH WINDS.

- TYPICALLY, A TORQUE HAS BEEN APPLIED TO THE COLLECTOR AND/OR DRIVE TO SIMULATE WIND LOAD.

- COLLECTORS OF DESIGN WHICH SURVIVED THESE TESTS HAVE BEEN SEVERELY DAMAGED IN THE FIELD, APPARENTLY DUE TO WIND-INDUCED OSCILLATIONS.

- IN THIS CASE, THE MANUFACTURER MODIFIED THE COLLECTOR STRUCTURE TO PREVENT OSCILLATION.

- RECOMMENDATION = WIND-INDUCED OSCILLATIONS NEED TO BE CONSIDERED IN THE DESIGN.

# OTHER ENVIRONMENTAL EFFECTS

- HIGH AMBIENT TEMPERATURES

  ELECTRONICS CABINETS AND EQUIPMENT SKIDS CAN BECOME EXCESSIVELY HOT IF NOT PROPERLY SHADED OR VENTILATED.

  EXAMPLE - THE TEMPERATURE INSIDE A CABINET SHADED BY AN ENCLOSURE REACHED 120 F WHEN AMBIENT TEMPERATURE WAS ONLY 85 F. THE TEMPERATURE INSIDE THE SHADED, BUT NOT WELL VENTILATED, ENCLOSURE WAS 99 F.

- SUNLIGHT

  ALARM AND CONTROL PANEL LIGHTS AND LED'S CAN BE NEARLY IMPOSSIBLE TO SEE IN BRIGHT SUN. SHADING IS REQUIRED.

  PLEXIGLASS OVER CONTROL PANELS LEADS TO A GREENHOUSE EFFECT AND GREATLY INCREASED TEMPERATURES.

- MOISTURE/CONDENSATION

  COLLECTORS CAN FROST UP OR BECOME COVERED WITH CONDENSATION WHEN ROTATED OUT OF STOW. MOISTURE MAY REMAIN ON COLLECTOR, ADVERSELY AFFECTING PERFORMANCE FOR SOME TIME. IT CAN BE MORE PROFITABLE TO DELAY OPERATION UNTIL THE COLLECTORS HAVE WARMED ABOVE THE DEWPOINT; HOWEVER, THERE ARE NO CONTROLS AT PRESENT TO PERFORM THIS FUNCTION AUTOMATICALLY.

  COLLECTORS WHICH HAVE NO BACK SHEET ARE MUCH MORE LIKELY TO ATTRACT CONDENSATION OR FROST IN THE STOW POSITION THAN THOSE WITH BACKSHEETS.

  COLLECTORS WHICH ARE NOT STOWED FULLY INVERTED TEND TO COLLECT A LOT OF DIRT ON THE PORTION OF THE MIRROR WHICH IS CLOSE TO THE GROUND.

  COLLECTORS MIRRORS ALSO ARE SOILED BY DIRT CARRIED IN THE RAIN FROM SHOWERS WHICH ARE TOO BRIEF TO WASH THE AIR CLEAN AND THEN RINSE THE MIRRORS.

# ENVIRONMENTAL DAMAGE TO REFLECTIVE SURFACES

## STRESSED GLASS

- STRESSED GLASS (CHEM-COR) MIRRORS ON A 2 METER PARABOLIC COLLECTOR DURING DEVELOPMENT TESTING HAD BEEN DEMONSTRATED TO SURVIVE HAIL (0.75 INCHES AT 55 FPS).
- THIRTEEN MIRRORS HAVE FAILED IN THE MISR QTS, APPARENTLY DUE TO WIND-BORNE DEBRIS SUCH AS ROCK AND TUMBLEWEEDS.
- SUCH DEBRIS MAY CAUSE DAMAGE WHEREAS HAIL DOES NOT BECAUSE THE DEBRIS MAY HAVE SHARP POINTS.
- DEBRIS-CARRYING WINDS ASSOCIATED WITH "DUST DEVILS" ARE OFTEN HIGHLY LOCALIZED AND OFTEN ARE NOT DETECTED AT ALL BY THE SYSTEM WIND SENSOR.
- DAMAGE HAS OCCURRED BOTH IN AND OUT OF THE PROTECTIVE STOW POSITION.
- RECOMMENDATION - DEVELOPMENT TESTING SHOULD INCLUDE SUCH DEBRIS AS WELL AS HAIL.

## ENVIRONMENTAL DAMAGE TO REFLECTIVE SURFACES
(CONTINUED)

### THIN-GLASS/STEEL LAMINATES

- THIN-GLASS/STEEL LAMINATES HAVE FAILED AT THE ADHESIVE BOND BETWEEN THE GLASS AND THE STEEL.

- THE EFFECT IS PROBABLY ACCELERATED WITH TEMPERATURE.

- ABOVE AMBIENT TEMPERATURE WILL OCCUR WHEN COLLECTORS ARE IN STOW, AS THEY ARE MOST WEEKENDS AT THE MISR SITE, ESPECIALLY WHEN THERE IS NOT A BACKSHEET ON THE COLLECTOR.

- DELAMINATION HAS ALSO BEEN OBSERVED IN COLLECTORS WHICH HAVE BACKSHEETS AND ALSO WHICH HAVE BEEN OPERATED ESSENTIALLY CONTINUOUSLY AND ARE THEREFORE NOT EXPOSED TO SUN ON THE BACK SIDE.

- RECOMMENDATIONS

  ALTERNATE ADHESIVES - EPOXY HAS BEEN TESTED, BUT IS MORE EXPENSIVE TO APPLY.

  ALTERNATE REFLECTIVE SURFACES - SAGGED GLASS, FILM.

# CONTROLS

- ALL MISR SYSTEMS WERE REQUIRED TO HAVE A RAINWASH CAPABILITY

  A RAINWASH CAPABILITY MEANS THE ABILITY TO POSITION ALL OF THE COLLECTORS FACING UP FROM A CENTRAL CONTROL.

  THE HELIOSTATS AT THE CENTRAL RECEIVER TEST FACILITY HAVE NEVER BEEN WASHED EXCEPT BY RAIN.

  MANUAL INITIATION WAS A REQUIREMENT SINCE AN OPERATOR MUST EXERCISE JUDGMENT CONCERNING THE PROBABLE DURATION OF THE RAIN AND POSSIBLE SEVERE WEATHER CONDITIONS.

  ALL SYSTEMS DISCONTINUE THE RAINWASH ATTITUDE DUE TO HIGH WINDS AND, IN SOME FASHION, PROTECT THE COLLECTORS FROM ACCIDENTAL FOCUSING WITHOUT FLOW.

  SOME OF THE SYSTEMS AUTOMATICALLY RESUME NORMAL SOLAR OPERATION WHEN INSOLATION IS ABOVE MINIMUM LEVELS.

  SIMPLE, REMOTE ACTUATION IS DESIRABLE SINCE AN OPERATOR MAY BE RELUCTANT TO STAND OUT IN THE RAIN WHILE ESTABLISHING THE RAINWASH CONFIGURATION.

## CONTROLS
(CONTINUED)

- LIGHT SWITCHES

LIGHT SWITCHES ARE USED TO DETERMINE WHETHER INSOLATION IS SUFFICIENT FOR SYSTEM OPERATION.

THE LIGHT SENSOR MUST VIEW THE PORTION OF THE SKY THROUGH WHICH THE SUN PASSES DURING THE YEAR. WHEN A LARGE PORTION OF THE SKY IS VIEWED, INDIRECT LIGHT ON A BRIGHT, CLOUDY DAY CAN CAUSE THE SENSOR OUTPUT TO EXCEED ITS THRESHOLD LEVEL.

THE MOST EFFICIENT SENSORS HAD SOME TYPE OF TRACKING ABILITY TO LIMIT THE ACTIVE FIELD OF VIEW. IN ONE CASE, THIS WAS ACHIEVED ELECTRONICALLY WITH NO MOVING PARTS.



- LOCAL CONTROLS

FEATURES FOUND TO BE CONVENIENT INCLUDE:

NON-MOMENTARY SWITCHES FOR MANUAL ROTATION OF COLLECTORS, ALTHOUGH MOMENTARY SWITCHES ARE PROBABLY SAFER.

THE ABILITY TO ROTATE THE COLLECTOR THROUGH FOCUS WITHOUT THE COLLECTOR ACQUIRING THE SUN.

A LOCAL CONTROL THAT ALLOWED AUTOMATIC POSITIONING OF A DRIVE GROUP FOR SPRAY WASHING.

WITH THE EXCEPTION OF A SYSTEM WHICH USED POWER-CABLE CARRIER-FREQUENCY CONTROL TECHNOLOGY, AN ENTIRE SYSTEM HAD TO BE SHUT DOWN IN ORDER TO BLOCK ELECTRICAL CONTROL SIGNALS FROM ENTERING A LOCAL CONTROLLER DURING REPAIR. A SINGLE MULTI-PIN PLUG WITHIN THE CONTROLLER SERVED THIS FUNCTION IN ONE CASE.

# DRIVE SYSTEMS

- RELIABILITY

  RELIABLE DRIVE SYSTEMS ARE ESSENTIAL.

  ONE SET OF RECEIVERS WERE RUINED ON A MISR SYSTEM DUE TO A MOTOR CONTROLLER FAILURE.

- MANUAL BACKUP

  IN THE EVENT OF A DRIVE SYSTEM FAILURE, A MANUAL BACKUP CAN ALLOW AN OPERATOR TO ROTATE THE COLLECTOR TO SAFE STOW.

- MECHANICAL STOPS

  MECHANICAL STOPS TO STOP THE ROTATION OF A COLLECTOR IN THE EVENT OF FAILURE OF A LIMIT SWITCH OR OTHER DRIVE SYSTEM COMPONENTS IS ESSENTIAL.

  THE MECHANICAL STOP SHOULD BE DIRECTLY TIED TO THE COLLECTOR. AT MISR, A DRIVE CHAIN JUMPED A COG, AND BECAUSE THE MECHANICAL STOP WAS PART OF THE CHAIN AND NOT THE COLLECTOR, IT DID NOT PREVENT THE COLLECTOR FROM BEING DESTROYED BY OVERDRIVING ITS LIMIT.

# INTERNATIONAL DISH SYSTEM DEVELOPMENT

Leonard D. Jaffe

Jet Propulsion Laboratory
Pasadena, CA 91109

Americans working on development of solar power systems are sometimes unaware of the very significant work underway in other countries. Several papers are presented describing innovative and advanced projects that are in progress overseas.

# DEPLOYMENT OF A SECONDARY CONCENTRATOR TO INCREASE THE INTERCEPT FACTOR OF A DISH WITH LARGE SLOPE ERRORS

Ugur Ortabasi and Evan Gray,
Solar Energy Research Centre, University of Queensland, St. Lucia,
Queensland 4067, Australia
and
Joseph O'Gallagher,
Enrico Fermi Institute,
University of Chicago, Chicago, Illinois, 60637, U.S.A.

## ABSTRACT

We report on the testing of a hyperbolic trumpet non-imaging secondary concentrator with a parabolic dish having slope errors of about 10 mrad. The trumpet, which has a concentration ratio of 2.1, increased the flux through a 141-mm focal aperture by 72%, with an efficiency of 96%, thus demonstrating its potential for use in tandem with cheap dishes having relatively large slope errors.

## INTRODUCTION

Recent studies have clearly demonstrated the potential of parabolic dish/receiver/heat engine systems to achieve high solar-to-electricity conversion efficiencies. Part of the reason for this success is the intrinsic ability of parabolic dishes to produce high solar fluxes at a very small focus. A compact receiver and a directly-coupled heat engine located at the focal area form a powerful conversion system with minimal heat losses. Temperatures in the order of 850° - 1200°C are easily generated and maintained. With the advent of modern heat engines and ceramic lined receivers, overall efficiencies higher than 40% are anticipated.

One of the major cost factors in the manufacturing of these systems is the parabolic dish itself. To achieve high concentration levels that can be maintained under heavy windloads the structural requirements on these dishes are very high. In addition, the necessity of a perfectly specular surface and minimum slope errors require very strict manufacturing tolerances and high precision. Obviously the cost of such a concentrator is too high and will always be detrimental to its economic feasibility.

Previous studies by Winston and O'Gallagher (Ref. 1) have demonstrated that a secondary non-imaging concentrator deployed at the focal plane of a parabolic dish can significantly improve the optical performance by increasing the intercept factor. Experiments conducted by the authors of Ref. 1 have shown that a trumpet with a concentration ratio of 2.1 can increase the energy flux into the receiver by more than 30% for a dish of medium quality. Otherwise stated, it is possible to design a trumpet which will increase the compound concentration ratio of a primary dish with given slope errors by a factor of about 2, with an improvement in intercept factor depending on the shape of the actual distribution of slope errors. This means in commercial terms that the dish tolerances normally required to obtain high temperatures may be significantly relaxed, and the cost of the dish reduced. The combination of "sloppy dish" and secondary concentrator has been proposed by SERC (Ref. 2) and a preliminary study of the effects of a secondary concentrator on system efficiency has been made by Jaffe (Ref. 3).

In the light of these findings, the Solar Energy Research Centre (SERC) of the University of Queensland and the Enrico Fermi Institute (EFI) have recently embarked on a joint research programme to further develop the sloppy dish/trumpet combination. This paper reports the beginning of our combined efforts, in which the trumpet built by EFI was tested on SERC's Omnium-G parabolic dish with a focal ratio of f = 0.67, located in Brisbane, Australia. The same trumpet tested at JPL was used for this experiment. It is formed from copper with cooling coils brazed around the throat section. The whole trumpet is silver plated and the inside polished.

The trumpet was designed for the Omnium-G parabolic dish at JPL, which concentrates 98% of the reflected energy into a focal aperture of 203 mm. SERC's dish has a broader flux distribution, with a considerable amount of energy arriving outside an aperture of 300 mm.

## EXPERIMENTAL PROCEDURE

To best match the trumpet to the dish, the 18 individual petals were realigned to maximise the flux in a 203-mm receiver aperture. This was done using an extension of a diagnostic technique described by Dennison and Argoud (Ref. 4) in which a target of concentric coloured annuli was illuminated at the focus and viewed from a distance. The focus was shifted after alignment to account for the finite viewing distance. In our case, we made a target consisting of a 203-mm bullseye surrounded by four differently coloured quadrants. The dish was viewed through a telescope in daylight from a building 300 m away, and the petals were each adjusted to maximise the area reflecting the colour of the bullseye. The colour coding of the quadrants gave unambiguous information about the adjustments necessary to realign each petal. We estimated from the final image that about 50% of the reflected light would pass through a 203-mm focal aperture.

Cold-water calorimetry was employed to measure both the distribution of flux in the focal plane and the effectiveness of the trumpet. The calorimeter was a cavity receiver, shown in Figure 2, which was water cooled according to the schematic diagram, Figure 3. The receiver was built at SERC to intercept as much of the beam as possible, and includes a preheating coil of diameter 500 mm on the front face, which was covered throughout the experiment. Water flow was measured by recording the angular speed of a previously-calibrated positive-displacement pump. The temperature rise across the colorimeter was measured by matched deep-insertion platinum resistance thermometers, and flow mixing devices were inserted in the pipes immediately ahead of the measuring points. $T_{out} - T_{in}$ was recorded until it stabilised, a time of about 20 minutes, before the data were accepted.

A water-cooled aperture plate consisting of five removable nesting annuli was used for the measurement of flux distribution. Two of the available apertures, namely 140.7 mm (5.5 inches) and 203.2 mm (8 inches), correspond to the physical exit aperture and the virtual entrance aperture of the trumpet respectively (Ref. 1). The other apertures available are 100 mm, 250 mm and 300 mm.

All the water pipes, including the preheating coil on the face of the SERC receiver, were heavily insulated with an alumina-fibre blanket to prevent stray heat flows. The interspace between the aperture plate and receiver mouth was

sealed with the same material to minimise convective losses.

$T_{out}-T_{in}$ was measured with the dish off the sun to account for any differences in the thermometers and direct heating of the receiver by the sun. Direct insolation was measured with an Eppley normal-incidence pyrheliometer calibrated to 1%. All data were recorded as minute by minute averages and then further averaged over periods of up to one hour.

All the measurements were made under very clear skies, with direct insolation from 800 to 1000 W/m². Although the zenith angle varied from 8° to 50° during the measurements, the diffuse radiation was only 8 to 10% of the direct, so no correction for variation in air mass was considered.

The energy collected by the receiver is

$$E = \dot{m}\, C\, \Delta T = I_D\, A\, \eta\, \phi$$

where

$\dot{m}$ = mass flow
C = specific heat
$\Delta T$ = $T_{out} - T_{in}$
$I_D$ = direct insolation
A = effective dish area
$\phi$ = receiver intercept factor

$\eta$ is an overall efficiency, including dish reflectivity and the effective absorptivity of the receiver cavity, which is assumed constant. Radiation and convection losses are ignored because receiver temperature was limited to about 50°C maximum at the rear surface and 40°C maximum at the front. There must, however, be an increasing convection loss at the larger apertures.

## EXPERIMENTAL RESULTS

Values of $\eta\phi$ are given in Table 1 and the derived flux distribution is shown in Figure 4.

| APERTURE | $\eta\phi$ |
|---|---|
| 100 mm | 0.075 ± .005* |
| 140.7 mm (5.5") | 0.116 ± .001 |
| 203.2 mm (8.0") | 0.209 ± .002 |
| 250 mm | 0.289 ± .002 |
| 300 mm | 0.351 ± .001 |
| * excluding uncertainty in insolation | |

Table 1. Collection efficiency at various receiver apertures

The irregular shape of the flux distribution may be ascribed to the variation in focal length among the 18 separate petals comprising the Omnium-G dish. The large amount of energy captured at diameters between 141 mm and

203 mm is probably due to the method of aligning the dish to maximise throughput in an 8-inch aperture rather than at a central point. The very low values of $\eta\phi$ are due to the poor reflectivity of the dish, whose aluminium ("Alzac") surface has been weathered for 4 years, and to the very broad beam at the receiver.

A preliminary measurement with the bare receiver, including the preheater, gave an overall value for $\eta\phi$ of about 0.5, so assuming $\phi \to 1$ at an aperture of 500 mm, $\eta \cong 0.5$. This suggests a value for $\phi$ of about 0.42 at an aperture of 203 mm. Using Aparisi's equation (Ref. 5) for slope errors, which is a good approximation at f = 0.67, the dish slope error is about 10 mrad. This is a rough estimate since Aparisi's equation assumes a Gaussian distribution of slope errors, whereas the measured distribution is irregular, but it serves to confirm the poor quality of the mirror.

The trumpet concentrator was then mounted and another calorimetric measurement made. The face of the receiver was completely insulated from the outer edge to the trumpet exit. The measured total efficiency was

$$\eta\phi = 0.200 \pm .001$$

excluding the uncertainty of 1% in the absolute value of the direct insolation. The intercept improvement relative to the 141 mm aperture plate is thus (0.200/0.116) - 1, or (72 ± 1)%. The previous measurements by Winston and O'Gallagher (Ref. 1) with this trumpet produced an intercept gain of 33%. The larger improvement with SERC's dish is due to the broad, flat-topped flux distribution. The overall trumpet efficiency is .200/.209, or (96 ± 1)%, in excellent agreement with the value found by Winston and O'Gallagher for the same trumpet.

The high trumpet efficiency is encouraging because in our measurements the trumpet walls reflected a much greater fraction of the total receiver flux than in the previous test. The trumpet throat slightly shades a 141 mm disk at the focal plane, so the energy reflected by its walls is slightly greater than that which would otherwise arrive at the receiver between 141 mm and 203 mm, namely 42% of the total in the 203 mm aperture. The integrated reflectance of the trumpet is thus greater than 90%. Compared to the reflectance of polished silver of about 93%, this indicates that a very high proportion of the energy actually redirected by the trumpet is reflected only once.

## CONCLUSION

We have demonstrated the effectiveness of the hyperbolic trumpet secondary concentrator in greatly improving the intercept factor of a dish with slope errors of about 10 mrad. We now propose to investigate the cost/quality tradeoff and design an optimised sloppy dish/secondary trumpet system.

## REFERENCES

1. R. Winston and J. O'Gallagher in proceedings of the Fourth Parabolic Dish Solar Thermal Power Program Review, Pasadena, 1982, p 221 (U.S. Department of Energy).

2. U. Ortabasi. "A novel method to improve optical performance of parabolic dish concentrators". Proposal to National Energy Research, Development and Demonstration Council (Australia), 1983.

3. L.D. Jaffe. "Optimisation of dish solar collectors with and without secondary concentrators", 1982. (U.S. Department of Energy).

4. E.W. Dennison and M.J. Argoud in proceedings of the Fourth Parabolic Dish Solar Thermal Power Program Review, Pasadena, 1982, p 177 (U.S. Department of Energy).

5. L. Wen, *et al*. Trans. ASME, J. Solar Energy Engineering, 102, 305 (1980).

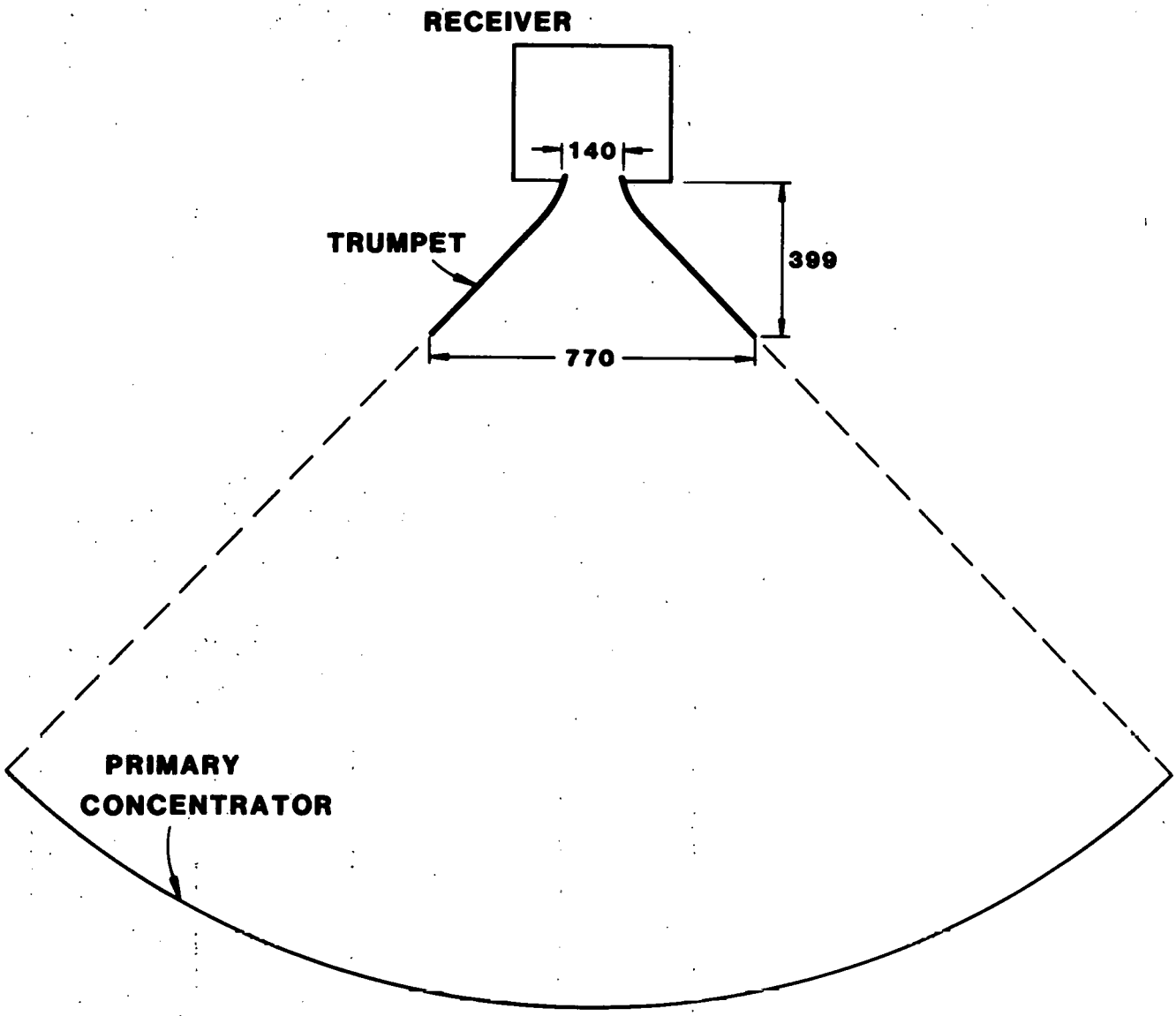


Figure 1: Trumpet concentrator configuration. Dimensions in millimetres

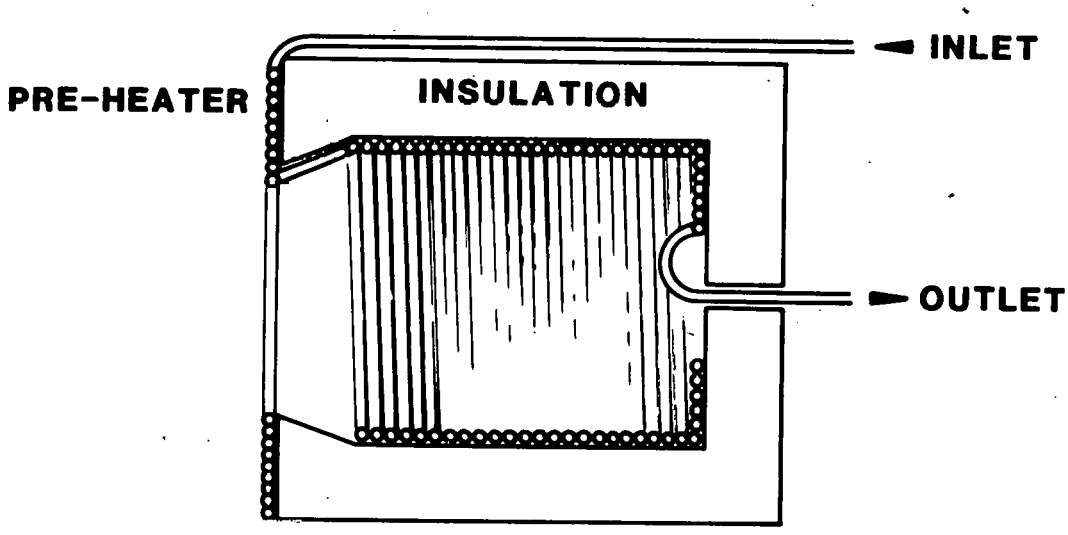


Figure 2: Cavity receiver

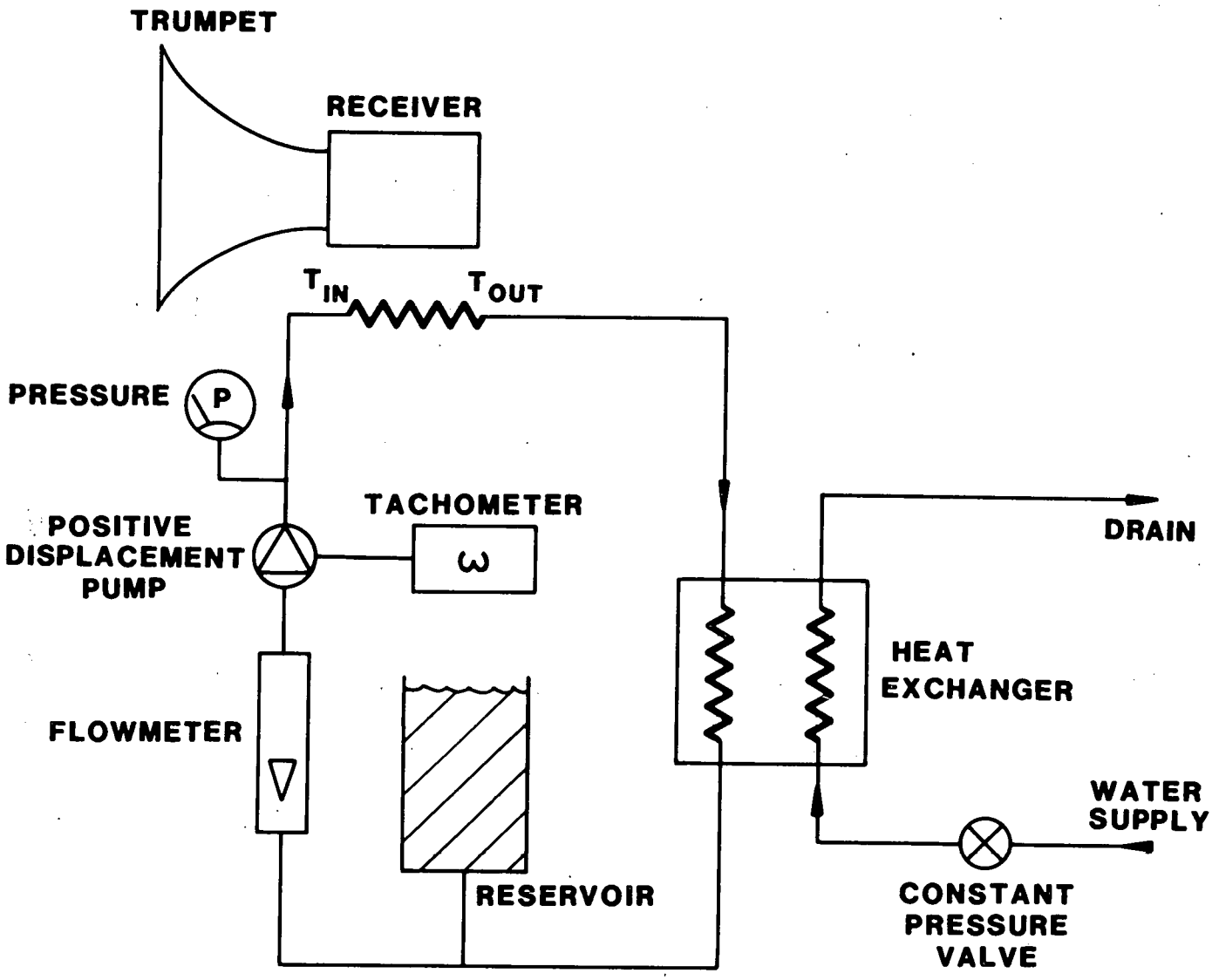


Figure 3: Receiver cooling scheme for cold calorimetry

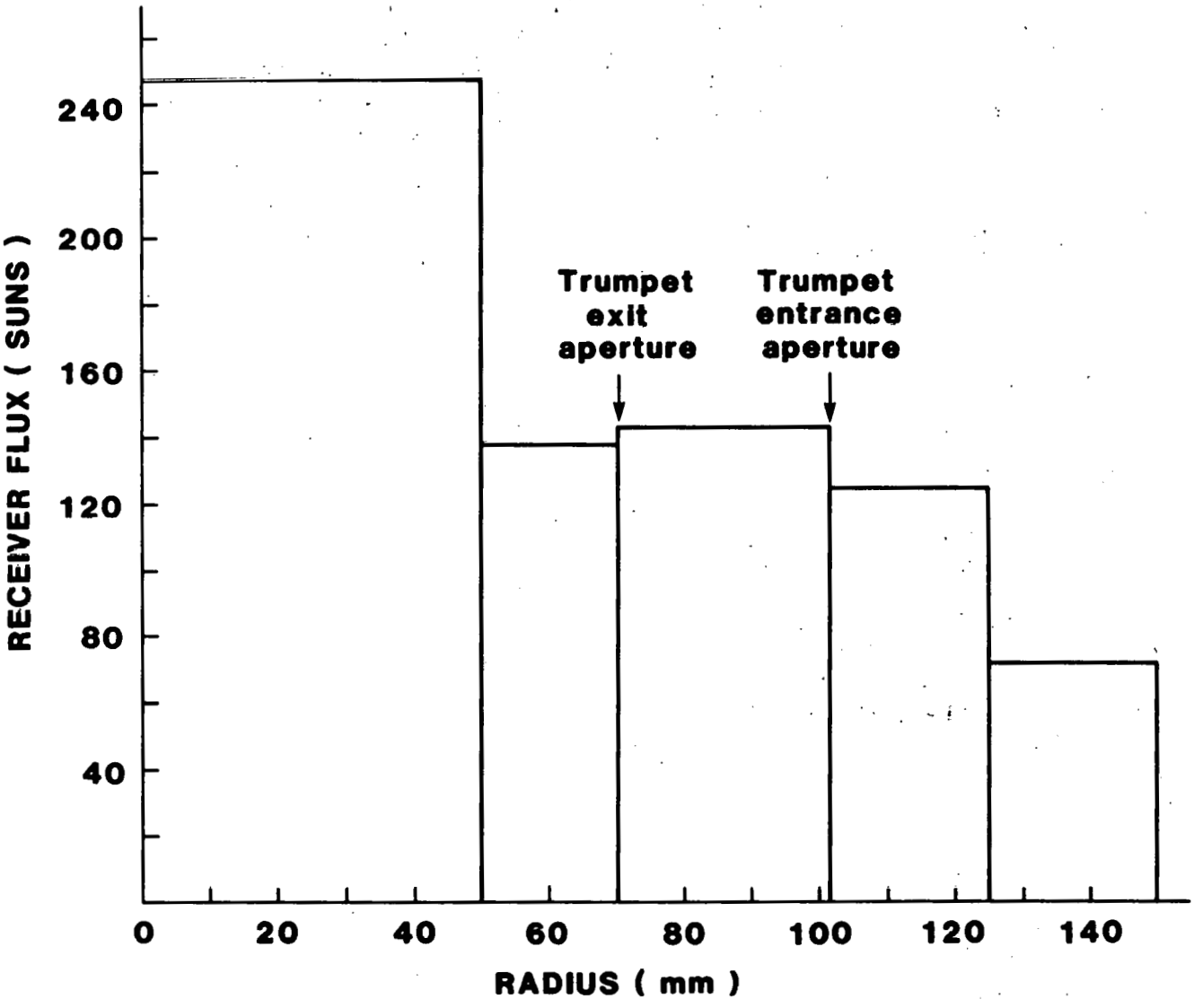


Figure 4: Radially averaged receiver flux distribution, measured by cold calorimetry

# Recent Advances in Design of Low Cost Film Concentrator and Low Pressure Free Piston Stirling Engines for Solar Power

Jürgen + Hans Kleinwächter
BOMIN-SOLAR GmbH
Lörrach, West-Germany

William Beale
Sunpower Inc.
Athens, Ohio, USA

The rapid development of free piston stirling engine technology in combination with low weight pneumatically formed plastic film concentrators makes possible solar thermal power plants with a combination of high performance and low cost. Recent improvements in the system allow the production of 10 kW of net electric power to the grid from a dish of approximately 7.3 meter diameter without the need for a cover dome. This system is believed to be practical and cost effective in Sahara environments.

The main power unit is a single cylinder low pressure 50 Hz free piston engine with hydrodynamic gas bearings of a simple and durable design. This machine is capable of high efficiency and long life without severe constraints on dimensional accuracy of its moving parts. Lower power versions of this machine have been successfully tested and have met their design performance goals.

The alternator driven by the engine has high power density and efficiency at least equal to that of rotary alternators presently available. If desirable, the alternator can be designed to deliver three phase power. Since reciprocating mass of the alternator is low, the operating frequency can be achieved without recourse to gas springing other than that available from the working gas, thus permitting a very simple and durable engine-alternator combination without stringent demands of axial alignment or other mechanical perfections.

It is believed that the combination of simple, low cost concentrator with a single cylinder, low pressure free piston engine and an efficient and durable alternator forms a leading combination for the production of electric power from solar energy.

## System Conception

Parabolic dish concentrators in combination with stirling engines represent the most promising thermodynamic solar-electricity system.

Beside its potential to deliver efficiencies from sunlight to electricity of over 25 %, there exist also good possibilities to build cost efficient, modular solar power stations.

In general high performing technical systems are more complex and thus expensive as systems dealing with low efficiencies and non sophisticated technology.

It was the main line of BOMIN-SOLAR's and Sunpower's thinking to overcome this law by developing a power station combining a low weight pneumatically formed plastic film concentrator with a single cylinder free piston stirling engine.

Both components are of extremely simple conception and once fully developed will be inexpensive in mass production. However, the development of simple high efficient inexpensive film concentrators and free piston stirling engines requires very complex studies in the field of materials, analytic understanding and structural design. Only the result looks simple, whereas the way to it is very complicated. That's the difference between simple and primitive technology.

The first part of the paper describes the status and recent advances of the plastic film concentrator, the second part the similar situation for the free piston stirling engine.

## 1. Plastic Film Concentrators

As we described during the last parabolic dish meetings our company is developing since 1972 parabolic dish mirrors by stretching plane, metalized plastic membranes over hollow, drum shaped structures. By forming pneumatically the membrane with slight over or underpressures (Fig. 1, Fig. 2) we got concentration ratios over 1000 (Fig. 3) and thus an enough good optical performance to produce with good efficiencies temperatures over 700°C needed for stirling operations (Fig. 4). Beside the pneumatically formation of dish type concentrators we also investigated the possibilities to deform the membrane by electric, magnetic or photonic means (Fig. 5).

We then studied the possibility to build excentric parabolic dishes with non circular circumferances by utilizing the same membrane technology. The result was the Fix-Focus concentrator (fig. 6) which led to a very attractive combination with a Beale free-cylinder stirling water pump. (fig. 7)

The material problem of the membrane was solved by utilizing the fluorpolymeric material Hostaflon-ET from the Hoechst company (table 1). The chemical inertness of this plastic film is on the one hand the

the reason for most of its outstanding properties like long life time without degradation, but leads on the other hand to difficulties in metallizing and assembling the membranes.
Adequate technologies were developed.

The basic economic arguments for thin film parabolic dishes are their simplicity in production and their low weight. As big dishes with thin membranes of 100 µm thikness are sensible to wind-loads, it is consequent to protect them under transparent domes (fig. 8). The disadvantages of this combination are however the extra costs for the dome, the reduction of the light-flux reaching the mirror (≤ 10 %), and the danger of burning parts of the dome cover during an accidental walk-off of the hot spot.

This situation led to recent developments and advances in our parabolic dish program.

## 2. Recent Advances

The fig 9 shows one membrane section of an elastically deformed film concentrator. The relationship between the two main radiuses of curvature $\rho_I$ and $\rho_{II}$, the two corresponding tensions $\sigma_I$ and $\sigma_{II}$, the membrane thickness $S$ and the normal tension $P$ is given by equation 1:

$$\frac{\sigma_I}{\rho_I} + \frac{\sigma_{II}}{\rho_{II}} = \frac{P}{S} \qquad \text{equation 1}$$

For a parabolic dish with the focal length and the equation

$$z = \frac{x^2}{4f} \qquad \text{equation 2}$$

The ratio of the main radiuses of curvature is given by

$$\rho_I = 2f\left[1+\left(\frac{x}{2f}\right)^2\right]^{1/2}$$

$$\rho_{II} = 2f\left[1+\left(\frac{x}{2f}\right)^2\right]^{3/2}$$

$$\longrightarrow \boxed{\frac{\rho_{II}}{\rho_I} = 1+\left(\frac{x}{2f}\right)^2} \quad \text{equation 3}$$

Only in the summit of the curvature ($x \ll f$) the ratio of $\frac{\rho_{II}}{\rho_I} \longrightarrow 1$ that means in this region the membrane shape is spherical, whereas in the outer regions $\frac{\rho_{II}}{\rho_I} > 1$ the membrane becomes more and more cylindrical.

For this reasion, in order to get a perfect parabolic shape, the ratio between $\frac{\sigma_I}{\sigma_{II}}$ must be depending from $x$ so that

$$\frac{P}{S} = \frac{\sigma_I}{\rho_I} + \frac{\sigma_{II}}{\rho_{II}}$$ equation 4

which leads to the necessity of an unisotropic prestretching of the membrane.

We developed the thechnology of unisotropic prestretching of membranes as well for the general case of excentric parabolic dishes (fig. 1o) as for the mostly required case of rotational parabolic dishes (fig.11).

It is shown, that the membrane is divided in several sectors whose lining is formed by clamping profiles (fig. 12) with multiple function.

-1) They permit the unisotropic prestretching of the film membrane as indicated in fig 11.

-2) As indicated in fig 13 the junction line between two film' membranes is in general disturbed because pasted seams or weld seams represent unhomogenities. Fig 14 shows that the clamping profiles compensate this disturbance and are individually adjustable by regulating screws.

-3) As a membrane parabolic dish concentration is functionally represented by the equation

$$\left(\frac{w_r}{w_o}\right)' = -2\frac{0.9}{a^2}r - 4\frac{0.1}{a^4}r^3$$ equation 5

and thus in its peripheric regions steeper than a real parabola, this divergency is also corrected by the clamping profiles.

-4) The division of the membrane into several smaller sectors by said clamping profiles stabilizes the mirror against wind forces and prevent flopping, especially when during non-operation times the membrane forming pneumatic pressure is interrupted. Consequently a profile reinforced plastic thin film concentrator of big dimensions can be free standing without protection dome.

As a first prototype we realized a 3 m diameter dish with profile reinforcement of the two parallel welded seams (fig. 15). Besides the wind stabilizing effect the result was a much higher concentration ratio as for the free membrane case.

The second prototype with a sectoral profile reinforcement has a diameter of 3,5 m (fig. 16) and has the capacity to produce concentration ratios > 5ooo.

Basing on these experimental results we are now planning to combine

a sectorial profile reinforced parabolic dish with a 1o $kW_{el}$ free piston stirling generator as described in chapter 2.

The technical datas of this stirling dish concentrator are:

| | |
|---|---|
| Insolation: | 9oo $W/m^2$ |
| Reflectivity: (Hostaflon-ET with silver back layer) | 0,9 |
| Cavity efficiency: | 0,9 |
| Stirling overall efficiency: (Heat to electric) | 0,38 |
| Total efficiency: | 27,3 % |
| Diameter of mirror: | 7,2 m |
| Concentration ratio: | 15oo |
| Diameter of hot spot: | 18,6 cm |
| Tracking mecanism: | astronomical mounting |

The expected ex factory costs are given in the following table

| component price in U.S.Dollars \ number of mirrors, power in MW | 1oo mirrors 1 MW | 1ooo mirrors 1o MW | 1oooo mirrors 1oo MW |
|---|---|---|---|
| 1o KW free piston stirling generator | 19oo | 14oo | 1ooo |
| 7,2 m mirror structure | 5ooo | 4ooo | 3ooo |
| 1oo $m^2$ plastic film and reinforcement structure | 5ooo | 3ooo | 2ooo |
| Astronomic mounting | 4ooo | 3ooo | 25oo |
| Foundings | 5ooo | 3ooo | 2ooo |
| Costs per installed $KW_{el}$ peak | 2.o9o $ | 1.44o $ | 1.o5o $ |

Rough economical analyses basing on a yearly production of 10000 units (100 $MW_{el}$) located at a site with 2500 KWh/m2year insolation

| | |
|---|---|
| Yearly average system efficiency = | 25 % |
| Life time = | 20 years |
| Price per $m^2$ of system = | 258 $ |
| Rate of interest = | 10 % |
| Yearly costs (y.c.) per $m^2$ of system = | 25,8 $ |
| Selling price of $KWH_{el}$ to customer = | 10 cents |
| Yearly production of electric energy per $m^2$ of system (y.p.) | 625 $KWH_{el} \hat{=} 62,5$ $ |

Conclusion: y.p. > y.c. = economical

Fig.1

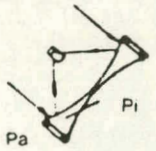


Pi < Pa

**Underpressure mirror**

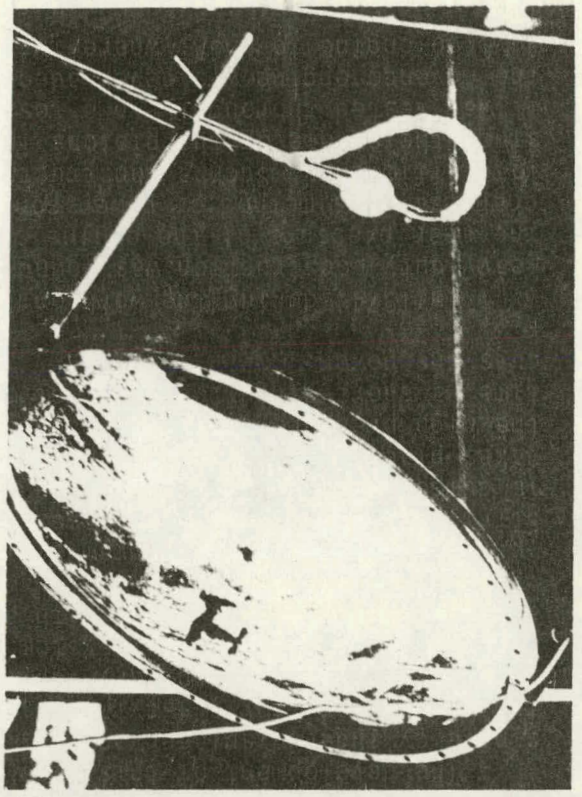

Fig.2

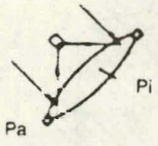


Pi > Pa

**Overpressure mirror**

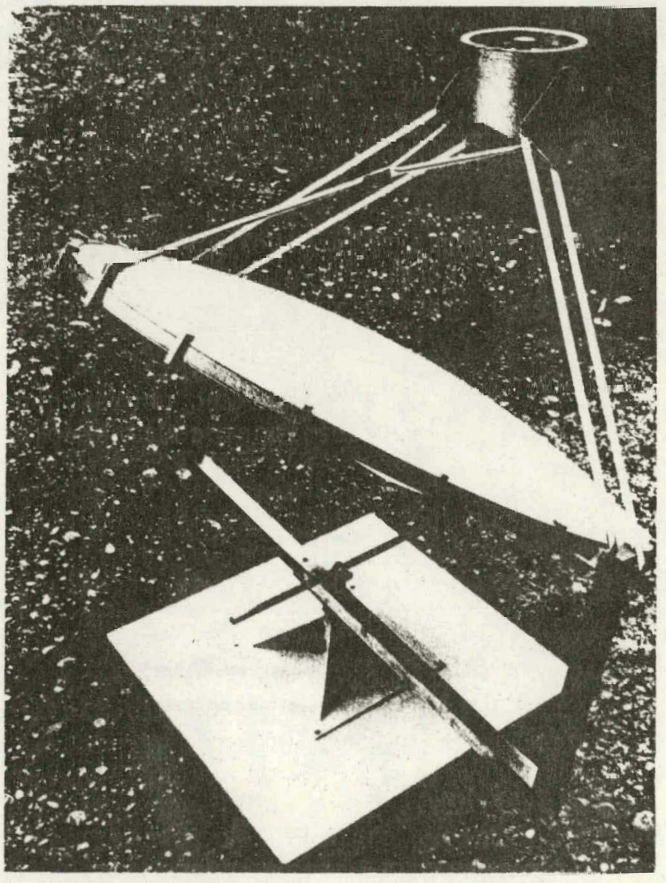

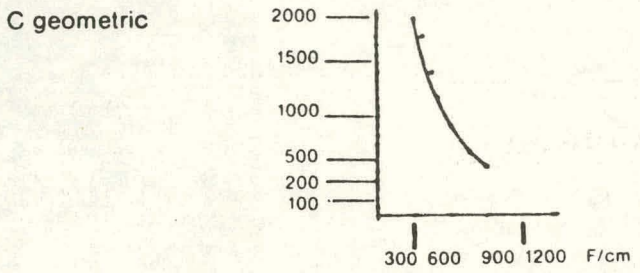


Fig 3 Concentration ratio of a 3 m underpressure mirror as a function of the focal length F.

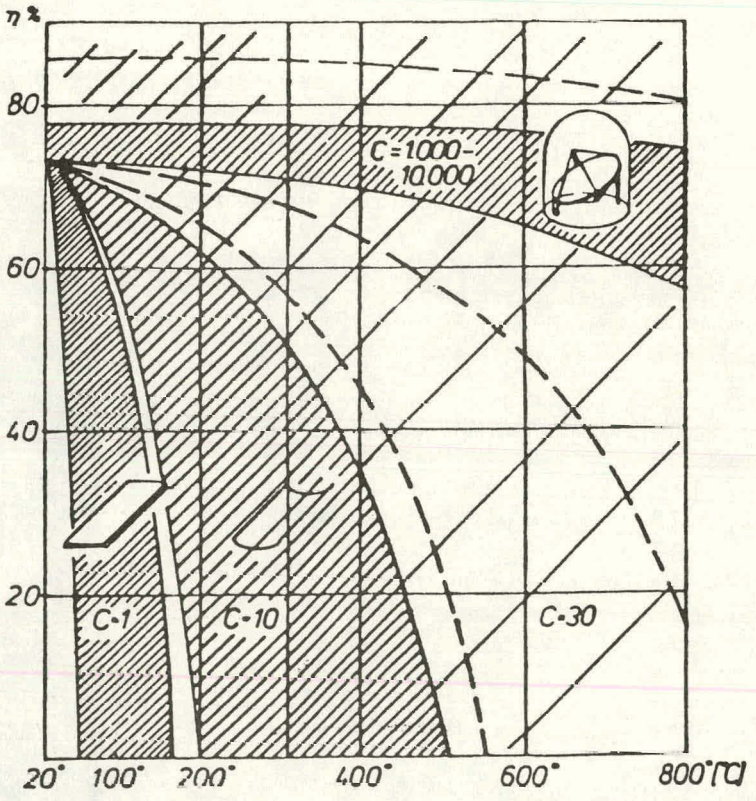


Fig 4 Efficiencies of transformation from solar radiant energy into thermal energy as a function of the temperature and of the optical concentration

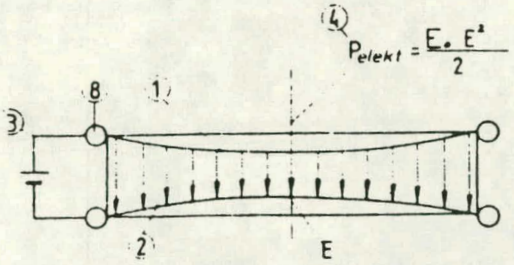


electric field deformation

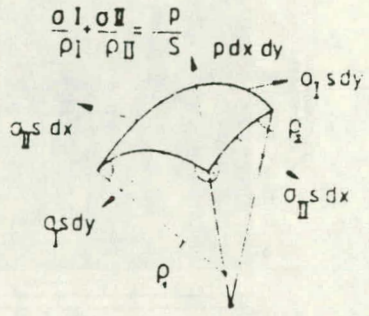


membran section

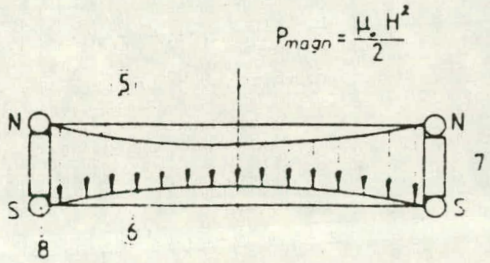


magnetic field deformation

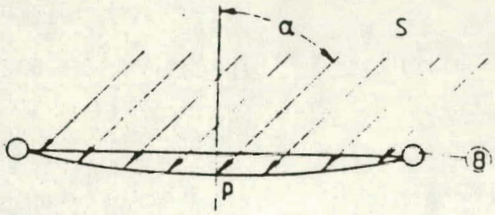


$p \cdot \frac{2 S \cos \alpha}{c}$

photonic deformation

Fig. 5 Different possibilities to deform film membranes

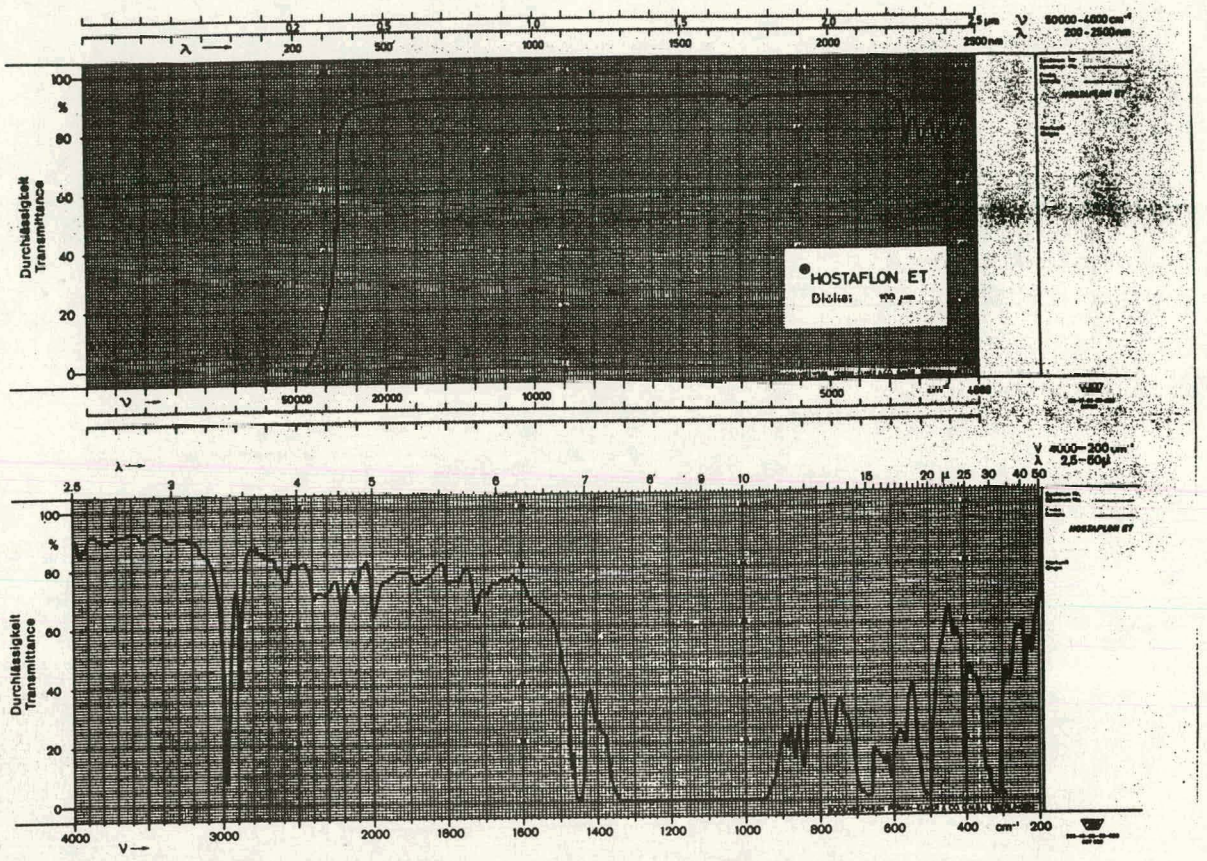


| | | |
|---|---|---|
| Thermal operation | | - - 190° - + 150° C |
| Melting range | | - 265° - 278° C |
| Transparency (100 µm foil) | | - 95 %, 10 % of diffuse light |
| Tensile strength | (at 23° C) | 53 N/mm² |
| Yield stress | " | 30 N/mm² |
| Breaking extension | " | 300 % |
| Tear strength | " | 440 N/mm² |

The foil is weldable and metallizable. Therefore it is used not only for the dome-covering but also for the foil mirror.

Table 1 Properties of Hostaflon-ET film

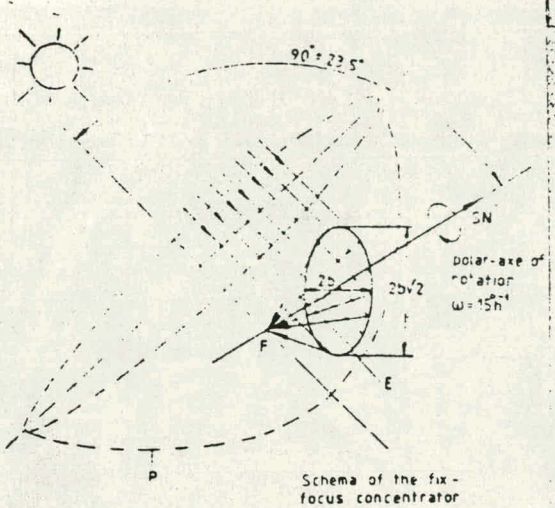


Schema of the fix-focus concentrator

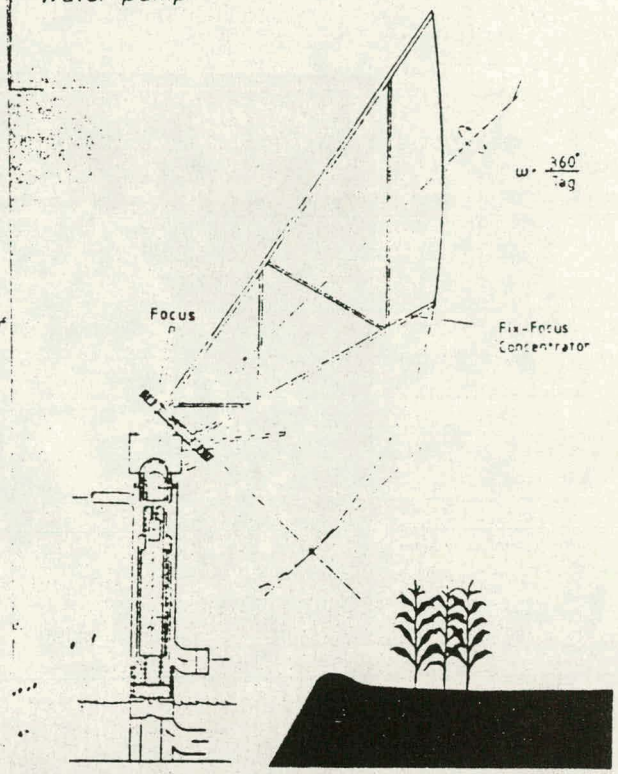


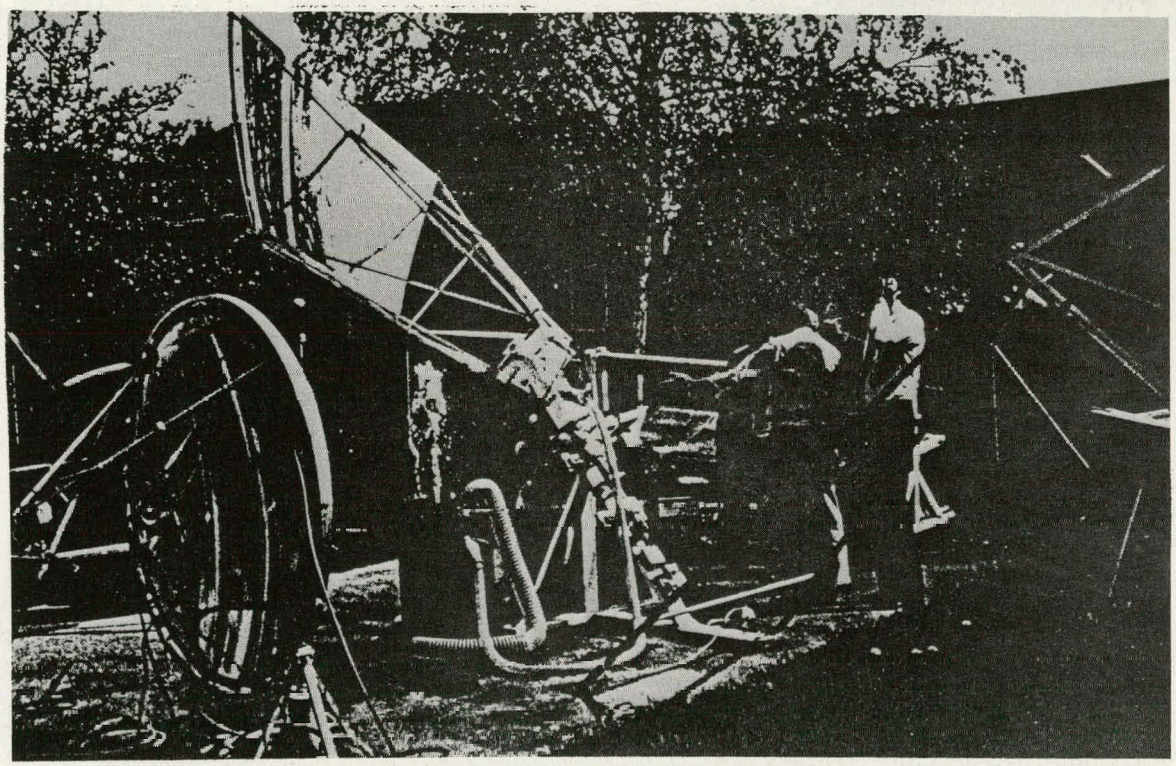

Fig. 6 and Fig. 7

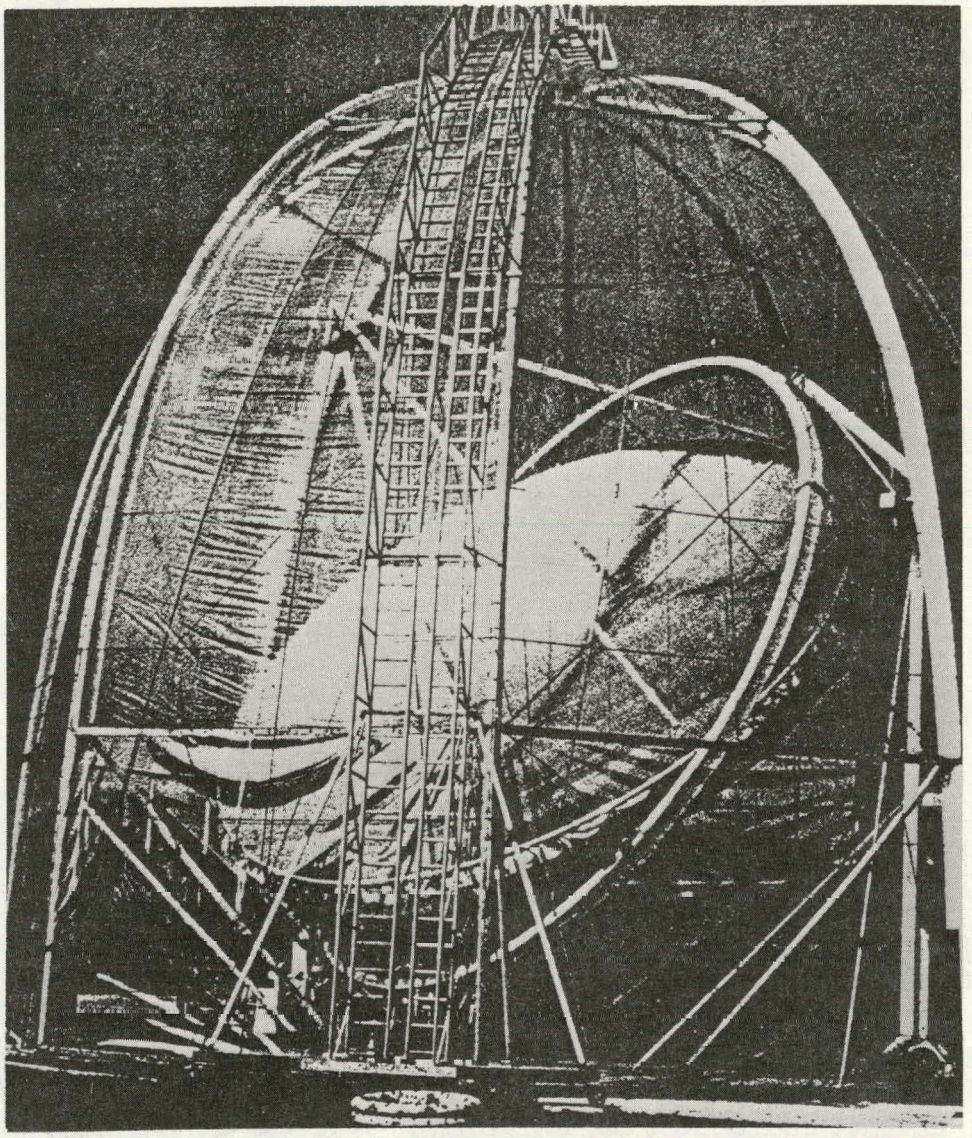

Fig. 8 lo m diamter film dish under dome

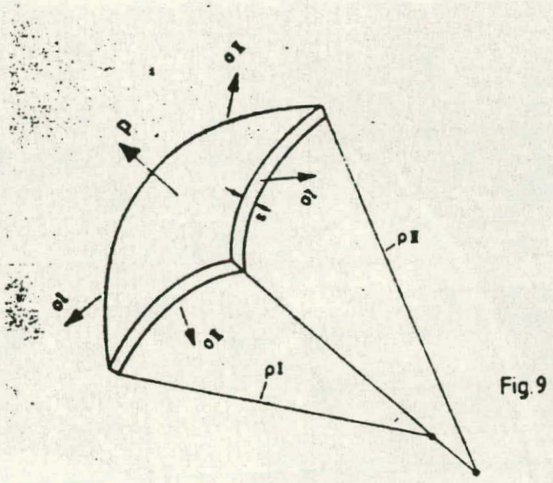


Fig. 9 Membrane section

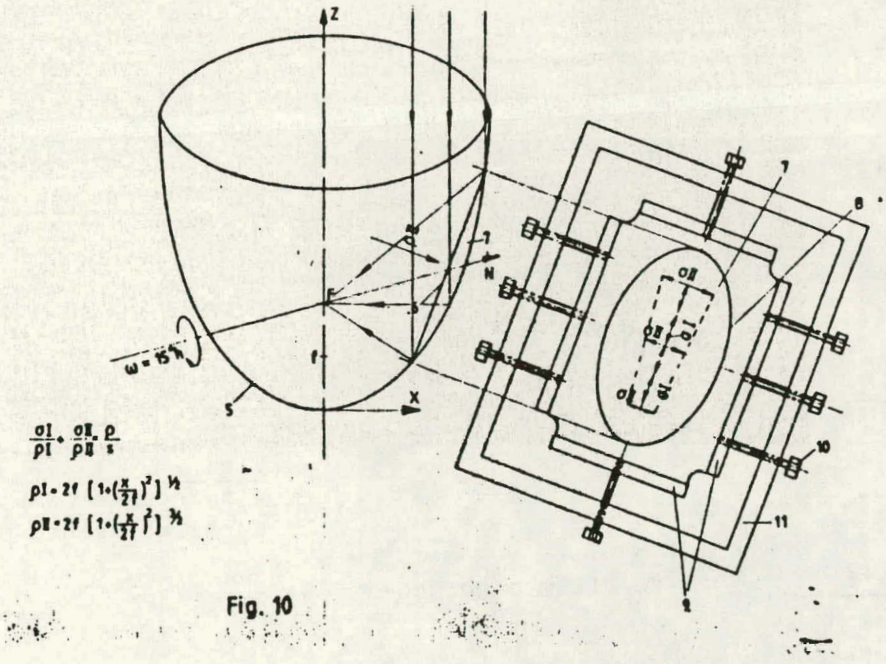


Fig 10 Prestretching of excentric film dish

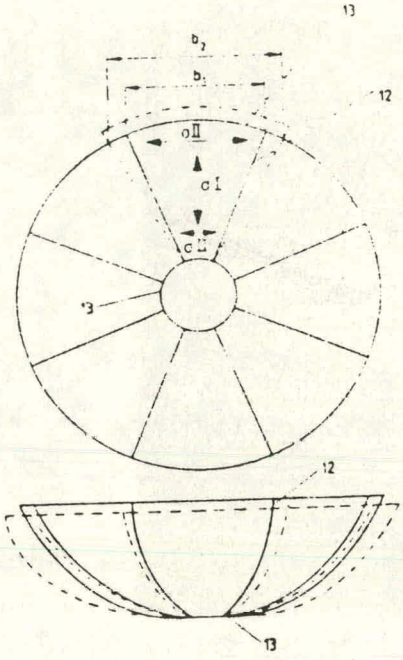


Fig. 11

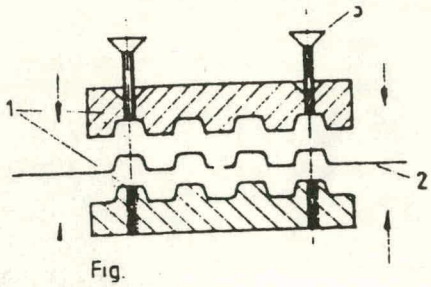


Fig.

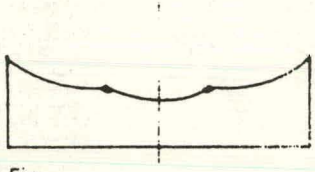

Fig

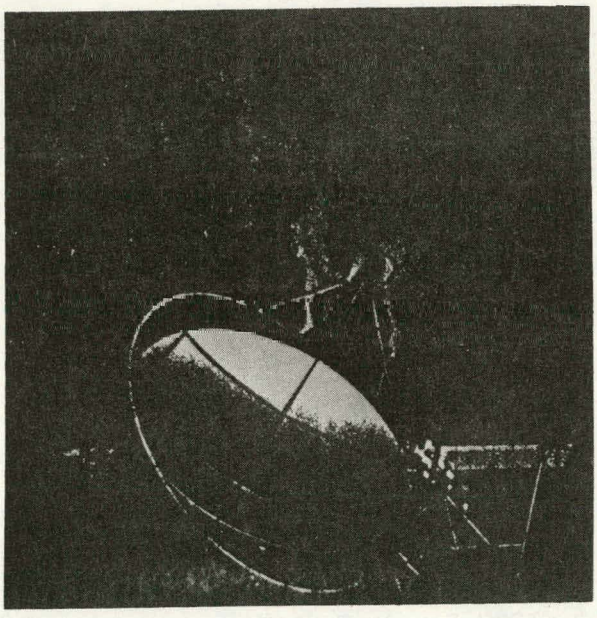

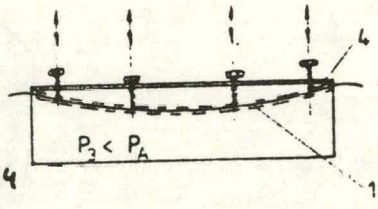


fig.14

Fig. 15 3 m film dish with reinforcement of the parallel welded seams

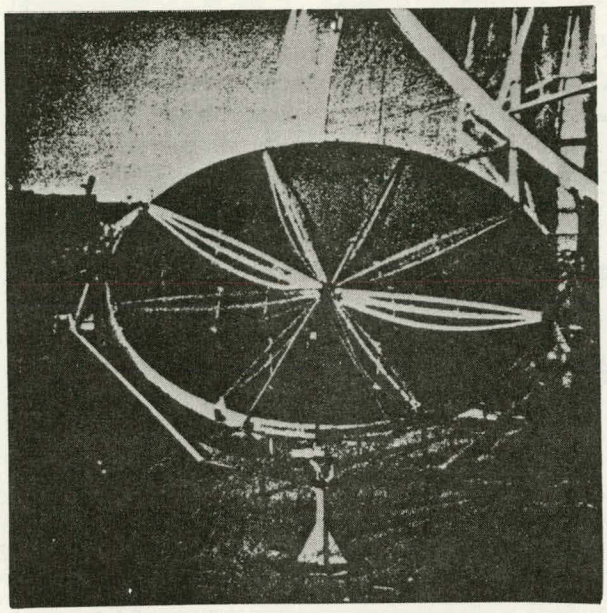

Fig. 16 3,5 m dish with sectorial reinforcement

References


Hencky "Über den Spannungszustand in kreisrunden Platten mit verschwindender Biegesteifigkeit" Zeitschrift für mathematische Physik, Vol. 63, 1915

Beale et al. IECEC meeting 1983

a) The development of a 1 KW electrical output free piston stirling engine alternator unit

b ) The free piston stirling engine - 2o years of development

Kleinwächster H.+J. "Solar driven stirling engines water pumping, cooling, electrification in rural areas and for future space stations" Proceedings comples meeting October 1983, Freiburg

## DESCRIPTION OF ENGINE-ALTERNATOR

The free piston engine-alternator described here is a first attempt at a design above 3kW. As such it represents only the beginning of what can be expected of machines of this type. But never the less, its promise is evident from its simplicity and projected performance. The performance given in the table below is derived from computer simulations using the Sunpower SYM-4 code, which has demonstrated its predictive capability within about 10% in power and efficiency over a very wide range of designs from 100 watt linear alternators to very low temperature ratio heat pumps.

Table of Performance Characteristics of 10kW Solar FPSE As Predicted by Computer Simulation

| | |
|---|---|
| Power Output | 10kW (e) |
| Engine Thermal Efficiency (Shaft Power/Heat to Head) | 40%+ @ 700°C Heat Temperature |
| Frequency (Hz.) | 50 |
| Working Fluid | Helium at 20 Bar |
| Cooling | Water @ 50°C |
| Engine-Alternator Dimensions | |
| Weight | 150kg |
| Diameter | 440mm |
| Length | 830mm |

ENGINE - The engine is a conventional free piston engine except in its pressure, which is relatively very low in comparison to its predecessors, large diameter, short stroke, thin wall and high frequency. (Figure 1). The advantages of such design include large heater head surfaces appropriate for the external heat transfer rates available, large piston diameter in correct ratio to the alternator size needed to match the power and high working space spring rates necessary to oscillate the piston and magnets at the desired frequency.

The moving parts of the engine are aligned precisely on a central rod, which also serves as a bearing surface for the displacer and its gas spring and a location for the alternator stator.

## HEATER-ABSORBER

The heater-absorber designed for the first prototype incorporated a flat surface exposed to solar radiation with integral involute gas passages between the regenerator hot end and a central connection to the expansion space. Other arrangements can readily be fitted-tubes, inverted cup quartz windows, or many others. Further work is in progress to locate the heater head design with the greatest overall performance.

ALTERNATOR - The alternator is of rectangular layout, with the stator winding normal to the engine axis. This arrangement was the lightest for its power which could be found, and in addition, was very easy to make with conventional laminations.

The moving magnets are directly connected to the piston of the engine and represent the minimum reciprocating mass possible for such an alternator, an important consideration, since the reciprocating mass determines the necessary spring rate, which in turn reflects on the thermodynamics of the working cycle and the system efficiency, as well as the mechanical complexity of the machine.

In the configuration used for the first prototye, the magnet bearing members slide on flat surfaces with contact, and a solid lubricant is used to minimize friction and wear. In designs requiring life above 10,000 hrs., it becomes desirable to use gas film lubrication, which on such flat surfaces with very light loads, is easily provided.

Alternative designs include those which are axisymmetric, with the alternator winding axis co-linear with the engine axis. This arrangement permits the use of hydrodynamic gas lubrication by way of spun piston and displacer, which method is somewhat less failure prone than the hydrostatic, with its auxiliary gas pump and very small orifices. The spinning effect is achieved by the impingement of the cooler port gas flow on small turbine blades milled into the facing surfaces of the piston and displacer. A trivial amount of cycle power is diverted to effect the spinning action.

## COOLING

The necessary cooling can be done by a rear mounted cylindrical heat exchanger and axial fan, with the coolant, which may be the same fluid as the working gas, moving from the engine internal cooler to the external heat exchanger either by way of a circulating pump, or in the case of a boiling coolant, by vaporization and condensation with gravity return.

If the cycle rejected heat is to be used for some other purpose, then the necessary conduit must be arranged from the ground to the engine.

## ADVANTAGES OF THE FPSE OVER CRANK DRIVE MACHINES FOR SOLAR APPLICATIONS

The free piston promises at least the following advantages over the crank type Stirling engine for Solar applications:

Since it is a single cylinder machine with essentially one working space, there is no possibility of flow maldistribution as can happen between the four working spaces of the double acting four cylinder crank type engine. Such flow unbalances can cause one of the heater tube sections to become hotter than the others and force a lower average working temperature in the four cylinder machine.

The free piston engine has only two essential moving parts, and is as a result much simpler and easier to make than the crank machine. Not only are the parts fewer, but they are also simpler, since the clearances on the sliding surfaces are quite generous, on the order of 50 to 70 microns.

There is no need for any liquid lubricant, with its attendant requirement for total exclusion from the working spaces.

There is no high pressure seal, and the seals that are used are not required to have close fits, since a small amount of blowby is acceptable, for the reason that it does not represent a loss of working fluid, nor does it carry with it any liquid contaminant. The only consequence of seal leak in the free piston machine is a slight degradation of performance.

The linear alternator of the free piston machine can be made to be very efficient and at the same time quite light for its power. Over 90 percent efficiency and a specific weight of about 6kg/kW for the alternator are readily and economically achievable.

The response of the FPSE to vrying thermal input is such that minimal control action is necessary. In the case of a direct grid connection, all that is required in the way of a control circuit is a disconnect which acts when alternator voltage is below line voltage.

It is not necessary to change pressure to match the engine to varying heat input, since the internal dynamics are such that temperature rise results in a very rapid rise in power capability, thus limiting temperature and efficiency variation to a low range as power varies between half and full power.

Since there is little mechanical friction in the FPSE, it will run to a low temperature difference. Usually about 100 degrees difference between source and sink suffices to keep it oscillating. This characteristic minimizes the need for restart during periods of varying solar input.

SUMMARY

The free piston Stirling-linear alternator has been shown to be scalable to power levels of tens of kilowatts in a form which is simple, efficient, long lived and relatively inexpensive. It avoids entirely the vexing problem of high pressure shaft seals, and its control requirements are not severe nor do they represent a significant threat to durability. Linear alternators have demonstrated high efficiency and moderate weight, and are capable of delivering 3 phase power from single machines without great increases of cost or complexity. There remains no apparent impediments to the commercial exploitation of the free piston engine for solar electric power generation.

ENGINE - ALTERNATOR LAYOUT

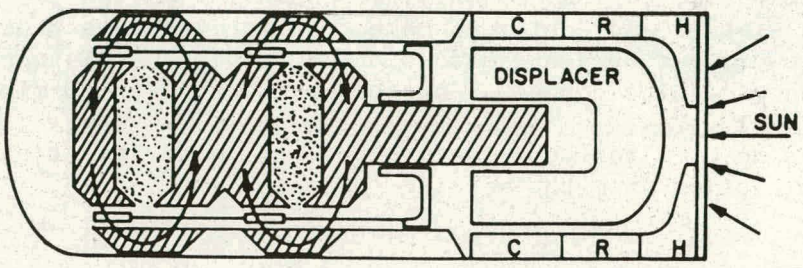

# THE BASE ENGINE FOR SOLAR STIRLING POWER

Roelf J. Meijer and Ted M. Godett
Stirling Thermal Motors, Inc.
Ann Arbor, MI 48104

## ABSTRACT

A new concept in Stirling engine technology is embodied in the "Base Engine" now being developed at Stirling Thermal Motors, Inc. This is a versatile energy conversion unit suitable for many different applications and heat sources.

The Base Engine, rated 40 kW at 2800 RPM, is a four-cylinder, double-acting variable displacement Stirling engine with pressurized crankcase and rotating shaft seal. It incorporates remote-heating technology with a stacked-heat-exchanger configuration and a liquid metal heat pipe connected to a distinctly separate combustor or other heat source. It specifically emphasizes high efficiency over a wide range of operating conditions, long life, low manufacturing cost and low material cost.

This paper describes the Base Engine, its design philosophy and approach, its projected performance, and some of its more attractive applications.

## BACKGROUND

In 1972, Ford Motor Company obtained a worldwide exclusive license from N.V. Philips of the Netherlands for the Stirling engine, covering virtually all applications, including automotive.

Under this license agreement the Research Lab of N.V. Philips was to design and build four 175 HP engines, two of which would be installed in Ford Torino automobiles [1]. See figures 1 and 2.

In 1976 the two Stirling powered Torinos and the older Philips Stirling bus, equipped with a 4-cylinder rhombic drive Stirling engine [2], were successfully demonstrated for three days in Dearborn, Michigan.

A few years later, in 1978, Ford terminated its Stirling engine activities to make manpower available for short-term technological problems, and a year later Philips stopped work on the Stirling engine.

Upon these events, Stirling Thermal Motors, Inc. (STM) was founded in the United States to continue the work done at Philips, so that the results of the years of research and development work at Philips, which had resulted in a technical breakthrough since its last license agreement in 1968, would not be lost.

STM's main purpose upon its foundation was to develop commercial Stirling engines. Philips Laboratories had only made laboratory models for research. The only engine made for a special purpose was the one for Ford. When this particular engine was made, Philips was confronted with the practical reality of designing and building a Stirling engine for the most complex application imaginable - an automotive engine. During this time it was discovered that some components of the engine might form obstacles for commercialization because of their complexity and vulnerability.

From 1974 on, a real breakthrough was made in avoiding these complexities. This made a more simple four-cylinder, double-acting Stirling engine possible.

Unfortunately, by this time it was too late to incorporate these improvements into the Ford engine. The intent was to use these new developments in a second-generation Ford engine. This, though, was not done before Ford dropped its Stirling engine program. The engines being built by earlier licensees of Philips were based on designs older than the Ford engine. Their configurations had been frozen for several years. It was therefore impossible to utilize the new improvements.

From the outset STM was convinced that the time was ripe for commercialization of the Stirling engine, because all the ingredients for a simple, inexpensive and reliable engine with a long service life were present.

## GENERAL APPROACH, BASIC APPLICATIONS

STM's general approach is based on the conclusion that we should avoid competition with existing internal combustion engines, at least in the beginning. We should rather find markets where the IC engine can not be used and where the use of the Stirling engine would be very economical, making use of the unique properties of the Stirling engine. Of the many possible applications, we gave particular attention to the following two:

- o Solar energy conversion
- o Prime mover for heat-driven heat pump.

If the manufacturing cost of the engine could be sufficiently low, particularly in mass production, the market in these fields alone could be vast.

## TECHNICAL APPROACH

The whole drive of STM is to commercialize the Stirling engine. This means that the engine must be simple, reliable, inexpensive, and it should have a long life. None of these requirements should have an adverse effect on the performance of the engine.

More than three years of designing, discussions with suppliers and vendors, component testing and price calculations, led to the Base Engine. Studies for NASA have shown that the Base Engine's configuration is suitable for a whole range of power sizes up to 500 hp.

Special emphasis was placed on the flexibility of the the engine to adapt readily to a wide range of specific applications, duty cycles and heat sources.

Consequently, remote-heating technology is an integral part of the development effort, making it possible to divide the engine into a thermal conversion unit and a distinctly separate external heating system. Different heat sources coupled to the same "thermal converter" will adapt the engine to different applications and enhance commercial introduction since most of the development complexity and cost is in the thermal conversion unit.

A liquid metal heat pipe [3] is used to transport the heat from the heat source to the expansion heat exchanger of the thermal converter.

So far, most of the development effort has concentrated on the thermal converter, which is designated STM4-120RH (4 cylinders, 120 $cm^3$ swept volume per piston, remote heated) and referred to as the Base Engine.

## ADVANTAGES OF REMOTE HEATING

One of the obstacles for mass-production of the Ford-Philips engine was the heater head. This was built as an integrated unit for the four cylinders (Figure 3). The huge mass of heat resistant material was very expensive and made the brazing cycle much too long. The reason for this large amount of material is that the tubular-expansion heat exchanger common to direct-flame Stirling engines must accomodate the relatively difficult heat transfer from the flue gas to the walls of the heat exchanger tubes. It is, therefore, characterized by a complex cage geometry as well as volume and flow-path length which are much larger than those required for the relatively easy heat transfer from the tube walls to the working fluid of the engine.

By contrast, an expansion heat-exchanger heated by the condensing metal vapor with a large film coefficient in a heat pipe can be ideally sized to suit the requirements of the working fluid and can be shaped in the most convenient manner for ease of fabrication (Figure 4).

Of course, this itself does not solve the difficult external heat transfer problem, but rather shifts it to the evaporator section of the heat pipe where the size necessary for adequate heat transfer does not affect the thermodynamic section and is easily realized since the heat pipe does not have to support the high cycle pressure.

For solar applications a solar receiver will be the evaporator of the heat pipe system.

Remote heating thus offers a number of advantages in addition to the flexibility with which it endows the engine:

- It brings about major simplifications to the heat-exchanger design. The so-called heat-exchanger-stack configuration, designed to take advantage of the high film coefficient of the condensing metal vapor, is considerably less expensive and more suitable for mass production.

- It brings about considerable improvement of the engine performance by permitting the heater design to be ideally suited to the thermodynamic requirements.

- The uniform temperature throughout the confines of the heat pipe enclosure eliminates hot spots on the heater and thus enhance both the efficiency and the reliability of the engine.

## NEW POWER CONTROL SYSTEM

Up to this time, the preferred method for changing power has been changing the pressure inside the engine, because the torque of the engine is approximately proportional to the mean pressure of the working gas [4].

The development of this type of power control at Philips was done with a single cylinder displacer engine, where this type of power control was acceptable. However, for a 4-cylinder, double acting engine it became quite cumbersome, particularly when very rapid changes are required, as in automotive applications. This type of system included many check valves, activator valves, and a storage bottle, along with a high pressure hydrogen compresser.

Figure 5 shows a diagram of the power control system of the Ford-Philips Stirling engine. Power increases when the working gas (in this case hydrogen) is dumped from the high pressure storage bottle into the engine. The reverse takes place when the gas is pumped out of the engine into the storage tank with the high pressure compressor. But because this is a slow process, during this time, a short-circuit power control - which is a loss-control - instantaneously cuts the power.

In 1974, during the work on the automotive engine, a relatively simple, heavy duty construction was found to vary the power [5], [6], [7]. In this case the mean pressure of the engine stays the same, but the stroke of the pistons changes. This method of power control has the further advantage of high part load efficiency. Such a construction could be used only with a swashplate drive since the stroke of the pistons is controlled by the angle of the swashplate. It was tested thoroughly in a test rig and applied in the Advenco engine, but the Advenco engine was never adequately tested. Philips eventually sold the Advenco engine to NASA, where further testing was done.

Figure 6 illustrates schematically the variable swashplate mechanism. The swashplate is mounted on a part of the shaft which is tilted an angle $\alpha$ from the main shaft axis. The swashplate is mounted in such fashion that its centerline makes an angle $\alpha$ with the tilted shaft axis and it can be rotated relative to and about the tilted shaft axis in order to change its angle, and, with this, the stroke of the pistons.

The swashplate angle variation affected by its rotation about and relative to the engine shaft, is accomplished with a rotary actuator. This is a hydraulic vane motor comprising two diametrically opposite vanes attached to the shaft and two attached to the housing as shown in the cross-section of the swashplate-power control of the Base Engine [8], [9],(Figure 7). Thus, two pairs, A and B, of diametrically opposite chambers are formed. Rotation of the

stroke converter housing relative to the shaft is affected by pressurizing one pair and relieving the other. The rotation is transmitted to the swashplate via a bevel gear to which the actuator housing is attached. The supply and return lines to the actuator are concentric tunnels in the shaft connected to a solenoid actuated proportional valve mounted outside the crankcase. Figure 8 shows a practical model of a variable swashplate in two positions.

The torque applied by the actuator to the swashplate in order to maintain a certain angular position depends on whether it was rotated to such position in the positive or in the negative direction. Rotation in the negative direction requires less torque since the engine torque itself in this case acts to increase the swashplate angle.

Figure 9 shows the actuator torque as a function of the swashplate angular position relative to the shaft. The curves labeled $M_+(\psi)$ and $M_-(\psi)$ refer to that torque for the positive and negative direction of rotation respectively. The third curve, $\gamma(\psi)$ shows the corresponding swashplate angle. The curve $M_-(\psi)$ reverses its sign within its range of definition. The point of sign reversal is an unstable control point to be avoided by narrowing the range of definition to exclude it. In the case of the Base Engine, shown in Figure 10, the angle $\alpha$ is 12.5° yielding maximum theoretical swashplate angle of $2\alpha = 25°$ corresponding to 180° rotation. The maximum swashplate angle of interest is only 22°, corresponding to a narrower range of definition (124°) within which the torque $M_-(\psi)$ does not change sign.

Loss of hydraulic power will result in the gas forces bringing the swashplate to a position perpendicular to the main shaft axis reducing the piston stroke to zero - an automatic safety feature.

## SEALS

In a 4-cylinder, double-acting Stirling engine there are two types of dynamic seals:

- Dynamic seals as piston rings to divide the four cycles from each other; and
- Dynamic reciprocating seals on the piston rods, in order to contain the high pressure working gas in the engine. These seals should also prevent oil penetration into the cylinders from the lubricated drive.

For the dry-running piston rings, a good solution is found in using a reinforced PTFE material.

However, the different types of reciprocating seals for the piston rods are still not reliable. Philips developed the rolling diaphragm seal, but this was shown, in the Ford-Philips engine, to be vulnerable in non-laboratory environments.

STM was able to avoid the gas containment function of these reciprocating seals entirely.

The new power control, with its variable swashplate, made it possible to enclose the relatively small drive with a pressure hull and to use a commercially available rotating shaft seal. Preventing oil penetration into the cylinders is, in this case, much easier, and has already been thoroughly tested in other engines.

## SPECIAL FEATURES

Amenability to dynamic balancing and the ease of starting the engine are two additional features of the variable swashplate drive and power control elaborated upon in this section.

DYNAMIC BALANCING is achieved by adjusting the swashplate moments of inertia to the reciprocating mass. This is done in a manner enforcing perfect dynamic balance at a certain swashplate angle within its range of variation. At different angles unbalanced moments will appear, but since perfect balance automatically occurs at zero angle, these will be very small.

STARTING of the engine can be accomplished by heating up the expansion heat exchanger and the regenerator and then suddenly using the control pressure to increase the swashplate angle. This will cause the pistons to move in their normal way causing the engine to immediately develop sufficient power to perpetuate the motion. An accumulator fed by the hydraulic pressure pump will be used for that purpose.

Obviously, such a simple procedure may be used only for such applications as solar conversion since no accessories are required for the combusiton. In other cases only a very small starter motor is required to power the accessories needed for combustion, such as the air blower. When the engine has reached its correct temperature the accumulator pressure may be used to quickly increase the angle, having the engine self-start as mentioned above.

## DESCRIPTION OF THE ENGINE

A layout drawing of the Base Engine STM4-120RH is shown in Figure 10. This engine is distinguished by two major features:

- Variable swashplate drive and power control contained in a pressurized "crankcase" with a commercially available rotating shaft seal containing the working fluid and making it possible to avoid the reciprocating rod sealing problem; and

- Remote heating, featuring heat-exchanger-stack configuration and liquid metal heat pipe heat transport system.

The cross heads are long in order to reduce contact forces and to relieve their bridge section from having to sustain any appreciable bending moment.

The drive components are supported and located by two aluminum castings forming the major building blocks of the engine (see Figure 11).

The crankcase pressure containment is formed by a commercially available rotating shaft seal placed in a seal-housing which also supports the thrust bearing, and by a pressure hull placed over the entire crankcase and bolted to the aluminum casting. The pressure hull serves no structural function other than containing the crankcase pressure.

The front casting also incorporates the cold part of the thermodynamic section, namely, the cylinders, coolers, cold ducts and coolant passages. Four identical assemblies, one for each cycle, form the hot portion of the thermodynamic section, as described in the previous section. These are made of the iron-based alloy CRM-6D sized to endow the engine with creep failure life well in excess of 50,000 hours at full load.

Table 1 summarizes some of the important features and parameters of the Base Engine.

## PERFORMANCE

A set of engine parameters governing the performance of the thermodynamic section was selected for the Base Engine through an extensive and painstaking effort to tailor the engine performance to the design approach described above.

This approach required a high level of efficiency to prevail over a wide range of operating conditions, making the engine suitable for any duty cycle. Hundreds of different combinations of engine parameters were simulated before the optimal set was selected and established the design base of the engine.

The result is shown in Figure 12 as two performance maps at mean cycle pressure levels of 11 MPa and 6.3 MPa respectively. Figure 12a shows that between the power levels of 8 kW and 40 kW the shaft efficiency is between 45% and 47% (excluding auxiliaries and collector efficiency). Over a wide power range the efficiency hardly hanges with the engine speed.

For applications requiring less power, a smaller charge of helium may be used with very little effect on the efficiency. This is shown in Figure 12b for an engine charged to 6.3 MPa to provide power output of no more than 25 kW. This will greatly enhance the life of the engine.

Major contributions to the high efficiency of the Base Engine are derived from the heat-exchanger-stack configuration, the variable stroke power control and the design of the drive mechanism.

The heat-exchanger-stack configuration adds more freedom to the set of

parameters governing the thermodynamic performance. These can be exploited to facilitate tailoring of the performance characteristics of the engine.

The variable-stroke power control inherently inhibits degradation of the efficiency at part load since power reduction is accomplished partly through the addition of void volume or, equivalently, reduction of the pressure wave amplitude, which is beneficial to the indicated efficiency.

Figure 13 schematically illustrates the Base Engine with solar receiver, solid fuel combustion, and with a liquid or gaseous fuel combustor.

## REFERENCES


1. Norman D. Potsma, Ford Motor Company & Rob van Giesel and Frits Reinink, N.V. Philips, Holland, The Stirling Engine for Passenger Car Application, Paper 730648, SAE, Chicago, Illinois, June 1973.

2. R.J. Meijer and C.L. Spigt, Philips Research Labs, Eindhoven, The Potential of the Philips Stirling Engine for Pollution Reduction and Energy Conservation. Paper presented at the Second Symposium on Low Pollution Power Systems Development, organized by the Committee on the Challenge of Modern Society of the North Atlantic Treaty Organization in Dusseldorf, Germany, November, 1974.

3. G.A.A. Asselman and D.B. Green, Heatpipes I & II, Philips Technical Rev.33, 104-113, Nov. 1973 No. 4 and 138-148, 1973, No. 5.

4. R.J. Meijer, The Philips Hot Gas Engine with Rhombic Drive Mechanism, Philips Techn. Rev. 20, 245-262, 1958/9, No.9.

5. R.J. Meijer and A.P.J. Michels, Conceptual Design of a Variable Displacement Stirling Engine for Automotive Propulsion, Paper 789351, Proceedings, 13th IECEC, October 1978.

6. J. Vos, Design Characteristics of an Advanced Stirlng Engine Concept, Paper 799257, Proceedings 14th IECEC, Boston, August 1979.

7. R.J. Meiejr and B. Ziph, A Variable Angle Wobble Plate Drive for a Stroke Controlled Stirling Engine, Paper 799258, Proceedings, 14th IECEC, Boston, August 1979.

8. R.J. Meijer and B. Ziph, Variable Displacement Automotive Power Train, Proceedings, 5th International Automotive Propulsion Systems Symposium, Dearborn, MI, April 1980.

9. B. Ziph and R.J. Meijer, Variable Stroke Power Control for Stirling Engines, Paper 810088, SAE, Detroit, Michigan, February 1981.

10. Roelf J. Meijer and Benjamin Ziph, A New, Versatile Stirling Energy Conversion Unit, Paper 829299, Proceedings, 17th IECEC, Los Angeles, California, August 1982.

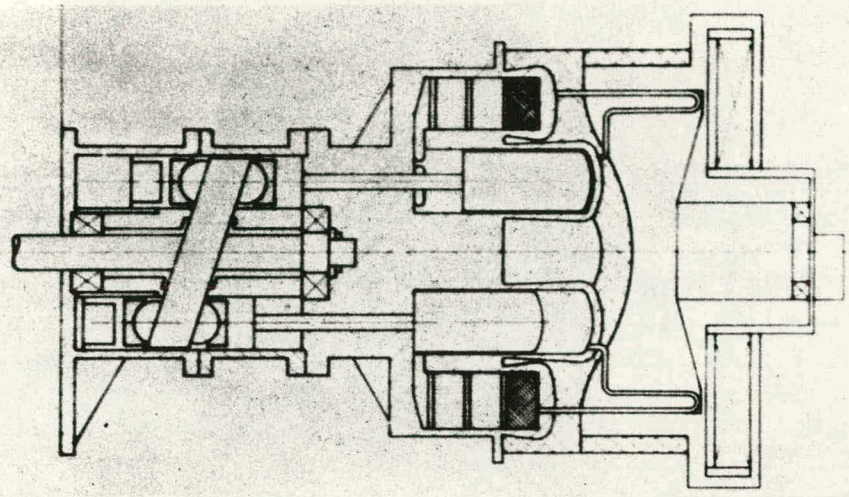

Figure 1

Schematic of the Ford-Philips Torino engine. This is a 4-cylinder double-acting Stirling engine with swashplate drive. Two of the four cylinders and two of the four cooler-regenerator units are shown in cross-sections. In these engines the movement of the pistons is transmitted to the main shaft by a swashplate.

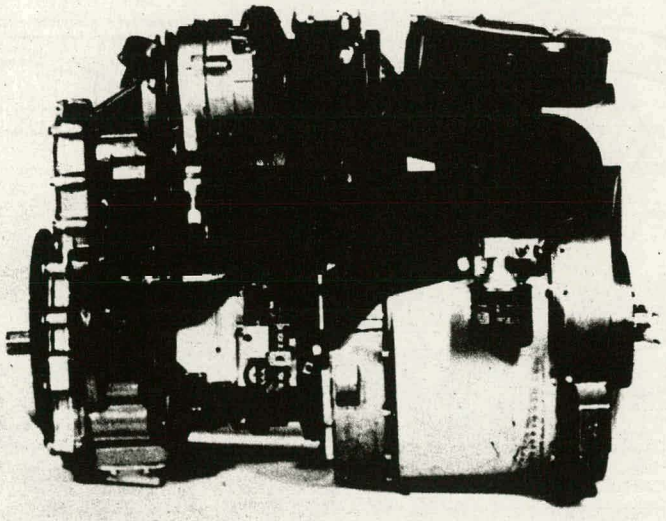

Figure 2

A 175 HP 4-cylinder double-acting type Stirling engine with swashplate drive to be mounted into a Ford Torino automobile (1975).

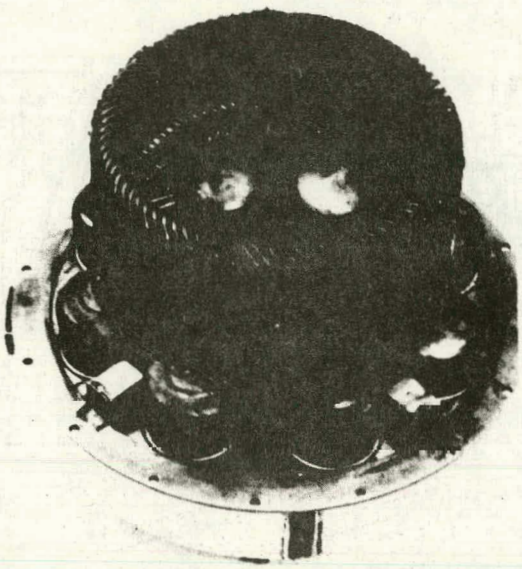

Figure 3
An example of the integrated direct-flame-heated heater head (from the Ford-Philips engine)

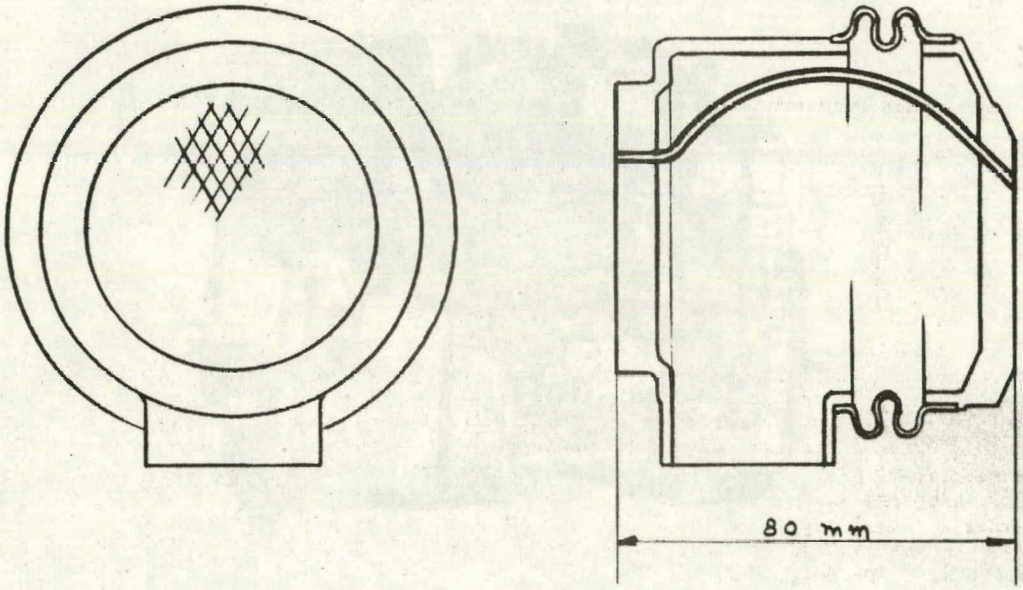


Figure 4
Expansion heat exchangers of the Base Engine. There is one per cylinder. These will later be electron-beam welded in the heat exchanger stack. The tubes are curved, enclosed in a flexible cannister, and brazed to two end plates.

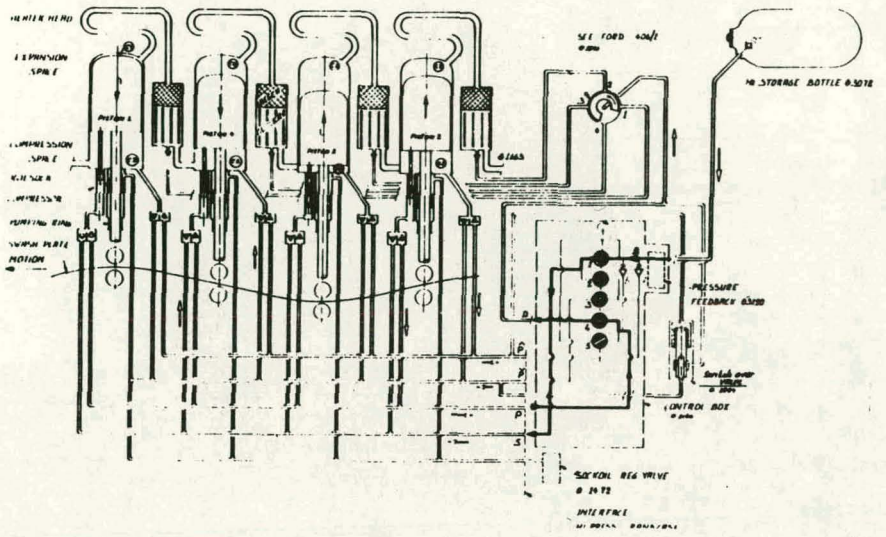

Figure 5

Power control system for the Ford-Philips Stirling engine. The torque of the engine is controlled by the pressure of the working gas. For more power, the woking gas from the storage bottle is supplied to the engine. For less power, small hydrogen compressors (connected to the bottoms of the pistons) are pumping the gas out of the engine and back into the storage bottle.

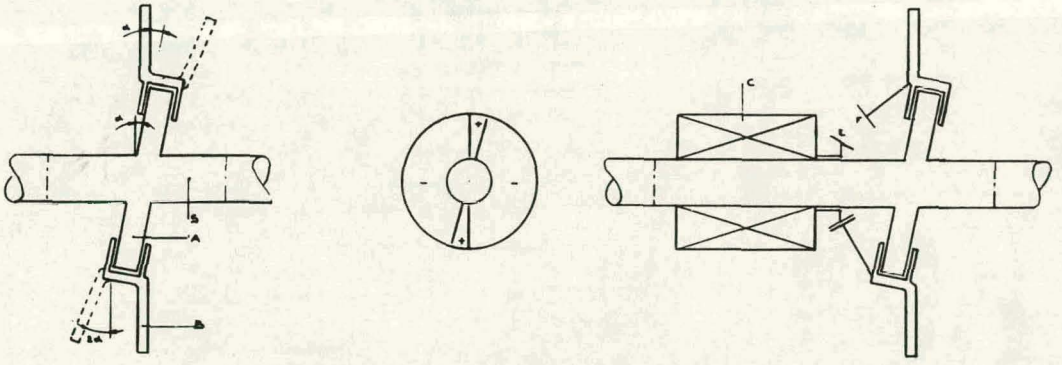

Figure 6

Schematic of the variable swashplate mechanism, showing the principle of changing the angle of the swashplate, which it makes with the shaft from 0 to $2\alpha$. The small plate A is fixed on the shaft S with an angle $\alpha$. The engine swashplate (drawn here as a solid line) is perpendicular on the shaft S. This situation, $\alpha - \alpha = 0$, means that the strokes of the pistons are zero. When the engine swashplate B is turned 180° relative to the small plate A, the angle then becomes represented by the dotted lines. In this case the strokes of the pistons are maximal. By turning B relative to A between 0° and 180° any angle of the swashplate between 0 and $2\alpha$ can be obtained, so the strokes of the pistons can be changed from zero to maximum. C is a hydraulic vane mechanism, the housing of which can turn in one or the other direction depending on which chambers are pressurized and which are not. The oil is fed via two channels in the shaft S. The turning of the housing is transmitted to the engine via the bevel gears E and F.

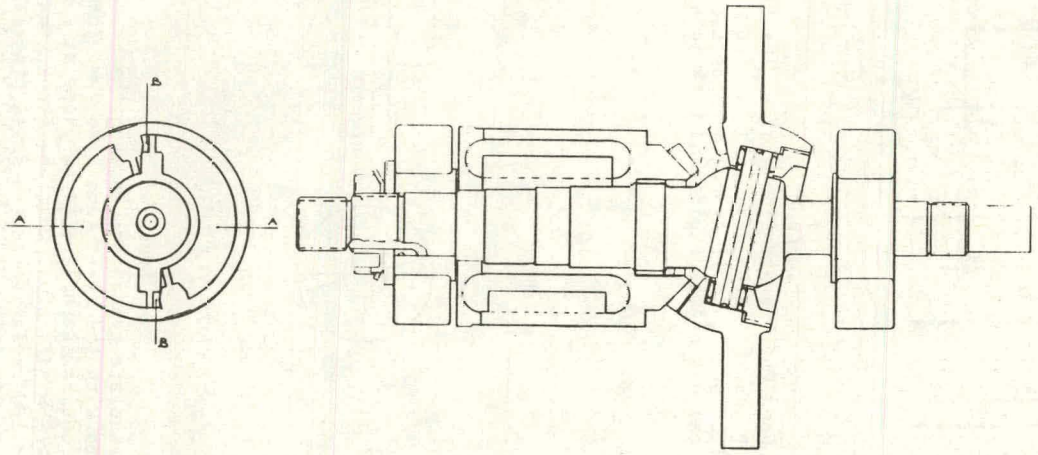

Figure 7

Cross-section of the rotary actuator of the Base Engine. The torque caused by the hydraulic vane-motor will turn the swashplate relative to the shaft via pinion and bevel gears.

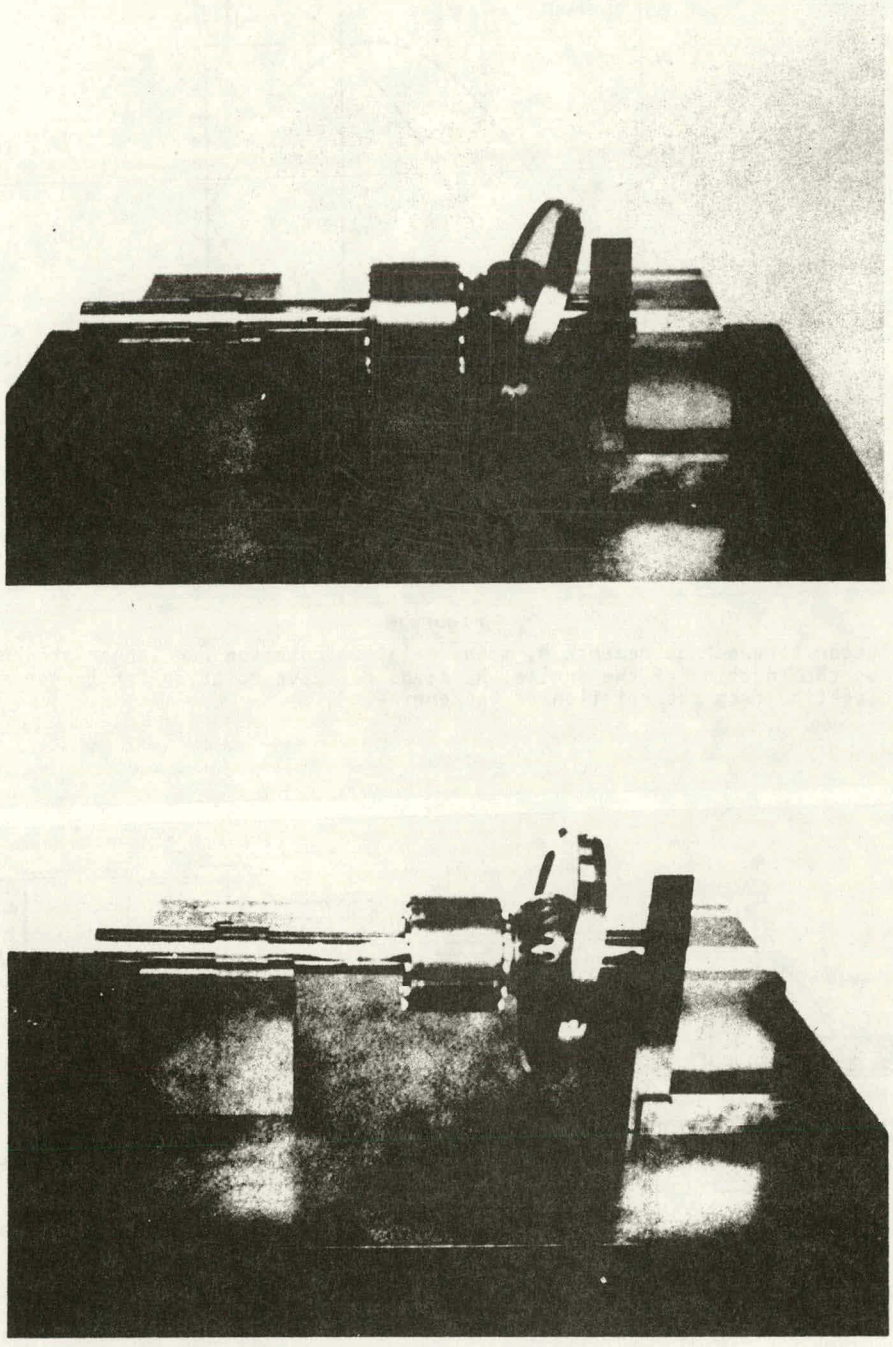

Figure 8
Practical model of a variable swashplate, shown in two positions.

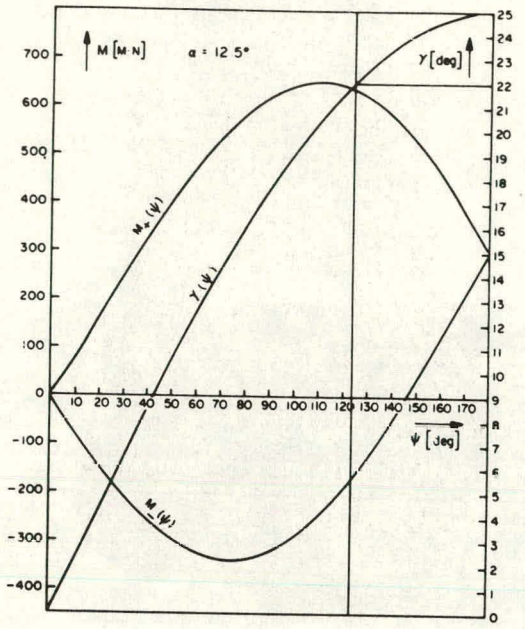


Figure 9

Rotary actuator torque requirements $M_+$ means relative rotation for larger stroke in the same direction as the rotation of the engine. $M_-$ means relative rotation for larger stroke in the opposite direction from the rotation of the engine.

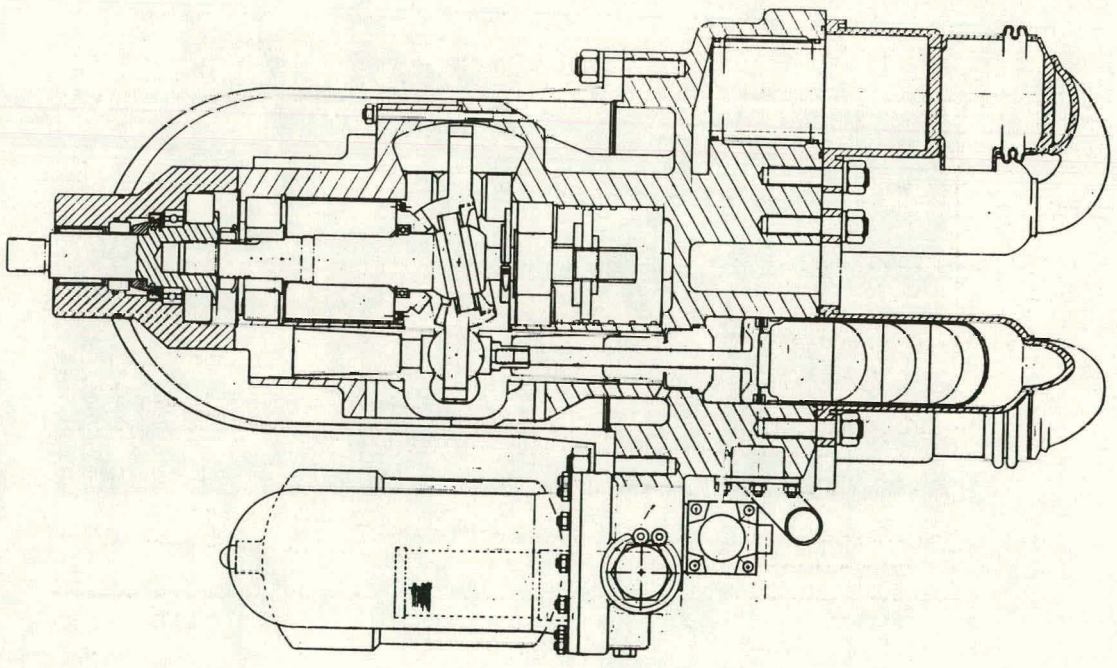

Figure 10

Layout of the Base Engine (STM4-120RH)

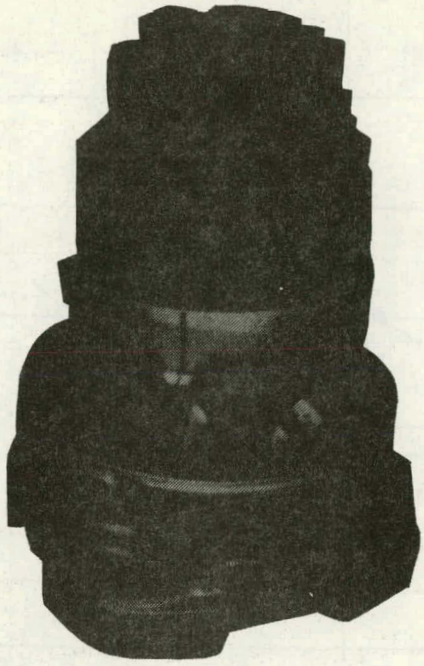

Figure 11

The aluminum castings for the front (bottom) and rear (top) parts of the crankcase. The front part incorporates the cold part of the thermodynamic section, mainly the cylinders, coolers, cold ducts and coolant passages.

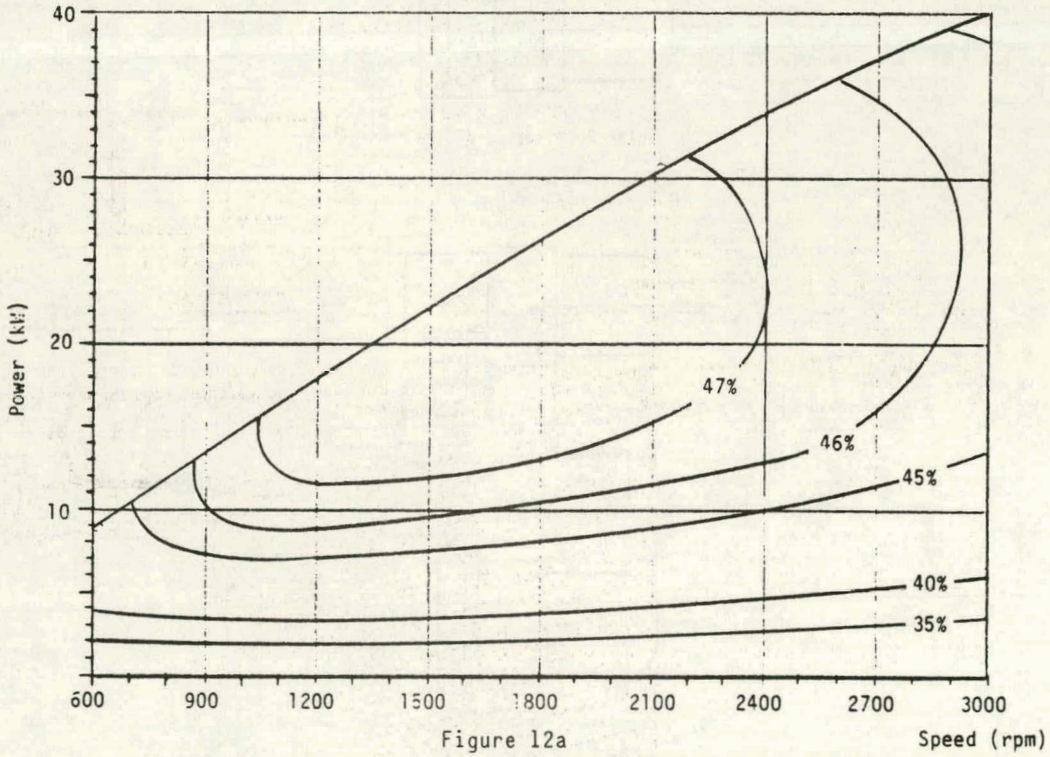


Figure 12a

Performance map of the STM4-120RH with mean pressure of 11 MPa showing lines of constant efficiency.

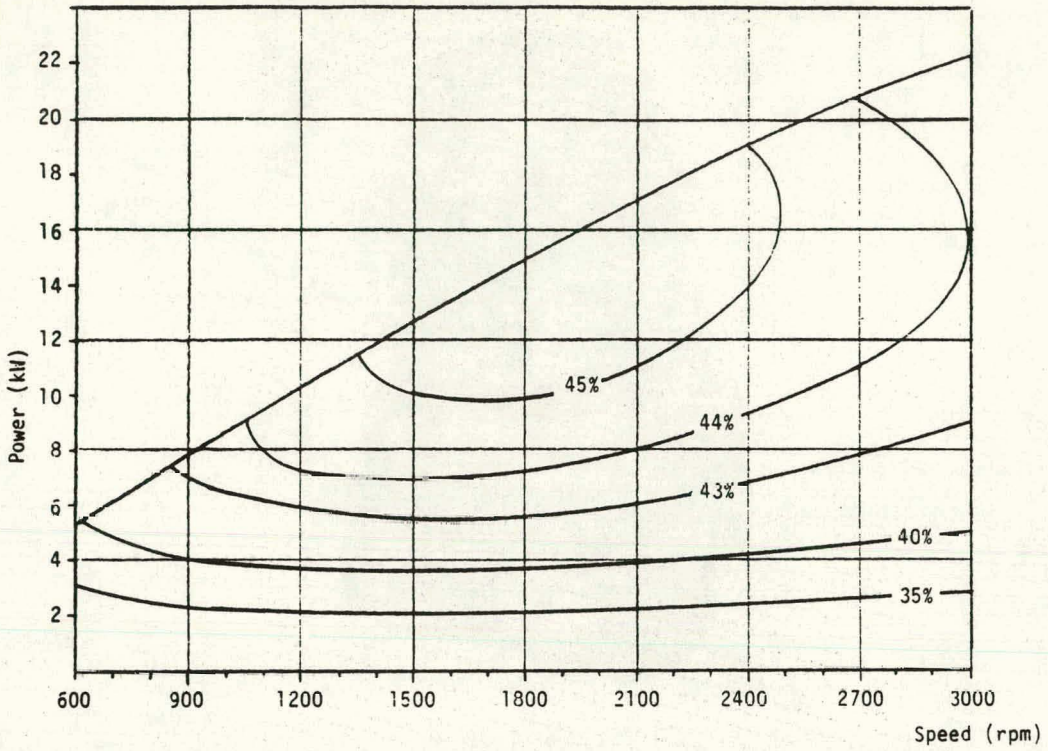


Figure 12b

**Performance map of the STM4-120RH with reduced mean pressure (6.3 MPa) showing lines of constant efficiency.**

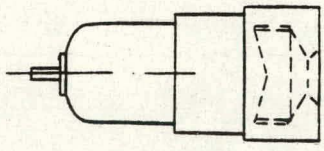

Solar Receiver

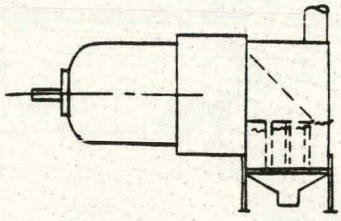

Coal Powder

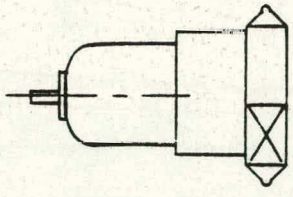

Liquid and Gaseous Fuels

Figure 13

The Base Engine with Different Heat Sources

| | |
|---|---|
| Arrangement: | Four double-acting cylinders symmetrically arranged about a common axis. One heat exchanger assembly per cylinder. |
| Bore: | 56 mm |
| Maximum stroke: | 48 mm |
| Overall length: | 635 mm |
| Cross sectional dimensions: | Largest cross-section is 300 mm in diameter |
| Total estimated weight: | 75 kg |
| Working fluid: | Helium |
| Mean cycle pressure: | 11 MPa |
| Heater temperature: | 800°C |
| Power control: | Piston stroke variation by means of a variable swashplate with a maximum angle of 22° |
| Heat transport: | Sodium heat pipe |
| Gas containment: | Crankcase pressurized to mean cycle pressure and sealed with a rotating shaft seal |
| Oil containment: | Reciprocating rod oil scraper |
| Materials: | Iron-base CRM-6D, CG-27 heater tube material |

Table 1 - Important Features and Parameters of the Base Engine

# TESTING AND INSTRUMENTATION OVERVIEW

Darrell L. Ross

Jet Propulsion Laboratory
Pasadena, CA 91109

Four papers were presented in the Testing and Instrumentation session: 1) Special Pyrheliometer Shroud Development, 2) Rapid Test Bed Concentrator Alignment Techniques, 3) PDC-1 Sun Position Calculation, and 4) Recent Solar Measurements Results. Each paper is described briefly below.

The paper on "Special Pyrheliometer Shroud Development", presented by Dr. Edwin Dennison, member of the Technical Staff at JPL, concludes that it is possible to build an insolation measurement system which is proportional to the thermal power at the focal plane for dishes that is accurate over a wide range of sky conditions.

The paper on "Rapid Test Bed Concentrator Alignment Techniques", presented by Maurice Argoud, Member of the Technical Staff at JPL, details a method of aligning the 220 mirror facets on a Test Bed Concentrator in one or two nights, instead of one to two weeks.

The paper on "PDC-1 Sun Position Calculation", presented by Dr. John Stallkamp, Member of the Technical Staff at JPL, presents the several computational approaches to providing the local azimuth and elevation angles of the sun as a function of local time and then the utilization of the most appropriate method in the PDC-1 microprocessor.

The paper on "Recent Solar Measurements Results", presented by Darrell Ross, Task Manager for Test and Evaluation at the PDTS, describes the effects of the El Chichon volcanic eruption in Mexico in 1982 on the insolation levels at the PDTS.

# Special Pyrheliometer Shroud Development

E. Dennison
Jet Propulsion Laboratory
California Institute of Technology
Pasadena, California 91109

Introduction The need for simple methods to compensate for circumsolar radiation became very important during the spring of 1982 when large amounts of dust appeared in the upper terrestrial atmosphere as a result of a volcanic eruption in Mexico. Prior to this time definitive calorimeter measurements at the JPL Parabolic Dish Site (PDTS) at the Edwards Test Station were limited to times when the insolation was greater than 950 W/sq.M, i.e., times when the amount of circumsolar radiation was negligible. This limitation was used because of the inconsistent data which was found at low elevation angles and on days of high circumsolar radiation.

After the appearance of the volcanic dust the maximum insolation was less than 900 W/sq.M and the amount of circumsolar radiation was significant. In addition, there was a very substantial increase in the presence of high thin cirrus clouds which added significant errors to the calorimeter measurements. The presence of circumsolar radiation is clearly shown in Figure 1. In this photograph of the PDC-1 concentrator the image of the sun is covered by the calorimeter and the bright halo around the calorimeter is the circumsolar radiation.

Insolation measurements are used to analyze atmospheric conditions, evaluate potential thermal power sites, and to determine the amount of input power to a power conversion unit. For the latter, the insolation measurements are used as an interpolation parameter between calorimeter measurements.

To insure that the insolation values accurately represent the input power to a power conversion unit it is important that the Field Of View (FOV) of the concentrator aperture and the insolation radiometer are

---

*The work described in this paper was carried out or coordinated by the Jet Propulsion Laboratory, California Institute of Technology, and was sponsored by the U.S. Department of Energy through an agreement with the National Aeronautics and Space Administration.

the same. The word "radiometer" will be used to refer to both radiometers and pyrheliometers. If the calorimeter and the power conversion unit have the same aperture, the radiometer can be used to normalize all power measurements to a standard insolation value x (1000 W/sq.M for the JPL data).

This report covers the calculations, implementation, and results of the JPL use of this approach. Three instruments were used to measure the insolation: an Eppley Normal Incidence Radiometer (NIP) and two versions of the cavity radiometer developed by J. M. Kendall, Sr. at JPL. One of the Kendall radiometers was of the Mark VI windowless design used for calibration of radiometers and the other was the Mark III quartz window design used for routine field measurements. The shrouds used to limit the FOV of the radiometers were designed to simulate the FOV of the PDC-1 concentrator with the Cold Water Cavity Calorimeter (Figure 2).

Field of View Calculations The quantitative description of the FOV of a concentrator or radiometer will be referred to as the Angular Acceptance Function (AAF). The AAF is the fraction of the radiation coming from a point source at an infinite distance as a function of the angular distance of the point source from the optic axis of the concentrator or radiometer. The AAF does not depend on the angular size of sun but only on the geometric parameters of the concentrator or radiometer. The AAF will be 1.0 for a source on the optic axis and will decrease continuously from an inner limiting angle to zero at the outer limiting angle. The form of a concentrator AAF is different from the AAF of a radiometer because of the respective optical geometries. As a result the radiometer AAF cannot be matched exactly to the concentrator but the differences between these functions can be made acceptably

Concentrator AAF One practical method for calculating the AAF of a solar concentrator was developed by Prof. G. F. Trentelman of Northern Michigan University using vector analysis. It has been found that in practice it is convenient to represent the AAF as a function of the ratio of the tangent of the source angle divided by the tangent of the receiver radius angle (receiver radius divided by the concentrator focal length). This parameter will be referred to as the "radius number." In this form the AAF changes substantially with the concentrator f-number (focal length divided by diameter) and insignificantly with receiver aperture. When the AAF is expressed in terms of these dimensionless parameters it can be easily applied to any paraboloidal concentrator with any receiver aperture (Figure 3). Slope errors cause some change in the AAF but in most cases these effects appear to be small.

Radiometer AAF The AAF of a radiometer can be calculated directly from the aperture and detector radii, the aperture/detector separation, and the angular distance of the point source from the optic axis. This calculation is based on the assumption that the detector aperture is uniformly sensitive. With the ratio of the front aperture to the

detector aperture and the tangent of the receiver aperture times the aperture/detector separation as free parameters the radiometer AAF can be calculated as a function of the radius number.

Matching Radiometer AAF to Concentrator AAF One practical method for finding the radiometer parameters which make the radiometer AAF fit the concentrator AAF is to use an interactive computer program. By a careful choice of parameters it is possible to make the radiometer AAF rapidly converge on the concentrator AAF. Because the concentrator AAF is determined from a finite number of rays, it can be fitted to a polynomial to give a smooth representation of the data. In practice this does not significantly change the radiometer parameters.

Experimental Results To verify the expected advantages of using a FOV limiting shroud on an insolation radiometer, a series of calorimeter measurements were made using the PDC-1 concentrator and the shrouded radiometers. One of the radiometers was an Eppley NIP mounted on the concentrator. The other radiometers were of the Kendall type and were attached to an equatorial mount with a clock drive. The boresight alignment images were checked frequently during the measurement period to insure that no erroneous data resulted from tracking errors.

The thermal power measured by the calorimeter and the insolation measured by the radiometers was plotted for each measurement period. To test the validity of this technique, the calorimeter values were divided by each of the radiometer values and the results were also plotted. These ratios gave the net power output of the concentrator normalized to 1000 W/sq.M under sky conditions which varied from light haze to thin cirrus clouds. No completely clear days occurred during the time these tests were made. There is no reason to believe that the normalized power values would differ from these values for completely clear skies. During the passage of the cirrus clouds the normalized power values showed a substantial variation over short periods of time as a result of long time constant of the calorimeter relative to the time constants of the radiometers.

Figures 4a and 5a show the radiometer data plots for two different days and Figures 4b and 5b show the corresponding plots of the direct and normalized power measurements. Figure 5b demonstrates that the normalized power is relatively constant under a wide range of sky conditions. The value of the normalized power in this figure was too high because of a faulty flow meter. This problem was corrected and the normalized power values shown in Figure 4b more accurately represent the performance of the PDC-1 concentrator.

The insolation values measured with these modified radiometers were lower than the values which would have been obtained with standard radiometers. However, the purpose of these measurements was to determine the relationship between the radiometers and the net power throughput

of the concentrator with a specific aperture. This calibration would have been used to determine the operating efficiency of the power conversion unit which was to have been used with this concentrator.

During this limited test program it was not possible to make a direct comparison between these shrouded radiometers and standard radiometers. However, this test program did demonstrate that the normalized power output of the PDC-1 concentrator was constant under a wide range of sky conditions.

Recommendations Because this program to evaluate the effectiveness of approach to insolation measurements was limited, it is recommended that these experiments be repeated with other concentrators and radiometers. These tests should be made with a wide range of sky conditions and solar elevation angles using both a standard and a shrouded NIP. These data would be very useful for determining the accuracy of existing NIP records. Finally, it is recommended that future site surveys be made with both standard and FOV limited NIP instruments to insure that proposed solar power systems are suitable for the proposed sites. This is most important when the proposed site has a substantial number of days with strong haze or thin clouds.

Conclusions This technique of matching the FOV of an insolation radiometer to the FOV of a specific concentrator and receiver aperture appears to be both practical and effective. It would appear that the efficiency of a power conversion unit will be too low if the insolation is measured with a radiometer which has a FOV which is larger than the FOV of the concentrator.

Author's Note An expanded version of this report with the AAF algorithms will be published at a later date.

Figure 1 PDC-1 with Cavity Calorimeter

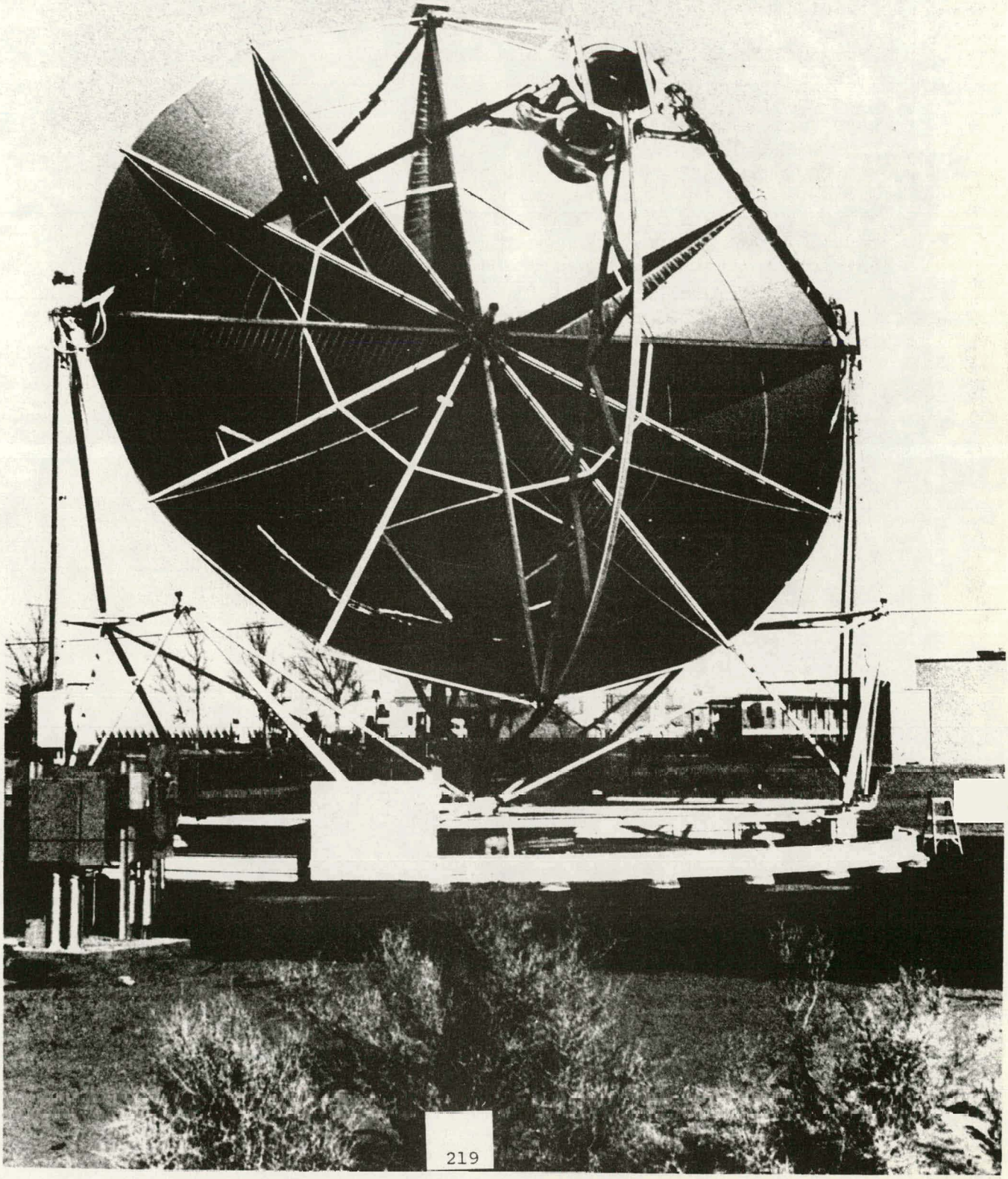

Figure 2 Radiometer with Shroud

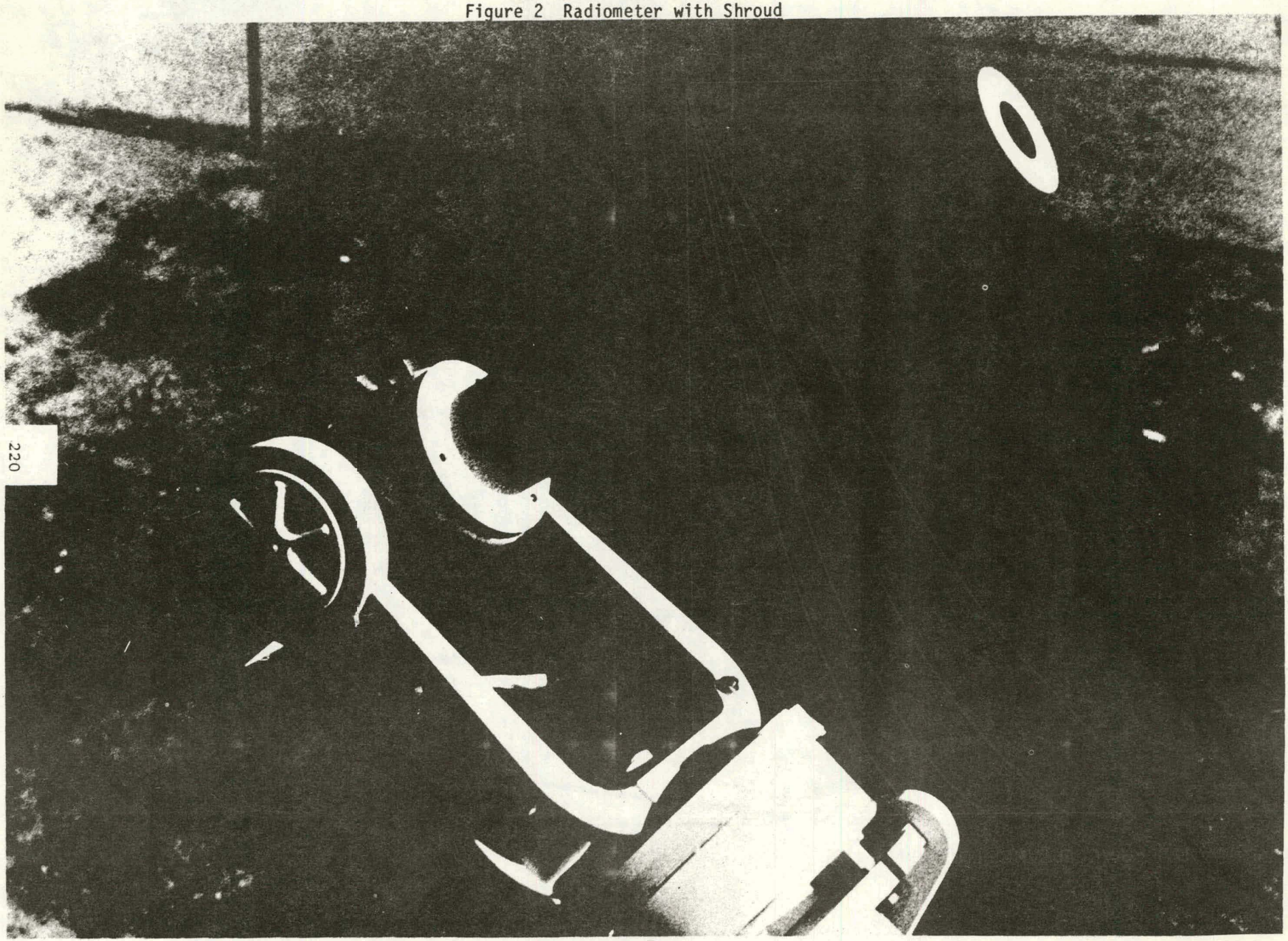

Figure 3

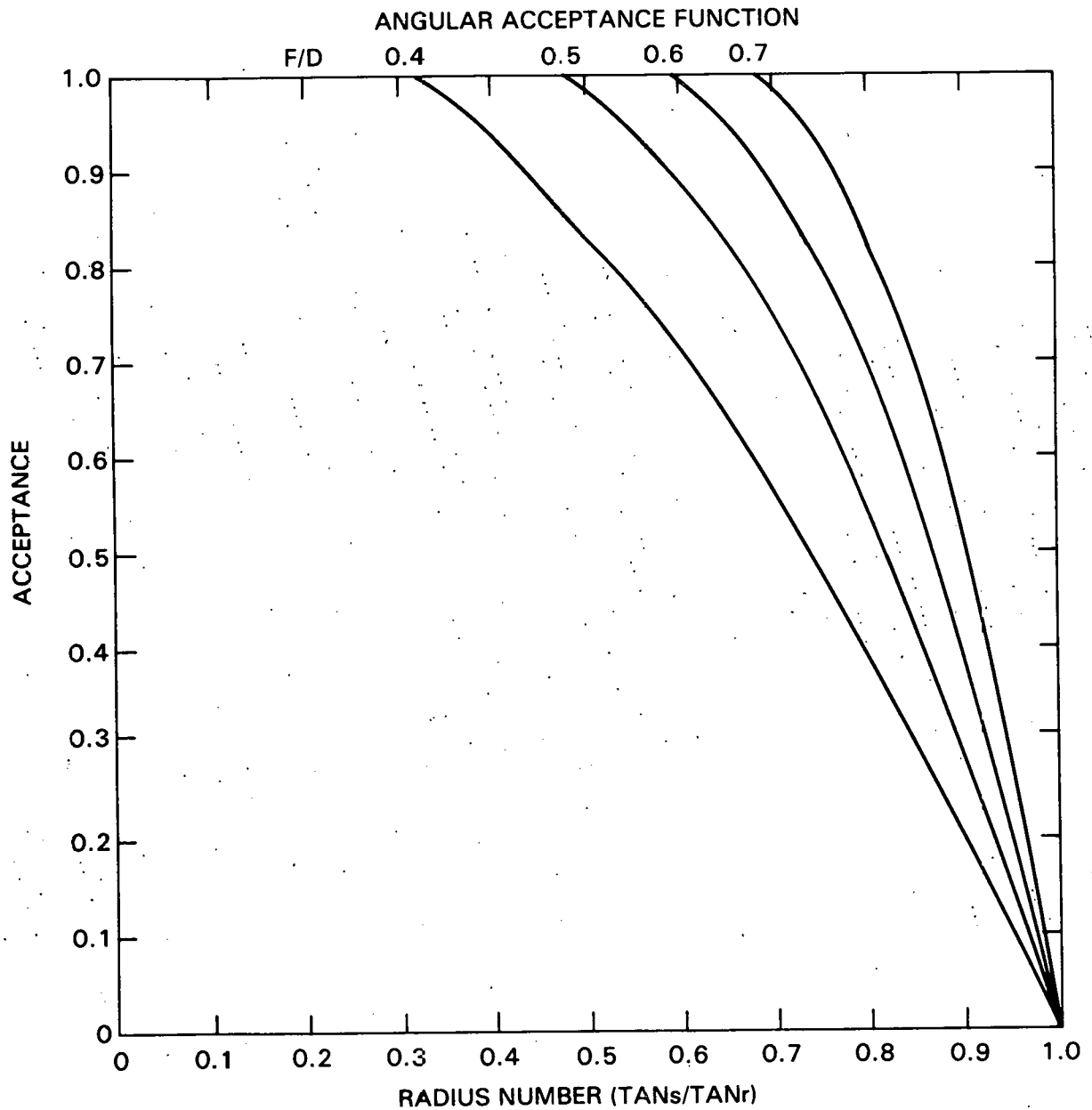
ANGULAR ACCEPTANCE FUNCTION
F/D
0.4
0.5
0.6
0.7
ACCEPTANCE
1.0
0.9
0.8
0.7
0.6
0.5
0.4
0.3
0.2
0.1
0
0
0.1
0.2
0.3
0.4
0.5
0.6
0.7
0.8
0.9
1.0
RADIUS NUMBER (TANs/TANr)

Figure 4a

PDC1: CWCC 100% MIRR.

TEST RUN: CW0192 14-JUL-83

TIME INTERVAL BETWEEN SCANS: 30 SEC.

NUMBER OF SCANS: 194

1. EPPLEY DISH
   W/M2 CHNL NO. 204
2. KENDALL NIP
   W/M2 CHNL NO. 203
3. KENDALL STD
   W/M2 CHNL NO. 215

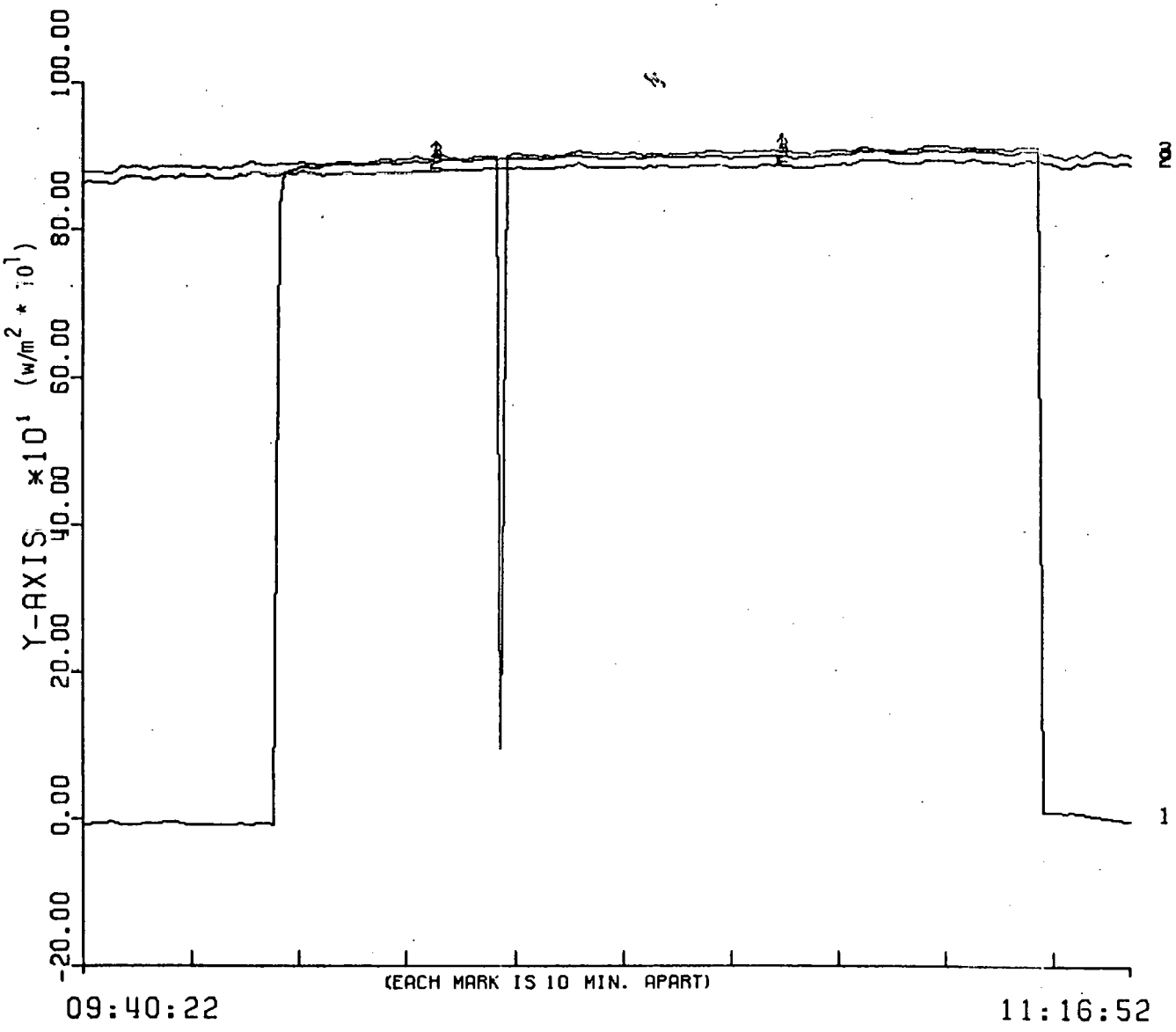

Figure 4b

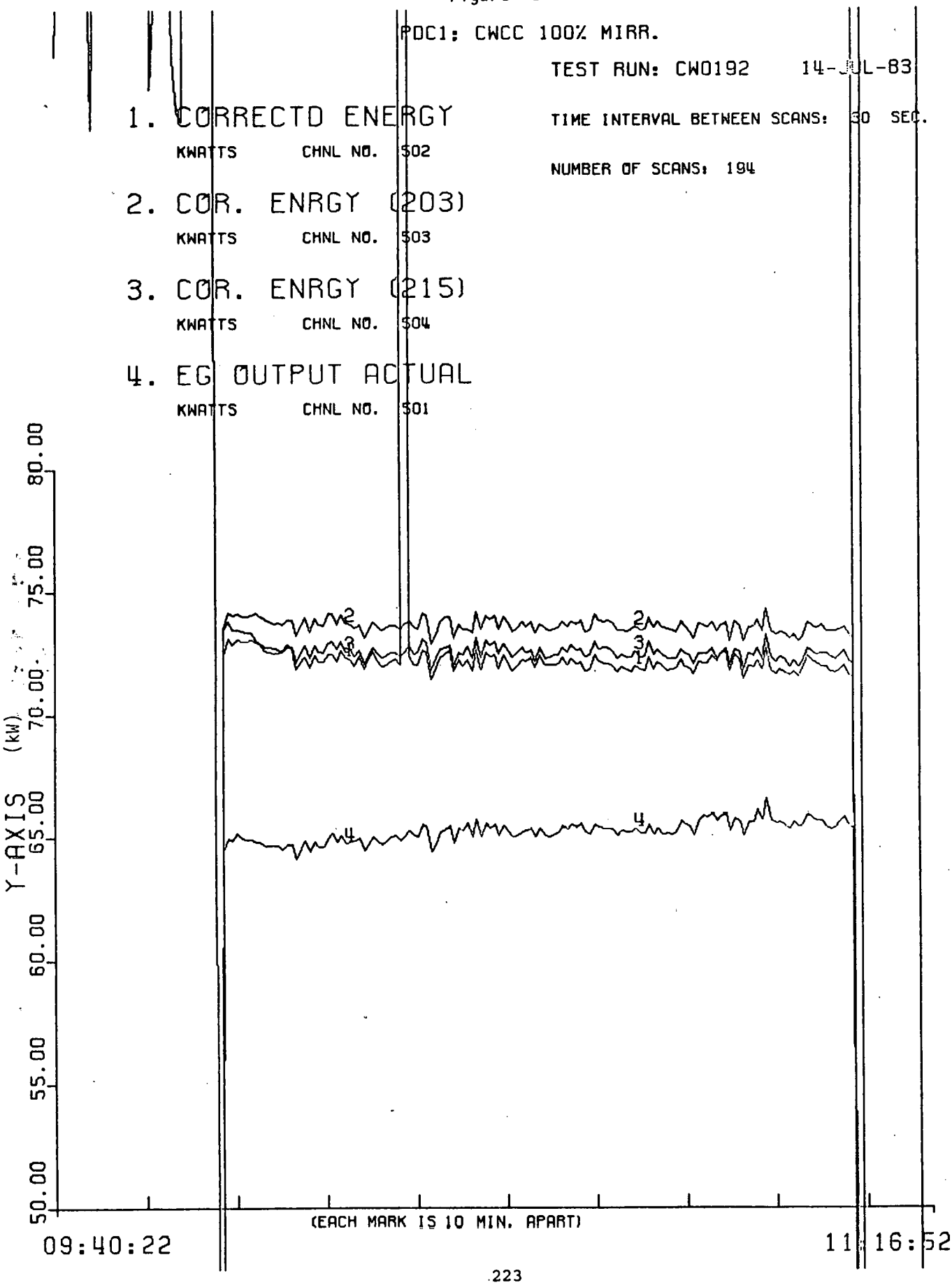
PDC1: CWCC 100% MIRR.
TEST RUN: CW0192 14-JUL-83
TIME INTERVAL BETWEEN SCANS: 30 SEC.
NUMBER OF SCANS: 194
1. CORRECTD ENERGY
KWATTS CHNL NO. S02
2. COR. ENRGY (203)
KWATTS CHNL NO. S03
3. COR. ENRGY (215)
KWATTS CHNL NO. S04
4. EG OUTPUT ACTUAL
KWATTS CHNL NO. S01
Y-AXIS (kW)
80.00
75.00
70.00
65.00
60.00
55.00
50.00
(EACH MARK IS 10 MIN. APART)
09:40:22
11:16:52

Figure 5a

PDC1: CWCC 100% MIRR.

TEST RUN: CW0178 22-FEB-83

TIME INTERVAL BETWEEN SCANS: 30 SEC.

NUMBER OF SCANS: 642

1. EPPLEY DISH
   W/M2 CHNL NO. 204
2. KENDALL NIP
   W/M2 CHNL NO. 203
3. KENDALL STD
   W/M2 CHNL NO. 215

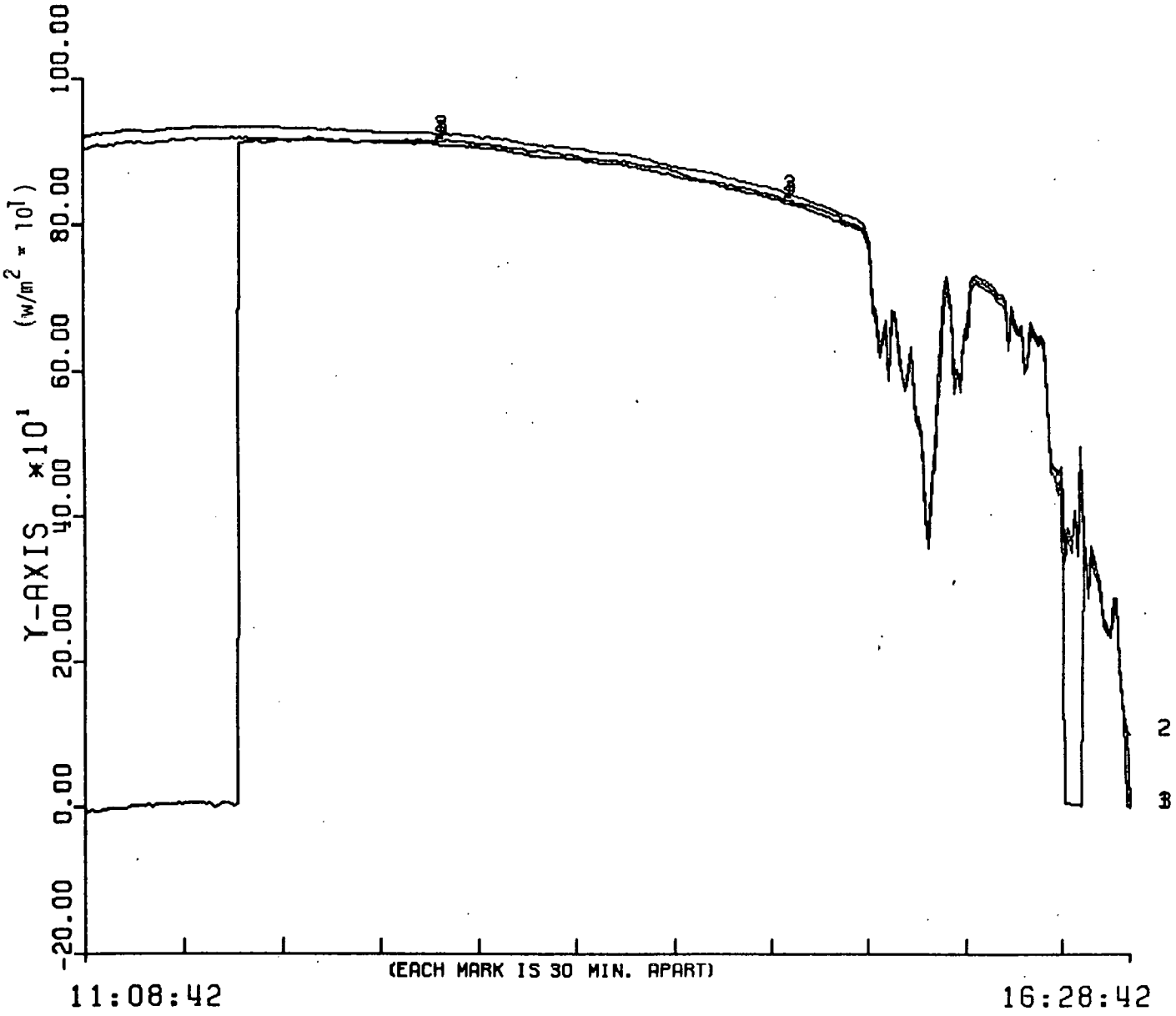

Figure 5b

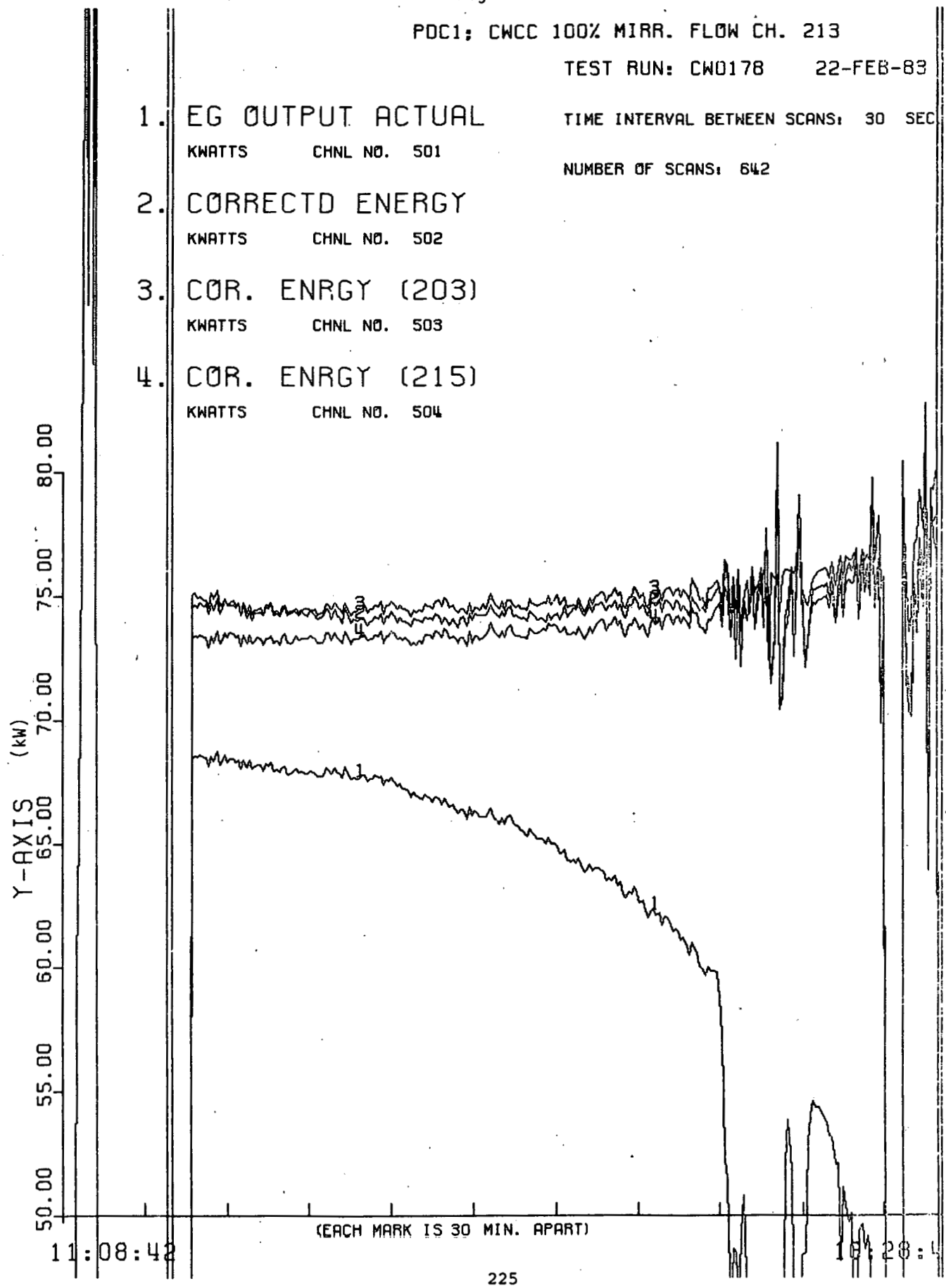
PDC1: CWCC 100% MIRR. FLOW CH. 213
TEST RUN: CW0178 22-FEB-83
1. EG OUTPUT ACTUAL
KWATTS CHNL NO. 501
TIME INTERVAL BETWEEN SCANS: 30 SEC
NUMBER OF SCANS: 642
2. CORRECTD ENERGY
KWATTS CHNL NO. 502
3. COR. ENRGY (203)
KWATTS CHNL NO. 503
4. COR. ENRGY (215)
KWATTS CHNL NO. 504
Y-AXIS (kW)
80.00
75.00
70.00
65.00
60.00
55.00
50.00
(EACH MARK IS 30 MIN. APART)
11:08:42
16:28:42

# RAPID TEST BED CONCENTRATOR (TBC) ALIGNMENT TECHNIQUES

Maurice J. Argoud

Jet Propulsion Laboratory
Pasadena, California

A new, labor and cost saving method was developed to eliminate the procedure of covering all (220) mirrors and uncovering them one-by-one in sequence to adjust each to the focal plane. This latest method being used to align mirrors of a parabolic solar concentrator utilizes a computer-derived target of discreet images made up of individual mirror reflections on a plane in front of the intended, nominal, focal point. Incorporating this computer technique increases accuracy and gives potential to develop flux distributions required by different receiver designs.

# Implementation of the Sun Position Calculation in the PDC-1 Control Microprocessor

John A. Stallkamp
Jet Propulsion Laboratory
California Institute of Technology
Pasadena, California 91109

Abstract:

The major portion of this paper presents the several computational approaches to providing the local azimuth and elevation angles of the sun as a function of local time and then the utilization of the most appropriate method in the PDC-1 microprocessor. The full algorithm, in FORTRAN form, is felt to be very useful in any kind or size of computer. It was used in the PDC-1 unit to generate efficient code for the microprocessor with its floating point arithmetic chip. The balance of the presentation consists of a brief discussion of the tracking requirements for PDC-1, the planetary motion equations from the first to the final version, and the local azimuth-elevation geometry.

## Introduction, Result, Nomenclature:

THE PDC-1 (Parabolic Dish Concentrator-1) is the first of a planned sequence of concentrators for dish-electric applications. It was designed by General Electric and uses injection molding techniques with plastic reflecting surfaces. The reflecting structure is a load bearing, integral part of the structure. A start-stop, on-off, control system is used to drive the elevation over azimuth configuration. The PDC-1 unit was fabricated and errected at Edwards Test Station (ETS) by Ford Aerospace and Communications Corp. (FACC).

The body of this paper is a mathematical derivation that will be given in a line item format. A minimum of comment and connective verse is used; some of the material and comment from the oral presentation is omitted as not necessary or rearranged for better continuity here.

The abstract adequately says what was done and why. The end result is the FORTRAN code and is the ultimate, almost stand alone, useful output of this presentation. Ordinary mathematical and computer language is freely used and this should not cause difficulties. There is no hope for a standardized or consistent nomenclature or notation for this field as is admitted by no less than the "Explanatory Supplement for the Ephemeris" in Section 1G.

Derivation and Discussion:

1. Requirement: Provide local azimuth and elevation angles of the sun.

2. Input: Local latitude, longitude and date/time. Date/time is the elapsed time from a recent epoch, viz., January 0, 19xx at 0 hours UT (Universal Time). The year is selectable; the required data are given in the Astronomical Almanac.

3. Accuracy: 0.01 degree.

4. Initial Approach: Paper by Robert Walraven (1). Paper was followed by corrections in subsequent issue (2).

5. Microprocessor for PDC-1 Concentrator: Advanced Micro Devices Model Am 95/4006 with an Am 9511 APU (Arithmatic Processing Unit). The ephemeris calculation was to be done at each concentrator in floating point, 32 bit, arithmetic and converted to fixed point integer units, 4096 counts per 90 degrees, for use in the control algorithm.

6. Am 9511 APU:

Fixed-Floating point capability: Discussed in Item 5 above.

Stack I/O Operation: Tedious to code but thoroughly adequate.

All direct and inverse trigonometric available: Inverse functions slow, 5000 to 8000 cycles, compared with less than 200 for multiplication.

Error return available for bad operation request, e.g., divide by zero: Not used in initial code but should have been. Not needed in final version.

7. Decision Point: When delivered to JPL, at a minimum the microprocessor code needed to be modified because of lack of complete selection of quadrant for an Arctan operation and potential divisions by zero. Walraven's equations as finally given seemed to be more complicated than needed; several computational simplifications, combinations and omission of some small correction terms should be accomplishable. The planetary motion equations resulting from the new analysis were identical with those given in recent issues of the Astronomical Almanac.

8. Final Planetary Motion Equations from The Astronomical Alamanac:

GMST = Greenwich mean siderial time

from page B6: "... holds during 1981: on days of year d at t hours UT, GMST = 6.6383211 hours + 0.0657098235 d + 1.0073791 t"

From page C20: "SUN, 1981"
"...coordinates of the sun to a precision of 0.01 deg"
"d = ... day of year ... + fraction of day from 0 hours UT"
"Mean longitude of Sun ... L = 279.575 deg + 0.985647 d"
"Mean anomaly: g = 356.967 deg + 0.985600 d"
"Ecliptic longitude: $\lambda$ = L deg + 1.916 sin g + 0.020 sin 2g"

The epoch numbers, 6.6383211 hours, 279.575 and 356.967 deg are for January 0, 1981 at 0 hours UT. These are the three numbers that are updated to change to a different epoch. All other numerical values are constant.

9. Ecliptic to Equatorial Coordinates:

RA = Right Ascension = equatorial longitude
DEC = Declination = equatorial latitude
$\epsilon$ = Obliquity of the Ecliptic
= 23.442 deg (1981) = 23.443 deg (1974)

The constants cos $\epsilon$ and sin $\epsilon$ are available and may be updated (need is questionable) from page C20 of the AA.

$$\sin DEC = \sin \epsilon * \sin \lambda$$
$$\tan RA = \cos \epsilon * \tan \lambda$$

Local Hour Angle = Greenwich Mean Sidereal Time - West Longitude - Right Ascension

NLHA = - NLA = Negative Local Hour Angle
= RA - GMST + West Longitude
= RA - LMST (Local Mean Sidereal Time)

Before looking at these equations, consider how the results are to be used in the final calculation of local azimuth and elevation.

10. Spherical Triangle Equations: See Figure 1.

When all the complementary angles are removed, the law of cosines gives the elevation angle, and then the law of sines gives the azimuth angle.

$$\sin ELV = [\sin LAT] * [\sin DEC] + [\cos LAT] * [\cos DEC * \cos NLHA]$$

$$\sin AZM = [\cos DEC * \sin NLHA] \quad [\cos ELV]$$

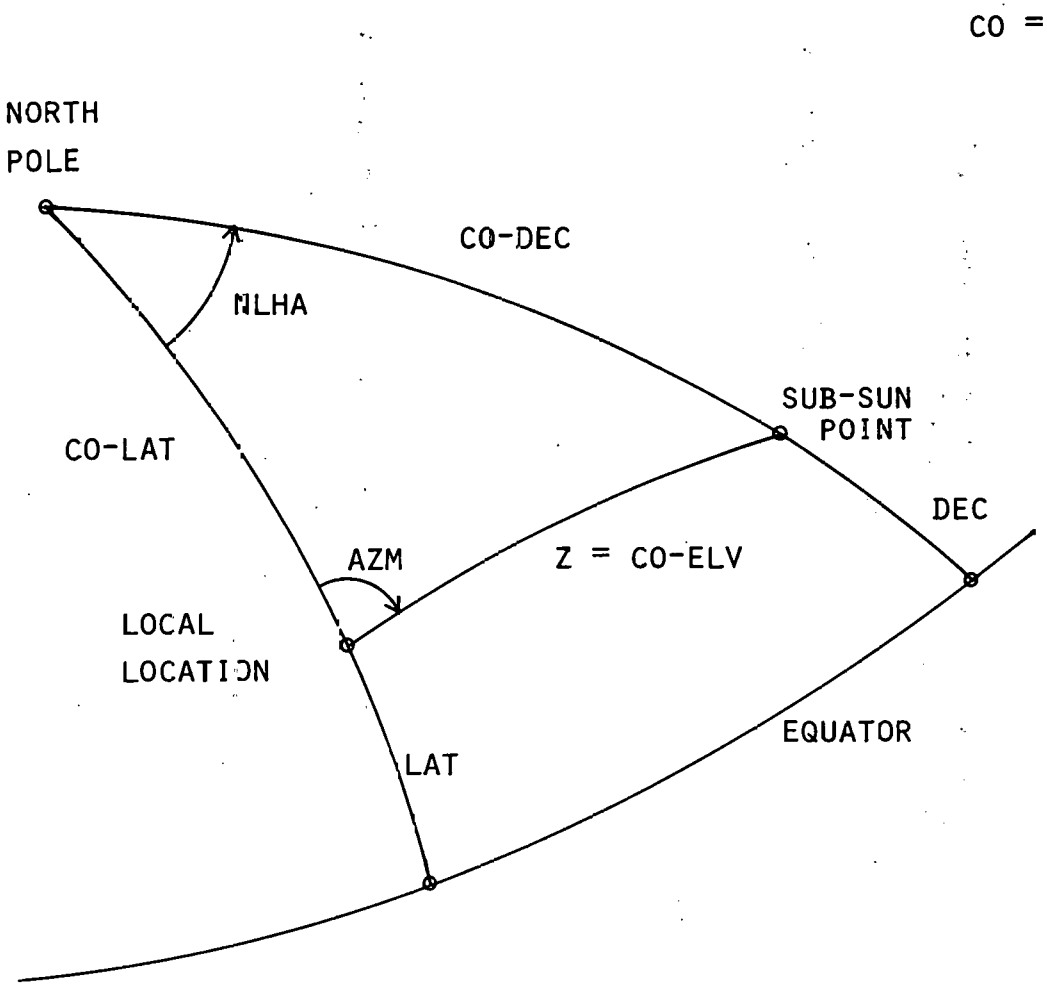


FIGURE 1 SPHERICAL TRIANGLE

11. Quadrant Selection:

$-90. \leq ELV \leq +90.$ From sign of sin ELV equation

$0. \leq AZM \leq 360.$ Two steps required.

IF(SIN(NLHA).GT.ZERO) $0. < AZM < 180.$
IF(SIN(LAT) * SIN(ELV).LT.SIN(DEC)) $90. < AZM < 270.$ (Walraven's paper)

12. Bracketed Quantities in Item 10:

Numerical values of the terms in [ ] are required for the computations. The terms sin LAT and cos LAT are local constants. The angular measure of DEC and NLHA are not required nor is the numerical value of cos DEC if the bracketed numerical forms can be obtained otherwise.

13. Obtaining the Variable Input Terms of the Spherical Triangle Equations of Item 10 from the Equations of Item 9:

[sin DEC] = sin $\epsilon$ * sin $\lambda$ is obtained directly.

The other bracketted variable terms in the equations of Item 10 are obtained from:

NLHA = RA - LMST
tan RA = cos $\epsilon$ * tan $\lambda$
RA and must be in the same quadrant

from which

sin RA = (cos $\epsilon$ * sin $\lambda$ )/DENOM
cos RA = cos $\lambda$ /DENOM
DENOM = + SQRT ($\cos^2\epsilon$ * $\sin^2\lambda$ + $\cos^2\lambda$)

14. Some Available Computational Approaches for RA Leading to the Bracketted Terms:

School Boy: Do inverse tangent directly,
Select quadrant,
Continue,

Delta Angle: Let RA = $\lambda$ + A,
Solve for A,
Continue,
(Expect automatic quadrant selection)

Trigonometric Sum Identity: NLHA = RA - LMST
sin NLHA = sin RA * cos LMST
-cos RA * sin LMST
(Expect avoidance of arc-trig operation and other simplifications)

15. School Boy Examples:

Large Computer:

```
SINRA = COS(ϵ) * SIN(λ)
COSRA = COS (λ)
   RA = ATAN2(SINRA, COSRA)
 NHLA = RA - LMST
```

The ATAN2 double argument input subroutine does the entire job and is not bothered by COSRA = 0.

Small Computer:

```
      SINRA and COSRA as above
      RA = ATAN(SINRA/COSRA)
or    RA = ATAN(COS(ϵ) * TAN(λ))
```

Now must protect from COSRA = 0 or large TAN(λ) and also must complete quadrant selection.

16. Delta Angle: With RA = λ + A expand sin RA and cos RA equations of Item 13.

$$\sin A = -\sin\lambda * \cos\lambda * (1-\cos\epsilon)/\text{DENOM}$$
$$\cos A = \cos^2\lambda * (1 - \tan^2\lambda * \cos\lambda)/\text{DENOM}$$

$$\tan A = -\tan\lambda * (1-\cos\epsilon) \Big/ (1 + \tan^2\lambda * \cos\epsilon)$$

This actually has excellent computational properties: A is small, sign (quadrant) is automatically selected, and, when tan λ is larger than the available computational range, set A to its obvious value of zero and skip ahead.

17. The Denominator: Expand DENOM of Item 13 and substitute for $\sin\epsilon * \sin\lambda = \sin \text{DEC}$.

$$\text{DENOM}^2 = \cos^2\epsilon * \sin^2\lambda + \cos^2\lambda$$
$$= \cos^2\epsilon * (\sin^2\lambda * \sin^2\epsilon) \Big/ \sin^2\epsilon + 1 - (\sin^2\lambda * \sin^2\epsilon) \Big/ \sin^2\epsilon$$
$$= 1 - \sin^2\text{DEC} * (1 - \cos^2\epsilon) \Big/ \sin^2\epsilon$$
$$= 1 - \sin^2\text{DEC} = \cos^2\text{DEC}$$

$$\text{DENOM} = +\cos \text{DEC}$$

DENOM was defined as a positive quantity and the plus sign is appropriate since the absolute value of DEC is less than or equal to ϵ = 22.4 deg.

18. The Trigonometric Sum Identity: This can now be used to obtain the remaining bracketted terms in a direct manner. We now have:

$$\sin RA = (\cos \epsilon * \sin \lambda) / \cos DEC$$
$$\cos RA = \cos \lambda / \cos DEC$$

$$\cos DEC * \cos RA = \cos \epsilon * \sin \lambda$$
$$\cos DEC * \sin RA = \cos \lambda$$

$$[\cos DEC * \cos NLHA] = \cos DEC * \cos (RA - LMST)$$
$$= \cos \lambda * \cos LMST + \cos \epsilon * \sin \lambda * \sin LMST$$

$$[\cos DEC * \sin NLHA] = \cos DEC * \sin (RA - LMST)$$
$$= \cos \epsilon * \sin \lambda * \cos LMST - \cos \lambda * \sin LMST$$

19. PDC-1 Implementation: The trig sum expansions of Item 18 are used.

Do not need angular measure of RA or DEC or numerical measure of cos DEC.

Only arc-trig functions are at end for obtaining angular measure of elevation and azimuth. Quadrant selection discussed in Item 11.

Minimum number of direct trig operations, sin g , sin 2g , sin $\lambda$ , cos $\lambda$ , sin LMST and cos LMST.

No division by zero (no division in main part of program) or other dangerous steps requiring protection except again at end for obtaining the azimuth angle itself. In the PDC-1 microprocessor the few protective steps are done; these would be specific to each computer.

Large sections of the original Am 9511 floating point code went away. The FORTRAN code given in Table 1 is thought to be remarkably short, concise and easy to follow.

20. FORTRAN Code:

Table 1 is schematic FORTRAN code. The line "TIME =" is the start of the formal calculations; this code is full FORTRAN and is directly useable when statement numbers are supplied for the several GOTO commands. The lines preceeding the "TIME =" line provide for input constants and parameters; some of these lines will need to be modified to suit the particular computer being used. The quantities DN and TM are assumed to be supplied from other subroutines; suitable common statements for these and the AZM and ELV output angles must be supplied or other Input/Output provisions made.

References:

(1) Solar Energy, Vol. 20, pp. 393-397. Pergamon Press 1978. Printed in Great Britain.

(2) Solar Energy, Vol. 22, pp. 195. Pergamon Press 1979. Printed in Great Britain.

```
DN                  : DAY NUMBER SINCE EPOCH
TM                  : LOCAL STANDARD TIME, HOURS
PI = 3.14159
RAD = PI/180.
GMSTO = 6.622408    : EPOCH GREENWICH SIDEREAL TIME
MAO = 356.711       : EPOCH MEAN ANOMALY
SEMLO = 279.336     : EPOCH SUN ECLIPTIC MEAN LONGITUDE
COSEPS = 0.91747    : EPS=OBLIQUITY OF ECLIPTIC
SINEPS = 0.39781    :    = 22.4XX DEG
ECC1 = 1.916        : ELIPTIC ORBIT CORRECTION
ECC2 = 0.020        :    PARAMETERS
RATE = 0.985647     : SIDEREAL RATE
RATM = 0.985600     : MEAN ANOMALY RATE
TZ = 8.             : TIME ZONE (PACIFIC HERE)
LAT = 34.992        : LOCAL LATITUDE DEGREES (ETS HERE)
LON = 117.873       : LOCAL LONGITUDE DEGREES (ETS HERE)
SINLAT = SIN(LAT * RAD)    : SUPPLIED OR CALCULATED
COSLAT = COS(LAT * RAD)    : SUPPLIED OR CALCULATED
TIME = DN + (TM + TZ) / 24.  :ELAPSED TIME IN DAYS
DELTA = RATE * TIME          :ELAPSED SIDEREAL ANGLE
MAR = RAD * (MAO + RATM * TIME)  :MEAN ANOMALY
SELD = SEMLO + DELTA + ECC1*SIN(MAR) + ECC2*SIN(2.*MAR)
SINRA = SIN(SELD * RAD)      :=SIN(SUN ECLIPTIC LON)
SINDEC = SINRA * SINEPS      :=SIN(DEC)
SINRA  = SINRA * COSEPS      :=SIN(RA) * COS(DEC)
COSRA = COS(SELD * RAD)      :=COS(RA) * COS(DEC)
GMSTD = 15. * (GMSTO + TM + TZ) + DELTA  :IN DEG
LMSTR = RAD * (GMSTD -LON)   :=NLHA = NEGATIVE LOCAL
SINLMS = SIN(LMSTR)          :  HOUR ANGLE IN RADIANS
COSLMS = COS(LMSTR)
SINELV = SINLAT*SINDEC+COSLAT*(COSRA*COSLMS+SINRA*SINLMS)
COSELV = (1.-SINELV**2.)     :=COS SQUARED HERE
IF(COSELV.LT.0)  GOTO (END)  :ERROR, ABANDON CALCULATION
COSELV = SQRT(COSELV)        :NOW IS COS(ELV)
ELV = ASIN(SINELV) / RAD     :=ELEVATION IN DEGREES
IF(COSELV.EQ.0)  GOTO (END)  :FINISHED, AZM NOT DEFINED
SINAZM = (SINRA*COSLMS-COSRA*SINLMS) / COSELV
COSAZM = (1.-SINAZM**2.)     :=COS SQUARED HERE
IF(COSAZM.LT.0)  GOTO (END)  :ERROR, ABANDON CALCULATION
AZMR = ASIN(SINAZM)          :=AZIMUTH IN RADIANS
QUAD = SINLAT*SINELV-SINDEC  :QUADRANT SELECTION
IF(QUAD.LT.0)  GOTO (+3)     :TO LINE IF(AZMR.GT.0)
AZMR = PI -AZMR
GOTO (+3)                    :TO LINE  AZM = AZMR / RAD
IF(AZMR.GT.0)  GOTO (+2)     :TO LINE  AZM = AZMR / RAD
AZMR = AZMR + 2. * PI
AZM = AZMR / RAD             :=AZIMUTH IN DEGREES
END
```

TABLE 1. SCHEMATIC FORTRAN

# RECENT SOLAR MEASUREMENTS RESULTS AT THE PARABOLIC DISH TEST SITE*

Darrell L. Ross

Jet Propulsion Laboratory

California Institute of Technology

Pasadena, California

ABSTRACT

After the Mexican volcanic eruptions of March 28, April 3 and 4, 1982, the question of its effect on insolation levels at the Parabolic Dish Test Site (PDTS) naturally arose. It was decided to look at this question in three steps: First to determine the impact, if any, on total direct normal energy (by month) at the PDTS for the summer of 1982 as compared to the summer of 1981 (after and before the explosion respectively). Secondly, we would look at the effect on peak insolation levels for the same period of time. The results of the first step were the following: A drop of 20%, 9% and 18% in total direct normal energy for the months of June, July and August 1982 respectively, as compared to the same months in 1981 was experienced. For the second step we found a decrease of 4.0%, 5.8% and 7.7% in peak direct normal insolation levels for the months of June, July and August 1982 respectively, as compared to the same months in 1981 (where the peak levels for each month were determined by averaging the top 3 days for each month). The most striking difference noted between the summer of 1981 and 1982 was the following: There were 29 days in June, July and August of 1981 where the insolation level exceeded 1,000 $W/m^2$. For the same period in 1982 there were no days that were in excess of 1,000 $W/m^2$. The third and final step was to compare the results of the summer of 1983 (a year after the explosion) with the summer of 1982. The results show only one day in excess of 1,000 $W/m^2$ during the summer of 1983 (this was in July 1983, a hiatus of thirteen months since the last one). Clearly, the answer to the original question is that the Mexican volcanic explosion had a significant impact on insolation levels at the PDTS and, furthermore, it has been quite long lasting. The data would seem to suggest that the volcanic explosion had little effect on PDTS insolation until the first of June 1982.

---

*The work described in this paper was carried out or coordinated by the Jet Propulsion Laboratory, California Institute of Technology, and was sponsored by the U. S. Department of Energy through an agreement with the National Aeronautics and Space Administration.

## INTRODUCTION

The Parabolic Dish Test Site (PDTS) was established in 1978 for the Department of Energy by the Jet Propulsion Laboratory (JPL), an operating Division of Caltech. It was established for the purpose of testing and evaluating parabolic dishes at the component, subsystem and system (or module) level. The PDTS is located on Edwards Test Station (A JPL facility), which in turn is located on Edwards Air Force Base. The test site is situated approximately a hundred miles north of Los Angeles. Figure 1 shows two identical Test Bed concentrators, 11 meters in diameter (on the right) and a single 12 meter diameter concentrator (on the left) designated Parabolic Dish concentrator Number One.

Since the El Chichon volanic eruption in Mexico on March 28, April 3, and 4, 1982, there have been reports from various solar sites in the United States of its effect. It was decided to determine the effect (if any) of these eruptions on insolation levels at the PDTS. Having this data would then enable a comparison to be made of volcanic effects at solar sites throughout the United States.

The approach employed to make this comparison was to compare the direct normal energy at the PDTS for the summers of 1981, 1982 and 1983, or in other words compare data for a year before the explosion, the summer shortly after the explosion and a year after the explosion. Secondly, determine the effect on peak insolation levels for the same period of time.

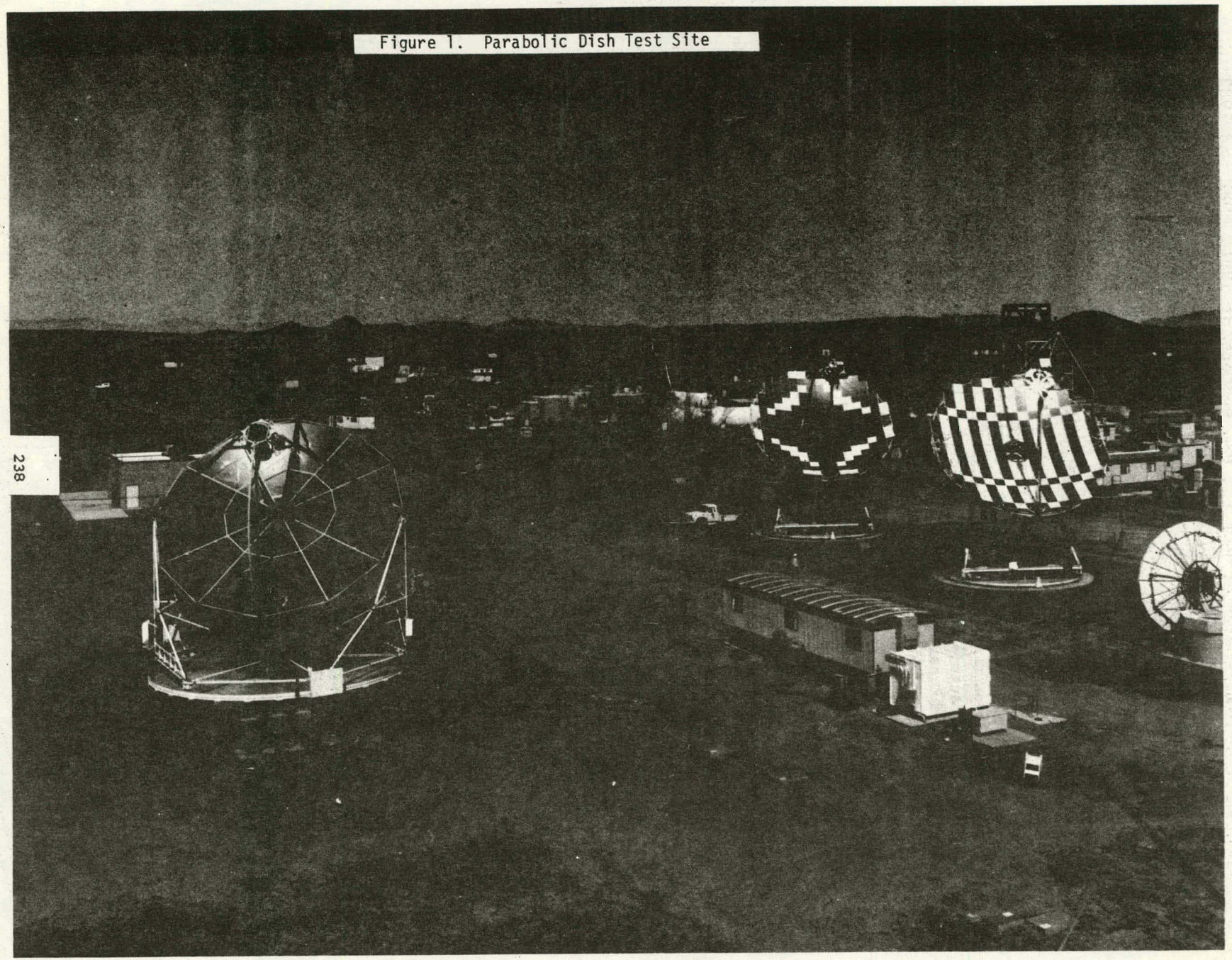

Figure 1. Parabolic Dish Test Site

Direct Normal Energy

The direct normal energy levels for the summers of 1981, 1982 and 1983 were compiled and are as shown in Table 1 below:

TABLE 1

COMPARISON OF DIRECT NORMAL ENERGY AT
ETS FOR THE SUMMERS OF 1981, 1982 and 1983

| | 1981 kW-HR/SQ-METER/DAY | 1982 kW-HR/SQ-METER/DAY | 1983 kW-HR/SQ-METER/DAY |
|---|---|---|---|
| June | 10.93 | 8.78 | 9.62 |
| July | 10.09 | 9.21 | 10.05 |
| August | 9.44 | 7.71 | 7.68 |

This data was obtained with the use of a Kendall Pyrheliometer (Absolute cavity Radiometer) that was mounted at the PDTS. This instrument is part of the weather station that was set up at the PDTS in support of the solar program. Insolation measurements have been taken since October 1978. Other instrumentation has been added over the years, such as: wind speed and direction, ambient temperature, barometric pressure and dew point.

Note that there was a significant drop during the summer of 1982 as compared to 1981 (19.7%, 8.7% and 18.3% for June, July and August respectively). For the summer of 1983 vs. 1981, the comparable numbers are: 12.0%, 0.4% and 18.6%. This indicates a significant increase in energy available in June 1983 (as compared to June 1982) and a return during July 1983, to the energy levels available prior to the volcanic explosion . Although not shown in Table 1, there was a large increase in energy level in May 1983 over May 1982 and in fact larger than May 1981. This can be seen in Table 3 in the Appendix. August of 1983, however, again shows a significant decrease from August of 1981 and virtually comparable to August of 1982. August of 1983 was, however, quite a stormy month and this undoubtedly had a significant impact on the energy available. Subsequent months will determine whether the energy levels are back to normal or not. Unfortunately, it will not be possible to make this assessment at the PDTS, since the weather station was shut down permanently early in September 1983.

Peak Direct Normal Insolation

The peak direct normal insolation levels for the summers of 1981, 1982 and 1983 are as shown in Table 2 below:

TABLE 2

COMPARISON OF PEAK DIRECT NORMAL INSOLATION LEVELS AT ETS FOR THE SUMMERS OF 1981, 1982, 1983

| | 1981 AVG. FOR TOP 3-DAYS W/SQ-METER | 1982 AVG. FOR TOP 3-DAYS W/SQ-METER | 1983 AVG. FOR TOP 3-DAYS W/SQ-METER |
|---|---|---|---|
| June | 1025 | 984 | 956 |
| July | 1026 | 967 | 995 |
| August | 1040 | 960 | 967 |

This data was measured with the same Kendall Pyrheliometer that was used to acquire the energy data in Table 1.

Again, it is to be noted that there was a significant drop in peak insolation levels during the summer of 1982 as compared to the summer of 1981 (4.0%, 5.8% and 7.7% for June, July and August respectively). Comparing the summer of 1983 with 1981, the corresponding numbers are: 6.7%, 3.0% and 7.0%. This data indicates a significant increase in peak insolation levels during July 1983 (as compared to July 1982), but still 3% below the peaks of 1981 for the same month. As was the case with the energy levels (indicated in Table 1), however, there was again a drop in insolation levels in August 1983 to a level comparable with August 1982 and 7.0% below August 1981. Since August of 1983 was quite a stormy month, this almost certainly contributed to lower insolation levels.

The most striking difference observed between the summer of 1982 and 1981 is the decrease in the number of days in 1982 and 1981 where the peak insolation was 1,000 $W/m^2$ or greater. During the summer of 1981 (June, July and August), there were 29 days greater than or equal to 1,000 $W/m^2$, while in 1982 for the same months there were no days of 1,000 $W/m^2$ or greater. For the same months in 1983, there was 1 day of 1,000 $W/m^2$ or greater. Further, there was a hiatus of 13 months

(from June 1982 through June 1983) during which the insolation level did not equal or exceed 1,000 $W/m^2$. For a tabulation of this data for all of 1981 and 1982 and 8 months in 1983, see Table 4 in the appendix.

## Conclusions

Clearly, the answer to the original question is that the Mexican volcanic explosion had a significant impact on energy and insolation levels at the PDTS and, furthermore, it has been quite long lasting. The first really significant decrease in energy and insolation levels occurred in June 1982 when the energy level decreased by 19.7% while the peak insolation levels went down by 4.0%. June of 1982 was also the first month (of 13 consecutive months) when peak insolation levels did not equal or exceed 1,000 $W/m^2$.

Signs of a recovery from the effects of the volcanic explosion began to appear in May of 1983, when the energy level exceeded that of May 1981 as well as May 1982. A return to almost normal levels (pre-volcanic explosion levels) occurred in July 1983 followed by a fairly large decrease occurring in August of 1983 because of stormy weather. Peak insolation levels did not show signs of recovery until July of 1983 when the first day above 1,000 $W/m^2$ occurred. July was also the first month in 1983 that registered an increase in average insolation levels over 1982. The average level in July 1983 did not, however, reach equal levels or an increase over 1981. While average insolation levels did decline in August 1983, the average was still slightly above August 1982.

In summary, it would appear that energy and insolation levels are improving at the PDTS, but have not quite reached normal or pre-volcanic levels. At this time the data would seem to suggest a return to normal energy and insolation levels will occur in the very near future.

TABLE 3

COMPARISON OF TOTAL DIRECT NORMAL ENERGY AT THE PDTS FOR 1981, 1982, AND 1983

| | 1981 kW-HR/SQ. METER/DAY | 1982 kW-HR/SQ. METER/DAY | 1983 kW-HR/SQ. METER/DAY |
|---|---|---|---|
| JANUARY | 4.87 | 6.14 | 4.73 |
| FEBRUARY | 6.43 | 5.15 | 3.98 |
| MARCH | 7.12 | 5.69 | 6.01 |
| APRIL | 8.90 | 8.17 | 6.50 |
| MAY | 8.68 | 8.42 | 9.29 |
| JUNE | 10.93 | 8.78 | 9.62 |
| JULY | 10.09 | 9.21 | 10.05 |
| AUGUST | 9.44 | 7.71 | 7.68 |
| SEPTEMBER | 8.80 | 6.70 | |
| OCTOBER | 7.65 | 6.44 | |
| NOVEMBER | 6.00 | 4.88 | |
| DECEMBER | 5.40 | 3.99 | |
| | 94.31 | 81.28 | |

$\frac{94.31}{12} = 7.86$ $\frac{81.28}{12} = 6.77$

TABLE 4

COMPARISON OF PEAK DIRECT NORMAL INSOLATION LEVELS

FOR 1981, 1982 AND 1983

| | 1981 | | 1982 | | 1983 | |
|---|---|---|---|---|---|---|
| | AVG. FOR TOP 3-DAYS $W/M^2$ | # OF DAYS AT OR ABOVE 1,000 $W/M^2$ | AVG. FOR TOP 3-DAYS $W/M^2$ | # OF DAYS AT OR ABOVE 1,000 $W/M^2$ | AVG. FOR TOP 3-DAYS $W/M^2$ | # OF DAYS AT OR ABOVE 1,000 $W/M^2$ |
| JANUARY | 1053 | 11 | 1045 | 9 | 932 | 0 |
| FEBRUARY | 1073 | 17 | 1019 | 4 | 958 | 0 |
| MARCH | 1065 | 15 | 1051 | 13 | 964 | 0 |
| APRIL | 1021 | 8 | 1034 | 5 | 966 | 0 |
| MAY | 1013 | 5 | 1002 | 2 | 951 | 0 |
| JUNE | 1025 | 8 | 984 | 0 | 956 | 0 |
| JULY | 1026 | 11 | 967 | 0 | 995 | 1 |
| AUGUST | 1040 | 10 | 960 | 0 | 967 | 0 |
| SEPTEMBER | 1026 | 7 | 966 | 0 | | |
| OCTOBER | 1018 | 5 | 977 | 0 | | |
| NOVEMBER | 1004 | 2 | 948 | 0 | | |
| DECEMBER | 1001 | 3 | 889 | 0 | | |

# Appendix: Attendee List

**FIFTH PARABOLIC DISH SOLAR THERMAL POWER PROGRAM REVIEW**

**December 6-8, 1983**

**INDIAN WELLS, CALIFORNIA**

ABBIN, Joseph P. (505) 844-8590
Division Supervisor
Sandia National Laboratories
Division 2541
Albuquerque, NM 87185

ALGER, Donald L. (216) 433-4000
Engineer
NASA
21000 Brookpark Road
Cleveland, OH 44135

ALHORN, Leland (505) 262-2247
Executive Director
N. M. Solar Industry Dev. Corp.
Suite 705 5301 Central Ave. NE
Albuquerque, NM 87108

ALMSTROM, Sten H. 46/40100950

United Stirling AB
Box 856
20180 Malmo, SWEDEN

ALPER, Marshall E. (213) 577-9325
Mgr., Solar Energy Program (FTS) 961-9325
Jet Propulsion Laboratory
4800 Oak Grove Dr., MS 502-307
Pasadena, CA 91109

ALVIS, Robert L. (505) 844-8573
Member Technical Staff (FTS) 844-8573
Sandia National Laboratories
Box 5800
Albuquerque, NM 87185

ARGOUD, Maurice J. (213) 577-9266
Member Technical Staff (FTS) 961-9266
Jet Propulsion Laboratory
4800 Oak Grove Dr., MS 506-328
Pasadena, CA 91109

ATKINSON, John H. (714) 635-5591
President - Technical Director
Advanced Solar Power, Inc.
2201-A East Winston Road
Anaheim, CA 92806

AUBRY, Ronald G. (219) 747-5117
Chief Engineer
Deltatemp Energy Corp.
4208 Earth Drive
Fort Wayne, IN 46809

BARBER, Robert E. (303) 421-8111
Vice President
Barber-Nichols Engr. Co.
6325 W. 55th Avenue
Arvada, CO 80002

BATTON, Bill (303) 421-8111
Senior Project Engineer
Barber-Nichols Engr. Co.
6325 W. 55th Avenue
Arvada, CO 80002

BAXTER, Hal (505) 846-0781
Project Engineer
Sandia National Laboratories
P. O. Box 5800
Albuquerque, NM 87185

BEALE, William T. (614) 593-2221
Technical Director
Sunpower, Inc.
6 Byard Street
Athens, OH 45701

BLAND, Timothy J. (815) 226-6771
Principal Eng., Thermodynamic Resrch
Sundstrand Advanced Technology Grp
4747 Harrison Ave., PO Box 7002
Rockford, IL 61125

BLUM, Edward H. (202) 822-3650
Vice President
Merrill Lynch Capital Markets Grp
1828 L St., NW - Suite 906
Washington, DC 20036

BOWYER, James M. (213) 577-9406
Member Technical Staff (FTS) 961-9406
Jet Propulsion Laboratory
4800 Oak Grove Dr., MS 507-228
Pasadena, CA 91109

CALAHAN, H. Donald (202) 755-2403
Program Manager (FTS) 755-2403
NASA Headquarters
Code RJE
Washington DC 20546

CAMERON, Christophor P. (505) 844-0363
Member of Technical Staff (FTS) 844-0363
Sandia National Laboratories
P. O. Box 5800
Albuquerque, NM 87110

CEDILLO, Raymond (213) 572-1505
Project Mgr., Solar Dish Prog.
Southern California Edison
P. O. Box 800
Rosemead, CA 41770

CHAMPION, Roscoe L. (505) 844-8643
Member Technical Staff (FTS) 844-8643
Sandia National Laboratories
Box 5800
Albuquerque, NM 87185

CHINGARI, Gastone (202) 296-1610
Manager, International Programs
IIT Research Institute
1825 K Street, N.W.
Washington, DC 20006

CLARK, Jeffrey S. (219) 747-5117
President
Deltatemp Energy Corp.
4208 Earth Drive
Fort Wayne, IN 46809

COBB, Sanford, Jr. (612) 733-6913
Sr. Rev. Spec.
3M Company
235-2D15 3M Center
St. Paul, MN 55144

CURTIS, George D. (808) 748-8788
Technical Director
Hawaii Natural Energy Institute
2640 Dole Street
Honolulu, HI 96822

DANZIGER, Robert N. (213) 657-8652
President
Sunlaw Energy Corporation
8530 Wilshire Blvd. #401
Beverly Hills, CA 90211

DARNELL, Alfred J. (213) 700-5514
Member Tech Staff, Proj. Scientist
Energy Technology Engineering Cntr
PO Box 1449
Canoga Park, CA 91304

DAVIS, S. Bear (603) 885-3212
Manager, Systems Design
Sanders Associates
95 Canal Street, MER-15-2350
Nashua, NH 03061

DEFFENBAUGH, Danny M. (512) 684-5111
Mgr., Thermal Energy Systems x2384
Southwest Research Institute
6229 Culebra Rd.(PO Box 28510)
San Antonio, TX 78284

DENNISON, Edwin W. (213) 577-9228
Member Technical Staff (FTS) 961-9228
Jet Propulsion Laboratory
4800 Oak Grove Dr., MS 506-328
Pasadena, CA 91109

DIXON, Howard H. (714) 896-3081
Dir, Program Engineering-Energy
McDonnell Douglas Astronautics Co.
5301 Bolsa Avenue
Huntington Beach, CA 92647

DROHER, Joseph J. (213) 700-5031
Member Technical Staff
Energy Technology Engineering Cntr
PO Box 1449
Canoga Park, CA 91304

ELFE, Thomas (404) 894-3650
Sr. Research Scientist
Georgia Institute of Technology
EES/EMSL
Atlanta, GA 30332

ENDICOTT, Donald L. (714) 896-3572
Engineering
McDonnell Douglas Astronautics Co.
5301 Bolsa Avenue
Huntington Beach, CA 92647

FALLER, Richard J. (714) 896-3678
Program Manager
McDonnell Douglas Astronautics Co.
5301 Bolsa Avenue
Huntington Beach, CA 92647

FELLOWS, Merrilee (213) 572-6597
Research Scientist
Southern California Edison
P. O. Box 800
Rosemead, CA 91770

FLYNN, Gregory, Jr. (313) 465-5576
Consultant
Carborundom
PO Box 164
St. Clair Shores, MI 48080

FUJITA, Toshio (213) 577-9407
Member Technical Staff (FTS) 961-9407
Jet Propulsion Laboratory
4800 Oak Grove Dr., MS 507-228
Pasadena, CA 91109

GAIA, Mario 39-2-2364582
Professor, Dept. of Energetics/ISREP
Politecnico di Milano
Piazza Leonardo DaVinci, 32
20133 Milano, ITALY

GODETT, Ted M. (313) 995-1755
Chief Design Engineer
Stirling Thermal Motors
2841 Boardwalk
Ann Arbor, MI 48104

HAGEN, Terry (213) 640-2429
Sr. Engineer
Advanco Corp.
999 N. Sepulveda Blvd.
El Segundo, CA 90245

HALBERT, David (915) 698-8800
(FTS) 729-4011
La Jet Energy Company
3131 Antilley Road
Abeleine, TX 79604

HALLARE, Bengt G. (703) 549-7174
President
United Stirling, Inc.
211 The Strand
Alexandria, VA 22314

HENSEL, Samuel L. (617) 835-6282
Mgr., Heat Transfer/Thermal Eng.
Electronic Space Systems Corp.
175 West Boylston Street
West Boylston, MA 01583

HOBGOOD, John M. (714) 635-5591
V.P., Product Development
Advanced Solar Power, Inc.
2201-A E. Winston Road
Anaheim, CA 92806

HOLBECK, Herbert J. (213) 577-9294
Task Manager (FTS) 961-9294
Jet Propulsion Laboratory
4800 Oak Grove Dr., MS 506-328
Pasadena, CA 91109

HOLGERSSON, Sten H. 46-(40)-100950
Program Mgr., Solar Stirling Engine
United Stirling
Box 856
Malmo, S-024017 SWEDEN

HOOPES, John R. (213) 449-2171
Project Engineer x 2342
Jacobs Engineering Group, Inc.
251 S. Lake Avenue
Pasadena, CA 91101

HUNKE, Robert W. (505) 846-7819
Distinguished Member, Tech. Staff (FTS) 846-7819
Sandia National Laboratories
Box 5800
Albuquerque, NM 87185

HUNT, Arlon J. (415) 486-5370
Physicist, Solar Energy Group (FTS) 451-5370
Univ.of California,Bldg.90,Rm.2024
Lawrence Berkeley Lab,
Berkeley, CA 94720

JAFFE, Leonard D. (213) 577-9312
Project Systems Engineer (FTS) 961-9312
Jet Propulsion Laboratory
4800 Oak Grove Dr., MS 506-418
Pasadena, CA 91109

JASTER, Paul A. (612) 733-1898
Senior Project Engineer
3M
OTC, Bldg. 223-4N-08, 3M
St. Paul, MN 55144

JENCKES, Thomas A. (415) 820-2000
Supervising Research Engineer
Pacific Gas & Electric Co.
3400 Crow Canyon Rd.
San Ramon, CA 94523

JOHNSON, Richard (213) 512-4551
Engineering Specialist
AiResearch Mfg. Co.
2525 190th St.
Torrance, CA 90509

KANEFF, Stephen (062) 49-2462
Prof.& Head, Dept. of Eng. Physics
Australian National University
Res.School of Physical Sciences
GPO4,Canberra ACT,2601 AUSTRALIA

KEARNEY, David W. (619) 481-8044
Vice President
Insights West
14022 Condesa Drive
Del Mar, CA 92014

KICENIUK, Taras (213) 577-9419
Experiment Manager (FTS) 961-9419
Jet Propulsion Laboratory
4800 Oak Grove Dr., MS 506-328
Pasadena, CA 91109

KINOSHITA, George S. (505) 846-7817
Member Technical Staff (FTS) 846-7817
Sandia National Laboratories
Box 5800
Albuquerque, NM 87185

KLEINWACHTER, Jurgen H. (49) 07621 5093
Dr., Dipl. Phys., Tech. Director
Bomin-Solar
D7850 Lorrach, Industriestr 8
Lorrain, 7850, W. GERMANY

KRENZ, Dennis L. (505) 846-5203

U. S. Department of Energy
Box 5400
Albuquerque, NM 87115

LARSSON, Anders
President
United Stirling
Box 856
Malmo, SWEDEN

LEMPERLE, Gerold (0049)711-6862-390
Dipl.-Ing.
DFVLR
Pfaffenwaldrigg 38-40
D-7000 Stuttgart 80, W. GERMANY

LEONARD, James A. (505) 844-8508
Div. Supvr, Dist. Receiver Research (FTS) 844-8508
Sandia National Laboratories
Box 5800
Albuquerque, NM 87185

LIVINGSTON, Floyd R. (213) 577-9416
Member Technical Staff (FTS) 961-9416
Jet Propulsion Laboratory
4800 Oak Grove Dr., MS 506-328
Pasadena, CA 91109

LUCAS, John W. (213) 577-9368
Asst.Mgr.,Thermal Power Systems Proj (FTS) 961-9368
Jet Propulsion Laboratory
4800 Oak Grove Dr., MS 502-419
Pasadena, CA 91109

LUDTKE, Norman F. (313) 755-4400
Vice President x268
Pioneer Engineering & Mfg. Co.
2500 E. Nine Mile Road
Warren, MI 48092

LUKENS, Larry L. (505) 844-1042
Member Technical Staff
Sandia National Laboratories
Division 2541
Albuquerque, NM 87185

MACCHI, Ennio E. (392) 2362678
Professor
Politecnico
Piazza Leonardo da Vinci 32
Milan, 20131 ITALY

MACIEJ, Dennis P. (213) 277-4520
Lead Technician, PDTS
Jet Propulsion Laboratory
4800 Oak Grove Dr., ETS
Pasadena, CA 91109

MACKAY, Robin (213) 417-6836
Dir., Industrial Power Mkt. Dev.
Garrett Corp.
9851 Sepulveda Blvd.
Los Angeles, CA 90045

MANATT, Scott A. (213) 417-6824
Gov't Relations Representative
Garrett Corporation
9851 Sepulveda Blvd.
Los Angeles, CA 90009

MANCINI, Frank (602) 255-3682
Associate Director
Arizona Solar Energy Commission
1700 W. Washington, Room 502
Phoenix, AZ 85007

MARRIOTT, Alan T. (213) 577-9366
Mgr., Thermal Power Systems Project (FTS) 961-9366
Jet Propulsion Laboratory
4800 Oak Grove Dr., MS 502-419
Pasadena, CA 91109

MARTIN, David E. (913) 864-4078
Director, Applied Energy Research
Univ.of Kansas Cntr for Research
2291 Irving Hill Dr.,Campus West
Lawrence, KS 66045

MARTIN, Dr. A. B. (213) 640-2429
Contracts Manager
Advanco
999 N. Sepulveda Blvd.
El Segundo, CA 90245

MARTIN, Robert L. (816) 753-7600
Soleras Project Manager
Midwest Research Institute
425 Volker Blvd.
Kansas City, MO 64110

MEIJER, Roelf J. (313) 995-1755
President
Stirling Thermal Motors
2841 Boardwalk
Ann Arbor, MI 48104

MENARD, Wesley A. (213) 577-9278
Section Mgr. (FTS) 961-9278
Jet Propulsion Laboratory
4800 Oak Grove Dr., MS 507-228
Pasadena, CA 91109

MENNA, Pietro 6968-3153
Chemical Engineer
ENEA/Casaccia
ENEA/Casaccia Fare IST
Rome, 00060 ITALY

MILLER, Joel (505) 844-1775
Member of Technical Staff
Sandia National Laboratories
Org. 1523
Albuquerque, NM 87185

MOLANO, Rafael A. (415) 781-4211
Engineer x4006
Pacific Gas and Electric Co.
77 Beale Street, Rm. 2361
San Francisco, CA 94106

MOORE, Douglas M. (404) 894-3412
Research Engineer II
Georgia Institute of Technology
EES/TAL
Atlanta, GA 30332

MORSE, Howard (415) 964-3200

Acurex Corporation
PO Box 7555, 555 Clyde Ave.
Mountain View, CA 94039

MURPHY, Lawrence M. (303) 231-1050
Group Manager
Solar Energy Research Institute
1617 Cole Blvd.
Golden, CO 80401

NAJEWICZ, David J. (518) 785-2284
Sr. Project Manager
Mechanical Technology Inc.
968 Albany-Shaker Rd.
Latham, NY 12110

NELVING, Hans G. 01146-40-100950

United Stirling AB
Box 856
Malmo, S 20180 SWEDEN

O'GALLAGHER, Joseph J. (312) 962-7757
Sr.Res.Assoc.,Enrico Fermi Institute
University of Chicago
5640 Ellis Ave.
Chicago, IL 60637

O'NEILL, Mark J. (214) 272-0515
Executive Vice President
Entech
P. O. Box 612246
DFW Airport, TX 75261

OTTS, John, V. (505) 844-2280
Div. Supv. - CRTF/DRTF
Sandia National Laboratories
Kirtland AFB
Albuquerque, NM 87185

OWEN, William A. (213) 577-9315
Member Technical Staff (FTS) 961-9315
Jet Propulsion Laboratory
4800 Oak Grove Dr., MS 506-328
Pasadena, CA 91109

PAPPAS, George M. (505) 846-5205
(FTS) 846-5205

US Department of Energy
P. O. Box 5400
Albuquerque, NM 87115

PERCIVAL, Worth H. (703) 549-7174
Technical Director
United Stirling, Inc.
211 The Strand
Alexandria, VA 22314

PERKINS, Robert (714) 896-3073
Mgr., Plant Support Subsystems-SFDI
McDonnell Douglas Astronautics Co.
5301 Bolsa Avenue
Huntington Beach, CA 92647

PEROW, John (213) 572-1825
Engineer
Southern California Edison Co.
2244 Walnut Grove Ave.
Rosemead, CA 91770

POTTHOFF, Robert (619) 235-7724
Engineer
San Diego Gas & Electric Co.
PO Box 1831
San Diego, CA 92112

RAFINEJAD, Dariush (415) 964-3200

Acurex Corporation
555 Clyde Avenue, P.O. Box 7555
Mountain View, CA 94039

RANNELS, James F. (202) 252-1623
Senior Physical Scientist (FTS) 252-1623
US Department of Energy Hdqtrs.
8906 Longmead Ct.
Burke, VA 22015

RASBAND, J. Lynn (801) 535-4281
Mgr., Advance Development
Utah Power and Light Co.
PO Box 899
Salt Lake City, UT 84110

RASBAND, J. Lynn (802-535-4281
Mgr. of Advance Development
Utah Power & Light Company
1407 W. No. Temple St. POB 899
Salt Lake City, UT 84110

ROBILLARD, Geoffrey (213) 577-9135
Asst. Lab Dir., Civil Programs Off. (FTS) 961-9135
Jet Propulsion Laboratory
4800 Oak Grove Dr., MS 502-317
Pasadena, CA 91109

ROGAN, James E. (714) 896-3296

McDonnell Douglas Astronautics Co.
5301 Bolsa Avenue
Huntington Beach, CA 92647

ROGERS, Bill (518) 271-7743
Senior Design Engineer
Power Kinetics, Inc.
1223 Peoples Ave.
Troy, NY 12180

ROSE, Thomas K. (612-574-5404
Mgr., Government Business Group
ONAN
1400 73rd Ave., N.E.
Mineapolis, MN 55447

ROSS, Darrell L. (213) 577-9317
Group Supervisor (FTS) 961-9317
Jet Propulsion Laboratory
4800 Oak Grove Dr., MS 507-228
Pasadena, CA 91109

ROY, Aharon (57) 664-786
Professor, Dept. of Chem. Engg.
Ben-Gurion University of Negev
Box 653
Beer-Sheva, 84105, ISRAEL

RUSSO, Richard E. (415) 486-4258
Stf Scientist, Lawrence Berkeley Lab (FTS) 451-4258
University of California
1 Cyclotron Rd., Bldg.90,Rm.2024
Berkeley, CA 94720

SAN MARTIN, Robert L. (202) 252-9275
Dep. Asst. Sec. - Renewable Energy (FTS) 252-9275
US Department of Energy
1000 Independence Ave., SW
Washington, DC 20585

SCHAEFER, John (415) 964-3200

Acurex Corporation
555 Clyde Ave., P.O. Box 7555
Mountain View, CA 94039

SCHUELER, Donald G. (505) 844-4041
Mgr., Solar Energy Dept. 6220 (FTS) 844-4041
Sandia National Laboratories
PO Box 5800
Albuquerque, NM 87185

SCHWINKENDORF, William E. (505) 848-5313
Associate Mgr, Energy Engineering
BDM Corporation
1801 Randolph Rd., SE
Albuquerque, NM 87106

SEARS, Dana A. (612) 574-5546
Project Engineer, Vanguard Module
Onan Corp.-Advanco Corp.
1400 73rd Ave., NE
Minneapolis, MN 55432

SELCUK, M. Kudret (213) 577-9300
Member Technical Staff (FTS) 961-9300
Jet Propulsion Laboratory
4800 Oak Grove Dr., MS 507-228
Pasadena, CA 91109

SHACHAR, Shaul S. (213) 700-3388
Engineer
Rockwell International

Canoga Park, CA 91304

SKVARNA, Paul E. (213) 572-2192
Senior Research Engineer
Southern California Edison Co.
2244 Walnut Grove Ave.
Rosemead, CA 91770

SLEMMONS, Arthur (415) 859-3162
Senior Research Engineer
SRI, International
333 Ravenswood Avenue
Menlo Park, CA 94025

SORON, John E. (518) 271-7743
President
Power Kinetics, Inc.
1223 Peoples Avenue
Troy, NY 12180

SOUTH, Jack (716) 665-6422
Senior Executive
Falconer Glass Industries
500 Work Street
Falconer, NY 14733

SOUVA, Gene C. (213) 417-6875
Dir., Space & Defense Mkt. Dev.
Garrett Corp.
9851 Sepulveda Blvd.
Los Angeles, CA 90045

SPIEGEL, Joseph M. (213) 577-9420
Section Manager (FTS) 961-9420
Jet Propulsion Laboratory
4800 Oak Grove Dr., MS 506-328
Pasadena, CA 91109

STALLKAMP, John (213) 577-9032
Member Technical Staff (FTS) 961-9032
Jet Propulsion Laboratory
4800 Oak Grove Dr., MS 502-207
Pasadena, CA 91109

STEIN, Charles K. (213) 354-8090
Member Technical Staff (FTS) 792-8090
Jet Propulsion Laboratory
4800 Oak Grove Dr., M3 126-310
Pasadena, CA 91109

STOLPE, John (213) 572-1556
Supervising Research Engineer
Southern California Edison
2244 Walnut Grove Avenue
Rosemead, CA 91770

THAYER, Mac (614) 592-3021
President
Sunpower, Inc.
6 Byard Street
Athens, OH 45701

UNDERWOOD, Arthur F.
Engineering Consultant

74 Lakeview Drive
Palm Springs, CA 92264

WAISMAN, Joseph L. (714) 896-3950
Director, Energy Programs
McDonnell Douglas Astronautics Co.
5301 Bolsa Avenue
Huntington Beach, CA 92647

WASHOM, Byron J. (213) 640-2429
President
Advanco Corp.
999 N. Sepulveda Blvd., #314
El Segundo, CA 90245

WATERBURY, Stuart S. (505) 848-5304
Associate Staff Member
BDM Corporation
1801 Randolph Rd., SE
Albuquerque, NM 87106

WEINBERG, Carl J. (415) 820-2000
Chief Dpl. Engineering Research
Pacific Gas & Electric Co.
3400 Crow Canyon Road
San Ramon, CA 94596

WEINSTEIN, LeRoy (714) 896-5098
Prog.Mgr., Collector Subsystems
McDonnell Douglas Astronautics Co.
5301 Bolsa Avenue
Huntington Beach, CA 92647

WEISIGER, Joe (505) 846-5207
Program Coordinator (FTS) 846-5207
US Department of Energy
P. O. Box 5400
Albuquerque, NM 87115

WELLS, David N. (703) 549-7174
Systems Integrator
United Stirling, Inc.
211 The Strand
Alexandria, VA 22314

WENDLING, Don (213) 640-2429
Purchasing Manager
Advanco Corporation
999 N. Sepulveda Blvd.
El Segundo, CA 90245

WILLCOX, William W. (213) 700-8200
Member of Technical Staff IV
Rockwell International, ESG
8900 DeSoto Avenue
Canoga Park, CA 91304

WILLIAMS, Tom A. (415) 422-3371
Research Engineer (FTS) 532-3371
Sandia TPI/Battelle PNL
Sandia/Livermore Labs, Div. 8454
Livermore, CA 94550

WOOD, Douglas E. (206) 627-1627

Solar Steam, Inc.
625 Commerce St., Suite 400
Tacoma, WA 98402

WOODBURY, John P. (213) 165-7462
PDTS Manager
Jet Propulsion Laboratory
4800 Oak Grove Dr., ETS
Pasadena, CA 91109

YOUNGBLOOD, Wallace W. (205) 837-4411
Senior Research Engineer
Wyle Laboratories
7800 Governors Drive, West
Huntsville, AL 35807

YUNG, David T.L. (613) 993-9224
Research Engineer
National Research Council-Canada
Div. of Energy, R92
Ottawa, K1A-OR6, CANADA

ZIPH, Benjamin (313) 995-1755
Vice President
Stirling Thermal Motors
2841 Boardwalk
Ann Arbor, MI 48104

☆U.S. GOVERNMENT PRINTING OFFICE: 1984 -746-081/2642 REGION NO. 4